Importance de la structure spatiale de la strate arborée sur les fonctionnements carboné et hydrique des écosystèmes herbe-arbre. Exemple d'une savane d'Afrique de l'Ouest

Guillaume SIMIONI

4 février 2002

Table des matières

I Contexte et démarche **9**

1 Contexte et démarche de cette étude **11**

II Variabilité spatio-temporelle et interspécifique des fonctionnements carboné et hydrique d'un écosystème de savane **20**

2 La savane de Lamto, Côte d'Ivoire **24**

3 Echanges gazeux foliaires de deux espèces d'arbre et de deux espèces d'herbe de savane **30**

4 Dynamiques foliaires de deux espèces d'arbre de savane **47**

5 Variabilité spatio-temporelle de la production herbacée **63**

III Construction d'un modèle 3D pour l'étude des fonctionnements carboné et hydrique des systèmes herbes-arbres **70**

6 Première version de TREEGRASS **73**

7 Seconde version de TREEGRASS **96**

IV Effets de la structure spatiale du couvert arbre sur les fonctionnements carboné et hydrique d'un écosystème de savane **121**

8 Effets potentiels de la structure spatiale de la strate ligneuse sur la NPP et le bilan hydrique en savane **124**

9 Déterminisme des effets de la structure spatiale de la strate ligneuse sur les fonctionnements carboné et hydrique. **144**

10 Conclusion et perspectives **159**

Note

This is a short desription of the manuscript for non french language readers.

Some parts of the documents are in French, some others, in the form of papers, published or to be published, are in English. All figures are in English.

The PhD thesis is entitled :

“Importance of the tree layer spatial structure on carbon and water function in tree/grass systems. Exemple of a West African savanna.”

It is organized the following way :

Part 1 :

An introduction in French to present the context and the approach (chapter 1).

Part 2 :

Presentation of the field work done to provide data needed to parameterize or test the model, and that are not documented for the site of Lamto. This part comprises 4 chapters : an introduction in French to the site of Lamto (chapter 2), two papers in English (chapters 3 and 4), and chapter 5 in French that describes the spatial and temporal courses of grass standing biomass, necromass, and phytomass.

Part 3 :

Two chapters corresponding to the TREEGRASS model construction, in the form of two papers in English. The first version (chapter 6) is anterior to the field campaign described in Part 2, and was parameterized and tested with already existing data sets. The paper describing the second version (chapter 7) is still under progress.

Part 4 :

Simulation experiments, in the form of two papers. For the first paper (chapter 8) the first version of TREEGRASS was used. The last version of TREEGRASS was used in the second paper (chapter 9). This second paper is still under progress.

Conclusion - Perspectives

In French

Remerciements

Docteur Eh oui, après trois années de mue progressive, le vieil étudiant devient jeune docteur. Or on ne devient pas docteur tout seul.

Bref, je me dois maintenant, et me fais un plaisir de placer un petit “merci” à tous ceux et celles qui y sont pour quelques chose dans cette thèse. Par qui commencer ? La première persone citée va se sentir flattée, alors que les derniers risquent de me casser la gueule, sans parler de ceux que je risque d'oublier (c'est compliqué à faire, les remerciements). Une solution pourrait consister à citer en premier les personnes que je vois souvent, et garder pour la fin celles qui sont loin.

Le lecteur l'a sans doute compris, l'ordre qui suit n'a pas d'importance.

Je vais donc commencer par remercier des ouvriers anomymes qui ont mis en place le mât servant pour les liaisons radio, à côté de la station de géophysique de Lamto. De la haut, avec la vue qu'on a sur la réserve, on se dit qu'il y a de bons côtés à faire une thèse en écologie.

Jacques + Xavier : Cette thèse n'aurait pas vu le jour, n'aurait pas pu se dérouler, et pas non plus se terminer, sans Jacques et Xavier. Tout deux ont pleinement assumé mon encadrement depuis mon DEA.

Je dois à Jacques Gignoux d'avoir guidé mes débuts en modélisation, sur le terrain, et dans les arcanes de SAS. Il est pour moi un de ces chercheurs qui ont toujours l'air (j'insiste sur “ont toujours l'air”) de planer un peu, avec seulement de fugaces passages dans le monde réel. Un exemple : “Jacques, j'ai besoin d'un ordinateur pour faire des simulations.” ... “Jacques, j'ai besoin d'un ordinateur pour faire des simulations !” ... “Jacques, je ne vais pas pouvoir finir cette thèse sans ordinateur ! ! !”. Une fois le message passé, Jacques surgit avec un ordinateur à chaque bras. Et on ne croirait pas comme ça, quand on le croise dans un couloir, mais Jacques a dix bras.

Xavier Le Roux est toujours d'une lucidité exaspérante. C'est énervant de devoir admettre qu'il a presque tout le temps raison, surtout quand il faut que je recommence une figure que j'ai passé deux heures à paufiner. Grâce à Xavier (à Jacques aussi d'ailleurs), cette thèse aura en quelque sorte été écrite deux fois. Merci bien ! Heureusement, si je ne sais pas ce que vaut cette version, la précédente était nettement moins bien. Xavier est une sorte de docteur vicelard qui mêt toujours le doigt là où ça fait bien mal. Et comme j'étais un thésard masochiste, j'écoutais toujours ses douloureux conseils.

Jacques et Xavier sont aussi des compagnons de route. Barcelone, Clermont-Ferrand, Montpellier, Les Houches, Lamto, Santa-Barbara... Bon, je m'arrête, après on va dire que les thésards ne font que du tourisme.

Que ce soit là bas ou ici, ils ont toujours été là.

Directeur Je remercie Luc Abbadie de m'avoir accueilli au sein de son laboratoire, et d'avoir accepté d'être mon directeur de thèse. Tout le monde le sait déjà, mais je n'y résiste pas, Luc est le plus fameux "tonton flaggeur" que Lamto ait connu, juste en dessous de N'Dri. Là c'est moi qui vais me faire flagger ! Mais bon, elle est fini cette thèse, alors je peux m'y risquer. N'empêche que l'état abbadiesque, qui, au passage, n'est pas l'appanage d'une seule persone, met du piquant dans les soirées de Lamto, surtout quand les abeilles s'en mêlent.

N'Guia Kloa : Je remercie le recteur de l'université d'Abobo Adjamé d'avoir autorisé les expériences de terrain présentée dans cette thèse.

Je remercie chaleureusement les anciens et nouveau directeurs de la station d'écologie de Lamto, respectivement Roger Vuattoux et Souleymane Konaté pour m'y avoir accueilli. Et pour le reste aussi, les histoires le soir au coin du feu et la bonne bouffe (merci Roger), la sortie en brousse la nuit au moment du feu et les coups de main pour les manips (merci Souley). Souley, c'est sympa quand t'es là (on aimerait te voir plus souvent quand on est à Lamto).

Je salue Philippe X et Mikael Augros, VSN de la station de géophysique, pour les nombreux coups de main lors de mes séjours à Lamto. Je remercie aussi l'ancien directeur, Pascal Roudil, pour m'avoir permi de "tirer" une ligne électrique depuis la station de géophysique jusque sur ma parcelle, et pour l'évènement qu'a constitué son mariage dans la petite communauté de Lamto.

Je m'agenouille devant les employés de la station d'écologie de Lamto. Leur connaissance du terrain et leur gentillesse m'ont été précieuses. Merci à Lazare et Gérard, qui donnent ses lettres de noblesse à la popotte de Lamto. Merci à Germain pour son dévouement et son sourire ! Et désolé pour tous ces aller-retours improvisés Lamto-Abidjan.

Je ne saurais être trop reconnaissant envers Konan N'Dri Alexis, Koumé N'Guessan François, et Savadogo Sadare Prosper, qui ont assumé tous les suivis sur les arbres, l'herbe, et le sol. Travailler avec vous a été un réel plaisir, partagé j'espère, et les moments en dehors du travail aussi. Je m'en veux un peu de vous avoir parfois demandé de faire des trucs assez tordus. Merci également aux personnes avec qui j'ai passagèrement travaillé à Lamto : Konan Marcel, Loukou Kouakou Martin, Kouassi Kouassi Etienne, et Apo. Je me dois aussi de remercier ceux des employés de la station de géophysique, qui ont construit les échaffaudages en bambou autour des arbres.

Je tiens aussi à remercier un jeune réparateur d'appareils photo dont, honte à moi, j'ai oublié le nom. Sur une caisse en bois, sur un trottoir d'une rue d'Abidjan, il a complètement démonté et réparé mon appareil (une nuit de travail). C'est grâce à lui que j'ai pu faire les photos hémisphériques qui constituent une plaque tournante de mes expériences de terrain.

Divers Des truc tordus, j'en ai fais un tas, comme, je l'immagine, tous les étudiants en thèse, quels qu'ils soient. Je me souviens être resté tard certaines nuits au labo du PIAF à Clermont-Ferrand, pour "coudre" des thermocouples sur des feuilles de silicone (ah, le silicone !), pour construire des capteurs de flux de sève. C'est une partie des expériences de terrain qui n'apparaît pas dans ce manuscrit. Et c'est à Christian Bodet que je dois de savoir faire de mes mains ces choses indispensables à tous être humain normalement constitué. Je remercie aussi Thierry Améglio (PIAF Clermont-Ferrand) et Charles Va-

lancogne (INRA Bordeaux) pour leurs conseils concernants les mesures de flux de sève et le choix du matériel. J'apprécie la disponibilité de Christian. Il aurait du m'accompagner à Lamto, mais a eu un empêchement. C'est Adrian Walcroft, Néo Zélandais de son état, qui l'a remplacé. Expert es échanges gazeux foliaires, il est venu faire une partie des mesures avec le LI-COR. Si les capteurs de flux de sève sont des engins de torture pour les arbres, le LI-COR est un engin de torture pour l'infortuné expérimentateur qui doit en faire l'usage. Pour 250000 F HT, LI-COR inc., Cary, USA, vous livre un appareil qui peut vous pousser tout droit au suicide. Je suis donc d'autant plus reconnaissant à Adrian et admire le calme avec lequel il a accompli sa tâche. Travailler avec lui a été réconfortant.

J'ai aussi fait des manips en France, au labo. Du genre broyage et pesées de feuilles. C'est Raphaëlle Appé, stagiaire en maîtrise qui avait commencé cet infâme travail, et c'est moi qui l'ai fini (berk), avec l'aide de Philippe Breton. Je tiens là à remercier Daniel Benest qui a encadré ces manips de labo avec un grand souci d'organisation.

Après il y a eu les manips in silico ! Et de longues, longues heures à programmer, compiler, débugger, débugger, débugger, débugger... et simuler. Ormi l'aspect conceptuel, car TREEGRASS a été conçu avec Jacques et Xavier, l'aspect technique fut plutôt un travail solitaire. Il faut quand même citer quelques interventions d'Hervé Sinoquet (INRA-PIAF, Clermont-Ferrand), dont on a intégralement pompé le modèle de bilan radiatif, et de mon cousin Gregory Pineau. Greg, malgré son jeune âge, est un de ces gurus Unix capables de mettre à genoux les machines les plus obtues. Il fait cela en tapant au clavier quelque formule ésotérique unixienne, dont seuls les gurus Unix ont le secret, et qui appaise immédiatement un processeur rebelle. Greg a été de bon conseil pour programmer en C++, même si, en définitive, le résultat final le ferait hurler.

Je remercie Eric Dufrêne, du labo d'écologie d'Orsay, pour les discussions terre-à-terre sur l'allocation et la respiration, et pour m'avoir permi d'utiliser le Leaf Area Meter.

Je remercie aussi l'ensemble de mes collègues de travail du laboratoire d'écologie de l'ENS. L'atmosphère sympathique au sein du labo est précieuse.

Jury Je remercie les membres du jury d'avoir accepté de juger ce travail. En particulier François Houllier (CIRAD-AMAP) et Joao S. Pereira (Institut d'Agronomie de Lisbone), tous deux rapporteurs, ainsi que Michael B. Coughenour (NREL, Colostate), qui a fait le chemin exprès depuis le Colorado. Je remercie Bernard Saugier et Jean-Yves Pontallier d'avoir accepter de me prêter un vidéo-projecteur (alors que je n'ai pu obtenir d'utiliser celui de mon propre labo...).

Perso Je me permet maintenant une petite digression.

En général, à lire les pages de remerciements, c'est à croire qu'une thèse est systématiquement une mine de super expériences, scientifiques ou humaines. Je ne pense pas qu'il faille s'attarder sur sa vie privée, mais je pense qu'une thèse demande souvent une implication importante, et que cela déborde du cadre purement professionel. Moi, ma thèse m'a en partie coûté la femme que j'aimais, et que j'aime toujours. Je la remercie néanmoins de m'avoir quitté, car cela m'a ouvert les yeux sur certaines choses. Maintenant que j'ai compris, tu peux revenir ! Bon, ce n'est pas drôle. Et il y a des sujets plus graves, sinon moins importants.

Pendant que je faisais tranquillement des mesures en brousse, des civils étaient abattus à Abidjan, à 200 km à peine. Leur sacrifice a permi de bouter hors du pays un dictateur en puissance. On parle peu de toutes ces morts anonymes pour la liberté. Je leur rend hommage ici.

Ma famille, elle, ne m'a jamais quitté, et j'en remercie les membres pour leurs encouragements. Avec une petite note pour les cousins(es) ayant vécu plus ou moins longtemps dans la grande cité (Charlotte, Greg, Stéphane). Je remercie aussi les amis proches d'être de proches amis.

Préambule

Les systèmes herbes-arbres regroupent divers types de formations végétales mixtes (présence d'herbes et d'arbres). Les fonctionnements carboné et hydrique de ces systèmes restent malconnus. Dans le contexte des changements globaux, au nombre desquels on trouve l'augmentation de la teneur en carbone atmosphérique et des modifications des régimes des pluies et des températures, cette lacune doit être comblée. Il est en effet aujourd'hui important de pouvoir prédire les rôles des écosystèmes dans les cycles du carbone et de l'eau, et les systèmes herbes-arbres, au nombre desquels les savanes, occupent de vastes surfaces. Ces systèmes accueillent également une grande proportion de la population mondiale. Et donc la gestion des ressources dans ces systèmes, et l'interêt agricole des associations herbes-arbres doivent être étudiés.

Dans un contexte plus conceptuel, ces systèmes proposent un certain nombre de défis aux écologues, notamment concernant la coexistence herbes-arbres, les interactions plantes-animaux, ou encore l'impact de l'espace dans les interactions entre organismes.

Cette thèse ne vise pas à déterminer quelles quantités de carbone ces systèmes sont susceptibles de stocker, ni si oui ou non ils présentent un intérêt agricole. Elle ne vise pas non plus à apporter de réponse à la question de la coexistence herbes-arbres. Il s'agit ici d'explorer le déterminisme de la production primaire et du bilan hydrique de ces systèmes, en focalisant sur un aspect singulièrement peu étudié en écologie fonctionnelle : la structuration spatiale de la végétation.

En première partie, l'importance des systèmes herbes-arbres, l'intérêt de les étudier, leur hétérogénéité spatiale, et le contexte et la démarche qui ont guidé ce travail sont présentés. La deuxième partie concerne le site d'étude et les travaux de terrain menés dans la réserve naturelle de Lamto (Côte d'Ivoire). Une troisième partie décrit l'élaboration du modèle de simulation TREEGRASS, outil principal d'investigation. Enfin, la quatrième partie présente les résultats des expériences menées avec TREEGRASS sur l'étude des effets de la structuration spatiale de la strate arborée sur les fonctionnements carboné et hydrique à Lamto.

Première partie

Contexte et démarche

Chapitre 1

Contexte et démarche de cette étude

1.1 Les écosystèmes herbes-arbres

Les écosystèmes herbes-arbres sont caractérisés par la coexistence d'une strate herbacée surmontée d'une ou plusieurs strates arbustive et/ou arborée. Ces systèmes se rencontrent à l'état naturel sous forme de savanes (Figure 1.1) ou résultent d'activités anthropiques, comme les vergers et les systèmes sylvopastoraux. Les systèmes dits silvopastoraux sont des associations herbes-arbres utilisées à des fins agronomiques, notamment pour l'élevage. L'occupation du sol par les seules savanes est estimée à 20% des terres émergées (Scholes et Hall 1996), et à 40% des zones tropicales (Solbrig et al. 1990). Bien qu'approximatifs, ces chiffres attestent de l'importance de l'étendue de ses systèmes, largement comparable à celle des forêts tropicales.

Ils présentent en outre une grande diversité par leur répartition géographique (zones tropicales à tempérées), par leurs caractéristiques climatiques (savanes humides à très sèches), et les espèces végétales que l'on y trouve.

Que ces systèmes soient naturels ou anthropiques, les processus sous-tendant leur fonctionnement sont similaires. A titre de référence, le reste de ce chapitre s'appuiera sur l'exemple des savanes.

1.2 La complexité des systèmes herbes-arbres

1.2.1 Aspects singuliers du fonctionnement

Les savanes présentent des processus fonctionnels analogues à l'ensemble des écosystèmes terrestres : productions primaire et secondaire, et décomposition de la matière organique par les organismes du sol. Mais certains aspects du fonctionnement se trouvent exacerbés en savane :

1. La biodiversité observée des acteurs de la production primaire, avec des groupes fonctionnels aussi distincts que les herbes et les arbres. La coexistence herbes-arbres représente la principale caractéristique des savanes.
2. L'impact majeur de perturbations telles que l'herbivorie et le feu.

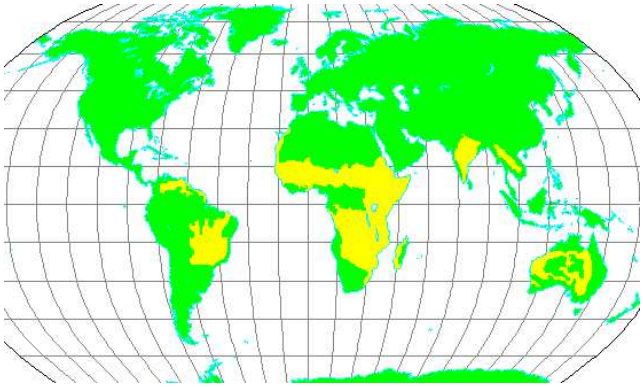

FIG. 1.1 – Extension géographique approximative des savanes tropicales (en jaune). Source : www.runet.edu/~swoodwar/classes/geog235/savanna/savanna.html.
Approximative geographical extension of tropical savannas (in yellow).

3. La forte hétérogénéité spatiale structurelle.

1.2.2 Biodiversité et coexistence herbes-arbres

La coexistence herbes-arbres a fait l'objet de nombreuses études (ex. Walker et Noy Meir 1982, Gignoux 1994, Jeltsch et al. 1996). Certaines ont souligné le rôle de l'herbivorie (Skarpe 1992), du feu (ex. Lacey et al. 1982, Gignoux et al. 1997), et de la compétition pour l'eau (ex. Eagleson et Segarra 1985) ou pour les nutriments (Skarpe 1992). Il n'y a pas de concensus général sur les conditions de cette coexistence et il est probable que ces conditions ne soient pas identiques dans tous les types de savane. Ainsi, les causes de cette coexistence et les conditions d'une éventuelle stabilité restent à déterminer.

Cette coexistence peut prendre plusieurs formes (rapport herbe/arbre très variable) et concerner des espèces plus ou moins éloignées. Ainsi, les espèces d'herbes et d'arbres coexistantes peuvent appartenir à des groupes métaboliques communs (incorporation du carbone suivant un métabolisme en C_3, cas fréquent au Sahel) ou distincts (arbres C_3, et herbes du goupe C_4, cas fréquent en savane humide). Herbes et arbres n'ayant pas les mêmes caractéristiques physiologiques, il est probable que le rapport herbes-arbres ait une forte influence sur la production primaire nette (NPP) et le bilan hydrique à l'échelle de l'écosystème. Les espèces d'herbe ou d'arbre peuvent par ailleurs différer par leurs modes d'alimentation hydrique (ex. Knoop and Walker 1985, Le Roux and Bariac 1998) ou azotée (ex. Lata 1999).

En dehors de la coexistence herbes-arbres, il a été montré dans différents écosystèmes que la biodiversité peut avoir un impact important sur le fonctionnement (ex. Naeem et al. 1994). La biodiversité est plus ou moins importante en savane, mais les effets de la biodiversité sur la NPP et le bilan hydrique ont été singulièrement peu abordés, indépendemment des études faites sur la coexistence herbes-arbres. Or il est probable que les différentes espèces au sein de chaque strate de végétation ne sont pas équivalentes. C'est vrai quand on compare différents types de savanes (ex. plantes plus ou moins adaptées à la sécheresse), mais aussi au sein d'une même savane (ex. Le Roux et Bariac 1998, qui ont montré des différences de comportements hydriques entre deux espèces d'arbre à Lamto, ou, au Vénézuela, la coexistence d'arbres à feuilles décidues et

d'arbres à feuilles persistantes (Medina 1982)).

1.2.3 Les perturbations

Le feu

Le feu, généralement d'origine anthropique, se produit à intervalles plus ou moins réguliers. Il détruit la partie épigée de la strate herbacée (y compris les plantules d'arbre s'y trouvant), et infuence notamment la phénologie des arbres et la démographie des plantes (Hochberg et al. 1994, Garnier et Dajoz 2001). Le feu a aussi un impact important sur les cycles biogéochimiques en savane, puisque le carbone et les minéraux contenus dans le combustible sont partiellement volatilisés (Delmas et al. 1995), ce qui constitue une perte pour le système.

L'herbivorie

Par la pression qu'elle exerce sur les végétaux, et par son influence sur les cycles des nutriments l'herbivorie peut avoir un impact important sur la production, (Owen Smith 1988, Leriche et al. 2001) et la biodiversité (McNaughton 1993) en savane.

La sécheresse

Les savanes présentent pour la plupart une saisonalité marquée, avec au moins une saison sèche et une saison des pluies. La sécheresse conditionne l'activité et la phénologie de la végétation (Wright and Cornejo 1990, Borchert 1994, Williams et al. 1997).

1.2.4 L'hétérogénéité spatiale

Les savanes présentent une forte hétérogénéité spatiale. On peut aborder cette hétérogénéité sous sa forme structurelle et sous sa forme fonctionnelle.

La structuration spatiale des végétaux (densité et agrégation des arbres) et des caractéristiques du sol (capacité de rétention d'eau, quantité de matière organique) participe de l'hétérogénéité structurelle. La répartition spatiale des arbres est fortement hétérogène (ex. San José et al. 1991, Skarpe 1991) avec un couvert discontinu. On retrouve des espèces plutôt isolées, d'autres plutôt en bosquet, et des mixtes (Gignoux 1994). Une même espèce peut en outre présenter des caractéristiques variables entre des individus isolés ou en bosquet (c'est le cas de l'architecture, Simioni et al. non publié). La strate herbe peut elle aussi, à une échelle fine (de l'ordre du mètre carré) être considérée comme discontinue avec, dans le cas de graminées perennes en touffes, de l'ordre de 80% de sol non occupé (César et Menaut 1974, Lata 1999). La structure du sol est également spatialement hétérogène. Par exemple les zones sous couvert arbre ou au niveau de buttes termitiques peuvent présenter de meilleures capacités de rétention d'eau (Mordelet et al. 1993, Konate et al. 1998) et de meilleurs stocks de matière organique.

Cette hétérogénéité structurelle influence le déroulement des processus de l'écosystème dans l'espace, et conditionne l'hétérogénéité fonctionnelle en contraignant la répartition spatiale des ressources et des perturbations. Les variables microclimatiques (température, humidité) sont spatialement hétérogènes (Breshears et al. 1997b, Breshears et al. 1998). Le microclimat qui peut être créé par un arbre en est un bon exemple.

L'ombrage occasioné par les arbres conditionne la quantité de lumière disponible pour la strate herbe. L'ombrage réduit aussi les pertes d'eau par évaporation ce qui, associé à de meilleures qualités hydriques du sol, peut augmenter la disponibilité en eau (Breshears et Barnes 1999). Les zones sous couvert arbre présentent également un sol généralement plus riche en nutriments (Weltzin and Coughenour 1990, Mordelet et al. 1993, Belsky 1994). Ces différents aspects influencent la production herbe sous couvert, mais aussi le recrutement des plantules d'arbres. Les buttes termitiques présentent aussi des conditions particulières qui vont influencer la croissance des végétaux, le recrutement des plantules (Barot et al. 1999), et à terme la végétation ligneuse et herbacée sur ces buttes (Abbadie et al. 1992). L'intensité des perturbations va dépendre étroitement de la structure spatiale du système. Le feu dépend en grande partie de la quantité de combustible. Il sera donc d'autant plus intense que la production herbacée est élevée. De même, l'herbivorie n'est pas uniforme dans l'espace, les herbivores sélectionnent des zones de nourriture favorables en termes de quantité, de qualité et d'accessibilité (Senft et al. 1987, Bailey et al. 1996). Les plantes seront plus ou moins sensibles à la sécheresse selon qu'elles se trouvent dans des zones plus humides, comme sous couvert arbre.

En retour, l'hétérogénéité fonctionnelle va influencer l'hétérogénéité spatiale. Le recrutement des plantules dépend du passage ou non du feu, des caractéristiques du sol, etc.

1.2.5 Des écosystèmes dynamiques

Les aspects particuliers du fonctionnement des savanes en font des systèmes pouvant changer de structure rapidement. La suppression ou la modification d'un des processus de fonctionnement peut engendrer des changements brutaux (ex. passage d'une savane à une forêt en 20 ans en supprimant le feu à Lamto, Devineau et Vuattoux 1984). En particulier, un phénomène général d'augmentation du couvert arbustif est observé ces dernières décennies (Polley et al. 1997, Archer et al. 2000). Les causes de ce phénomène restent hypothétiques : augmentation du CO_2 atmophérique qui favoriserait les plantes à métabolisme en C_3, changements dans le régime des feux, changement de la pression d'herbivorie, ces deux derniers pouvant être liés à des activités anthropiques.

1.2.6 Questions écologiques particulières au fonctionnement des savanes

Au cours des sections précédentes, de nombreux aspects des relations structure-fontion en savane ont été cités. Il apparaît clairement que de nombreux processus ont une importance sur la production primaire, le bilan hydrique et les cycles des nutriments. Mais les connaissances actuelles ne permettent pas une compréhension globale du fonctionnement des savanes. Des questions sont toujours sans réponse :

- La diversité des processus est-elles nécessaire au maintien des savanes, comme le suggèrent Jeltsch et al. (1996), ou certains processus sont-ils dominants ? Autrement dit, peut-on négliger certains processus ?
- Si des processus sont dominants, lesquels ? Et sont-ils les mêmes dans tous les types de savane et à toutes les échelles ? Ce qui revient à dire : à quels processus particuliers doit-on s'intéresser dans un contexte donné ?

En particulier, l'influence sur le fonctionnement de l'écosystème de l'hétérogénéité spatiale de la strate ligneuse, commune à tous les systèmes herbes-arbres, n'a été que partiellement étudiée.

1.2.7 Prédire la production primaire nette et le bilan hydrique des systèmes herbes-arbres : des enjeux pratiques à différentes échelles

Indépendemment de l'intérêt conceptuel que suscite le fonctionnement des savanes, des questions d'ordre pratique se posent à différentes échelles de temps et d'espace :

A l'échelle du biome : quelle est la part des savanes dans la production primaire mondiale, quel rôle peuvent-elles jouer sur la séquestration du carbone, et dans quelle mesure interagissent-elles avec le climat ? Vu leur étendue géographique et l'importance des émissions de carbone par les feux de savane (Menaut et al. 1991), pouvoir évaluer précisément le rôle des systèmes herbes-arbres dans le bilan carboné mondial est de toute première importance. Les modèles globaux requièrent des paramètres pour prédire la production à l'échelle des différents biomes (paramètres de photosynthèse ex. Haxeltine et Prentice 1996, ou d'efficiences de conversion de la lumière, ex. Ruimy et al. 1996). Or de tels paramètres pour des espèces de savane sont rares. Ces modèles se basent également sur des estimations par télédétection du couvert végétal. De telle mesures dans les systèmes herbes-arbres sont compliquées par l' hétérogénéité spatiale de la végétation, et des méthodes spécifiques doivent être developpées (Asner et Wessman 1997, Asner et al. 1998b). L'avènement de satellites capables de produire des images haute définition (avec une précision de l'ordre du mètre) devrait nettement faire progresser ce domaine.

A l'échelle du paysage : Au niveau du paysage, la transpiration du couvert végétal influence les quantités d'eau ruisselée et infiltrée dans le sol. La nature du couvert végétal peut donc influencer l'hydrologie. Les zones de savanes, où la pression démographique peut être importante, et où la disponibilité en eau peut-être problématique, ont pourtant peu fait l'objet de travaux conjoints entre écologistes et hydrologues (mais voir Boulain 2000).

A l'échelle locale : pour des besoins de conservation du milieu naturel, pratiques d'agroforesterie, monitoring... la demande est forte en outils de gestion, notamment pour les agriculteurs ayant choisi les systèmes silvo-pastoraux pour élever du bétail ou faire des cultures. Les interactions plantes-plantes et plantes-animaux sont alors au premier plan, mais de tels outils sont rares, et difficilement généralisables parce qu'empiriques (ex. GRASP, McKeon et al. 1990). Mieux comprendre les mécanismes agissants sur le fonctionnement de ces systèmes pourra sans aucun doute permettre de proposer des outils fiables.

1.3 Objectifs et démarche de la thèse

> *"To an observer B, an object A* is a model of an object A to the extent that B can use A* to answer questions that interest him about A."*

Minsky 1965

1.3.1 La modélisation comme outil d'investigation

Aux qualités généralement reconnues des modèles (outils de gestion, étude des propriétés des systèmes écologiques, états des lieux des connaissances, tests d'hypothèses scientifiques), Coquillard et Hill (1997) ajoutent qu'ils permettent de mettre à jour des "comportements écologiques incompréhensibles par la seule voie réductionniste". Cela semble particulièrement vrai en savane, où l'hétérogénéité spatiale et la complexité des processus handicapent fortement les approches expérimentales classiques. La réplicabilité des mesures pose problème (Jetsch et al. 1997). Par exemple, si deux parcelles présentent le même type de sol, d'autres facteurs, comme le recouvrement ligneux par exemple, rendront ces parcelles différentes. Il est de plus extrêmement difficile de focaliser sur un unique processus in situ. La modélisation apparaît alors comme un outil de choix pour étudier des écosystèmes aussi complexes que les savanes (Scholes and Archer 1997, Jeltsch et al. 1996).

1.3.2 Objectifs de ce travail

L'espace semble être une composante essentielle des savanes mais a été cependant peu étudié. Des travaux ont été menés pour mettre en avant le rôle de l'espace dans la démographie des arbres (Gignoux 1994, Barot et al. 1999), dans la coexistence herbes-arbres (Gignoux 1994, Jeltsch et al. 1996), et dans la dynamique à long terme de l'écosystème (Jeltsch et al. 1997). Mais l'impact de l'hétérogénéité spatiale de la végétation ligneuse sur la production primaire et le bilan hydrique n'a pas été abordé. Or si la strate arborée détermine pour une grande part l'accès aux ressources de la strate herbacée, on peut légitimement se demander si différents agencements spatiaux des arbres ne vont pas avoir des conséquences sur la productivité et l'évapotranspiration du système entier.

Il apparaît donc important d'étudier l'influence de la structure spatiale de la strate arborée (densité et agrégration des arbres) pour 1) l'identifier ou non comme déterminant majeur du fontionnement, et 2) le cas échéant, améliorer la qualité des prédictions des modèles de fonctionnement de systèmes herbes-arbres, quelles que soient les échelles de temps et d'espaces considérées.

Ce travail de thèse focalise sur l'importance de la structure spatiale de la strate arborée sur la production primaire et le bilan hydrique annuel. Cette étude se base sur une méthode par modélisation.

Les questions auxquelles ce travail de thèse propose de répondre sont :

1. Pour un écosystème de savane donné, au cours d'un cycle de végétation, la structure spatiale de la strate ligneuse peut-elle modifier les performances de l'écosystème, en terme de production primaire nette (NPP), de bilan hydrique, et d'efficiences d'utilisation des ressources (lumière, eau, azote) ?
2. Si oui, quelles sont les conditions de cette influence ?
3. Toujours au cas où une influence est montrée, peut-elle être prédite à l'aide des descripteurs habituels de végétation (par exemple l'indice foliaire (LAI)), ou est-il nécessaire de développer des méthodes spécifiques pour qu'elle soit prise en compte à des échelles de temps et d'espace plus grossières ?

1.3.3 Choix du modèle

Pour satisfaire aux objectifs fixés, le modèle utilisé doit :

1. être en trois dimensions afin de pouvoir prendre en compte la structuration spatiale : 1) les positions des plantes, 2) la conformation dans l'espace du feuillage et des racines, et 3) l'hétérogénéité des caractéristiques du sol.
2. décrire les mécanismes écophysiologiques liés à la production primaire (photosynthèse, respiration, allocation) et aux flux hydriques (évaporation et transpiration), et reproduire les influences environnementales sur ces mécanismes.
3. être basé sur les individus, niveau auquel se déroulent les mécanismes influençant la démographie, et également permettant d'étudier l'importance de l'agrégation des individus. Plusieurs études ont montré l'intérêt de tenir compte des individus sur le fonctionnement de l'écosystème (Pacala and Deutschman 1995, Moravie et al. 1997). Ceci limite en outre le modèle à reproduire des parcelles de surfaces modestes, mais néanmoins pertinentes pour étudier les mécanismes opérant à l'échelle de l'écosystème (compétition entre individus).

Le choix du type de modèle est important. Un modèle trop empirique est clairement inadapté car il ne permettra pas d'étudier les processus. De plus, les besoins de pouvoir prédire NPP et flux d'eau, et de pouvoir hiérarchiser les processus suggèrent un modèle quantitatif. Selon Luo et Reynolds (1999), intégrer au sein d'une même approches de nombreux processus apparaît aujourd'hui indispensable pour aboutir à une compréhension intégrée du fonctionnement des écosystèmes, par exemple en réponse aux changement globaux.

Notre choix s'est donc porté sur l'utilisation d'un modèle mécaniste. Un tel modèle est cependant très exigeant en terme de données de terrain, que cela soit pour le paramétrer, le valider, où l'alimenter en variables d'entrée (ex. forçage climatique). Mais en retour, un tel modèle, pour peu qu'il soit convenablement paramétré et testé, doit permettre d'identifier et de quantifier les processus clés du fonctionnement.

Dans le cadre de ce travail, on considère le modèle comme un laboratoire virtuel.

1.3.4 Les modèles de systèmes herbes-arbres existants

Différentes approches ont été proposées à différentes échelles spatiales :

A l'échelle continentale : Les modèles globaux (voir Sellers et al. 1997) sont conçus pour prédire les flux d'eau et de carbone à l'échelle continentale ou planétaire, y compris pour les zones de savane. Ces modèles ne sont spatialement explicites que pour des tailles de pixels très élévées, de l'ordre du degré carré. Ces modèles disposent de paramétrisations insuffisantes pour les zones de savanes.

A l'échelle du paysage : Des modèles ont été conçus à l'échelle du paysage pour étudier le fonctionnement des savanes à plus ou moins long terme dans le cadre de changements climatiques (MCI, Daly et al. 2000) ou pour étudier la structure spatiale du paysage (SAVANNA, Coughenour 1994). MCI n'est pas un modèle spatialement explicite et fonctionne à des pas de temps élevés. SAVANNA inclue l'hétérogénéité spatiale à

l'échelle du paysage (distinction de zones boisées et herbacées), mais pas à l'échelle des individus. Ce modèle inclue cependant un paramètre d'agrégation des arbres, qu'aucune étude n'a permis de calibrer correctement (Coughenour, com. pers.).

A l'échelle de l'écosystème : Plusieurs approches existent à l'échelle de l'écosystème. On peut distinguer celles qui s'intéressent particulièrement à la coexitence herbes-arbres. Elles sont spatialement explicite. Le modèle de Jeltsch et al. (1996) est un automate cellulaire qui intègre un jeux complet de processus (influence climatique, herbivorie, feu). Il fonctionne à des échelles de temps de l'ordre de plusieurs siècles, et la description des flux de carbone et d'eau est très simplifiée. Les travaux menés autour de l'Ecological Field Theory (EFT, Walker et al. 1989), ont données lieu à des approches tridimensionnelles, décrivant des zones d'influence des plantes agissant sur la disponibilité des ressources. La résolution temporelle est là aussi très grossière.

Le modèle CENTURY-SAVANNA (Parton et al. 1993) est une adaptation du modèle CENTURY (Parton et al. 1988) pour gérer des systèmes herbes-arbres. C'est un modèle qui privilégie les mécanismes de recyclage de la matière organique du sol, et où la disponibilité des nutriments détermine de façon simple la croissance des plantes. Ce modèle n'est pas spatialement explicite.

A des échelles temporelles plus fines, on trouve des modèles développés comme outils de gestions (le modèle empirique GRASP, McKeon et al. 1990, le modèle herbes-arbres ALWAYS, Berjez et al. 1999) mais ils ne sont pas spatialement explicites.

Aucun de ces modèles n'est adapté aux objectifs de cette thèse.

1.3.5 L'approche du modèle TREEGRASS

La construction d'un modèle spatialement explicite et mécaniste représente un investissement important. Dans un contexte moins immédiat que celui de la thèse, pouvoir faire évoluer un tel modèle pour étudier des questions complémentaires sur le fonctionnement des savanes apparaît comme un moyen de rentabiliser à long terme l'investissement placé dans sa contruction.

Puisque de nombreuses questions persistent à différentes échelles de temps et d'espace, nous avons choisi de placer ce travail au sein d'une approche bottom-up. Dans un premier temps, à l'échelle de la thèse, cette approche se limite à étudier la structure spatiale de la végétation. A plus long terme, le modèle pourrait être complété pour évaluer l'importance d'autres mécanismes (l'importance de l'hétérogénéité de la matière organique du sol, par exemple). A terme, un tel modèle pourrait permettre d'étudier l'ensemble des processus importants opérant aux échelles spatiale et temporelle fines (compatibles avec les écosystèmes). Un tel modèle, pourrait servir de référence à l'élaboration de méthodes de changement d'échelle (simplifications *a posteriori*) de manière à pouvoir tenir compte des processus identifiés comme importants à une échelle fine dans une échelle plus grossière. Les simplifications inhérentes à un changement d'échelle s'accompagnent d'une complexification par ajoût de processus opérant à l'échelle la plus grossière. Par exemple, on ne peut prendre en compte de façon explicite la structure spatiale fine de la végétation à l'échelle du paysage, il faut donc la simplifier quand on passe de l'écosystème au paysage. En même temps, il est nécessaire d'ajouter une composante hydrologie, qui est susceptible d'interagir avec la végétation et donc d'influencer la NPP et le bilan hydrique à l'échelle du paysage.

Dans ce contexte, le modèle élaboré au cours de cette thèse, baptisé TREEGRASS, représente la première étape d'une approche modélisatrice susceptible d'aborder de nombreux aspects du fonctionnement des savanes.

1.4 Choix du site et plan de travail

Le travail de cette thèse s'articule autour de la construction et de l'utilisation du modèle TREEGRASS. Ce modèle nécéssitera de nombreuses données de terrain aux fins d'une part, de paramétrisation, et d'autre part, de validation. Le choix du site de référence doit donc s'orienter vers un site déjà fortement documenté.

La réserve de Lamto (Côte d'Ivoire) présente l'avantage d'un site de savane ayant fait l'objet de nombreuses études, notamment sur le sol et la végétation. Il fait en outre l'objet d'un suivi climatique permanent. Lamto a été récemment sélectionné comme site de référence d'une zone atelier de suivi des écosystèmes à long terme.

La production (César et Menaut 1974, César 1992, Mordelet 1993a, Le Roux 1995) et les flux d'azote (Abbadie 1984) au niveau de la strate herbacée ont été bien décrits. Mais les études ont essentiellement porté sur des zones hors couvert arbre. S'il a été montré une diminution de la production herbe sous couvert (Mordelet 1993a), l'ampleur de cette diminution n'a pu être corrélée à l'intensité du recouvrement arbre. Des données précises d'échanges gazeux foliaires (capacités photosynthétiques) font également défaut.

Les comportements hydriques (mode d'extraction de l'eau par les plantes) de la strate herbe et de deux espèces d'arbres (*Crossopteryx febrifuga* et *Cussonia arborea*) ont été étudiés (Le Roux et al. 1995, Le Roux et Bariac 1998).

Mis à part le comportement hydrique, la strate arborée a principalement été étudiée d'un point de vue démographique (Gignoux 1994, Barot 1999), mais il n'existe aucune donnée sur le développement du feuillage, sur les caractéristiques folaires, ou sur les échanges gazeux foliaires.

Dans cadre de la thèse, à des fins de paramétrisation ont été mesurées :

- les caractéristiques d'échanges gazeux foliaires pour deux espèces d'herbe (*Andropogon canaliculatus* et *Hyparrhenia diplandra*) et deux espèces d'arbres (*Crossopteryx febrifuga* et *Cussonia arborea*).
- la dynamique spatio-temporelle du feuillage arbre.

Un deuxième aspect concerne l'obtention d'un jeu de données robustes destinées à tester le modèle :

- suivi temporel de la croissance herbe, à différents niveaux de recouvrement arbre.
- suivi des teneurs en eau du sol dans les mêmes zones que le suivi herbe.

Ces travaux de terrain, mettant en évidence la variabilité spatio-temporelle des fonctionnements carboné et hydrique de la savane de Lamto, sont présentés dans la deuxième partie de cette thèse. La structure du modèle TREEGRASS, sa paramétrisation et les tests effectués, font l'objet de la troisième partie. La quatrième partie décrit les expériences par simulations destinées à satisfaire aux objectifs de cette thèse.

Deuxième partie

Variabilité spatio-temporelle et interspécifique des fonctionnements carboné et hydrique d'un écosystème de savane

Introduction aux études de terrain

Dans cette partie sont présentés les travaux de terrain effectués en vue de fournir des données pour paramétrer et tester le modèle TREEGRASS. La paramétrisation de ce modèle requiert des informations de base sur la physiologie (caractéristiques photosynthétiques, caractéristiques foliaires, et comportement hydrique) des plantes et les caractéristiques hydriques (point de flétrissement, capacité au champ) du sol.

Les caractéristiques hydriques du sol sont déjà bien documentées (le Roux 1995) et peuvent être aisément complétées par des mesures en saison sèche et en saison des pluies. La production de la strate herbe a déjà fait l'objet de plusieurs études concernant la concentration en azote foliaire (Abbadie 1984) et la dynamique annuelle de la croissance (Roland 1967, Abbadie 1983, Puyravaud 1990, Mordelet 1993a, Le Roux 1995). Des mesures de photosynthèse ont été faites sur une espèce d'herbe (Le Roux et Mordelet 1995) mais sont inadaptées pour paramétrer un modèle mécaniste de photosynthèse. Le Roux et al. (1995) et Le Roux and Bariac (1998) ont bien documenté les modes d'alimentation hydrique de la strate herbe.

La physiologie des arbres n'a fait l'objet que de très peu d'attention jusqu'à aujourd'hui. Le Roux et Bariac (1998) ont cependant montré que deux espèces d'arbres, *Crossopteryx febrifuga* et *Cussonia arborea*, présentent des comportements hydriques différents, le second puisant l'eau plus en profondeur que le premier. Des données non publiées de J.-C. Menaut sont également disponibles sur les relations allométriques des arbres en savane. Mais leurs caractéristiques foliaires (dynamique de la surface foliaire, teneur en azote, rapport poids-surface), restent inconnues, elles sont pourtant essentielles pour estimer l'assimilation de carbone par les plantes.

Aux fins de paramétrisation ont donc été mesurés :

1. les échanges gaseux foliaires de deux espèce d'herbe (*Andropogon canaliculatus* et *Hyparrhenia diplandra*) et de deux espèces d'arbre dominantes dans la savane de Lamto.
2. la dynamique annuelle des surfaces foliaires et des caractéristiques foliaires des deux espèces d'arbres.

Des expériences spécifiques ont été menées afin de produire un jeu de données adapté pour tester le bon fonctionnement du modèle. Des suivis ont été mis en place simultanément et sur les même parcelles que les expériences destinées à paramétrer TREEGRASS :

1. La croissance herbacée à différents niveaux de recouvrement arbre.

2. Les teneurs en eau du sol dans différents horizons sous et hors couvert arbre.

A ces suivis s'ajoute l'utilisation de photos hémisphériques permettant de caractériser le recouvrement arbre, et donc de relier la production herbacée et l'eau du sol au recouvrement arbre.

Ces expériences sont présentées sous forme de trois chapitres, les deux premiers sous forme de publications : (i) les mesures d'échanges gazeux foliaires, (ii) la dynamique foliaire et l'eau du sol des deux espèces d'arbre, et (iii) la variabilité spatio-temporelle de la production herbe. Ces chapitres sont précédés d'une description du site d'étude.

Chapitre 2

La savane de Lamto, Côte d'Ivoire

2.1 Localisation et climat

La réserve naturelle de Lamto est située en République de Côte d'Ivoire, à environ 200 km au nord d'Abidjan (6°13 N, 5°02 W). Cette localisation correspond au sud du "V baoulé", une zone de savane qui s'étend vers le sud dans la zone de forêt (Figure 2.1).

La réserve s'étend sur 2500 ha et correspond aux savanes de type guinéen, caractérisées par une pluviométrie annuelle élevée et répartie de façon bimodale. Ainsi, les 1200 mm annuels de pluie en moyenne se répartissent en une grande saison des pluies de mars à juillet et une petite saison des pluies de septembre à novembre.

La variabilité interannuelle des précipitations est importante avec des totaux annuels observés allant de 800 à 1400 mm.

2.2 Type de sol

La roche mère se compose de granite (socle précambrien), souvent affleurant. Les sols résultants de l'érosion de la roche mère sont des sols dits ferrugineux tropicaux (classification française, CPCS 1967), ou ferralsols (classification FAO, Delmas 1967, Riou 1974). Ces sols sont très sableux et peu argileux avec un pH acide (5-6.5). Ils sont généralement très pauvres en calcium, potassium, phosphore, et azote.

Delmas (1967) a pu distinguer différentes variantes de sols ferrugineux : sols ferrugineux de plateau et de haut de pente, sols ferrugineux de pente, plus limoneux, et des sols de bas de pente, hydromorphes très limoneux, saisonnièrement engorgés d'eau.

2.3 Le feu

Le feu est un facteur à part entière du milieu. Il est artificiellement déclenché, sous contrôle, vers la mi-janvier. Il détruit en grande partie la végétation herbacée épigée (César 1971) et les plantules d'arbres, alors que les arbres adultes sont moins exposés (les bourgeons se trouvant majoritairement au dessus du niveau des flammes). le feu semble jouer un rôle prépondérant dans la structure et la stabilité de la savane, en influant sur le rapport herbes/arbres (Menaut et al. 1993). Des parcelles non brûlées de

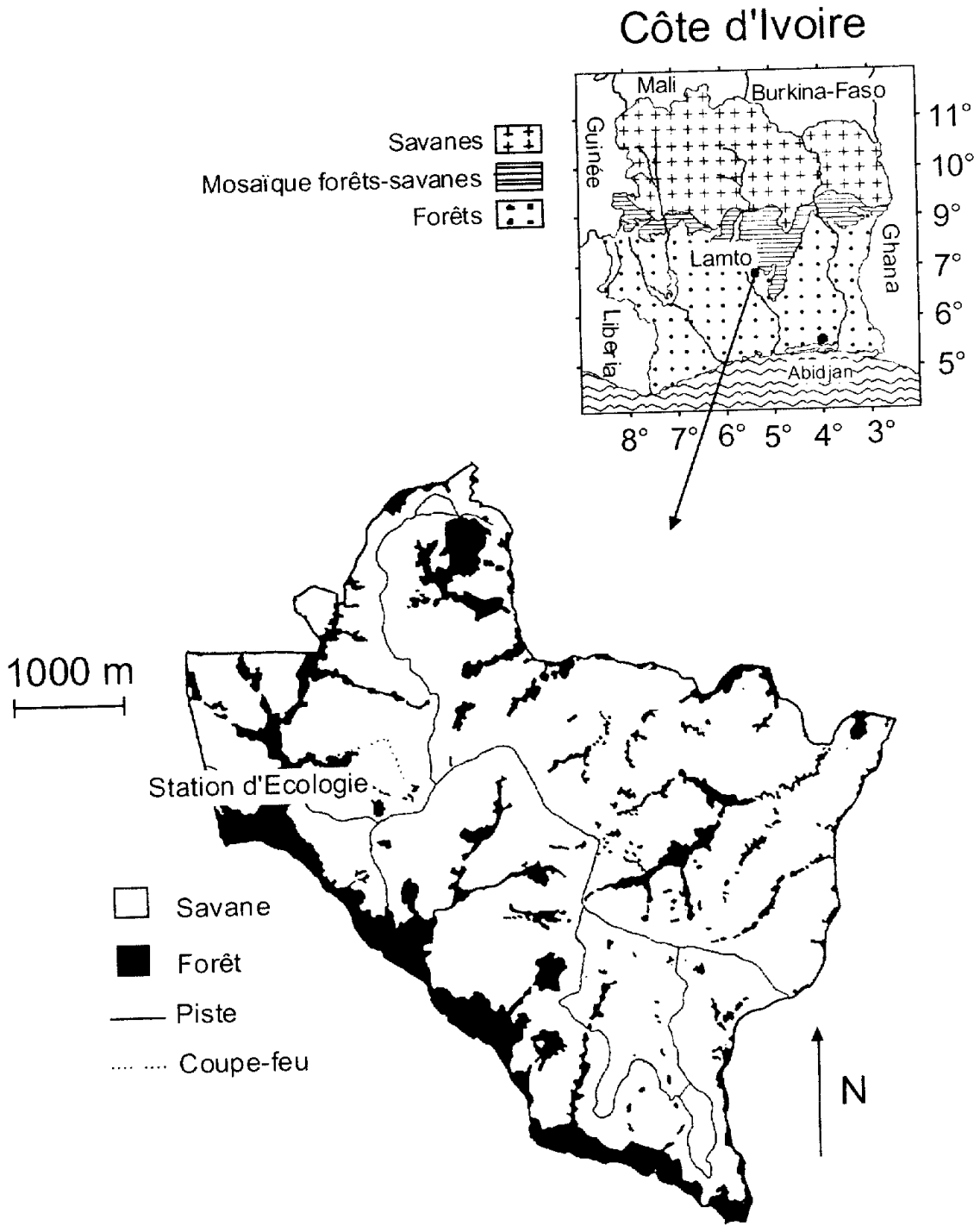

FIG. 2.1 – Carte de la végétation de la réserve de Lamto (Côte d'Ivoire) (d'après Gautier 1990a).
Vegetation map of the Lamto natural reserve (Ivory Coast) (after Gautier 1990a)

FIG. 2.2 – *Crossopteryx febrifuga*

Lamto ont été recolonisées par des espèces de forêt en moins de trente ans (Vuattoux 1970, 1976).

2.4 La végétation

la végétation est constituée d'une mosaïque de savanes séparées par des forêts galleries dans les bas-fonds (Menaut et César 1979, Gautier 1990b) (Figure 2.1). La végétation se répartie sur des plateaux, des bas-fonds et des zones de transition. Sur les plateaux, se trouvent des savanes boisées, sur les zones de transition (du haut de pente vers le bas) on trouve des savanes arbustives à Andropogonées, des savanes herbeuses à *Loudetia simplex*, et, dans les bas-fonds, des forêt galeries qui bordent les cours d'eau (marigots) temporaires ou permanents.

Le couvert ligneux des savanes a tendance à décroître du haut vers le bas de la pente. Il est dominé par quatres espèces : *Crossopteryx febrifuga*, *Cussonia arborea*, *Piliostigma thonningii*, et *Bridelia ferruginea.*

La strate herbacée est largement dominée par les graminées (75 à 99% de la biomasse totale, César 1971, César et Menaut 1974). Les principales espèces appartiennent aux genres *Hyparrhenia*, *Andropogon* et *Loudetia*.

FIG. 2.3 – *Cussonia arborea*

2.5 Les espèces étudiées

Les expériences ont porté sur deux espèces d'herbe, *Hyparrhenia diplandra* et *Andropogon canaliculatus* de la famille des Andropogoneae. Cette famille a été le point d'intérêt de nombreuses études menées sur la strate herbe (Menaut et César 1979, Abbadie 1984, Abbadie 1992, Le Roux 1995, Lata 1999, Leriche et al. 2001). Ces sont des graminées en touffe, appartenant aux plantes de métabolisme photosynthétique en C_4. Ces herbes sont non nitrifiantes (Lata 1999).

Les deux espèces d'arbres étudiées aux cours de cette thèse sont *Crossopteryx febrifuga* (Rubiaceae, Figure 2.2) et *Cussonia arborea* (anc. *Cussonia barteri*, Araliaceae, Figure 2.3).

2.6 Le site expérimental

Les expériences faisant l'objet des trois prochains chapitres ont été menées sur trois parcelles, proches les unes des autres :

1. Une parcelle "hors bosquet" de 75×35 m présentant trois vastes zones sans arbres et des individus isolés de *C. febrifuga* et *C. arborea* (Figure 2.4). Dans cette parcelle ont été suivis les arbres isolés, les placettes herbe hors couvert arbre, et les teneurs en eau hors couvert arbre.
2. Une parcelle "sous bosquet" de 50×25 m présentant deux bosquets d'arbres (Figure 2.5), dans lesquels ont été suivis les arbres en bosquet, les placettes herbes sous bosquet et les teneurs en eau du sol sous bosquet.
3. Une parcelle dite "damier" de 8×8 m comportant un individu *C. febrifuga* isolé (Figure 2.6). Dans cette parcelle, des placettes herbes situées à différentes distances

FIG. 2.4 – Photographie de la parcelle “hors bosquet”, les arbres disposant d’échaffaudages font partie du suivi.
Photograph of the “out of clump” plot. Trees with scaffoldings were part of the survey.

de l’arbre (différents niveaux de recouvrement) ont été suivies. L’arbre a aussi fait l’objet de suivi en temps qu’individu isolé.

Les mesures d’échanges gazeux foliaires ont eu lieu sur les parcelles “hors” et “sous bosquet”.

FIG. 2.5 – Photographie de la parcelle “sous bosquet”. On peut distinguer les deux bosquets où des arbres ont été suivi (à gauche et à droite).
Photograph of the “clump” plot, where took place the clump tree survey.

FIG. 2.6 – Photographie de la parcelle “damier” après le passage du feu. Noter la matérialisation de placettes de 1×1 m qui servira à délimiter les placettes pour le suivi de la croissance herbacée.
Photograph of the “grid” plot after fire. Note that the soil is marked out with squares, this will be used to delimit grass pixels for the grass growth survey.

Chapitre 3

Echanges gazeux foliaires de deux espèces d'arbre et de deux espèces d'herbe de savane

Leaf gas exchange characteristics and water- and nitrogen-use efficiencies of dominant grass and tree species in a West African savanna

à soumettre

G. Simioni, A. Walcroft, X. Le Roux, and J. Gignoux

Introduction

Information about photosynthetic characteristics and stomatal behaviour of plant species is required to predict carbon and water fluxes at the leaf, plant, ecosystem and biome levels (Schulze et al 1994). In the last decades, photosynthesis and stomatal conductance have been intensively studied for a wide range of species belonging to various ecosystems worldwide. Particular attention has been paid to the light-saturated photosynthetic rate (Amax) and stomatal conductance (g_s) (Schulze et al 1994, Woodward and Smith 1994, Kellilher et al 1995) and to the relationships between Amax, g_s, and the amount of nitrogen per unit leaf area (Field and Mooney 1986, Ellsworth et al. 1994, Reich et al. 1994, Schulze et al 1994). Published works on photosynthesis for dominant plant species in a given ecosystem or biome have generally ignored the biochemically-based modelling approaches proposed by Farquhar et al. (1980) for the C_3 pathway, and by Collatz et al (1992) for the C_4 pathway. This is surprising because those approaches can greatly improve the predictive capacity of photosynthesis models (Leuning 1990) and are largely used in large-scale schemes representing land surface-atmosphere exchanges (Sellers et al. 1997). Reviews on photosynthetic traits in the major terrestrial biomes show that no comprehensive data base is available for the dominant, coexisting species in savanna ecosystems (Schulze et al 1994, Woodward and Smith 1994) despite the large area they cover (3×10^6 km^2 in West Africa, Menaut et al

1991). These savannas often associate C_4 grass and C_3 tree species that are thus expected to exhibit contrasted photosynthetic traits (Ehleringer and Björkman 1977, Bolton and Brown 1980, Pearcy and Ehleringer 1984). These ecosystems can also undergo rapid changes in their structure, particularly the tree/grass balance (Archer et al. 2000). Because C_4 species generally exhibit higher photosynthetic water- and nitrogen-use efficiencies (WUE and NUE) (Sage and Pearcy 1987), a shift from grass- to tree-dominated savanna areas would probably entail strong changes in WUE and NUE at the ecosystem scale. A few field studies have quantified light-saturated net photosynthesis of grass species (Le Roux and Mordelet 1995, Anten et al 1998, Baruch and Bilbao 1999) or tree species (Sobrado 1991 and 1996, Medina and Francisco 1994, Fordyce 1995, Prior 1997) in humid savannas. Responses of g_s to air humidity have also been reported for a few humid savanna grass species (Baruch et al. 1985). However, no comprehensive approach allowing to compare the photosynthetic characteristics among major grass and tree species coexisting in a given humid savanna ecosystem (i.e. photosynthetic capacity, WUE and NUE) has been achieved to date. Furthermore, acclimation of leaf photosynthetic characteristics along light gradients within the canopy (i.e. variations between open areas or under tree clumps for grasses or intra tree crown variations) has not been documented for such species. This is a deterrent for the understanding and predicting of surface-atmosphere exchanges in the humid savanna zone. This is also a deterrent for the understanding of the coexistence of plant life forms in humid savannas. In this study, leaf photosynthesis and stomatal conductance were measured for two dominant perennial C_4 grass species (*Hyparrhenia diplandra* and *Andropogon canaliculatus*), and two dominant C_3 tree species (*Crossopteryx febrifuga* and *Cussonia arborea*) of the Lamto savannas (Ivory Coast). Our objectives were (1) to determine the photosynthetic capacities of the four species and parameterize biochemically-based models of photosynthesis for each, (2) to compare the stomatal responses to light and air humidity between the four species, and (3) to compare the photosynthetic water- and nitrogen-use efficiencies between these species. In particular, we tested whether differences in photosynthetic capacities, stomatal responses to environmental variables, and WUE and NUE were only explained by differences in the photosynthetic pathway and life forms (i.e. contrasts between trees and grasses), or whether significant differences could be observed between species sharing the same photosynthetic pathway and life form (i.e. importance of the specific composition of the grass and tree layers).

Materials and methods

Study area

The Lamto ecological reserve is located 5°02' W and 6°13' N. It belongs to the guinean savanna type, caracterised by a high annual rainfall (typically 1200 mm/year) following a bimodal seasonal distribution. A long dry period occurs from November to March, a long rainy season from March to July, a short dry season in August and a small rainy season from September to October. Vegetation at Lamto has been extensively described in Menaut and César (1979). It is a mosaic of gallery forests (following rivers and seasonal water streams) and savanna areas. The grass layer is dominated by C_4 perennial grasses, essentially from the genders *Hyparrhenia* and *Andropogon*, from the Andropo-

goneae family (about 80% of grass phytomass, Le Roux 1995), among which *Hyparrhenia diplandra* and *Andropogon canaliculatus*. The tree layer is dominated by four C_3 species among which *Crossopteryx febrifuga* and *Cussonia arborea*.

Photosynthesis models

Two photosynthesis models were used to characterise plant photosynthetic characteristics. These are the C_3 photosynthesis model of Farquhar et al. (1980) and the C_4 photosynthesis model of Collatz et al. (1992).

The C_3 photosynthesis model

The model used to derive C_3 plant photosynthetic parameters corresponds to the version of Harley et al. (1992) of the model proposed by Farquhar et al. (1980), without including the potential limitation due to the use of triose phosphate.

Net CO_2 assimilation rate A_n (μmol $CO_2 \cdot m^{-2} \cdot s^{-1}$) is expressed as :

$$A_n = (1 - \frac{0.5 \cdot O}{\tau \cdot C_i}) \cdot min(W_c, W_j) - R_d \tag{3.1}$$

where W_c (μmol $CO_2 \cdot m^{-2} \cdot s^{-1}$) is the carboxylation rate limited by the amount, activation state or kinetic properties of Rubisco, W_j (μmol $CO_2 \cdot m^{-2} \cdot s^{-1}$) is the carboxylation rate limited by the rate of RuP_2 regeneration, τ is the specitivity factor for Rubisco (Jordan and Ogren 1984), R_d (μmol $CO_2 \cdot m^{-2} \cdot s^{-1}$) is the rate of CO_2 evolution in light that results from processes other than photorespiration, and O and C_i (Pa) are the partial pressures of O_2 and CO_2 in the intercellular air spaces, respectively.

W_c follows competitive Michaelis-Menten kinetics with respect to O_2 and CO_2 :

$$W_c = V_{cmax} \cdot \frac{C_i}{C_i + K_c \cdot (1 + \frac{O}{K_o})} \tag{3.2}$$

where V_{cmax} (μmol $CO_2 \cdot m^{-2} \cdot s^{-1}$) is the maximum rate of carboxylation, and K_c and K_o (Pa O_2 and Pa CO_2) are Michaelis constants for carboxylation and oxygenation, respectively.

W_j is controlled by the rate of electron transport J (μmol$\cdot m^{-2} \cdot s^{-1}$) :

$$W_J = J \cdot \frac{C_i}{4 \cdot (C_i + \frac{O}{\tau})} \tag{3.3}$$

J depends on photosynthetically active photon flux density Q (μmol$\cdot m^{-2} \cdot s^{-1}$) :

$$J = \alpha \cdot \frac{Q}{\sqrt{1 + \frac{\alpha^2 \cdot Q^2}{J_{max}^2}}} \tag{3.4}$$

where J_{max} (μmol$\cdot m^{-2} \cdot s^{-1}$) is the light-saturated rate of electron transport, and α is the apparent efficiency of light energy conversion on an incident light basis (mol electrons per mol photons). The temperature dependence of R_d, τ, K_c, and K_o is described by :

$$(R_d,\, \tau,\, K_c,\, K_o) = e^{c - \frac{\Delta H_a}{R \cdot T_l}} \tag{3.5}$$

where ΔH_a (J·mol^{-1}) is the activation energy of the given parameter, R (8.3143 J·K^{-1}·mol^{-1}) is the gaz constant, T_l (K) is leaf temperature, and c is the dimensionless, scaling constant of the given parameter. Similarly, the temperature dependence of V_{cmax} and J_{max} is described by :

$$(V_{cmax}, J_{max}) = \frac{e^{c - \frac{\Delta H_a}{R \cdot T_l}}}{1 + e^{\frac{\Delta S \cdot T_l - \Delta H_d}{R \cdot T_l}}} \tag{3.6}$$

where ΔS (J·K^{-1}·mol^{-1}) is an entropy term, and ΔH_d (J·mol^{-1}) is the deactivation energy of the given parameter. To account for the linear relationships commonly observed between leaf photosynthetic capacities and the amount of leaf nitrogen per unit leaf area N_a (g N·m^{-2}), the scaling factors c for V_{cmax}, J_{max}, and R_d are linearly related to $ln(N_a)$ as :

$$c = a_N + b_N \cdot ln(N_a) \tag{3.7}$$

The C_4 photosynthesis model

The model used to derive C_4 plant photosynthetic parameters corresponds to the simplified model of Collatz et al. (1992).

Gross photosynthesis A is given as a function of Q, C_i, and T_l in a form of a pair of nested quadratic equations. The first equation is :

$$\theta \cdot M^2 - M \cdot (V_T + \alpha \cdot Q) + V_T \cdot \alpha \cdot Q = 0 \tag{3.8}$$

where V_T (μmol CO_2·m^{-2}·s^{-1}) is the temperature-dependent, substrate saturated rubisco capacity, α (mol·mol^{-1}) is the quantum efficiency (initial slope of the photosynthesis-light response), M (μmol CO_2·m^{-2}·s^{-1}) is the flux determined by the rubisco and light limited capacities, and θ is a curvature parameter that gives a gradual transition between Q and V_T limited fluxes. The limitation on the overall rate by M and the CO_2 limited flux is expressed likewise :

$$\beta \cdot A^2 - A \cdot (M + k_T \cdot \frac{C_i}{P}) + M \cdot k_T \cdot \frac{C_i}{P} = 0 \tag{3.9}$$

where k_T is the temperature-dependent pseudo-first order rate constant with respect with C_i, P is the atmospheric pressure (Pa), and β is analogous to θ and specifies the degree of co-limitation between M and the CO_2 limited flux. The smaller roots are the appropriate solutions for both quadratics. A_n is defined as :

$$A_n = A - R_T \tag{3.10}$$

where R_T is the temperature-dependent rate of leaf respiration.

Temperature dependencies follow :

$$V_T = \frac{V_{max} \cdot Q^{\frac{T_l - 25}{10}}_{10 - V_{max}}}{(1 + e^{0.3 \cdot (13 - T_l)}) \cdot (1 + e^{0.3 \cdot (T_l - 36)})} \tag{3.11}$$

$$R_T = \frac{R_d \cdot Q_{10-R_d}^{\frac{T_l-25}{10}}}{1+e^{1.3\cdot(T_l-55)}} \tag{3.12}$$

$$k_T = k \cdot Q_{10-k}^{\frac{T_l-25}{10}} \tag{3.13}$$

where $Q_{10-(V_{max},R_d,k)}$ are proportional increase of V_T, R_T, and k_T respectively, with a 10°C increase in temperature, T_l (°C) is leaf temperature, and V_{max}, k, and R_d are reference values for V_T, k_T, and R_T for 25°C.

The stomatal conductance model

Stomatal conductance was parameterised according to the empirical model proposed by Jarvis (1976). The model assumes that stomatal conductance, g_s, is affected by non-synergistic interactions between plant and environmental variables. While the model is able to handle multiple environment effects, this study focused on Q and the vapour pressure deficit at leaf surface (VPD_l) :

$$g_s = g_{sref} \cdot f(Q) \cdot f(VPD_l) \tag{3.14}$$

where g_{sref} is the reference stomatal conductance, defined as measured stomatal conductance under homogeneous environmental conditions.

Determination of the parameters of the C_3 photosynthesis model

Gas exchange measurements were done in March-April 2000 and in May 2001, using a LI-COR 6400 infra-red gaz analyser-leaf chamber system (LI-COR, Inc., Lincoln, NE USA) that allowed control of environmental conditions. A red light source was used during the 2000 period, while a blue-red light source was used for the 2001 measurements. No difference in the measurements due to the type of light source was noticed. Net CO_2 assimilation and transpiration rates, stomatal conductance, and CO_2 partial pressure in the substomatal spaces were calculated according to von Caemmerer and Farquhar (1981). Measurements were done on 12 *C. febrifuga* and 9 *C. arborea* leaves sampled on trees from various locations and of different sizes. Leaves were chosen to encompass full sunlight and shade conditions. All measurements were performed on fully expanded leaves.

For each leaf, an $A-C_i$ response curve at high irradiance (1000 to 1200 μmol·m^{-2}·s^{-1}) was used to infer the best fit V_{cmax} value by non-linear least square regression. Only data collected for C_i values below 20 Pa were used. Measurements for which carboxylation was not limiting (i.e. values below those predicted by Equations 3.1 and 3.2) were used to estimate J_{max}. Typically, for each response curve, the order of measurements was : 1) a reference value at ambient CO_2 (350-360 ppm), 2) a measurement at high CO_2 (1800 ppm), 3) several measurements while decreasing CO_2 down to 50-100 ppm, and 4) a respiration measurement at ambient CO_2 and in darkness. At least three points were collected for each CO_2 levels. Given the high sensibility of stomatal conductance to high atmospheric CO_2 concentrations, this scheme was not always respected and shifts between high and low CO_2 were often necessary to keep stomatal conductance open. We checked that no hysteresis occurred during the procedure. All measurements were

TAB. 3.1 – Parameter values used to derive photosynthetic parameters from field measurements. H92 refers to Harley et al. 1992. C refers to Collatz, pers. com.

parameter	value	unit	source
C_3 model :			
α	0.24	mol·mol^{-1}	H92
c_{K_c}	35.79	-	H92
c_{K_o}	9.59	-	H92
c_τ	-3.9489	-	H92
ΔH_{a-K_c}	80.47·10^3	J·mol^{-1}	H92
ΔH_{a-K_o}	14.51·10^3	J·mol^{-1}	H92
$\Delta H_{a-\tau}$	-28.99·10^3	J·mol^{-1}	H92
ΔH_{a-R_d}	84.45·10^3	J·mol^{-1}	H92
$\Delta H_{a-V_{cmax}}$	116.3·10^3	J·mol^{-1}	H92
$\Delta H_{a-J_{max}}$	79.5·10^3	J·mol^{-1}	H92
$\Delta H_{d-V_{cmax}}$	202.9·10^3	J·mol^{-1}	H92
$\Delta H_{d-J_{max}}$	201·10^3	J·mol^{-1}	H92
$\Delta S_{V_{cmax}}$	650	J·K^{-1}·mol^{-1}	H92
$\Delta S_{J_{max}}$	650	J·K^{-1}·mol^{-1}	H92
C_4 model :			
Q_{10-k}	1.8	-	C
$Q_{10-V_{max}}$	2.1	-	C
Q_{10-R_d}	2	-	C

done at leaf temperatures ranging from 28 to 33°C. Parameter values were corrected to avoid temperature effects, to a reference temperature of 31°C, using the temperature dependence equations 3.5 and 3.6 with parameters proposed by Harley et al. (1992) (see Table 3.1).

Determination of the parameters of the C_4 photosynthesis model

$A - C_i$ response curves were made as for C_3 plants on 11 leaves for *A. canaliculatus*, and 6 leaves for *H. diplandra*. Leaves were chosen to encompass full sunlight and shade conditions (i.e. for grasses in open areas or under tree clumps). α and θ were derived from $A - Q$ response curves (same as $g_s - Q$ curves, see below). No significant difference was found between the two grass species (P>0.05), thus mean values were used ($\alpha = 0.0657$ mol·mol^{-1}, $\theta = 0.7617$). β, V_T and k_T were computed from each $A - C_i$ curve by fitting Equations 3.8 and 3.9. No significant difference was found between species for β (P>0.05), thus equations were re-fitted to $A - C_i$ curves with a mean value for β of 0.915. R_T was estimated as for C_3 plants. Measurements were done at leaf temperatures from 29°C to 35°C. Parameter values were corrected to account for temperature effects : Equations 3.11-3.13 and Q_{10} parameters presented in Table 3.1 were used to estimate reference values at 31°C.

Figure 3.1 presents typical $A - C_i$ response curves obtained for the four species.

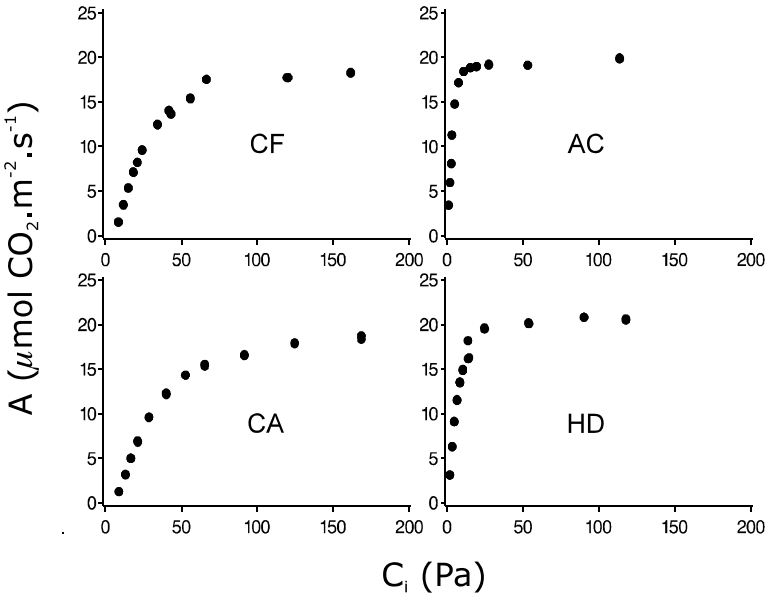

FIG. 3.1 – Examples of the response of net assimilation rate to variations in internal CO_2 partial pressure ($A - C_i$ response curves) for the two C_3 trees, *Crossopteryx febrifuga* (CA), and *Cussonia arborea* (CA), and the two C_4 grasses, *Andropogon canaliculatus* (AC), and *Hyparrhenia diplandra* (HD).

Determination of the parameters of the stomatal conductance model

$g_s - Q$ and $g_s - VPD_l$ response curves were obtained under ambient CO_2 (350-360 ppm) and for leaf temperatures ranging from 28 to 34°C. For each $g_s - Q$ curve, measurements were acquired at Q =1800, 1600, 1400, 1200, 1000, 800, 600, 400, 200, 100, 50, and 0 μmol·m^{-2}·s^{-1}, under VPD_l around 1 kPa. Each curve had a particular reference stomatal conductance, g_{sref-Q}, defined as the mean measured g_s at 1000-1200 μmol·m^{-2}·s^{-1}. g_{sref-Q} allowed to compare variations of the $\frac{g_s}{g_{sref-Q}}$ ratio with light for the different curves. For each $g_s - VPD_l$ curve, measurements were acquired at VPD_l values ranging from 1 or below, to as high as environmental conditions allowed (3 to 5 kPa). Q was maintained between 1000-1200 μmol·m^{-2}·s^{-1}. $g_{sref-VPD}$ was defined as mean g_s at VPD_l values of 1.4-1.6 kPa. 8, 5, 5, and 4 $g_s - Q$, and 5, 4, 6, and 5 $g_s - VPD_l$ curves were done for *C. febrifuga*, *C. arborea*, *A. canaliculatus*, and *H. diplandra* respectively.

For each species, a reference stomatal conductance g_{sref} was computed as the stomatal conductance measured at $Q = 1000 - 1200$ μmol·m^{-2}·s^{-1}, $VPD_l = 1 - 1.6$ kPa, $T_l = 29 - 34$ °C, and air CO_2=350-360 ppm. g_{sref} values from all response curves ($A - C_i$, $g_s - Q$, and $g_s - VPD_l$) corresponding to these conditions were used to compute g_{sref}. Measured g_{sref} were corrected for VPD_l effects using species specific $g_s - VPD_l$ relations described above.

Leaf analysis

All leaves on which gas exchange measurements were done were collected. Tree leaves were copied fresh to have a print of the fresh leaf surface. Tree leaf surfaces

were then measured using a leaf area meter (Delta T Devices, Hoddeston, U.K.) on leaf copies. Tree leaves were dried 3 days at 70°C and weighted. For each grass leaf, leaf exchange surface was calculated with measured leaf dimensions inside the LI-COR leaf chamber. A larger part of the leaf was collected to provide sufficient matter for nitrogen analysis. Each grass leaves was dried 3 days at 70°C and the leaf part corresponding to the leaf exchange surface was weighted.

All leaves were crushed using a 0.08 mm filter and leaf N concentration was measured using an elemental analyser (NA 1500 series 2, Fisons).

Calculation of water- and nitrogen-use efficiencies

Measurements from all response curves from which g_{sref} were computed were used to calculate photosynthetic WUE (ratio A_n/transpiration, in μmol $CO_2 \cdot$mmol^{-1} H_20) and NUE (A_n/N_a ratio, in μmol $CO_2 \cdot s^{-1} \cdot g^{-1}$ N). Only a few leaves were suitable for g_{sref} computation for *H. diplandra*, thus all grass g_{sref}, WUE and NUE data were pooled.

Statistical analyses

All variance and covariance analyses were performed with the SAS proc GLM procedure (SAS inst., Cary, USA). All regression analyses were performed using the SAS proc REG procedure.

Results

Photosynthesis parameters

For tree species, V_{cmax} and J_{max} were linearly correlated to N_a (Figure 3.2). Assuming similar intercepts between the two tree species for the $V_{cmax} - N_a$ relationship, a significantly higher slope was found for *C. arborea* (covariance analysis, P<0.05). Similarly, assuming similar slopes between the two species for the $J_{max} - N_a$ relationship, a significantly higher intercept was found for *C. arborea* (covariance analysis, P<0.05). R_d was not significantly correlated with N_a and was not found to be different between tree species (covariance analysis, P>0.05).

For grass species, no species effect was found for any parameter, and no nitrogen effect was detected for R_d (analysis of covariance, P>0.05). A weak relation suggests an increase of V_{max} with N_a (P=0.08), while k increased significantly with N_a (P<0.05) (Figure 3.2).

Stomatal conductance

g_{sref} increased with N_a for *C. febrifuga* and grasses, while no significant relation was found for *C. arborea*. Analysis of covariance showed no significant difference between grasses and *C. arborea*, while *C. febrifuga* exhibited lower g_{sref} values (Figure 3.3).

Stomatal conductance decreased with decreasing Q for all species (Figure 3.4). As non-linear response have generally been observed (Jarvis 1976), data were fitted using a logarithmic relationship (that gave the most accurate fit for the pooled four species). This common relation allowed to test species effect. Analysis of covariance showed no

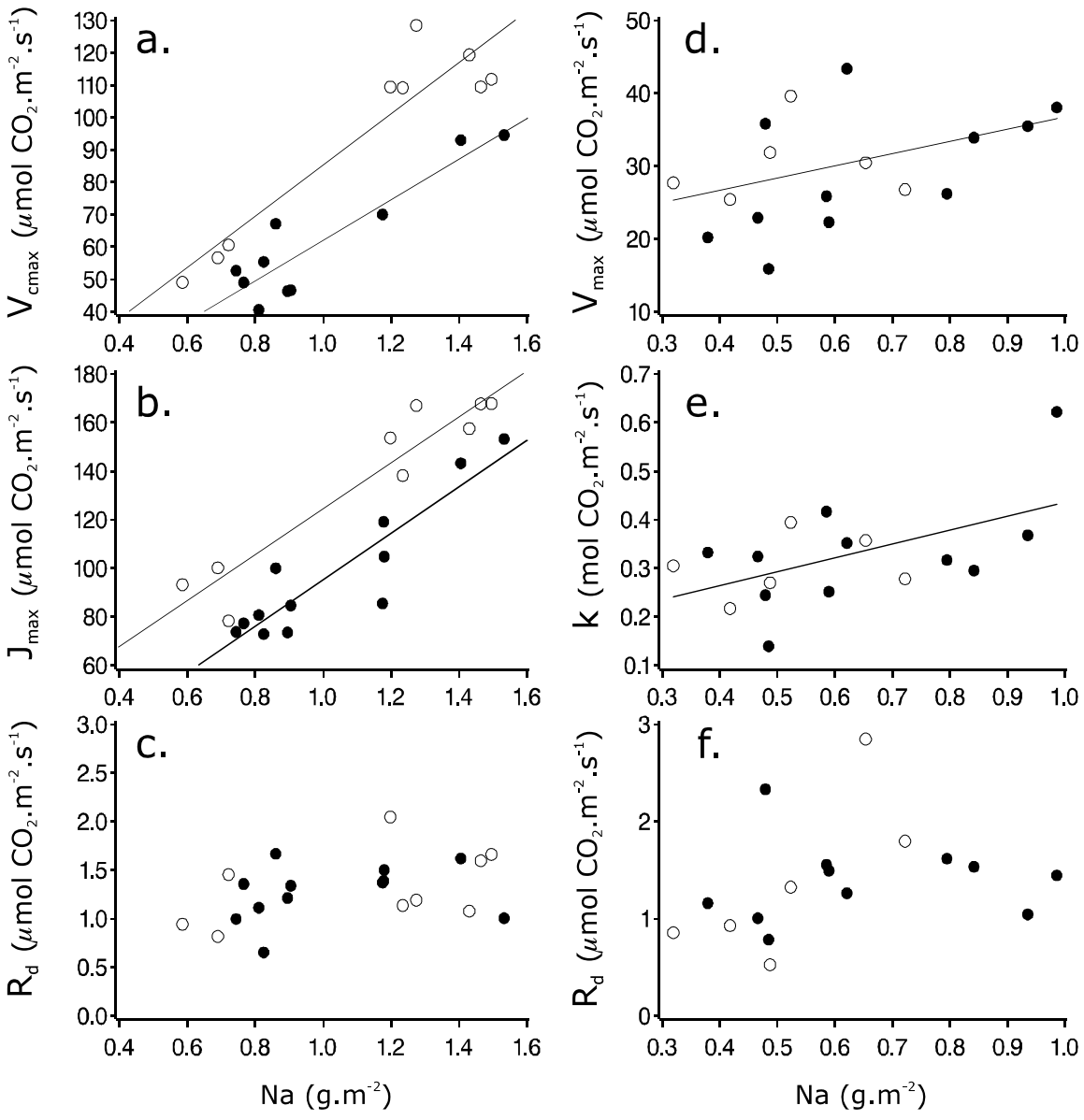

FIG. 3.2 – Variations of (a., b., and c.) the C_3 photosynthesis model parameters for *Crossopteryx febrifuga* (CF, •) and *Cussonia arborea* (CA, ○), and of (d., e. and f.) the C_4 photosynthesis model parameters for *Andropogon canaliculatus* (AC, •) and *Hyparrhenia diplandra* (HD, ○), with nitrogen per unit leaf area (N_a). Values were corrected to a reference temperature of 31°C for all species. Lines represent significant (P<0.05) regression fits per species for C_3 plants, and for pooled species for C_4 plants (except for $V_{max} - N_a$: P=0.08). Regression coefficients are for $V_{cmax} - N_a$: 0.83 for CF and 0.88 for CA ; for $J_{max} - N_a$: 0.82 for CF and 0.90 for CA ; for $V_{max} - N_a$: 0.18 ; and for $k - N_a$: 0.29.

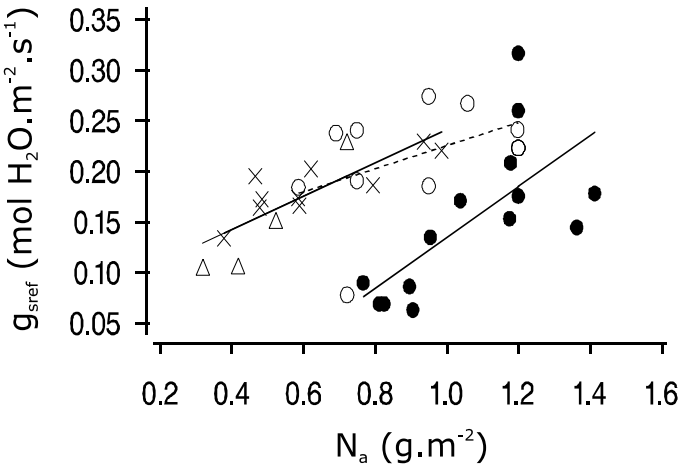

FIG. 3.3 – Reference stomatal conductances of *Crossopteryx febrifuga* (•), *Cussonia arborea* (○), *Andropogon canaliculatus* (×), and *Hyparrhenia diplandra* (△), as a function of leaf nitrogen per unit leaf area (N_a). Plain lines represent significant regression fits for *C. febrifuga* and for grasses. The dashed line represents a non significant regression fit for *C. arborea*.

difference between *A. canaliculatus*, *H. diplandra*, and *C. febrifuga*, but *C. arborea* fit had significantly different slope and origin (P<0.05). *C. arborea* maintained a higher g_s than other species at low irradiance, but the difference was small.

For all species, the stomatal conductance decreased with increasing VPD_l (Figure 3.5). To test eventual differences between species, an analysis of covariance was conducted, using a logarithmic relationship for all species (that gave the best fit for the pooled four species), shape of these fits are presented in Figure 3.5. The slope and the intercept obtained for *C. febrifuga* were significantly different from those obtained for the other species. *A. canaliculatus* had a significantly different slope from *H. diplandra* and from *C. arborea*, but these three species had similar intercepts. *H. diplandra* and *C. arborea* slopes and intercepts were not significantly different. These results, along with graphical comparison of the fits (Figure 3.5) suggest that for *C. febrifuga*, g_s decreased more at high VPD_l than for all other species (about 75% decrease at 3-4 kPa), g_s of *A. canaliculatus* showed the lowest decrease (less than 50% decrease at more than 4 kPa), and g_s of *H. diplandra* and *C. arborea* showed an intermediate decrease (about 60% decrease at 4 kPa).

Water and nitrogen use efficiencies

C. febrifuga WUE decreased with N_a, while no relation was found for all other species. Analysis of variance showed that *C. febrifuga* and *C. arborea* WUE were not significantly different (average values of 5.84 and 5.45 μmol $CO_2 \cdot mmol^{-1}$ H_20, respectively), but were lower than that of grasses (9.15 μmol $CO_2 \cdot mmol^{-1}$ H_20) (Figure 3.6).

Grass NUE decreased with N_a, but was much higher than tree NUE (ANOVA, P<0.05). *C. arborea* NUE (12.95 μmol $CO_2 \cdot s^{-1} \cdot g^{-1}$ N) was higher than that of *C. febrifuga* (8.7 μmol $CO_2 \cdot s^{-1} \cdot g^{-1}$ N) (Figure 3.6). Tree NUE was not correlated with N_a (P>0.05).

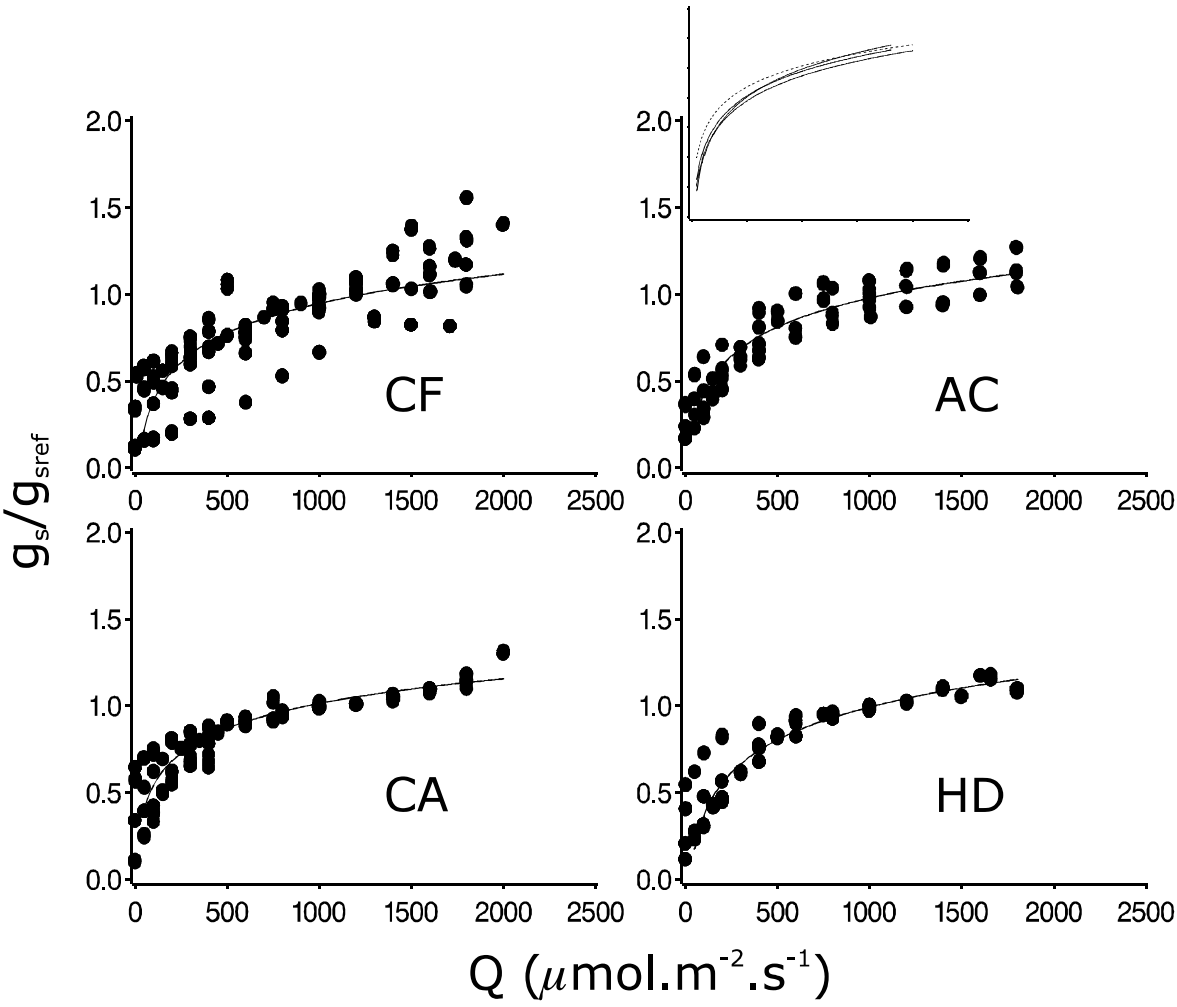

FIG. 3.4 – Stomatal conductance response to incident photosynthetically active radiation (Q), for *Crossopteryx febrifuga* (CF), *Cussonia arborea* (CA), *Andropogon canaliculatus* (AC), and *Hyparrhenia diplandra* (HD). Stomatal conductance is represented as the ratio of actual (g_s) to reference stomatal conductance (g_{sref}). Lines represent regression fits using a comon relation for all species. Regression coefficients are 0.66, 0.83, 0.86 and 0.88 for CF, CA, AC, and HD, respectively. The inset graph represents regression fits for all species. No difference was found between species except for CA, represented with a dashed line.

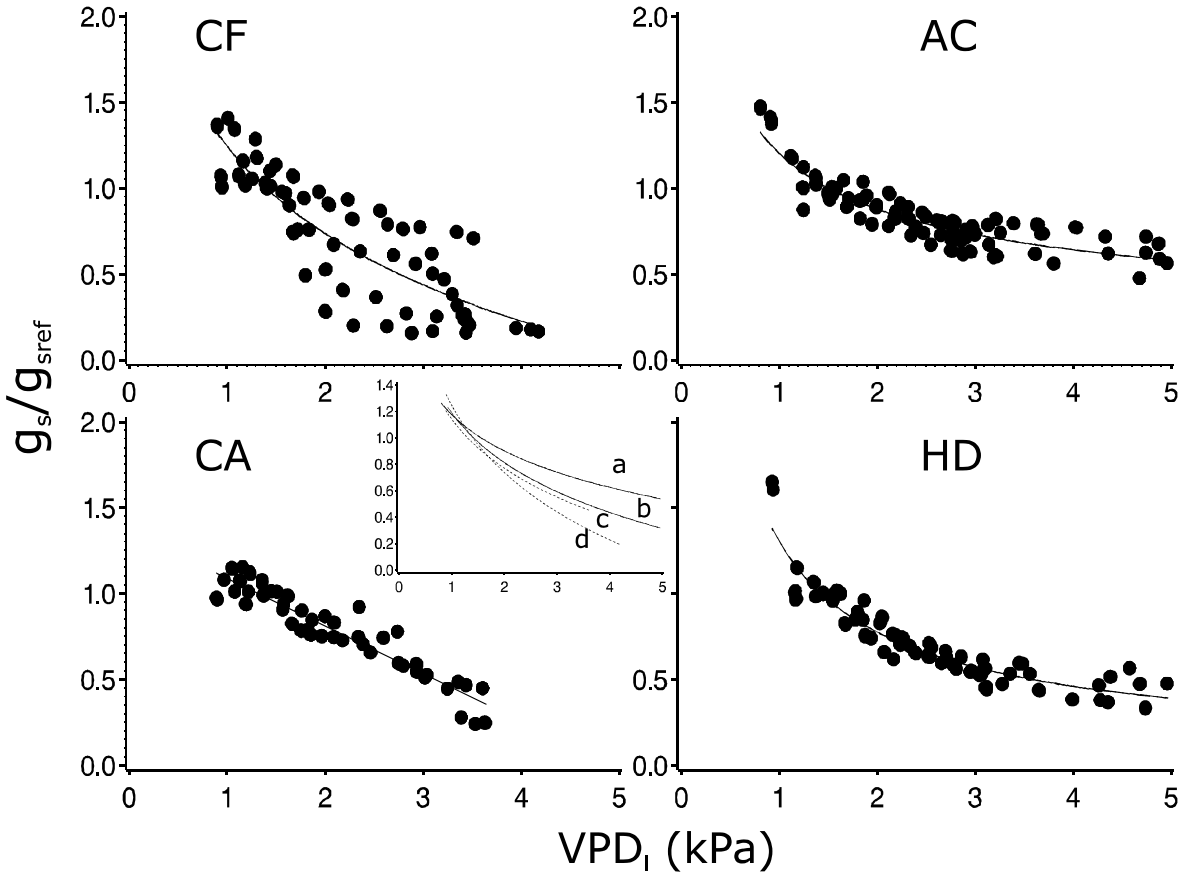

FIG. 3.5 – Stomatal conductance response to vapour pressure deficit at leaf surface (VPD_l) of *Crossopteryx febrifuga* (CF), *Cussonia arborea* (CA), *Andropogon canaliculatus* (AC), and *Hyparrhenia diplandra* (HD). Stomatal conductance is represented as the ratio of actual (g_s) to reference stomatal conductance (g_{sref}). Lines represent best regression fits. Regression coefficients are 0.72, 0.89, 0.80 and 0.88 for CF, CA, AC, and HD, respectively. The inset graph represents logarithmic fits for AC (a), HD (b), CA (c), and CF (d), that were used for statistical comparison between species.

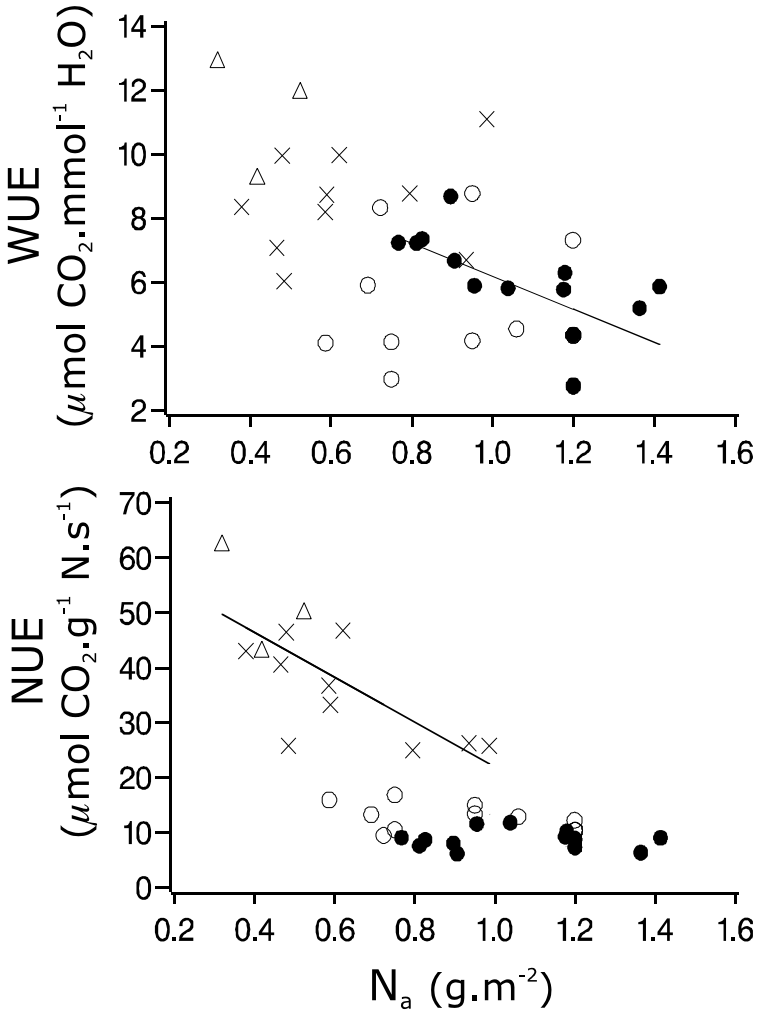

FIG. 3.6 – Variations of water use efficiencies (WUE), and nitrogen use efficiencies (NUE) of *Crossopteryx febrifuga* (•), *Cussonia arborea* (○), *Andropogon canaliculatus* (×), and *Hyparrhenia diplandra* (△), with the amount of nitrogen per leaf area (N_a). Plain lines represent significant regression fits (P<0.05) for WUE of *C. febrifuga*, and for NUE of grasses.

Discussion

Differences in gas exchange characteristics between C_4 grass and C_3 tree species of the Lamto savannas

Stomatal behaviour

We found no difference in g_{sref} that could be attributed to a difference in metabolic pathway. This lack of difference is not surprising because these four species are all shallow rooted (i.e. rely mostly on soil water from 0 to 170 cm below ground, Le Roux et al. 1995). g_{sref} of *C. arborea* is close to maximal stomatal conductance values reported in Schulze et al. (1994) for tropical trees. Tree g_{sref} are also in accordance with stomatal conductances of some Kenya savanna tree species (Hesla et al. 1985). *A. canaliculatus* and *H. diplandra* g_{sref} are lower than maximum stomatal conductance reported for temperate grasslands, tropical savannas, or tropical pasture (Schulze et al. 1994). Our results are in the range of values reported for some Kenya savanna grass species (Hesla et al. 1985), but are lower than maximum g_s measured in the rainy season on *Hyparrhenia rufa* in Venezuela (Baruch and Fernandez 1993).

We also found no diffence between C_4 grasses and C_3 trees in the response of g_{sref} to Q. The pattern of decrease of g_{sref} to VPD_l was more complex, but no clear distinction can be made between grasses and trees either in the shape or in the extent of the decrease.

Photosynthetic water and nitrogen use efficiencies

Conversely to stomatal characteristics, and in accordance with the literature (Pearcy and Ehleringer 1984), we found higher WUE for C_4 than for C_3 plants. *C. febrifuga* and *C. arborea* WUE values are in agreement with Sage and Pearcy (1987) for *Chenopodium album*, and with Bolton and Brown (1980) for *Festuca arundinacea*. *A. canaliculatus* and *H. diplandra* WUE values are in the range of those measured by Sage and Pearcy (1987) on *Amaranthus retroflexus*, and by Bolton and Brown (1980) on *Panicum maximum* .

The largely higher NUE we found for grasses are also in accordance with the literature comparing C_4 and C_3 species (Bolton and Brown 1980, Sage and Pearcy 1987b, Anten et al. 1998). *C. febrifuga* and *C. arborea* NUE values are lower than NUE of C_3 grasses of a Venezuelan savanna (Anten et al. 1998), but are in the range of values measured for *Chenopodium album* by Sage and Pearcy (1987). *A. canaliculatus* and *H. diplandra* NUE values are higher than NUE measured on *Amaranthus retroflexus* (C_4 annual, Sage and Pearcy 1987), but are in the range of values measured for *Hyparrhenia rufa* (Baruch et al. 1985, Anten et al. 1998).

These contrasts in photosynthetic characteristics between C_4 and C_3 pathways are explained by differences in the location of carboxylation sites and in the transport of atmospheric CO_2 to these sites (Edwards and Huber 1981).

Differences in gas exchange characteristics within C_4 grass and C_3 tree life forms of the Lamto savannas

Homogeneity among grass species

No difference in V_{max}, k, R_d, WUE, and NUE, were found between *A. canaliculatus* and *H. diplandra*. This homogeneity of grass photosynthetic characteristics is in accordance with the homogeneity of production patterns observed for perennial grasses at Lamto (César 1992, Mordelet 1993a, Le Roux 1995, Simioni 2001). k was related with N_a, but only a weak relation was found for V_{max}. Nontheless, we think that this relation is physiologically relevant, as photosynthesis, for a number of C_4 species, has been related with N_a (Bolton and Brown 1980, Sage and Pearcy 1987, Anten et al. 1995, Anten et al. 1998). Most studied species had higher N_a values than *H. diplandra* and *A. canaliculatus*. C_4 photosynthesis correlation with N_a was often seen when pooling results from many species (Field and Mooney 1986). However, detailed descriptions of photosynthetic properties of C_4 leaves are very scarce, and more studies should be done for species having constrasting N_a values, in order to have a better information on the relationship between photosynthesis parameters and N_a. When corrected for a temperature of 25°C, the mean V_{max} is 25 μmol·m^{-2}·s^{-1}. As well as the range of k values we observed, it is much lower than the value proposed by Collatz et al. (1992) for corn. These differences are probably due to higher N_a values for corn. R_d is generally correlated with N_a (Boot and den Bubbelden 1990, Anten et al. 1995), this was not the case in this study. This is probably due to measurement precision, as CO_2 fluxes associated with respiration are very low compared to fluxes associated with photosynthesis, and observed N_a values were very low. The mean R_d value found here is in accordance with Collatz et al. (1992) and is in the range of those presented by Anten et al. (1998) for C_3 and C_4 savanna grass species from Venezuela.

Only a few g_{sref} values could be derived from field measurements, and the similarity of g_{sref} within *A. canaliculatus* and *H. diplandra* has to be confirmed.

While the responses of g_s to Q was identical for the two grass species we studied, they differed when regarding stomatal conductance response to VPD_l. This difference occurred mainly at high VPD_l. Nontheless, it is likely that, in case of water stress (usually, high VPD_l values are observed during dry seasons), g_s will be more affected by plant water stress than by VPD_l. Thus the difference of response to VPD_l does probably not entail big differences in g_s between *A. Canaliculatus* and *H. diplandra*.

Contrasts between tree species

C. febrifuga and *C. arborea* exhibited contrasting photosynthetic characteristics. *C. arborea* had higher V_{cmax}, J_{max}, and NUE than *C. febrifuga*. Associated with identical R_d for the two species, this means that *C. arborea* has higher photosynthetic capacities than *C. febrifuga*, on a N_a basis. V_{cmax} and J_{max} values were high given the N_a, when compared to other studies (Harley et al. 1992, Le Roux et al. 1999a), but this is at least partly due to the high reference temperature (31°C), as optimal temperatures for V_{cmax} and J_{max} are generally higher than 30°C (Dreyer et al. 2001).

C. arborea displayed a higher g_{sref} than *C. febrifuga*. It is likely to be related to the water pools to which these species have access. Le Roux and Bariac (1998) showed that *C. arborea* has access to deeper soil layers and thus probably benefits better water

conditions, especially during dry periods. Plant water potential was found to respond to soil water potential in the 0-60 cm soil layer for *C. febrifuga* or in the whole soil profile (down to 170 cm) for *C. arborea*, thus indicating contrasting water stress behaviours. This may also account for the slowest decrease in g_{sref} for *C. arborea* than for *C. febrifuga* with increasing VPD_l. Conversely to generally observed patterns of g_{sref}, g_{sref} of *C. arborea* was not significantly correlated with leaf N_a. However, our data set lacks some measurements at high N_a (i.e. full sun leaves). The range of N_a should hence be enlarged for this species, to complete this study, and to seek a plausible $g_{sref} - N_a$ relation.

The slowest stomatal closure with decreasing incident Q of *C. arborea* compared to *C. febrifuga* may be linked with plant growth strategies. *C. febrifuga* is the only tree species at Lamto which seedlings can grow in open areas, while *C. arborea* seedlings grow under tree clumps (Gignoux 1994). *C. arborea* could thus be more adapted to shade conditions. Differences in $g_s - Q$ response between light adapted and shade tolerant species has already been reported for some savanna grass species (Amundson et al. 1995). These authors also found different responses of g_s to Q for the same species between leaves well exposed to light and shade leaves. However, the difference of response to Q between *C. febrifuga* and *C. arborea* was small, and its importance on plant performance is yet to be proved.

Because of its higher g_{sref}, *C. arborea* is expected to exhibit higher transpiration rates than *C. febrifuga*. This, along with similar WUE for the two tree species, probably confers *C. arborea* higher assimilation rates than *C. febrifuga*.

Importance of species functional diversity on ecosystem WUE and NUE

C_4 grasses and C_3 trees at Lamto did not exhibit similar resource use efficiencies. Thus the tree/grass ratio may be a critical aspect for savanna WUE and NUE. The two tree species also showed strong contrasts, hence the respective abundances of each species may also affect ecosystem performance. When assessing savanna production, techniques such as remote sensing provide green leaf area index (LAI) for a given surface, and leaf nitrogen concentration (N). But carbon assimilation in savannas not only depends on total green LAI and N, but also on how LAI and N are partitioned between C_4 grasses and C_3 trees, or between constrasting species of the same metabolic pathway. This problem is of importance when regarding the tree encroachment phenomenon observed worldwide (Archer et al. 2000), including Lamto (Gautier 1989). Our results suggest that a shift from grass to tree dominated savannas, would lower ecosystem NUE and WUE. Our results thus stress the need to account for species functional diversity to predict carbon and water fluxes at the vegetation-atmosphere interface in savanna ecosystems.

Annex - Equations of the significant relationships obtained

Photosynthesis relationships

C. febrifuga :

$c_{V_{cmax}} = 50.226 + 0.996 \cdot ln(N_a)$ R^2=0.75

$c_{J_{max}} = 36.224 + 0.942 \cdot ln(N_a)$ R^2=0.78

C. arborea :

$c_{V_{cmax}} = 50.546 + 0.988 \cdot ln(N_a)$ R^2=0.94
$c_{J_{max}} = 36.507 + 0.758 \cdot ln(N_a)$ R^2=0.88

grasses (25°C) :

$V_{max} = 15.64 + 13.28 \cdot N_a$ R^2=0.18 ; P=0.08
$k = 0.1044 + 0.2013 \cdot N_a$ R^2=0.29

$g_{sref} - N_a$ relationships :

grasses : $g_{sref} = 0.0755 + 0.1655 \cdot N_a$ R^2=0.68
C. febrifuga : $g_{sref} = -0.1176 + 0.2519 \cdot N_a$ R^2=0.52
C. arborea : $g_{sref} = 0.1106 + 0.1143 \cdot N_a$ R^2=0.19 ; P=0.21

$g_s - Q$ relationships :

A. canaliculatus : $\frac{g_s}{g_{sref}} = -0.6927 + 0.2416 \cdot ln(Q)$ R^2=0.86
H. diplandra : $\frac{g_s}{g_{sref}} = -0.69428 + 0.243578 \cdot ln(Q)$ R^2=0.88
C. febrifuga : $\frac{g_s}{g_{sref}} = -0.743789 + 0.244512 \cdot ln(Q)$ R^2=0.66
C. arborea : $\frac{g_s}{g_{sref}} = -0.410296 + 0.205952 \cdot ln(Q)$ R^2=0.83

$g_s - VPD_l$ relationships (VPD_l in kPa) :

A. canaliculatus : $\frac{g_s}{g_{sref}} = e^{0.185162 - 0.454798 \cdot ln(VPD_l)}$ R^2=0.80
H. diplandra : $\frac{g_s}{g_{sref}} = e^{0.267028 - 0.75122 \cdot ln(VPD_l)}$ R^2=0.88
C. febrifuga : $\frac{g_s}{g_{sref}} = 1.246853 - 0.736737 \cdot ln(VPD_l)$ R^2=0.72
C. arborea : $\frac{g_s}{g_{sref}} = 1.366645 - 0.277406 \cdot VPD_l$ R^2=0.89

Chapitre 4

Dynamiques foliaires de deux espèces d'arbre de savane

Spatial and temporal variations in leaf area index, specific leaf area, and leaf nitrogen of two co-occurring savanna tree species.

à soumettre

G. Simioni, J. Gignoux, X. Le Roux, and R. Appé

Abstract

Foliage growth, leaf nitrogen concentration, and specific leaf area (SLA) were surveyed during a complete vegetation cycle for two co-occurring savanna tree species : *Crossopteryx febrifuga* and *Cussonia arborea*. The study was conducted in the natural reserve of Lamto (Ivory Coast), on isolated and clumped trees. Leaf flush occurred before the beginning of the rainy season. Maximum leaf area index (LAI) computed on a projected canopy basis for tree individuals was strongly variable within species, but the mean, about 4, was similar for *C. febrifuga* and *C. arborea*. The seasonal courses of the ratio of actual to maximum LAI were close between individuals of each species, but differed between species. For *C. febrifuga*, clumped trees reached their maximum LAI before isolated trees. LAI of *C. arborea* trees was not different between clumped and isolated individuals, but maximum LAI was reached about two months later than *C. febrifuga*. Leaf fall was associated with decreasing soil water contents for *C. arborea*, but occurred without apparent link to soil moisture for *C. febrifuga*. Leaf nitrogen concentration, specific leaf area (SLA), and amount of leaf nitrogen per unit leaf area (N_a) decreased with time, but presented different patterns between species : SLA and N_a decreased later in the vegetation cycle for *C. arborea* than for *C. febrifuga*. For both species, N_a decreased, and SLA increased with decreasing leaf irradiance level whithin canopy. Effects of light on leaf characteristics were not different between isolated and clump trees. Given relationships between N_a and photosynthetic capacities obtained in a previous study for these species, our results show that 1) *C. arborea* maintains its foliage photosyntheti-

cally active later in the vegetation cycle than *C. febrifuga* ; and 2) both species are able to acclimate photosynthetic capacities to decreasing irradiance.

Introduction

Plant foliage is at the vegetation-atmosphere interface, and important regulations of transpiration and CO_2 assimilation occur at leaf surface (Sellers et al. 1997). Leaf area development and leaf characteristics are thus among the main factors influencing vegetation carbon and water fluxes and driving ecosystem production and water balance. In this context, leaf area index (LAI) is commonly used to characterize vegetation cover and to compute net primary production (NPP) in vegetation production models (e.g. Running 1994, Haxeltine and Prentice 1996, Kirschbaum 1999). Concurrently, many ecological studies have focused on amount of nitrogen per unit leaf area N_a (g $N \cdot m^{-2}$), and specific leaf area (SLA $cm^2 \cdot g^{-1}$). Indeed, N_a influences photosynthetic capacity (Field and Mooney 1986), and SLA (the leaf surface-to-mass ratio) is an index of dry matter investment per unit leaf area. N_a and SLA generally decrease with leaf age (Reich et al. 1992, Wilson et al. 2001). Furthermore, at a given soil N availability, leaf SLA and N_a generally acclimate to environmental light conditions (Gulmon and Chu 1981, Ellsworth and Reich 1992). This acclimation process can occur within the same plant canopy (Le Roux et al. 1999). At least, significant variations in N, N_a and SLA can be observed between species (Reich et al. 1999). Many studies have quantified spatial and temporal variations in LAI and leaf characteristics in forest ecosystems (e.g. Pierce and Running 1988, McWilliam et al. 1993, Reich et al. 1999). In contrast, comprehensive studies on the spatial and temporal variations in LAI and leaf characteristics are particularly scarce for the dominant species belonging to savanna ecosystems (but see Pressland 1975), although they cover a large part of terrestrial surfaces (20%, Scholes and Hall 1996). For instance, in the Lamto savanna (Ivory Coast), while the seasonal courses of the biomass, LAI, and N content of the grass layer have been surveyed (Abbadie 1984, Le Roux 1995), no similar studies have been conducted on tree species. This lack of data for savanna trees is probably due to the spatially heterogeneous structure of savanna vegetation (a discontinuous tree layer above a continuous grass layer). Surveys of tree LAI are indeed particularly tedious and time consuming in savannas, because most comfortable, and less destructive methods to measure LAI (based on remote sensing, e.g. Gamon et al. 1995, or radiation interception by foliage, e.g. Gower and Norman 1991) have been developed for closed canopies (i.e. forests or grasslands) but cannot be applied for heterogeneous canopies. Such a lack of data strongly restricts our ability to assess water and carbon fluxes in savanna ecosystems and to better understand competitive interactions between the main coexisting species of the tree layer in a given savanna ecosystem. In this study, the spatial and temporal variabilities of tree individual LAI and leaf SLA and N were surveyed for two coexisting and dominant tree species, *Crossopteryx febrifuga* and *Cussonia arborea* (anc. *C. barteri*), from the Lamto savanna. Both isolated trees and trees belonging to clumps were studied during one vegetation cycle. Leaves were collected on the same trees throughout the year at two contrasting irradiance levels, and N_a and SLA were measured. Concurrently, soil water content was measured at different depths in the same plots. At one date during the year, N, SLA, N_a and sky openness (an index of local irradiance) were measured in different locations of the tree crowns.

These data were used to test : (1) whether the temporal dynamics of LAI, N, N_a and SLA differ between the two species, and within each species between isolated trees versus trees belonging to clumps, (2) whether the temporal dynamics of LAI is strongly related to the dynamics of the soil water content, and (3) whether acclimation of leaf traits to the local light environment differed between species and between isolated trees versus trees belonging to clumps. Implications for the seasonal and spatial variations in tree carbon assimilation potential and for competitive interactions between tree individuals are discussed.

Materials and Methods

Study area

Measurements were conducted in the natural reserve of Lamto, Ivory Coast (6°13'N, 5°02'W). Mean monthly temperatures are constant throughout the year (27°C). Rainfall averages 1200 mm·year^{-1} and determines dry seasons (from November to March, and in August) and rainy seasons (from April to July, and from September to October). Soils are ferralsol (according to the FAO classification). Main features of the vegetation are described in Menaut and César (1979). Forests are present along streams, but most of the reserve is covered by savanna areas. In the savanna, the herbaceous layer is composed of perennial grasses. Tree density varies along the catena, from almost pure grassland in bottomlands to dense shrub facies on plateaus. The four dominant species of the tree layer include *Crossopteryx febrifuga* and *Cussonia arborea*, and can be found aggregated in clumps or isolated. Fire is set every year in early January.

Plant material

Crossopteryx febrifuga and *Cussonia arborea* display constrasting biologies. *C. arborea* roots allow extraction of water from deeper soil horizons than *C. febrifuga* (Le Roux and Bariac 1998). *C. arborea* has a higher photosynthetic potential (Simioni et al. 2001e). Two natural plots were chosen, one where trees were isolated and the other where trees were gathered into two clumps of mixed species. The two plots were 150 m from the Lamto geophysical station, where daily climate data were measured.

LAI estimation

The LAI survey was carried out during the 2000 vegetation cycle. 5 isolated and 2 clump *C. febrifuga* trees, and 4 isolated and 3 clump *C. arborea* trees were studied. Tree height ranged from 1.85 m to 6.8 m for *C. febrifuga*, and from 4 m to 6.8 m for *C. arborea*.

Tree foliage was assumed to be an assemblage of elemental leaf groups. LAI estimation was based on three measurements : 1) survey of leaf number for two leaf groups for each tree during the whole 2000 vegetation cycle ; 2) measurement of the total number of leaf groups in each tree, including their spatial location in the canopy, at one date during the year ; and 3) a survey of leaf individual area, to convert leaf numbers into leaf areas.

For each tree, two leaf groups were chosen, one well exposed to light, and one in shade parts of the canopy. For each leaf group, leaf number was counted every 2 weeks

from January to April, and from October to December, and every 4 weeks from May to September.

For each species, we searched for an estimator of group leaf number. For *C. febrifuga*, we found a good correlation between group leaf number and basal diameter (BD) of the supporting branch. For *C. arborea* a good correlation was found between group leaf number and the length of the supporting branch (LSB) corresponding to leaf insertion. These parameters were measured as part of the leaf group survey. Correlations at different periods of the vegetation cycle are presented in Appendix 1.

BD or LSB (depending on tree species) were measured on all leaf groups of each tree at one date during the year (from May to October 2000, depending on the tree). This allowed to estimate a total leaf number per tree at one point in the vegetation cycle, using BD/LSB-green leaf number relationships. For each tree, the ratio of the total number of leaves to the number of leaves of the surveyed groups was assumed to be constant throughout the vegetation cycle. This allowed to extrapolate temporal dynamics of total tree leaf number.

All tree leaf clumps were positioned in space as presented in Figure 4.1. A reference point and a reference direction were chosen. Each leaf clump base was positionned by measuring the distance from the leaf clump to the reference point, the height of the leaf clump base and the angle made by the leaf clump base, the reference point, and the reference direction. Angle measurement was done using a large 0-90° protractor, with a precision of 0.1°. Distance was measured with a decameter, and height with a decameter used as a plumb line. Tree height was computed as the heigth of the highest leaf clump base plus 50 cm (to account for leaf clump dimensions). Canopy cover (i.e. the projected area of the tree canopy) was computed as the horizontal surface delimited by the outer leaf clump positions, plus a margin of 50 cm.

Mean individual leaf area data was necessary to convert leaf numbers into leaf areas. All sampled leaves (see below) used for N, SLA, and N_a measurements were fully expanded when possible. These leaves did not represent the leaf size distribution with time, with many young leaves at the begining of the vegetation cycle, and mostly fully expanded leaves at the end. We thus made separate estimations of mean leaf individual area. Three times during the year (26 March, 21 May and 23 October 2000), 8 tree leaf clumps were collected on four independent trees for each species, in order to estimate mean individual leaf surfaces. Leaves were copied fresh, and leaf areas were measured on copies with a leaf area meter (Delta T devices, Hoddeston, U.K.). Relationships between leaf individual areas and time (Figure 4.2) allowed to convert total leaf number of each tree into total leaf area. Individual tree LAI was calculated as the ratio of total leaf surface to tree canopy surface.

Reproductive phenology

At each date corresponding to the LAI survey, the presence of flowers and/or fruits in trees was recorded.

Leaf sampling and analysis

For each species, leaves were collected on two of the isolated trees, and two of the clump trees that were used for the LAI survey, every month at the beginning of the

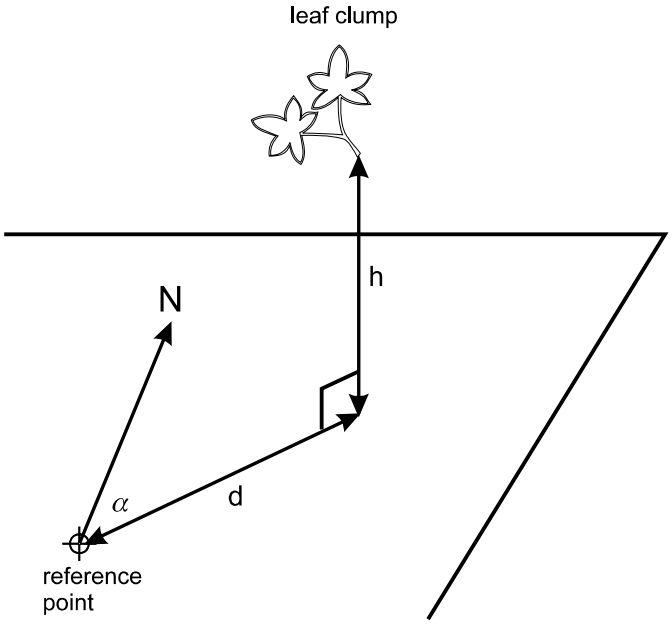

FIG. 4.1 – Method to measure the location of leaf clumps. Leaf clump base is characterized by its height h, distance d from a reference point, and angle α from a reference direction (e.g. North).

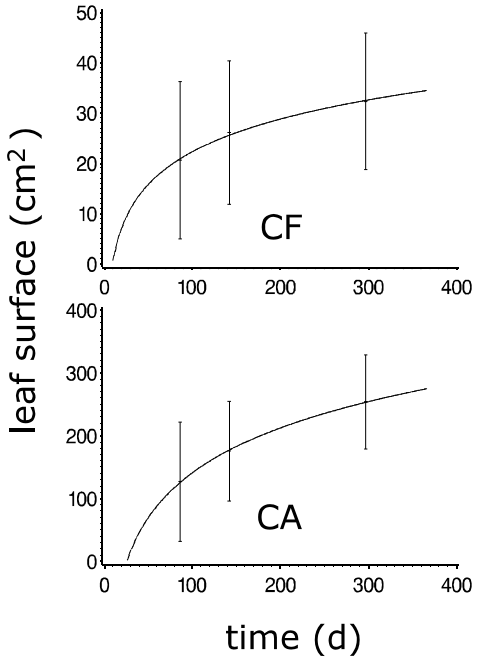

FIG. 4.2 – Temporal variations of mean individual leaf area for *Crossopteryx febrifuga* (CF) and *Cussonia arborea* (CA) during the 2000 vegetation cycle. Plain lines are best regression fits (P<0.05) through mean individual leaf areas calculated from sampling all leaf age classes. Bars represent standard deviations of measured leaf surface.

vegetation cycle, and every two months after. For each tree, two sun leaves and two shade leaves were collected on different branches than those used for the survey of leaf clumps. Leaves were copied fresh, dried 3 days at 70°C, and weighted. Leaf surface was measured on leaf copies with a leaf area meter. SLA was calculated as the ratio of leaf surface to leaf dry mass.

Dried leaves were crushed using a 0.08 mm filter. Leaf N concentration was measured with an elemental analyser (NA 1500 series 2, Fisons).

Spatio-temporal variations in photosynthesis

We used relationships obtained from Simioni et al. (2001e) between maximum carboxylation rate (V_{cmax}, in μmol $CO_2 \cdot m^{-2} \cdot s^{-1}$) at a leaf temperature of 31°C, and N_a for both species to estimate contrasts in photosynthesis due to variations in N_a.

Hemispherical photographs

In order to characterize the influence of leaf radiation environment on SLA and N_a, hemispherical photographs were taken from the 16th to the 26th of October 2000. 21 leaves for *C. febrifuga* and 20 leaves for *C. arborea* were chosen on various isolated and clump trees (independent of the LAI survey) to encompass a large range of radiation regimes. Just above each leaf, a shot was taken skyward with a Canon AL-1 camera equiped with a Canon fish-eye 7.5 mm lense. Additional photographs were taken for shade leaves, of both species, on trees growing in a dry forest area. Leaf mass, surface, and N were analysed as above. Photographs were analysed with the GLA software (Gap Light Analyser v.2.0, Fraser et al. 1999), that calculated an index of sky openness corresponding to percent of sky directly visible from the leaf (i.e. from the camera position). Leaf SLA measured for leaves from forest trees were in accordance with those measured in the savanna, however, N was significantly higher (data not shown), probably due to a higher soil fertility, and are not presented in the results.

Soil water content

Soil water was surveyed during the same period by the gravimetric method in the same plots than for the tree LAI survey. Measurements were made at four points, out of tree cover, in the isolated tree plot, and at four points under tree clumps. For each point, soil samples were collected at 8 depths (0 to 160 cm with 20 cm intervals).

Each sample was weighted fresh, dried 3 days at 100°C, and weighted dried. Difference between fresh and dry masses allowed to calculate the soil water content in %. This content was converted into mm, assuming an apparent soil density of 1.5 (Le Roux 1995).

Statistical analyses

All variance or covariance analyses were done using the SAS proc GLM procedure. All regression analyses were done using the SAS proc REG procedure (SAS inst., Cary, USA).

Results

Seasonal dynamics of LAI and soil water content

LAI was very variable between individual trees of the same species. Maximum LAI ranged from 2 to 7.4 with a mean of 4.2 for *C. febrifuga*, and from 2.2 to 5.6 with a mean of 4.0 for *C. arborea*. Maximum LAI was not correlated with tree height or canopy cover. Mean annual LAI was 2.4 and 2.27 for isolated and clump *C. febrifuga* trees, and 2.16 and 2.08 for isolated and clump *C. arborea* trees, respectively.

On the opposite, leaf area development (i.e. seasonal course of actual LAI/maximum LAI) was very homogeneous within species (Figure 4.3a. and b.). Repeated measure ANOVA showed differences between clump and isolated trees ($P<0.05$) for *C. febrifuga*, with an earlier leaf growth and leaf fall for clump trees. No difference was found between isolated and clump trees for *C. arborea*. The time between leaf emergence and maximum LAI was longer for *C. arborea* than for *C. febrifuga*. *C. arborea* reached maximum LAI about two months later than *C. febrifuga*. For both species, leaf fall occurred shortly after reaching maximum LAI.

Soil water contents were not significantly different out of or under tree clumps, except during the long dry season (day<100 and day>300) in the 0-60 cm soil layer (repeated measure ANOVA, $P<0.05$) (figure 4.3c. and d.). In the 0-60 cm layer, soil water content was high at the beginning of the year, due to precipitation in January, but decreased importantly afterwards before the soil was replenished during the rainy season, from day 100 to 200. It decreased again after day 300, once precipitation became scarce and the dry season started. Soil water contents in the 60-160 cm layer also decreased during the dry season and increased during the rainy season, with less amplitude than in the upper layer, and much more variability at a given date.

C. febrifuga and *C. arborea* trees started leaf growth under low soil water contents, and scarce precipitation. This suggests that trees started leaf growth using plant water storage. *C. febrifuga* leaf fall did not seem to be initiated by water stress, while the steep leaf fall of *C. arborea* corresponded to a steep decrease in water contents in all soil layers.

Reproductive phenology

The flowering period ranged from February to May for *C. febrifuga* trees, and from April to May for *C. arborea* trees. *C. arborea* trees produced fruits from May to August, after this period, no more fruits remained on the trees. Fruit growth started in April for *C. febrifuga*, and fruits remained on the trees until the end of the year, making difficult to assess when fruit growth really stopped.

Temporal and spatial variations of N, N_a, and SLA

Leaf N, N_a and SLA decreased after leaf growth initiation (Figures 4.4 and 4.5). Decrease in N was steep shortly after leaf initiation and less pronounced after day 100 for *C. febrifuga*, but much more progressive for *C. arborea*. A weak decrease in N_a was observed shortly after leaf initiation, and N_a remained quite constant for *C. febrifuga*. In contrast, N_a was constant during the first 100 days and decreased strongly from day 150 to 300 for *C. arborea*. SLA decreased exponentially for both species, but the decrease was more important for *C. febrifuga* than for *C. arborea*.

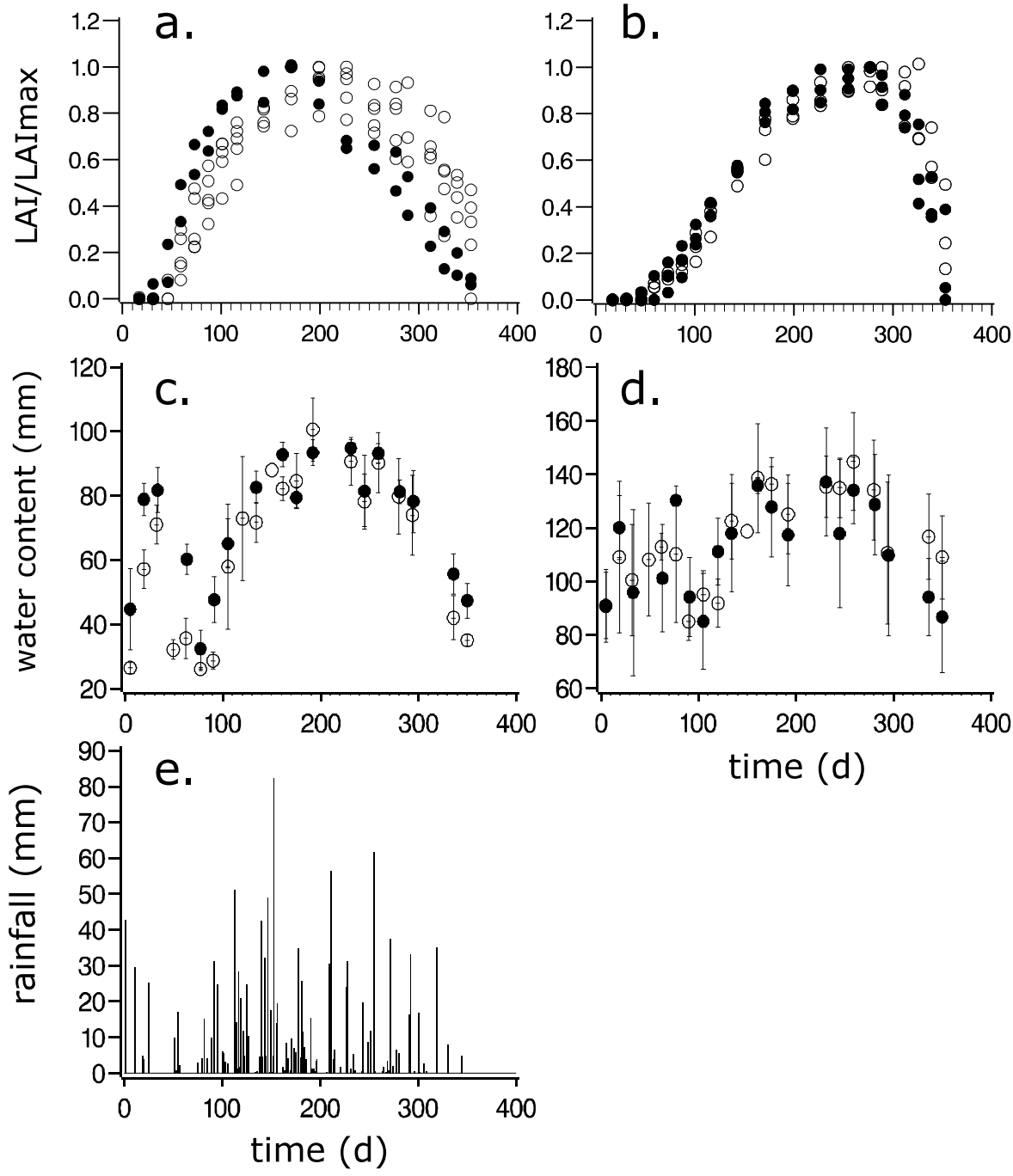

FIG. 4.3 – Temporal dynamics of individual tree leaf area index, soil water contents, and daily rainfall, during the 2000 vegetation cycle. a.) leaf area index (expressed as the ratio of actual (LAI) to maximum (LAImax) leaf area indices) of *Crossopteryx febrifuga* for 5 isolated (○) and 2 clump (●) trees. b.) leaf area index of *Cussonia arborea* for 4 isolated and 3 clump trees. c.) soil water contents in the 0-60 cm soil layer in open areas (○) and under tree clumps (●), bars represent standard deviations. d.) soil water content in the 60-160 cm soil layer. e.) daily rainfall.

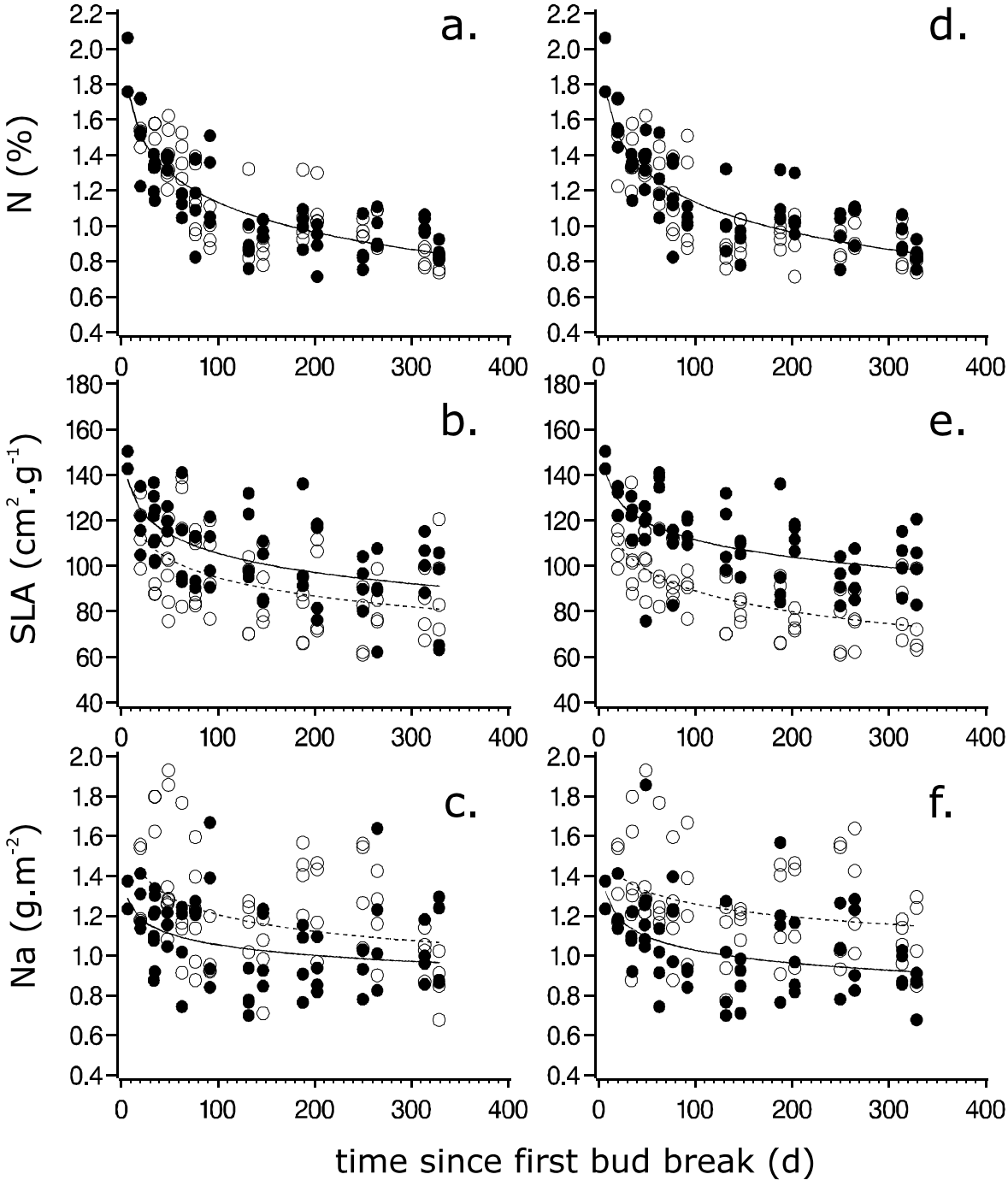

FIG. 4.4 – Temporal dynamics of leaf N concentration per unit mass (N), amount of N per unit leaf area (Na) and specific leaf area (SLA) of *Crossopteryx febrifuga*, since first leaf emergence. Open and closed symbols correspond to isolated and clump trees (a. b. and c.), or with sun and shade leaves (d. e. and f.), respectively. Plain lines represent best significant regression fits with time for either clump trees or shade leaves, and dashed lines represent best regression fits for either isolated trees or sun leaves ($P<0.05$).

Analyses of variance were conducted on residuals of N, N_a, and SLA regressions with time. For *C. febrifuga*, N residuals were not different between isolated and clump trees, and not different between sun and shade leaves (P>0.05). For *C. arborea*, N residuals were not different between isolated and clump trees (P>0.05), but were different between sun and shade leaves (P<0.05). For both species, N_a and SLA residuals were different between isolated and clump trees, and between sun and shade leaves (P<0.05).

SLA and N_a in relation to light environment

No effect of sky openness was found on N (not shown). For both species, N_a increased and SLA decreased with increasing sky openness (i.e. with decreasing leaf shading) in October 2000 (Figure 4.6). No difference was found between isolated and clump trees. Analyses of covariance indicated, at this period of the year, significantly higher N_a for *C. febrifuga* than for *C. arborea*, whereas no species effect was found for SLA.

Spatio-temporal dynamics of photosynthesis

Estimated V_{cmax} varied with time (as for N_a) but was higher for *C. arborea* than for *C. febrifuga*, except at the end of the vegetation cycle (Figure 4.7). Estimated V_{cmax} decreased with decreasing sky openness and was higher for *C. arborea* than for *C. febrifuga* (Figure 4.8). But the difference between the two species decreased with decreasing sky openness.

Discussion

Seasonal dynamics of LAI

C. febrifuga and *C. arborea* initiated leaf growth under unfavorable water conditions. This suggests that, for both species, leaf initiation occurred independently of soil water conditions. For a number of deciduous tropical tree species, stem rehydration occurs prior to the onset of the rainy season and allows leaf flushing (Williams et al. 1997). It is possible that *C. febrifuga* and *C. arborea* also use some endogenous mechanism to trigger leaf growth. Leaf growth time was relevant with leaf growth of some other deciduous tropical savanna species (Eamus 1999).

C. febrifuga leaf fall started early in the vegetation cycle, before any decrease in soil water. On the opposite, *C. arborea* leaf shedding corresponded to a steep decrease of soil humidity in both horizons, suggesting that for this species, once foliage development has started, it continues as long as water conditions are favorable. Williams et al. (1997) observed that for all deciduous species in an Australian tropical savanna, leaf fall occurred concurrently with decrease in soil moisture. *C. febrifuga* did not show such characteristics, and it seems that leaf fall is triggered by mechanisms yet to be studied. This result is not in accordance with Konate et al. (1998) that showed that *C. febrifuga* trees growing on termite mounds (i.e. with higher soil humidity) lost their leaves later than trees growing on ordinary soil. The early leaf shedding of *C. febrifuga* could be a mechanism to decrease transpiration before the onset of the long dry season and to preserve water for the next vegetation cycle. *C. arborea* is suspected to have access to a larger water pool

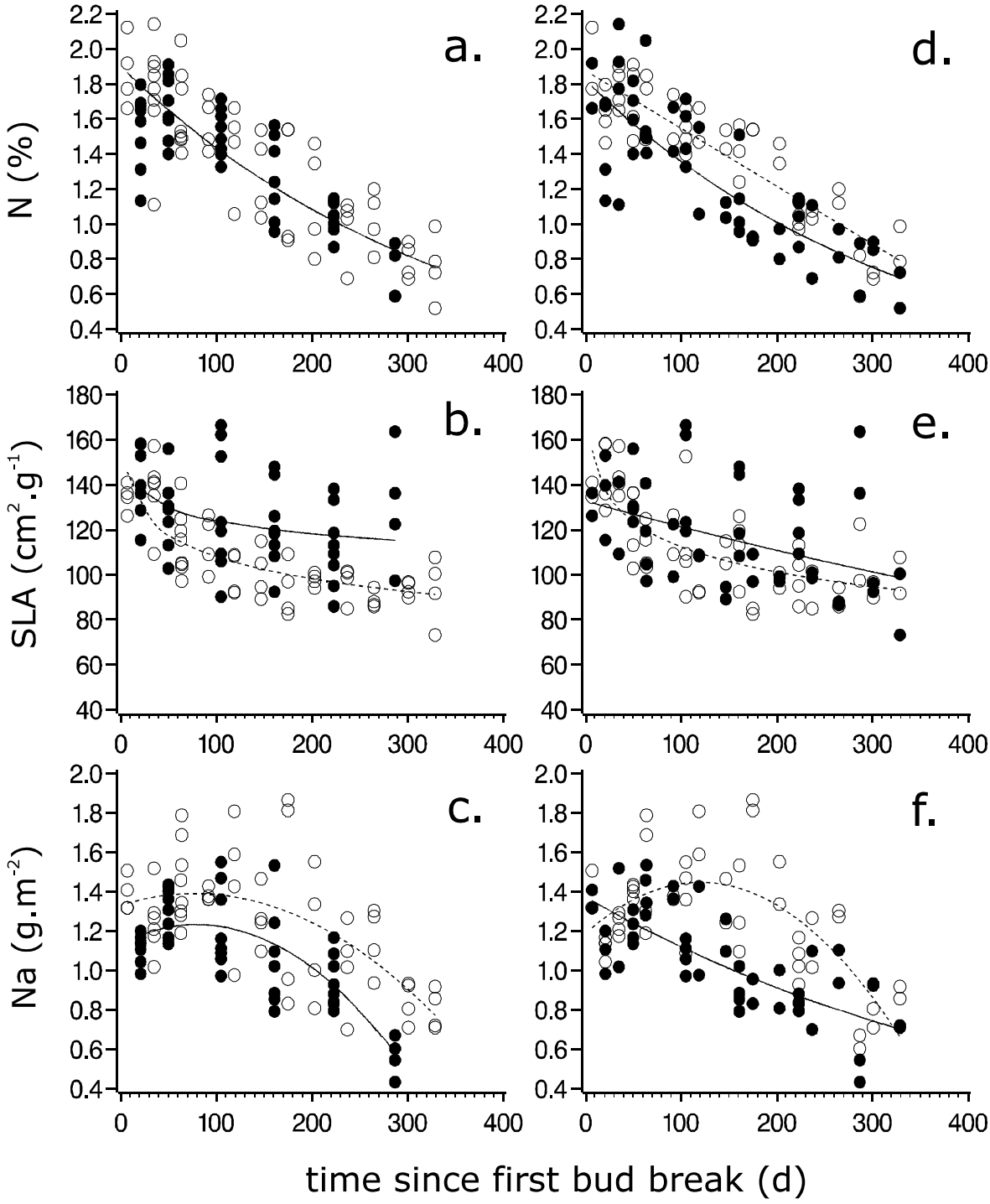

FIG. 4.5 – Temporal dynamics of leaf N concentration per unit leaf mass (N), amount of leaf N per unit leaf area (Na), and specific leaf area (SLA) of *Cussonia arborea*, since first leaf emergence. Legend as in Figure 4.4.

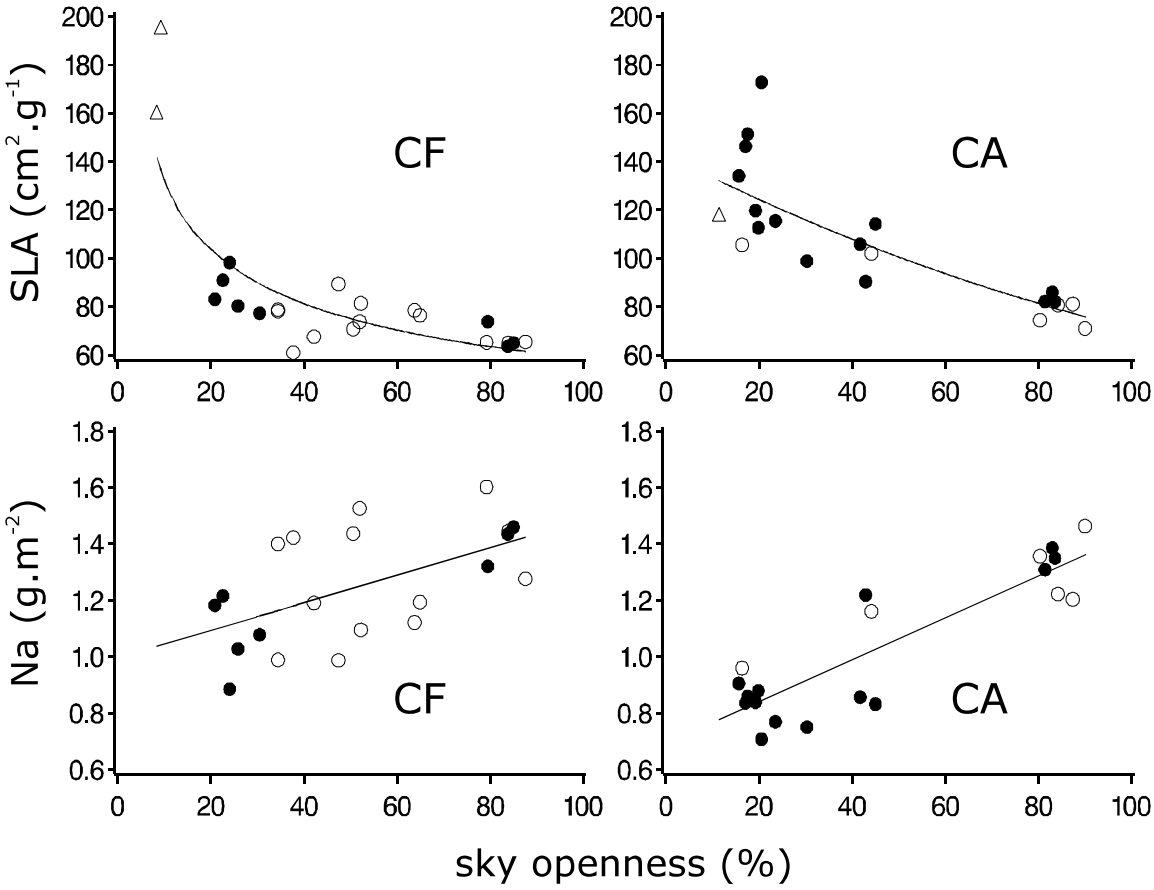

FIG. 4.6 – Effect of sky openness on specific leaf area (SLA) and amount of nitrogen per unit leaf area (Na) of *Crossopteryx febrifuga* (CF) and *Cussonia arborea* (CA). Measurements were done in October 2000, on isolated (○), clump (•), and forest (△) trees. Lines represent best significant regression fits ($P<0.05$). Regression coefficients are 0.72 and 0.32 for CF SLA and Na, and 0.74 and 0.78 for CA SLA and Na.

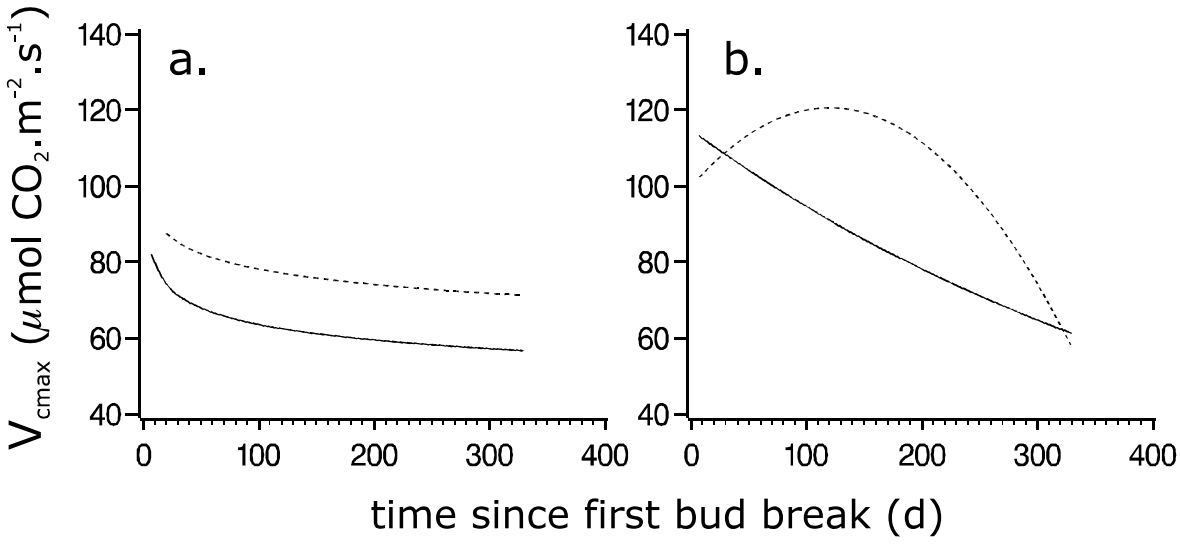

FIG. 4.7 – Estimated temporal dynamics of the maximum rate of carboxylation (V_{cmax}) at 31°C for sunlit (dashed lines) and shade (plain lines) leaves (a.) of *Crossopteryx febrifuga* and (b.) *Cussonia arborea*. V_{cmax} was calculated from relationships with leaf nitrogen per unit leaf area N_a (from data in Simioni et al. 2001e), and from regression fits of N_a with time (this study).

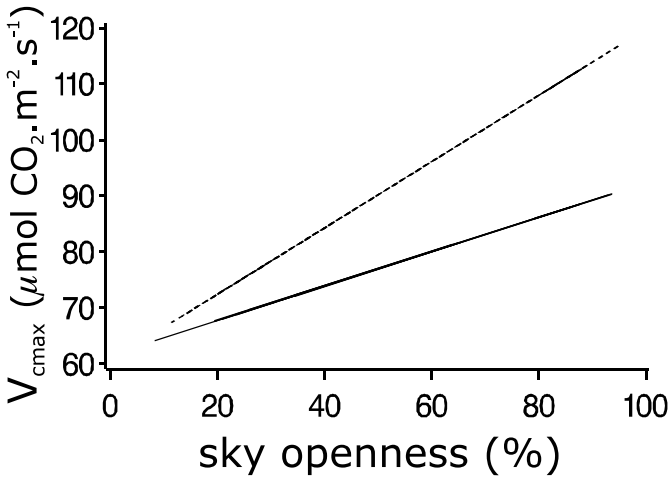

FIG. 4.8 – Estimated maximum rate of carboxylation (V_{cmax}) at 31°C with sky openness for *Crossopteryx febrifuga* (plain line) and *Cussonia arborea* (dashed line). V_{cmax} was calculated from relationships with leaf nitrogen per unit leaf area N_a (from data in Simioni et al. 2001e), and from regression fits of N_a with sky openness (this study). Sky openness was measured in October 2000.

than *C. febrifuga* (Le Roux and Bariac 1998), this species thus has a better potential to build leaf later.

There seems to be a temporal segregation of leaf development between species, *C. febrifuga* having most of its foliage from day 100 to 250, while *C. arborea* had most of its foliage from days 180 to 300. We can address the question of niche separation, as *C. febrifuga* individual in clumps, and thus that may be close to *C. arborea* trees, start foliage growth and leaf fall earlier than isolated trees. A possible reason could be competition for light. Allocation to reproductive parts is unlikely to influence leaf growth, as both species flowered and made fruits approximately at the same period. But the quantities of carbon allocated to flowers and fruits may differ between species.

The erratic maximum individual LAI, observed for both species, may be due to the growth history of each tree, as disturbances like fire or herbivory (*C. febrifuga* and *C. arborea* trees were subject to insect herbivory) can affect tree growth. The total N pool of a tree can also limit the amount of foliage a tree can grow, as building leaves requires nitrogen.

Seasonal variations in N, SLA, N_a, and photosynthetic capacities

N and SLA decline with leaf age, as a mechanism of leaf expansion (Field and Mooney 1983). N is high in young, not fully expanded leaves (Chapin and Kedrowski 1983, Millard and Nielsen 1989), and decreases by addition of structural material, and eventually, by N retranslocation from senescent leaves (Brady 1973). The resulting N_a declines with leaf age. In this study, leaf age was not measured, but, since most leaves were initiated in the first part of the foliage growth, the declines of N, N_a, and SLA with time since leaf emergence were well visible for both species. However, the shapes of decline were different between *C. febrifuga* and *C. arborea*. *C. arborea* maintained relatively higher N and N_a values with time. This allowed *C. arborea* trees to maintain photosynthetically active foliage later than *C. febrifuga*, as confirmed by estimated temporal variations of V_{cmax}. This is consistent with the higher LAI observed late in the vegetation cycle for *C. arborea*. The range of N_a values was similar for the two tree species, but *C arborea* has a higher photosynthetic capacity at given N_a (Simioni et al. 2001e). Thus *C. arborea* displayed a higher photosynthetic capacity than *C. febrifuga* except at the end of the vegetation cycle.

Higher SLA for *C. arborea* can be seen as an advantage for *C. arborea*, as it means a lower carbon investment in leaves. But *C. arborea* SLA does not account for the long leaf petioles, that correspond to 33% of the mass of the leaf itself, and thus increases importantly carbon investment in *C. arborea* leaves.

N can be influenced by N nutrition level (Tan and Hogan 1998), and a higher mineral N was found under tree clumps at Lamto than in open areas (Mordelet et al. 1993). However no difference was found in N between isolated and clump trees in this study.

Within canopy variations in N, SLA, N_a, and photosynthetic capacities

N content was different between sun and shade leaves for *C. arborea*. This means that for this species nitrogen allocation could be in favor of sun leaves. However such a result was not confirmed when analysing N of the leaves for which sky openness was computed.

Variations of N_a and SLA with the local leaf radiation regime (i.e. sky openness) is consistent with published results (Chabot et al. 1979, Gulmon and Chu 1981, Le Roux et al. 1999b) and has been understood as an important feature that increases the light use efficiency at the plant level (Field 1983).

Our results support the opinion of Le Roux et al. (1999b) that the maximisation of tree carbon gain should be studied by analysing patterns of investment in leaf dry mass per area rather than in leaf N concentration. Indeed, the decrease in V_{cmax} with decreasing sky openness was due to changes in SLA but not in N. This decrease can be interpreted as an acclimation process to adapt leaf photosynthetic capacities to the local light environment (Field 1983).

The correlations we found between N_a and sky openness, and between SLA and sky openness, were not affected by the type of tree (isolated or clumped), conversely to results of N_a and SLA dynamics during the vegetation cycle. Temporal dynamics were conducted on isolated and clump trees, and two types of leaves (sun and shade) were collected. But the radiation level for each leaf was not recorded, and a sun leaf of an isolated tree probably undergoes a higher irradiance level than a sun leaf of a clump tree, and a shade leaf of a clump tree is probably at a lower irradiance level than a shade leaf of an isolated tree. This may explain why N_a and SLA were different between isolated and clump trees for the temporal survey.

Sky openness was measured in October, when *C. febrifuga* LAI was below maximum. However light conditions for leaves at very low (highly shaded leaves) or very high (full sun leaves) sky opennesses probably did not undergo significant change since the period of maximum LAI. And these leaves greatly determine the relationship between SLA and sky openness, and between N_a and sky openness. In addition, even in case of changes in light conditions, reacclimation of leaves to these new light conditions may have occurred (Frack et al. 2001). Thus the difference of acclimation between the two species is not likely to be biased because of the date hemispherical photographs were taken.

In their reviews, Schulze et al. (1994) and Reich et al. (1999) did not mention dates at which leaves were sampled nor what kind of leaves were sampled. However, their reviews provide a comprehensive overview of N and SLA. Compared to other deciduous tree species worldwide, *C. febrifuga* and *C. arborea* have some of the lowest N ever measured for deciduous species, and are more similar to values measured for evergreen trees. *C. febrifuga* and *C. arborea* SLA are more in the range of observed SLA for deciduous trees, either temperate or tropical. This means that *C. febrifuga* and *C. arborea* N_a values must be low compared to most deciduous trees. Lamto infertile soils must explain these low N and N_a values. N retranslocation from senescing leaves is a common process in woody plants (e.g. Chapin and kedrowski 1983, Crane and Banks 1992). But at such low N values, N retranslocation from *C. febrifuga* or *C. arborea* leaves at the end of the vegetation cycle was not apparent, if any.

Conclusion

C. febrifuga and *C. arborea* displayed constrasting seasonal course of LAI, *C. arborea* reached its peak LAI and started leaf fall later than *C. febrifuga.* Seasonal courses of leaf N_a of were in accordance with seasonal LAI variations, allowing *C. arborea* to maintain high photosynthetic capacities late in the vegetation cycle.

SLA and N_a decreased with decreasing light availability within tree canopies, showing a strong ability of the two species to acclimate photosynthetic capacities to local light environments.

Both seasonal and within canopy estimated variations of photosynthetic capacities (calculated from leaf N_a) suggest that *C. arborea* performs higher photosynthetic rates than *C. febrifuga* in most conditions.

Acknowlegements

The authors are very debtfull to Konan N'Dri Alexis, Kouamé N'Guessan François, and Savadogo Sadare Prosper (Lamto Ecology Station), for participating in the field work. Rainfall data was provided by the Lamto Geophysical Station. We also wish to thank P. Breton and D. Benest (ENS, Paris) for their assistance in leaf N analysis.

This work was funded by the Programme National de Recherche en Hydrologie (INSU) and the Programme National Environnement, Vie & Société (CNRS).

Appendix 1-Leaf clump allometry

The following equations were used for predicting green leaf numbers (n_{GL}) from basal diameters (BD, mm) of the supporting branch of leaf clumps for *Crossoteryx febrifuga* or from length of the supporting branch corresponding to leaf insertion (LSB, cm) for *Cussonia arborea*. All leaf clumps were measured between May and October for *C. febrifuga* trees, and in May and August for *C. arborea* trees. Corresponding equations were used. For *C. febrifuga*, for all leaf groups for which BD was below 4 mm, n_{GL} was estimated using a regression fit including all month data with BD values below 4 mm.

C. febrifuga :

May : $n_{GL} = 26.58 \cdot BD - 95.87$ R^2=0.81

June : $n_{GL} = e^{2.18 \cdot BD - 0.0774}$ R^2=0.78

August : $n_{GL} = e^{2.484 \cdot BD - 0.9675}$ R^2=0.81

October : $n_{GL} = 11.93 \cdot BD - 42.74$ R^2=0.6

BD<4 mm : $n_{GL} = e^{2.482 \cdot BD - 0.625}$ R^2=0.86

C. arborea :

May : $n_{GL} = 1.148 \cdot LSB + 15.0697$ R^2=0.93

August : $n_{GL} = 1.189 \cdot LSB - 17.158$ R^2=0.88

Chapitre 5

Variabilité spatio-temporelle de la production herbacée

Introduction

La strate herbacée est composée principalement d'espèces perennes non nitrifiantes disposées en touffes. La dynamique annuelle de la production herbacée en zone ouverte (hors couvert arbre) à Lamto est bien documentée (Roland 1967, Monnier 1968, Abbadie 1983, Abbadie 1984, Puyravaud 1990, César 1992, Mordelet 1993a, Le Roux 1995). Des mesures ont également été menées sous couvert arbre (Mordelet 1993a).

Ces travaux sont tous basés sur des prélèvements destructifs (donc sensibles à une éventuelle variabilité spatiale intra-site), et ont été faits en différentes zones de la réserve. Ainsi, à la variabilité temporelle de la biomasse et de la nécromasse épigées est associée une variabilité spatiale inter-site. Ces deux éléments de variabilité sont confondus. Par ailleurs, la surface de prélèvement adoptée est variable, de 1 m^2 à plus de 16 m^2 (Roland 1967). Les herbes perennes sont diposées en touffes qui n'occupent pas toute la surface du sol. A l'échelle du mètre carré, la variabilité spatiale de la biomasse épigée peut donc être importante. Enfin, les mesures faites sous et hors couvert ne sont que qualitativement comparables, en l'absence de référence pour caractériser le couvert arbre.

César (1971) a montré qu'à partir de 5-6 m^2 de surface de prélèvement, les mesures sont plus fiables. Si des surfaces de cet ordre sont faciles à trouver hors couvert arbre, elle sont rares sous couvert. Une alternative consiste alors à utiliser plusieurs placettes de plus petites dimensions.

En vue de tester la capacité d'un modèle à reproduire la dynamique annuelle de la production herbe sous et hors couvert, il apparaît donc important :

- d'obtenir des mesures dans le temps de la biomasse et de la nécromasse herbacées, si possible grâce à un suivi non destructif (suivi des même placettes) dans différentes situations de recouvrement arbre.
- de pouvoir associer à ces mesures une caractérisation de l'intensité du couvert arbre, et donc de pouvoir quantifier l'effet du couvert arbre sur la production herbe.

Un suivi non destructif de la biomasse et de la nécromasse herbacée a été mis en place pour des placettes plus ou moins ombragées par la présence d'arbres. Pour chacune des placettes, le taux de recouvrement des arbres a été quantifié à l'aide de photographies

hémisphériques. L'ensemble de ces données a permis de caractériser la variabilité spatio-temporelle de la production herbacée au cours de l'année 2000.

Materiels et Méthodes

Suivi de la production herbe

Sur les parcelles "hors bosquet" (HB), "sous bosquet" (SB) et damier décrites au Chapitre 2, des placettes d'herbe de 1×1 m ont été choisies. Les placettes suivies se décomposent ainsi :

- 5 placettes pour chacune des trois zones ouvertes de la parcelle "hors bosquet" (soit 15 placettes hors couvert),
- 4 placettes sous chacun des deux bosquets de la parcelle "sous bosquet" (soit 8 placettes sous couvert arbre),
- 10 placettes sur la parcelle "damier", à différentes distances de l'arbre.

Le nombre de placettes compense la faible surface de celles-ci. Pour chacune des placettes, un suivi par point contact a été mis en place. Le principe du point contact est de compter le nombre de feuilles vivantes ou mortes touchant un piquet placé à la verticale dans le couvert. A l'intérieur de chaque placette, le comptage est fait tous les dix centimètres, soit pour 100 positions.

Le suivi a débuté juste après le passage du feu en janvier 2000. Il s'est poursuivi jusqu'en mai 2000. Après cette période, le couvert herbacé est devenu trop dense pour distinguer toutes les feuilles au contact du piquet. A chaque date de mesure, 4 placettes indépendantes furent aussi mesurées puis aussitôt récoltées pour calibrer des relations entre le nombre de brins vivants ou morts comptés et la biomasse, la nécromasse, ou la phytomasse de chaque placette.

Une récolte des placettes (échelonnée du 11 décembre 2000 au 4 janvier 2001, selon les placettes) a complété ce suivi. Afin d'estimer le taux de recouvrement basal des touffes d'herbe, les circonférences basales de chaque touffe ont été mesurées au moment de la récolte pour les placettes hors et sous bosquet. Pour chaque placette, biomasse et nécromasse furent séparées, séchées 3 jours à 70°C, et pesées.

Mesure de l'indice de trouée

Du 16 au 26 octobre 2001, des photographies hémisphériques furent prises au dessus de chaque placette d'herbe suivie, avec un appareil réflex Canon AL-1, équipé d'un objectif fish-eye Canon 7.5 mm. La prise des clichés s'est effectuée l'objectif de l'appareil dirigé vers le ciel. Les photos furent ensuite analysées à l'aide du logiciel GLA (Gap Light Analyser, Fraser et al. 1999), avec lequel un indice d'ouverture du ciel (pourcentage de ciel directement visible depuis l'objectif) fut calculé pour chaque placette.

Résultats

Calibration de la méthode point contact

De bonnes relations furent obtenues entre le nombre de feuilles vivantes (n_{FV}) et la biomasse, le nombre de feuilles mortes (n_{FM}) et la nécromasse, et entre le nombre total

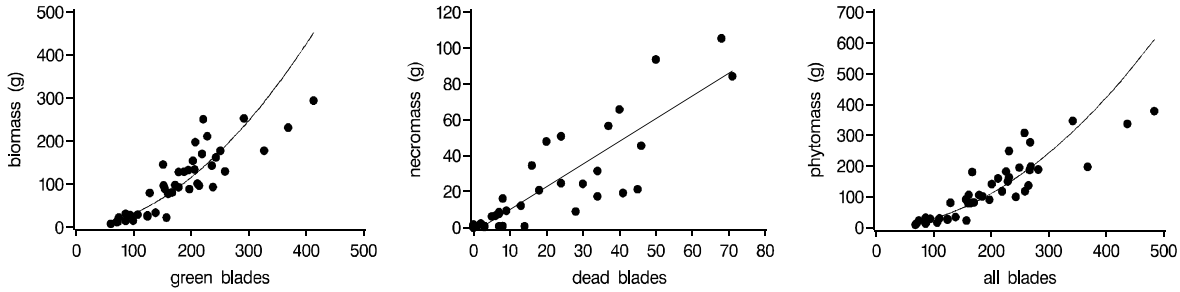

FIG. 5.1 – Relations entre la biomasse, la nécromasse, et la phytomasse épigées herbe, avec les nombres de contacts avec des feuilles vivantes, mortes, ou le nombre total de feuilles vivantes et mortes, mesurés par la méthode de point contact sur des placettes de 1×1 m. Les lignes représentent les meilleures corrélations (relations log-log pour biomasse et phytomasse, relation linéaire pour la nécromasse) (P<0.05).
Relationships between grass aboveground biomass, grass aboveground necromass, and grass aboveground phytomass, with the number of contacts with green blades, dead blades, and all blades counted with the Point Contact method. Lines represent best regression fits (log-log relationships for biomass and phytomass, and a linear relationship for necromass) (P<0.05).

de feuilles (n_{FT}) et la phytomasse pour les placettes récoltées indépendemment du suivi (R^2=0.83, 0.76, et 0.85, respectivement) (Figure 5.1) :

$$biomasse = e^{-5.21+1.87 \cdot ln(n_{FV})} \tag{5.1}$$

$$necromasse = -2.87 + 1.26 \cdot n_{FM} \tag{5.2}$$

$$phytomasse = e^{-5.57+1.94 \cdot ln(n_{FT})} \tag{5.3}$$

Relation Production-Indice de trouée

La comparaison entre biomasse, nécromasse, phytomasse ou surface basale des touffes des placettes lors de la récolte en fin de cycle, avec les indices de lumière mesurés par photos hémisphériques, a donné des relations significatives entre la production épigée herbe et l'environnement lumineux (Figure 5.2) avec R^2 =0.68, 0.49, 0.82 and 0.86 pour la biomasse, la nécromasse, la phytomasse et la surface basale des touffes, respectivement.

Variations temporelles de la production épigée de la strate herbacée

La variation temporelle n'a pu être mesurée par point contact que pour le premier tiers du cycle de végétation. En regroupant les placettes par classes d'indice de trouée, des variations importantes se manifestent dès le début du cycle en fonction de l'intensité du couvert arbre (Figure 5.3). La croissance est plus faible lorsque l'ombrage augmente.

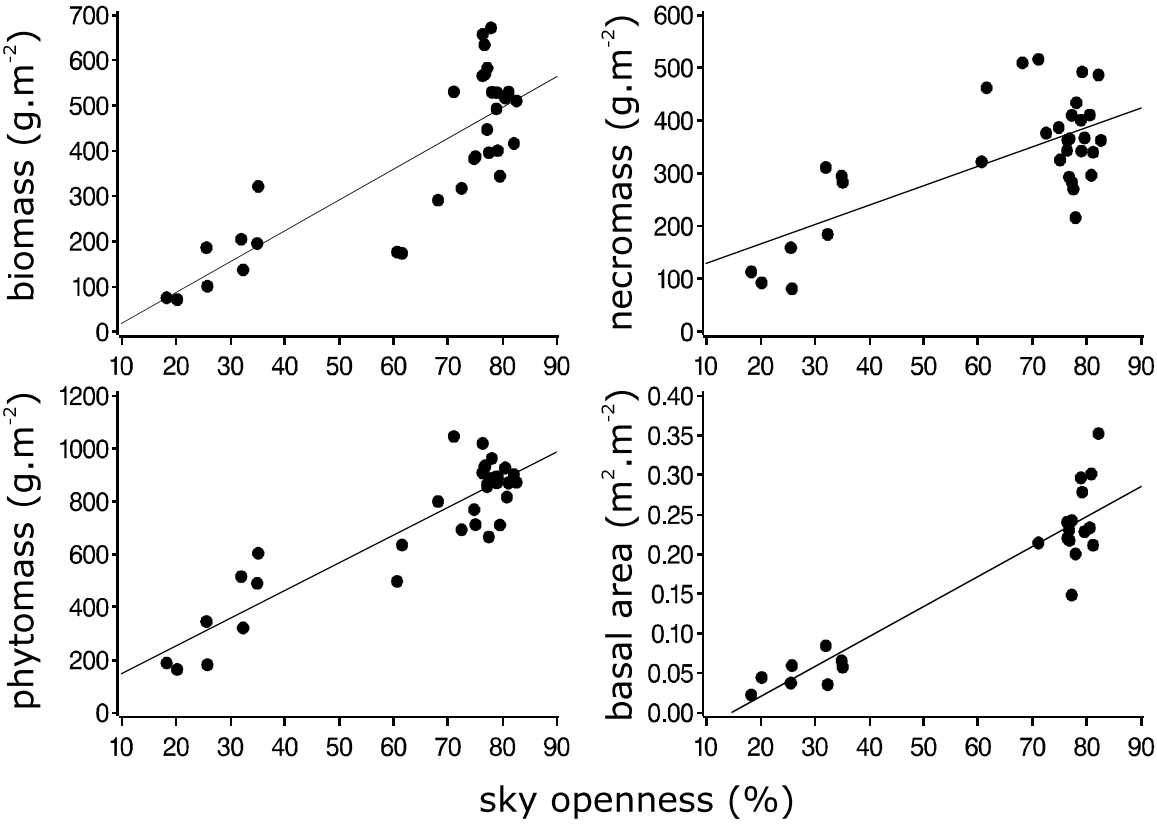

FIG. 5.2 – Relations entre indice de trouée (% de ciel libre) et biomasse, nécromasse, phytomasse, et surface basale des touffes de la strate herbacée. Les placettes ont été récoltées du 11 décembre 2000 au 4 janvier 2001. Les indices de trouée ont été mesurés du 16 au 26 octobre 2000. Les droites représentent des corrélations significatives à $P<0.05$. Relationships between grass aboveground biomass, necromass, phytomass, or tuft basal area, and sky openness (percent of sky not obstructed by tree foliage above grass). Grass plots were collected from 11th December 2000 to 4th January 2001. Sky opennesses were measured from 16th to 26th october 2000. Lines represent significant regression fits ($P<0.05$).

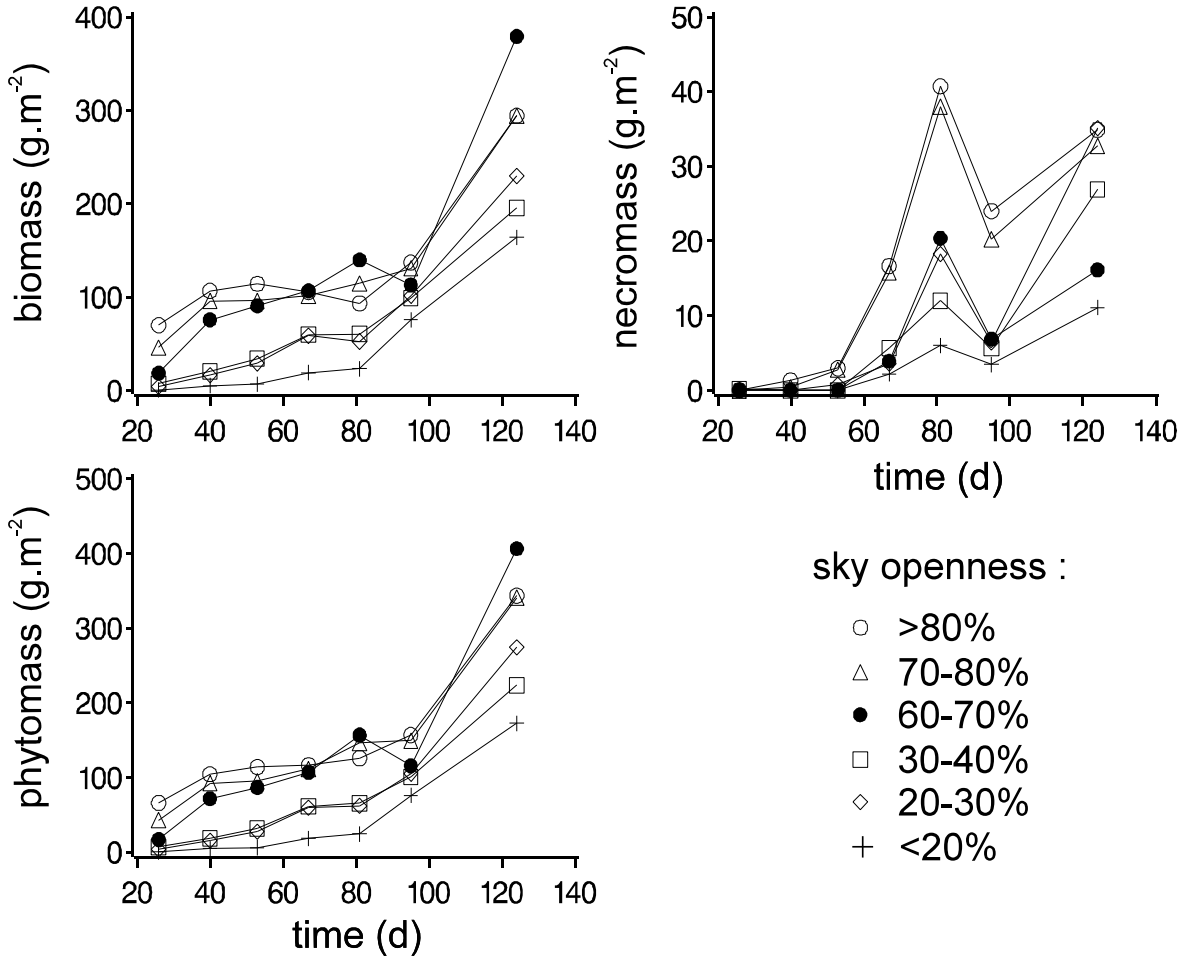

FIG. 5.3 – Biomasse, nécromasse et phytomasse épigées moyennes de la strate herbacée, par classe d'indice de trouée, en fonction du temps (début de l'année 2000).
Mean grass standing biomass, necromass, and phytomass temporal dynamics at the begining of the year 2000 and at different sky openness levels.

Discussion

La méthode de mesure par point contact s'est avérée fiable sans qu'il ait été besoin de tenir compte des espèces en présence. Cette méthode n'est cependant applicable que pour des couverts modérément développés, en dehors desquels on ne peut plus distinguer toutes les feuilles au contact du piquet. Cette méthode permet néanmoins de s'affranchir d'un suivi uniquement destructif et est simple à mettre en place.

L'intérêt de l'indice de trouée va au delà de la caractérisation de l'environnement lumineux à une date et un lieu donné. Lorsque mesuré, comme ici, alors que le feuillage arbre est encore important, il peut présenter un indice des conditions lumineuses sur l'ensemble du cycle de végétation. Les relations entre indice de trouée et biomasse ou nécromasse épigées sont moins bonnes que la relation indice de trouée-phytomasse épigée. Cela peut s'expliquer par le fait que les placettes d'herbe ont été récoltées sur une période de plusieurs semaines. Or en fin de cycle de végétation, la mortalité est importante, et le transfert biomasse vers nécromasse est rapide (voir les suivis de production herbe de Le Roux 1995). Certaines valeurs de biomasse en fin de cycle présentées ici sont donc probablement sous estimées, et certaines valeurs de nécromasse surestimées. La résultante en terme de phytomasse apparaît en revanche plutôt stable.

Le suivi temporel de la biomasse, de la nécromasse et de la phytomasse épigées indique que des différences apparaissent liées à l'indice de trouée mesuré en octobre. Cependant, en début de cycle, ces différences ont lieu alors que la croissance du feuillage arbre n'est pas achevée (voir Chapitre 4). Il est probable que l'accès à la lumière ne soit pas le seul facteur explicant les différences entre placettes correspondantes à différents niveaux d'indice de trouée. Si on considère la surface basale des touffes d'herbe comme un indice de leur développement racinaire, et donc de la quantité de réserves mobilisables pour démarrer la croissance, la plus faible surface basale des touffes sous couvert peut expliquer les différences de biomasse dès le début de la croissance.

La croissance herbe n'est pas constante, et dans le cas de l'année 2000, est affectée fortement par le stress hydrique. La saison sèche s'est prolongée jusqu'au début du mois d'avril (jour 100 environ) (voir mesures d'eau du sol au Chapitre 4), restreignant la croissance, quelles que soient les placettes, avec pour effet l'apparition de nécromasse. La croissance repart ensuite avec le début de la saison des pluies.

Conclusion

La méthode de point contact a permis, pour la première fois à Lamto, de suivre les variations temporelles de biomasse et nécromasse herbacées au cours d'un cycle de végétation en s'affranchissant de la variabilité spatiale (suivi des mêmes placettes). Les mesures par photos hémisphériques ont permis de quantifier le couvert arbre et son influence sur la croissance herbe. Ce jeux de données constitue un précieux moyen de tester la faculter de modèles spatiaux de fonctionnement de savane de reproduire la variabilité spatiale de la production herbacée.

Etudes de terrain - Conclusion

La photosynthèse, la conductance stomatique, le LAI, la SLA, et l'azote foliaire sont largement pris en compte dans des modèles à diverses échelles de temps et d'espace. Or de telles données sont rares pour des espèces de savane. L'ensemble des travaux de terrain présentés dans cette partie a permis d'obtenir des informations de base sur des espèces d'herbe et d'arbre sur un même site de savane. On a ainsi pu compléter les études déjà menées sur le site de Lamto, avec pour la première fois des mesures simultanées faites sur les arbres, l'herbe, et le sol sur les mêmes parcelles.

Ces expériences ont confirmé l'homogénéité du fonctionnement des espèces dominantes composant la strate herbacée, tant au niveau des échanges gazeux foliaires qu'au niveau de la production du couvert. A l'opposé, les deux espèces d'arbre étudiées présentent de forts contrastes en terme de capacités photosynthétiques, de conductances stomatiques, et de dynamiques foliaires. Ces contrastes s'ajoutent à ceux précédemment décrits concernant les comportements hydriques de ces espèces. Des contrastes encore plus forts, mais attendus, ont été montrés entre les espèces d'herbe, à métabolisme en C_4, et d'arbre, à métabolisme en C_3. Ces résultats confirment la nécessité de prendre en compte le rapport herbes-arbres dans l'estimation de la production et du bilan hydrique en savane, particulièrement si des plantes en C_4 et en C_3 coexistent. Ils suggèrent également de prendre en compte la composition spécifique du couvert arbre.

Troisième partie

Construction d'un modèle 3D pour l'étude des fonctionnements carboné et hydrique des systèmes herbes-arbres

Construction du modèle - Introduction

Cette partie décrit la construction de TREEGRASS, modèle spatialement explicite de production primaire et de bilan hydrique pour les systèmes herbes-arbres. Deux versions de ce modèle sont présentées, sous forme de deux publications.

La première version est antérieure aux études de terrain présentées aux chapitres précédents. Cette version est le fruit de l'expérience en modélisation acquise sur le site de Lamto (Le Roux 1995, Gignoux 1994), à laquelle a été associé le modèle spatialement explicite d'absorption du rayonnement et de transpiration RATP (Sinoquet et al. 2001). Si dans cette première version l'absorption du rayonnement et l'évapotranspiration sont très détaillés, les processus de production y sont très simplifiés. Une limitation forte de cette version est la non prise en compte de l'azote, élément fortement limitant dans les écosystèmes de savane. Cette version a été paramétrée et testée avec des jeux de données antérieurs aux expériences de cette thèse. C'est cette version qui est utilisée au Chapitre 8, pour l'étude des effets de la structure spatiale de la strate ligneuse sur la production primaire et le bilan hydrique à l'échelle de l'écosystème.

Dans la seconde version de TREEGRASS, les processus de production sont beaucoup plus détaillés. La photosynthèse est explicitement prise en compte ainsi que les facteurs l'influençant (dont l'azote foliaire et le stress hydrique), les dynamiques spatio-temporelles de l'azote foliaire et de la surface spécifique folaire sont également prises en compte. Cette deuxième version permet de simuler le fonctionnement annuel d'un système herbes-arbres en prenant en compte plusieurs espèces d'herbe et/ou d'arbre. Elle bénéficie en outre de données spécifiquement acquises dans le but de la paramétrer et de la tester. La publication de cette deuxième version est présentée sous une forme non définitive. Cette deuxième version du modèle est utilisée au Chapitre 9.

Chapitre 6

Première version de TREEGRASS

TREEGRASS : a 3D, process-based model for simulating plant interactions in tree-grass ecosystems

Ecological Modelling, 2000, 131 :47-63

G. Simioni[1], **X. Le Roux**[2], **J. Gignoux**[1] **and H. Sinoquet**[2]

1 Laboratoire Fonctionnement et Evolution des Systèmes Ecologiques, Université Paris 6 - CNRS - ENS, 46 rue d'Ulm, 75230 Paris, cedex 05, France

2 U.A. Bioclimatologie-PIAF (INRA-Université Blaise Pascal), Site de Crouelle, 234 avenue du Brezet, 63039 Clermont-Ferrand cedex 02, France

Abstract

The function and dynamics of savanna ecosystems result from complex interactions and feedbacks between grasses and trees, involving numerous processes (i.e. competition for light, water and nutrients, fire, and herbivory). These interactions are characterised by strong relationships between vegetation structure and function. Given the heterogeneous structure of savannas, modelling appears as a convenient approach to study tree-grass interactions. Most current models that describe carbon and water fluxes are not spatially explicit, which restricts their ability to simulate plant interactions at small scales in heterogeneous ecosystems. We present here a new 3D process-based model called TREEGRASS. The model aims at predicting, in heterogeneous tree-grass systems, plant individual radiation, carbon and water fluxes at a local spatial scale. It is run at a daily time-step over periods ranging from one to a few years. The model includes (i) a 3D mechanistic submodel simulating radiation and energy (i.e. transpiration) budgets, (ii) a soil water balance submodel, and (iii) a physiologically based submodel of primary production and leaf area development. The ability of TREEGRASS to predict the seasonal courses of grass dead and leaf mass, soil water content and light regime as observed in the field has been tested for grassy and shrubby areas of Lamto savannas (Ivory Coast). Simulations showed that the spatial distribution of primary production can be strongly affected by the spatial vegetation structure. Potential applications involve predicting net primary production and water balance from the individual to the ecosystem

and from the day to the annual vegetation cycle (e.g. effects of tree spatial patterns on carbon and water fluxes at the ecosystem level).

Key words : savanna, spatial patterns, primary production, water balance, radiation absorption, simulations

1. Introduction

Savannas are defined as ecosystems where a continuous grass layer and a discontinuous tree layer coexist (Scholes and Archer, 1997). Savanna ecosystems cover about 20% of continental surfaces (Scholes and Hall, 1996) and 40% of tropical land surfaces (Solbrig et al., 1990). In addition to their highly heterogeneous vegetation structure, these ecosystems are characterised by complex interactions between tree and grass individuals that compete for light, water and nutrient resources. Being able to predict grass and tree functioning separately does not enable to predict the functioning of the coupled tree/grass system. This restricts our ability to predict tree/grass stability and dynamics in savannas (Scholes and Archer, 1997).

Assessment of tree/grass interactions has mainly been addressed by field studies. Most of them have focused on the effects of trees on the biomass and primary production of the grass layer (e.g. Knoop and Walker, 1985 ; Stuart-Hill and Tainton, 1989 ; Weltzin and Coughenour, 1990 ; Belsky, 1994 ; Mordelet and Menaut, 1995), on the soil water balance (e.g. Knoop and Walker, 1985 ; Joffre and Rambal, 1988 ; Mordelet, 1993a and b ; Le Roux and Bariac, 1998) or on soil nutrient availability (e.g. Isichei and Muoghalu, 1992 ; Mordelet et al., 1993 ; Cruz, 1997 ; Rhoades, 1997). Though necessary, these studies do not point out the different processes that determine the integrated effect of one vegetation component on the other, but rather appear as a list of particular case studies.

Thus, for some authors, the only way to gain a comprehensive understanding of tree/grass coexistence and to account for the effect of vegetation structure on ecosystem physiology is to build specific models (Jeltsch et al., 1996 ; Scholes and Archer, 1997). During the last two decades, several modelling approaches have been proposed to simulate the functioning of tree/grass systems (Scholes and Archer, 1997). Some authors have developed models of tree/grass equilibrium that focused on the competition for soil water (Walker et al., 1981 ; Eagleson and Segarra, 1985). These models were generally based on a spatial segregation between grass roots exploiting mainly surface soil layers, and tree roots exploiting mainly deeper layers. More recently, simulation models predicting the effects of tree/grass interactions on grass and tree production have been developed. Among them, the GRASP model (Littleboy and McKeon, 1997) represents competition for water and nutrients, and the CENTURY-Savanna model (Parton and Scholes, unpublished), a tree/grass version of CENTURY (Parton, 1996), is based on competition for nutrients. These two models were designed to compute the bulk functioning of the tree and grass components of tree/grass systems, and use bulk information on vegetation structure (i.e. tree leaf and root biomasses or tree basal area computed at site scale) to drive tree/grass competition. The SAVANNA model (Coughenour, 1994) is a process-based model that is spatially explicit at the landscape scale (i.e. it is not individual based but each pixel is an association of one tree/grass zone and one pure grass zone). However, the choice of a relevant variable to define the respective size and dynamics of

these two areas is still unclear (Coughenour, pers. com.). To our knowledge, the only savanna model that accounts for tree individual spatial structure is the automaton model of Jeltsch et al. (1996). This model is suitable for predicting the effects of natural or man-induced disturbances on tree dynamics and tree/grass equilibrium, but was not designed to study the effect of vegetation structure on water or carbon fluxes in savannas. Other modelling studies have emphasized the importance of spatial patterns (Khorzukhin and Ter-Mikaelian, 1995 ; Pacala and Deutschman, 1995 ; Weishampel and Urban, 1996).

In this paper, we present a simulation model, named TREEGRASS, designed to test the effects of the fine scale vegetation structure (i.e. tree density, tree spatial distribution, crown shape and crown size distribution) on tree/grass interactions (i.e. water and carbon budgets at the site level). TREEGRASS takes into account competition for light and water in a mechanistic and spatially explicit way, and uses a biologically based approach to compute net primary production. The model is derived from three existing models : (1) the 3D RATP model (Radiation Absorption, Transpiration and Photosynthesis) (Sinoquet et al., 2000) that computes radiation and energy budgets within vegetation canopies ; (2) the PEPSEE model (Production Efficiency and Phenology in Savanna EcosystEms) (Le Roux et al., 1996) that simulates primary production and soil water balance ; (3) the MUSE simulation framework (MUltistrata Spatially Explicit model) (Gignoux et al., 1996) designed to represent an ecosystem as a set of individuals and their geometric features by a spatially explicit approach. In the next section, the TREEGRASS model is presented and is parameterised for a humid savanna ecosystem (Lamto, Ivory Coast). The ability of the model to simulate radiation absorption, primary production and soil water balance in pure grass and tree/grass areas is tested against field data. Limitations and possible applications of TREEGRASS are discussed.

2. The TREEGRASS model

The main original features of the 3D TREEGRASS model are that (1) trees are represented individually, (2) radial extensions of tree foliage and roots are taken into account, (3) the foliage and the root system are distributed into a grid of 3D cells, and (4) competition for light and water are treated mechanistically (i.e. most relationships used are biophysical). This model runs with a hourly/daily time step over one or a few vegetation cycles. The model has been developed in Borland Pascal 7. Processes considered in the model are presented in figure 6.1.

2.1. Main assumptions

The present version of TREEGRASS uses 5 major hypotheses :

1. Net primary production (NPP) is computed by the light use efficiency (LUE) approach (Monteith, 1972 and 1977) : one value for maximum LUE is used for trees and another value for grasses, while the same value is used for all the individuals on a site (maximum LUE values have to be determined from field measurements). The actual LUE is modulated by water stress. The assumption of the constancy of maximum LUE under different light regimes has recently been supported by the conceptual physiological model of Dewar et al. (1998).

2. The ratio of produced dry matter allocated to roots to the amount allocated to

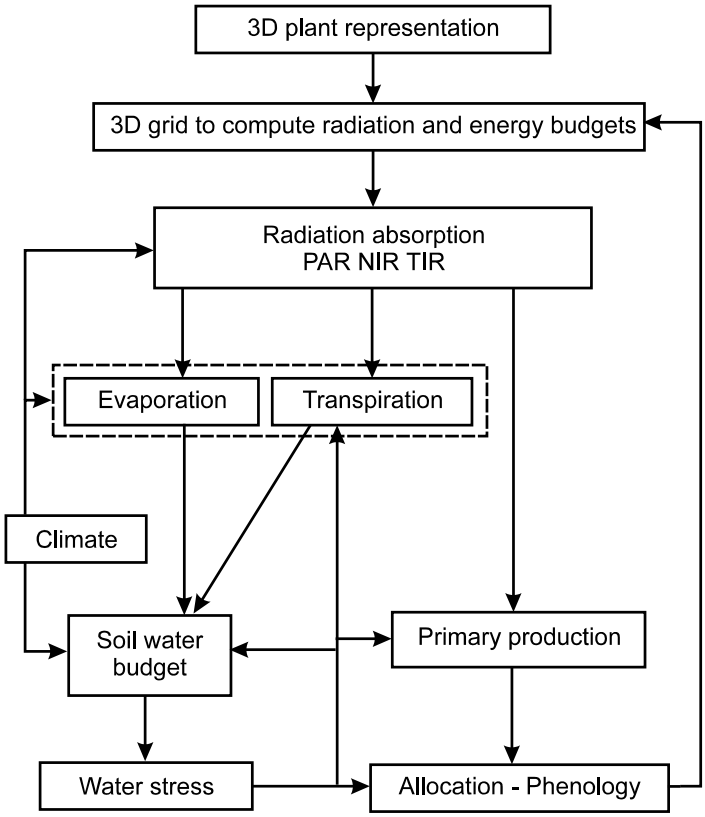

FIG. 6.1 – Processes computed in the TREEGRASS model

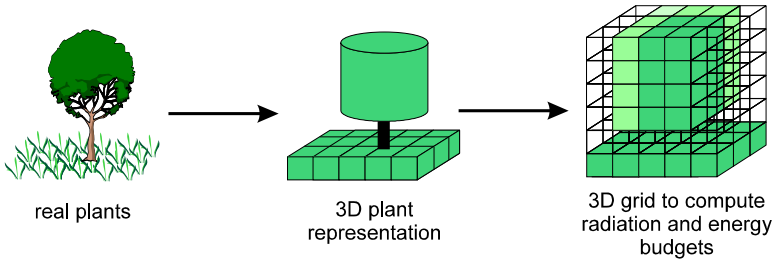

FIG. 6.2 – Spatial representation of plants in TREEGRASS. The second picture shows the simple plant structural features used to represent trees (i.e. simple cylindrical crown, crown radius, and total height and bole height). Though they do not appear on this figure, roots are represented in a similar way. the third picture represents the 3D grid used to compute the spatial distribution of plant foliage as used by the radiation/energy budget submodel (different levels of green correspond to different values of leaf area density (LAD)). Tree LAD is distributed using overlap coefficients between tree crown and cell volumes.

shoots is computed as a function of actual to maximum LUE values (Landsberg and Waring, 1997).

3. Over one vegetation cycle, tree architecture (crown volume and shape) is constant, and only the leaf area density (LAD) can change, tree dynamics and seedling growth are not implemented ;

4. Rainfall interception by the foliage is neglected ;

5. Climatic variables (wind, air temperature and humidity) are assumed to be spatially homogeneous on the site.

Nutrients, in particular nitrogen, can play an important role in tree/grass interactions (see Belsky, 1994, and Scholes and Archer, 1997), but they are not explicitly treated in TREEGRASS. The present model must be considered as a first version to which a soil organic matter submodel can be coupled, in order to include the nitrogen cycle.

Two additional hypotheses were made for the simulations presented in this paper :

1. for a given simulation, only one species of grass and one species of tree are considered ;

2. night transpiration is neglected (because of dew occurrence at night at the study site, Le Roux, 1995).

2.2. Spatial representation of the vegetation

Plants are distributed within a 3D grid of cells (figure 6.2). The grid is divided into an above ground part, where the foliage is distributed into vegetation cells, and a below ground part where roots are distributed into soil cells. One vegetation cell can contain different types of leaves (green or dead, grass or tree, individual i or j). In each cell, each leaf type is characterised by its LAD, inclination distribution and optical properties. Soil cells can contain roots of different plants as well.

A grass individual occupies one above ground cell and the soil cells underneath. Tree foliage and root crowns are assumed to have cylindrical shapes. Truncs and branches are not explicitely represented. Tree leaves and roots are spread into vegetation and soil

cells according to overlap coefficients between cylinders and cells. Two grass 'individuals' (i.e. plots) do not share any vegetation nor soil cell, which is in accordance with the spatial distribution of roots observed for grasses in humid savannas (Le Provost, 1993). In contrast, a tree can share cells with grasses or with other trees. In particular, a tree compulsorily shares soil cells with grass individuals.

2.3. Radiation absorption

The radiation submodel has been adapted from the RATP model (Sinoquet et al., 2000). Rays from several directions are directed into the cell grid. When a ray passes through a cell, it is attenuated following Beer's law, depending on the LAD and on the angular distribution of the vegetation entities (i.e. types of leaves) present in the cell. Intercepted radiation is shared between these entities, assuming that the leaves are randomly and uniformly distributed. Light interception by twigs and branches is neglected.

Radiation interception computed for each ray is used to calculate exchange coefficients between sources and receptors. Sky, foliage and soil are both sources (respectively of direct and diffuse radiation, and of transmitted or reflected radiation) and receptors. For one day, five representative sun directions are computed (corresponding to daytime 6, 9 and 12 A.M., and 3 and 6 P.M.). These directions vary with the day of year and latitude. For diffuse and reflected radiation, the direction space is divided into solid angles, centered around representative heights and azimuths. Incident diffuse radiation is calculated assuming a standard overcast sky luminance distribution (Moon and Spencer, 1942). Sources of reflected radiation are calculated considering that reflection and transmission are isotropic and depend only on the angular distribution of organs. Exchange coefficients between a source and a receptor are built in a progressive manner, adding the contribution of beams coming from the source when they meet the receptor.

These exchange coefficients are first calculated for diffuse and scattered radiation (depending thus only on the foliage characteristics and on the sky luminance distribution). For direct radiation, additional exchange coefficients are then computed for each time step, i.e. each sun direction. The first step is necessary only when the LAD of one individual has undergone a significant change. Hence, to save calculation time, exchange coefficients are computed only when a significant change in LAD (20% in our simulations) of at least one individual has occurred.

Radiation fluxes intercepted by each entity in each cell are computed by using the radiosity method (Ozisik, 1981) : the flux intercepted by a given receptor is a linear combination of fluxes coming from the whole set of sources weighed by the exchange coefficients between the sources and the receptor. Intercepted fluxes (including multiple scattering) are thus written as a system of linear equations. Solving this system allows us to calculate radiation fluxes. Details on the calculation can be found in Sinoquet and Bonhomme (1992) and in Sinoquet et al. (2000).

2.4. Transpiration and evaporation

Energy budget is computed in three dimensions to determine, for each entity in each cell, the organ temperature that balances fluxes of received and lost heat :

$$R_{n_{jk}} - H_{jk} - E_{jk} = 0 \tag{6.1}$$

where $R_{n_{jk}}$ is the net radiation absorbed by entity j in cell k, and H_{jk} and E_{jk} are sensible and latent heat fluxes lost by entity j in cell k. Energy budgets are established for shaded and sunny surfaces. Energy storage by the plant has been neglected. Net radiation absorption includes net balance for photosynthetically active radiation (PAR), near infra-red radiation (NIR), and thermal infra-red radiation (TIR) emitted by leaves and soil. For instance, net radiation absorption by the sunny surface e of entity j in cell k can be written :

$$R^e_{n_{jk}} = I^e_{jk}(PAR) + I^e_{jk}(NIR) + I^e_{jk}(TIR) - 2 \cdot \sigma \cdot (T^e_{jk})^4 \tag{6.2}$$

where $I(PAR)$ and $I(NIR)$ are PAR and NIR fluxes calculated by the radiation absorption submodel, $I(TIR)$ is the TIR absorbed by entity j in cell k, and the last term represents TIR emitted by the entity surface : T_{jk} is the surface temperature of entity j in cell k, and σ is the Stephan-Boltzman constant (5.67.10-8 $W{\cdot}m^{-2}{\cdot}s^{-1}{\cdot}K^{-4}$). Sensible heat flux can be written :

$$H^e_{jk} = \rho \cdot C_p \cdot g_b \cdot (T^e_{jk} - T_a) \tag{6.3}$$

where ρ, C_p, and g_b are respectively the air density ($kg{\cdot}m^{-3}$), the air specific heat ($J{\cdot}kg^{-1}{\cdot}K^{-1}$) and the aerodynamic conductance ($m{\cdot}s^{-1}$) that depends on wind speed ; T_a is the air temperature and T^e_{jk} is the sunny surface temperature of entity j in cell k. Similarly, the latent heat flux can be expressed as :

$$E^e_{jk} = (\rho \cdot \frac{C_p}{\gamma}) \cdot g_w \cdot (e^e_{sjk} - e_a) \tag{6.4}$$

where parameters γ and g_w are the psychrometric constant ($Pa{\cdot}K^{-1}$) and the leaf conductance ($m{\cdot}s^{-1}$), respectively, e^e_{sjk} is the saturating vapour pressure at temperature T^e_{jk} estimated with the Tetens formula (1930), and e_a is the air water vapour pressure.

g_w is the combination of aerodynamic and stomatal conductances of lower and upper leaf surfaces (g^e_{si} and g^e_{ss}). These conductances depend on microclimatic factors. In this work, leaves are hypostomatous, g_{ss} is considered as nil, and the model proposed by Jarvis (1976) is used to compute g_{si} :

$$g^e_{si} = g_{smax} \cdot f_{VPD} \cdot f_{PAR} \cdot f_{SI} \tag{6.5}$$

where g_{smax} is the maximum stomatal conductance, f_{VPD} is a linear function for vapour pressure deficit (VPD), f_{PAR} is a nonlinear function of PAR (Jarvis, 1976), and f_{SI} is a threshold function accounting for water stress (SI is the stress index, see section 2.5.3).

Similarly, an energy budget for each soil cell of the upper layer is calculated taking into account a conductive heat flux G into the soil :

$$R_{n_{ks}} - G_{ks} = E_{ks} + H_{ks} \tag{6.6}$$

where G_{ks} is calculated as a fraction of $R_{n_{ks}}$ in soil cell ks, according to vegetation phenology (Le Roux, 1995). As for leaves, solving the soil energy budget requires the

determination of the soil aerodynamic resistance and the soil surface resistance to water vapour transfer. The former depends on wind speed while the later depends empirically on the quantity of water evaporated since last rain in soil upper layer (Amadou, 1994).

The overall energy budget for sunny and shaded surfaces of each entity j in each cell k (including soil cells) makes an equation system in which surface temperatures are the unknowns. The energy budget is solved using the Newton-Raphson algorithm by successive iterations. Further details are given by Sinoquet et al. (2000).

Evaporation, transpiration and absorbed PAR obtained for each entity in each cell are summed up to calculate daily soil evaporation, and individual plant transpiration and absorbed PAR.

2.5. Soil water budget

Soil is divided into two strata, an upper layer (layer 1, the depth of which is defined so that this layer includes 90% of the grass roots), the layer 2 (down to the maximum plant rooting depth), plus the deep soil underneath.

2.5.1 Soil water extraction

Water evaporated is extracted from the soil upper layer cells. Water transpired by each individual is extracted from the soil cells occupied by the plant roots, using overlap coefficients between volumes of soil occupied by roots and soil cell volumes. The total transpiration T is extracted from layer 1 (T_1) and from layer 2 (T_2) for an individual; values for T_1 and T_2 depend on the water stress index and are calculated as :

$$\frac{T_1}{T} = (\frac{T_1}{T})_{max} \cdot f_{SI} \tag{6.7}$$

$$T_2 = T - T_1 \tag{6.8}$$

where $(\frac{T_1}{T})_{max}$ is a species specific parameter, the fraction of the plant total transpiration extracted in layer 1 under non-limiting water conditions. Transpirated water that can't be extracted from layer 1 or 2, because their wilting points are reached, is assumed to be pumped from the deep soil.

2.5.2 Run-off and drainage

Run-off occurs if precipitation P exceeds a threshold value P_0 and if the total LAI is below a threshold value LAI_0 (De Jong, 1983) :

$$RunOff = a \cdot (P - P_0) \tag{6.9}$$

where a is an empirical parameter.

Drainage (from layer 1 to layer 2, and from layer 2 to deep soil) is computed by a simple bucket model (i.e. drainage occurs when the soil water content of a given layer exceeds field capacity).

2.5.3 Water stress

In the model, for each plant, the stress index depends on the soil water content in layer 1, as Le Roux and Bariac (1998) found that water potentials of *Crossopteryx febrifuga*, a tree species, and *Hyparrhenia diplandra*, a grass species, were related with water potential in the 0-60 cm soil horizon. Each soil cell in layer 1 has a corresponding stress index :

$$R_1 \leq R_{l_1} \qquad f_{SI} = \frac{R_1 - R_{wp_1}}{R_{l_1} - R_{wp_1}} \tag{6.10}$$

$$R_1 > R_{l_1} \qquad f_{SI} = 1 \tag{6.11}$$

where R_1 and R_{l_1} are the actual and threshold values of soil water content in layer 1, and R_{wp_1} is the soil water content of layer 1 at wilting point.

In layer 1, a grass individual has its roots in only one cell, its water stress index is thus determined by the water content of this cell. On the opposite, the stress index for a tree individual is a combination of the stress indices of the different cells where its roots are present. All soil cells occupied by roots of a given tree contribute to its stress index in proportion to overlaps between the root crown volume and cell volumes.

2.6. Primary production and allocation

2.6.1. Fire

Fire occurs at a prescribed date, according to field obervations. To avoid to model the kinetics of the allocation from roots to shoots after fire for grasses (Le Roux et al., 1997), leaf biomass is initialised to a minimum value (10 g·m^{-2}), as proposed by Ciret et al. (1999). In a similar way, fire reduces individual tree LAI to 0.1 (on a projected crown area basis).

2.6.2. Dry matter production

The light use efficiency approach (Monteith, 1972 and 1977) is applied to each grass or tree individual :

$$TNPP = E_b \cdot APAR \tag{6.12}$$

where $TNPP$ is the total net primary production of the individual (g·unit^{-1} time), $APAR$ is the PAR absorbed by the plant (MJ·unit^{-1} time), and E_b is the conversion efficiency of $APAR$ into dry matter (g·MJ^{-1} APAR). E_b is given by :

$$E_b = E_{bmax} \cdot f_{SI} \tag{6.13}$$

where E_{bmax} is the maximum conversion efficiency (i.e. without water stress). One value of E_{bmax} is used for trees and one for grasses.

2.6.3. Allocation

The proportion of $TNPP$ allocated to shoots (η_s) is given by the empirical relation proposed by Landsberg and Waring (1997) :

$$\eta_s = 1 - \frac{\alpha}{1 + \beta \cdot \frac{E_b}{E_{bmax}}} \tag{6.14}$$

For example, with $\alpha = 0.6$ and $\beta = 0.5$, a plant allocates 60% of carbon to shoots when $\frac{E_b}{E_{bmax}}$ and thus $f_{SI} = 1$. This fraction decreases to 40% when the water stress is maximum (and when production tends to zero). Such an effect of drought on root/shoot allocation has been reported in field studies (e.g. Durand et al., 1989) and is in accordance with the functional equilibrium theory (Brouwer, 1983). For trees, a similar approach is used to compute root/shoot allocation. In addition, because tree above ground production is shared between leaves and branches/trunk, we assume that all the above ground growth is allocated to leaves as long as the plant has not reached its maximum LAI (each tree is given a maximum LAI value related to its size, see section 3.1.2).

2.6.4. Seasonal variations in biomass and necromass

For each grass individual, variations in biomass and necromass compartments are computed as (Le Roux, 1995) :

$$\begin{array}{rcl} B_t & = & B_{t-1} \cdot (1 - \Gamma_M) + TNPP \cdot \eta_s \\ N_t & = & N_{t-1} \cdot (1 - \Gamma_D) + B_{t-1} \cdot \Gamma_M \\ R_t & = & R_{t-1} \cdot (1 - \Gamma_R) + TNPP \cdot (1 - \eta_s) \end{array} \tag{6.15}$$

where B and N are above ground biomass and necromass (g·m^{-2}), Γ_M and Γ_D are above ground mortality and decomposition rates (g·g^{-1}·day^{-1}), and t is time (days). Because of the lack of mortality and decomposition data for roots in savannas, the root compartment is represented simply by a phytomass R (g·m^{-2}) with a constant decomposition rate Γ_R (g·g^{-1}·day^{-1}). For each tree individual, variations in the leaf biomass B_l are given by (LAI_{max} is the maximum tree LAI) :

$$\begin{array}{lll} if\ LAI < LAI_{max} \quad (before\ dry\ season)\ : & B_{l_t} = B_{l_{t-1}} \cdot (1 - \Gamma_M) + TNPP \cdot \eta_s \\ else\ : & B_{l_t} = B_{l_{t-1}} \cdot (1 - \Gamma_M) \end{array} \tag{6.16}$$

For grasses, above ground mortality and decomposition rates are assumed to be zero after fire until grass individual LAI reaches 1, and constant afterwards (Le Roux, 1995). For tree individuals, the leaf mortality rate is nil before the dry season, and depends on water stress during the dry season :

$$\Gamma_M = \chi \cdot (1 - f_{SI}) \tag{6.17}$$

where χ is the maximal mortality rate. Tree leaf fall is assumed to be instantaneous, i.e. there is no dead leaf accumulation within the tree foliage (Mordelet, 1993a). All the remaining green leaves fall after fire occurrence (Menaut, 1974).

Grass green LAI is computed according to specific leaf area values decreasing with increasing grass biomass values. A constant specific leaf area is used for grass dead leaves and tree green leaves (Le Roux, 1995).

3. Application of TREEGRASS to the Lamto savannas

3.1. Parameterisation of the model

The model has been parameterised for the humid savanna of Lamto, Ivory Coast (Menaut and César, 1979) (Tables 6.1 and 6.2).

3.1.1. Climatic data

Daily global radiation, rainfall and wind speed, and daily courses of air temperature and VPD measured at Lamto in 1991-92 (Le Roux, 1995) were used as input variables. A sinusoidal evolution of global radiation was assumed during the day, sampled at five sun positions. PAR was considered as a fixed amount of global radiation (48%) (Le Roux et al., 1997). Because the amount of diffuse radiation has not been rountinely recorded at Lamto, it was assumed constant and equal to 60% of global radiation (Gauthier, 1993). Atmospheric radiation was also assumed to be constant and equal to 350 $W{\cdot}m^{-2}$, according to measurements made at Lamto in 1991-92. Wind speed was assumed constant throughout the day. For each day, the model used five temperature and VPD values (recorded in 1991-92) corresponding to the five sun directions used.

3.1.2. Plant data

The C_4 perennial bunch grass species considered here was *Hyparrhenia* spp. (Andropogoneae). The tree type corresponded to a dominant, deciduous, shallow-rooted species present at Lamto : *Crossopteryx febrifuga*.

Each tree was characterised by its location (spatial position of the trunk), its total height (*Ht*, in meters), and cylindrical leaf and root crown shapes. The basal leaf crown surface (i.e. tree foliage projected crown surface, *CS*, in m^2) was given as (Gignoux, regression based on unpublished data) :

$$CS = 0.4372 \cdot Ht^{1.7228} \tag{6.18}$$

Bole height was assumed to be half of *Ht*. Root crown radius (*RCR*) depended on the leaf crown radius (*RC*) (Mordelet, 1993a) :

$$RCR = 1.5 \cdot RC \tag{6.19}$$

Maximum tree LAI was determined from CS as (Menaut, unpublished) :

$$LAI_{max} = 0.65 \cdot CS^{1.065} \tag{6.20}$$

Tree architecture was assumed to be fixed (i.e. there was no crown volume variation during a vegetation cycle). Grass green (LAI) and dead ($dLAI$) leaf area indices were computed from biomass B and necromass N according to measured specific green and dead leaf areas (Le Roux, 1995) :

$$LAI = (128 - 62 \cdot (1 - e^{-0.0102 \cdot B})) \cdot B \cdot 10^{-4} \tag{6.21}$$

$$dLAI = 0.0144 \cdot N \tag{6.22}$$

TAB. 6.1 – Sources and values of the TREEGRASS model parameters used for simulations of Lamto savannas (part 1).

Parameters	Values	References
Radiation profile		
PAR/global radiation ratio	0.48	Le Roux et al. 1997
Diffuse/global radiation ratio	0.60	Gauthier 1993
Atmospheric radiation ($W \cdot m^{-2}$)	350	Le Roux 1995
Leaf angular distribution		
Grass living leaves	erectophile	Le Roux et al. 1997
Grass dead leaves	planophile	Id.
Tree	spherical	NA
PAR absorbances		
Ground	0.76	Le Roux et al. 1997
Grass living leaves	0.78	Id.
Grass dead leaves	0.35	Id.
Tree	0.78	NA
PIR absorbances		
Ground	0.50	Le Roux et al. 1997
Grass living leaves	0.04	Id.
Grass dead leaves	0.05	Id.
Tree	0.10	NA
Soil layer depths (cm)		
Layer 1	60	Le Roux 1995
Layer 2	110	Id.
Soil water contents (mm)		
Layer 1 field capacity	104.6	Le Roux and Bariac 1998
Layer 1 threshold (R_{l_1})	60	Id.
Layer 1 wilting point (R_{wp_1})	30.9	Id.
Layer 2 field capacity	187	Id.
Layer 2 wilting point	100	Le Roux unpublished
Run-off		
Minimum precipitation (P_0 mm)	22	de Jong 1983
Maximum LAI (LAI_0)	2.5	Id.
a	0.1394	Id.

NA : not available

TAB. 6.2 – Sources and values of the TREEGRASS model parameters used for simulations of Lamto savannas (part 2).

Parameters	Values	References
Maximum stomatal conductances g_{smax} ($mmol \cdot m^{-2} \cdot s^{-1}$)		
Grass	230	Sueur 1995
Tree	230	NA
Maximum fraction of transpirated water extracted from layer 1 $(\frac{T_1}{T})_{max}$		
Grass	0.9	Le Roux 1995
Tree	0.7	Le Roux et al. 1995
Maximum aboveground conversion efficiencies ($g \cdot MJ^{-1}$ APAR)		
Grass	1.14	Le Roux et al. 1997
Tree	0.8	Bégué pers. com.
Fraction of production allocated to above groun parts (for trees and grass) (%)		
Without water stress	60	Durand et al. 1989
With water stress (minimum value)	40	Id.
Initialisations after fire		
Grass leaf biomass ($g \cdot m^{-2}$)	10	Ciret et al. 1999
Tree individual LAI	0.1	Id.
Others		
Grass mortality rate Γ_M (d^{-1})	0.012	Le Roux 1995
Grass decomposition rate Γ_D (d^{-1})	0.015	Id.
Grass phytomass decomposition rate Γ_R (d^{-1})	0.002	Id.
Grass dead specific leaf area ($cm^2 \cdot g^{-1}$)	144	Id.
Tree maximum leaf mortality rate χ (d^{-1})	0.04	NA
Tree specific leaf area ($cm^2 \cdot g^{-1}$)	90	Gauthier 1993, Medina 1982, Medina and Francisco 1994

NA : not available

Tree specific leaf area (SLA, table 6.2) has been measured by Gauthier (1993). Possible temporal evolution of tree SLA was neglected.

Published values of stomatal conductance for *Hyparrhenia* spp. under sub-optimal conditions ranged from 202 to 296 mmol·m^{-2}·s^{-1} (Simoes and Baruch, 1991) or from 120 to 275 mmol·m^{-2}·s^{-1} (Sueur, 1995). A maximal stomatal conductance of 230 mmol·m^{-2}·s^{-1} was used for the simulations. Very few stomatal conductances have been reported for savanna trees (see Schulze, 1994). Ullman (1985) observed maximal values up to 220 mmol·m^{-2}·s^{-1} for different acacia species in sahelian and saharian zones. Schulze (1994) gave values for different vegetation types : 145 mmol·m^{-2}·s^{-1} for monsoonal forests, 200 for sclerophyllous shrubland, 190 for temperate deciduous trees, 273 for tropical deciduous forests, and 207 for tropical rainforests. In the present study, we chose a maximum stomatal conductance of 230 mmol·m^{-2}·s^{-1}.

Values for fVPD and for fPAR were computed as :

For grass (Baruch et al. 1985) :

$$f_{VPD} = 1.25 - 2.5 \cdot 10^{-4} \cdot VPD \tag{6.23}$$

For trees (Le Roux et al., 1999a) :

$$f_{VPD} = 1.18 - 1.8 \cdot 10^{-4} \cdot VPD \tag{6.24}$$

(Le Roux et al., 1999a) :

$$f_{PAR} = \frac{0.030978 \cdot APAR}{1 + 0.030978 \cdot APAR} \tag{6.25}$$

where VPD is the vapour pressure deficit (Pa) and $APAR$ is the absorbed PAR for a given sun position.

Above ground maximal conversion efficiency has been measured at Lamto for grass (Le Roux et al., 1997), and in a dry savanna in West Africa for trees (Bégué, pers. com.) (table 6.2). E_{bmax} values were assumed to be twice the measured values of above ground maximal conversion efficiency (i.e. assuming a root : shoot ratio of 1 for production). Grass conversion efficiency was supposed to be constant under tree cover and in open areas. This is consistent with Cruz's results (Cruz, 1997) which showed that conversion efficiency did not differ under or out of tree cover for *Dichanthium aristatum*, a C_4 tropical grass species. Allocation parameters in eq. 6.14 were chosen so that plant allocated 60% of their assimilates to above ground parts without water stress and 40% with maximum water stress (Table 6.2).

3.1.3. Data for soil water storage and water flow

Values of soil water contents in layers 1 and 2 at field capacity and wilting point were estimated from field observations (Table 6.1). Aerodynamic soil resistance was prescribed. Soil surface resistance to water vapour transfer (SSR) depended on the amount of water evaporated since last rainfall from layer 1 (E_{cum}) (Amadou, 1994) :

$$SSR = 80 \cdot e^{0.23 \cdot E_{cum}} \tag{6.26}$$

The conductive heat flux G in the soil was a constant fraction of net radiation (R_n) of the soil-grass system (Le Roux, 1995) :

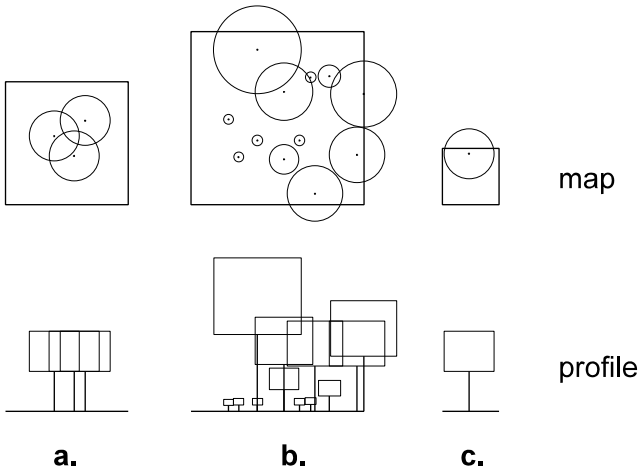

FIG. 6.3 – Tree-grass plots used to test the model. Tree trunks (dots and bars) and canopies (circles and rectangles) are represented. (a) Tree clump site (6×6 m). (b) Site corresponding to Gauthier's study (1993), rebuilt from tree structure data (8×8 m). (c) Site used to test the effects of cell dimensions (3×3 m). Trees in sites (a) and (b) were identical (3.61 m high, canopy area of 4 m^2).

$$\frac{G_{ks}}{R_{n_{ks}}} = 0.3 - 0.22 \cdot C_{ks} \tag{6.27}$$

$$C_{ks} = 1 - e^{-0.607 \cdot LAI} \tag{6.28}$$

where C_{ks} is the grass fractional cover over the soil cell ks.

According to Le Roux (1995), under non-limiting water conditions, grasses took up 90% of transpired water from layer 1 (i.e. transpiraiton fraction extracted from layer 1 $(\frac{T_1}{T})_{max} = 0.9$). The ratio $(\frac{T_1}{T})_{max}$ is 0.7 for trees (Le Roux and Bariac, 1998). Field data also showed that water stress should be calculated from water content in layer 1 for both grasses and trees (Le Roux and Bariac, 1998).

Runoff was computed when threshold values for daily precipitation ($P_0 = 22$ mm) and LAI ($LAI_0 = 2.5$, including grass dead LAI) were reached, as observed by De Jong (1983) at Lamto.

3.2. Simulations performed

The model was tested by comparing its outputs with measured data. Simulations were performed using :

(1) a pure grass site (i.e. one grass individual) for which TREEGRASS outputs of seasonal dynamics of grass above ground biomass and necromass, and seasonal courses of soil water contents in layers 1 and 2 were tested against 1991-92 field data from Le Roux (1995) ;

(2) a tree clump site (a 6×6 m site with a clump of 3 trees at the center, see figure 6.3a.) for which TREEGRASS outputs of the seasonal course of soil water content in layer 1 under tree cover were tested against 1991-92 field data from Le Roux (1995) ;

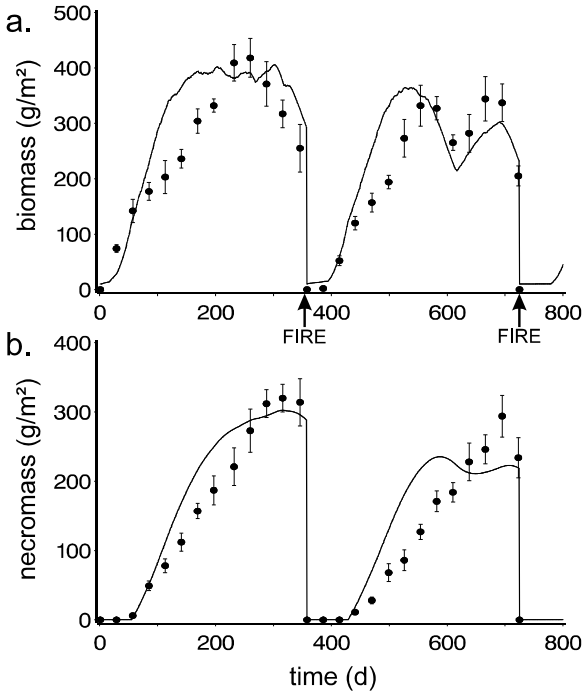

FIG. 6.4 – Measured (•) (le Roux 1995) and simulated (lines) seasonal courses of grass above ground biomass (a) and necromass (b) in an open (pure grass) site, during two annual vegetation cycles. Bars represent one standard deviation.

(3) a tree/grass site corresponding to the site where radiation absorption was studied at Lamto (figure 6.3b.) for which TREEGRASS outputs of tree radiation absorption were tested against field data from Gauthier (1993).

For each test, the model was run using climatic data measured in 1991-92. Cell basal dimensions were 1x1m (cell basal dimensions refers to the side length of the square basis of a cell). In addition, and in order to assess possible effects of cell basal dimensions, simulations were carried out with the tree/grass site of figure 6.3c., using different cell sizes. Finally, in order to illustrate possible effects of the tree spatial structure on spatial production patterns, two other simulations were conducted with distinct tree spatial distributions.

4. Results

4.1. Pure grass site

Although the model slightly overestimated primary production at the beginning of each cycle, the seasonal dynamics of biomass and necromass were adequately simulated (figure 6.4). The water stress effect in the middle of the 1992 vegetation cycle was satisfactorily simulated. Over the two years, measured and simulated biomasses and necromasses were well correlated (R^2=0.83, $F_{1,26}$=130.6, P=0.0001 for biomass ; and R^2=0.88, $F_{1,26}$=193.2, P=0.0001 for necromass). The seasonal courses of soil water contents in layers 1 and 2 were also adequately simulated by the model (figure 6.5). Measured and

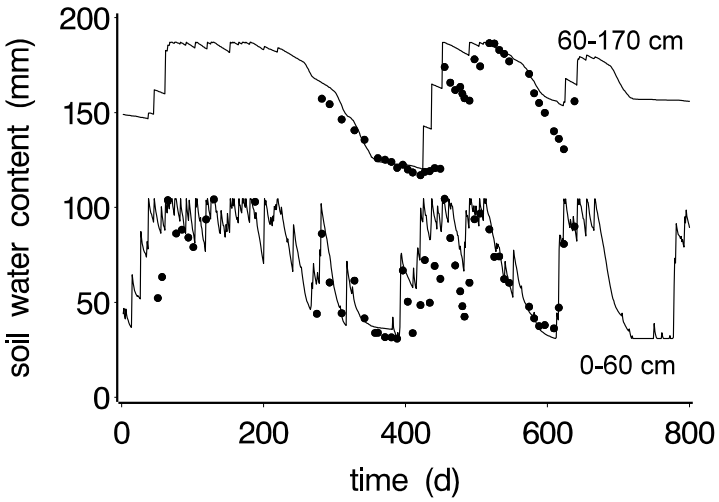

FIG. 6.5 – Measured (•) (Le Roux 1995) and simulated (lines) seasonal courses of soil water contents in the two upper soil layers (0-60 cm and 60-170 cm) in an open (pure grass) site, during two annual vegetation cycles.

simulated soil water contents were well correlated (R^2=0.64, $F_{1,37}$=66.6, P=0.0001 for layer 1, and R^2=0.75, $F_{1,37}$=113.3, P=0.0001 for layer 2). Nonetheless, soil water content in layer 1 was overestimated at the beginning of the vegetation cycle and early drainage was thus simulated from layer 1 to layer 2 around day 425.

Mean values of annual above ground and total NPP computed by TREEGRASS, using 1991-92 climatic data, were 15.3 t·ha^{-1} and 25.8 t·ha^{-1}, respectively. These numbers were close to values reported for Lamto savannas : 12.7 t·ha^{-1} for above ground NPP (Le Roux, 1995), 9.6 t·ha^{-1} for below ground NPP (Abbadie, 1983), and from 21.5 to 35.8 t·ha^{-1} for total NPP in savanna grasslands (Menaut and César, 1979).

4.2. Tree clump site

Measured and simulated soil water contents under tree clump were well correlated (R^2=0.68, $F_{1,34}$=73.4, P=0.0001), despite an overestimation at the beginning of the vegetation cycle (figure 6.6).

Simulated grass above ground NPP under tree clump corresponded to 45% of the above ground NPP in open areas (not shown). Simulated grass above ground NPP under tree clump was therefore slightly lower than that observed by Mordelet and Menaut (1995) who reported a value of 63%.

4.3. PAR absorption by trees

Figure 6.7 shows the PAR absorption efficiency of trees in relation to tree total LAI. For low tree LAI (under 0.4), the model, which does not account for PAR absorption by woody parts, underestimated tree PAR absorption efficiency. Above a tree LAI of 0.4, tree PAR absorption efficiency was correctly simulated. The model gave sets of different tree LAI for which PAR absorption efficiencies were identical. This is because, as reported

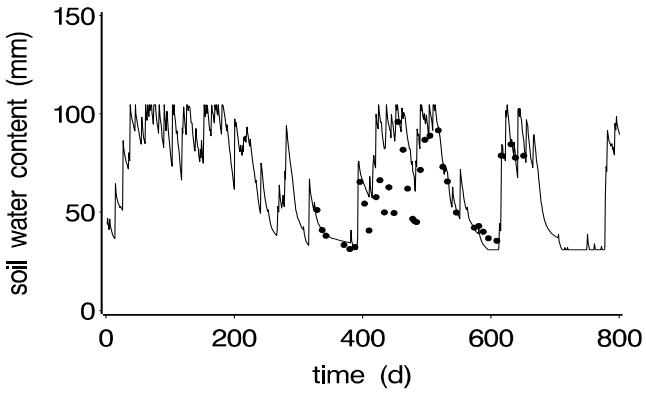

FIG. 6.6 – Measured (•) (Le Roux 1995) and simulated (lines) seasonal courses of soil water content in the upper layer (0-60 cm) under a tree clump, during two annual vegetation cycles.

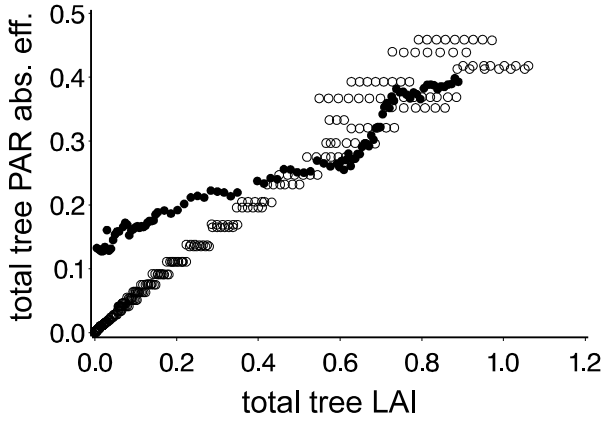

FIG. 6.7 – Measured (•) (Gauthier 1993) and simulated (◦) total tree PAR absorption efficiency as a function of total tree LAI.

earlier in the model description, new LAI values are used in the radiation absorption submodel only if, for at least one plant, a change of 20% has been reached. For a given value of tree LAI, there were also different values of tree PAR absorption efficiencies because the simulation was done for two vegetation cycles, and in each cycle, tree LAI increased and decreased (leaves expanded and fell). The tree LAI threshold of 0.4 was reached between two to three months after fire occurrence, depending on the year.

4.4. Effects of cell basal dimensions

Compared to PAR absorption efficiency or water fluxes, NPP was the most sensitive variable to cell basal dimensions. Total grass NPP increased from 12.79 to 14.34 $t{\cdot}ha^{-1}$ (12.1% variation) when cell basal side size decreased from 3 to 0.375 m respectively (figure 6.8a.). On the opposite, total tree NPP decreased from 15.00 to 12.97 $t{\cdot}ha^{-1}$ (13.5% variation) (figure 6.8b.). Total NPP decreased little with decreasing cell basal di-

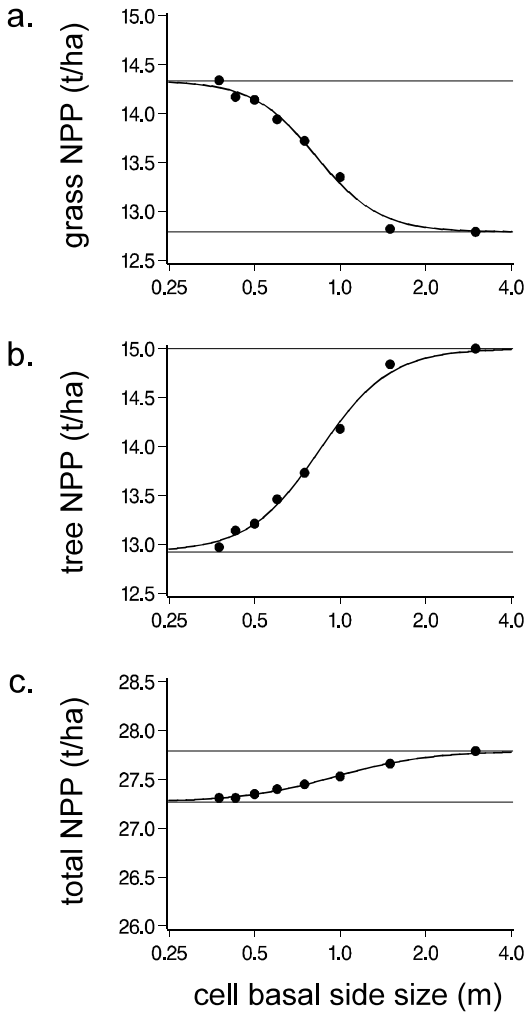

FIG. 6.8 – Effects of cell basal dimensions on (a) grass, (b) trees, and (c) total net primary productions (NPP) simulated over on vegetation cycle (1991). Logarithmic scale is used for cell basal side size. Dots represent simulations, thick lines represent non linear regressions and thin lines are regression asymptots. All figures are at the same scale.

mensions (1.7% variation) (figure 6.8c.). Thus changing cell basal dimensions affected primarily the NPP distribution between the grass and tree components more than the overall production.

In the case of a cell size of 6×6 m, as whole site dimensions were 3×3 m, the system was homogeneous (i.e. one grass layer fully overlapped by one tree layer). When cell size decreases, one can expect model outputs to reach an asymptotic state as the model approaches a cell size of zero (i.e. a continuous description of space). We fitted a logistic curve through non linear regression (PROC NLIN, SAS Inst., 1990) to NPP values as a function of log(cell basal side size). Values of NPP obtained for the maximal cell size (3×3 m) were used as asymptotes for the logistic curves (i.e. top asymptotes for total and tree NPP, basal asymptote for grass NPP). The nonlinear fit algorithm converged in all cases and gave the following estimates for asymptotes corresponding to a cell size

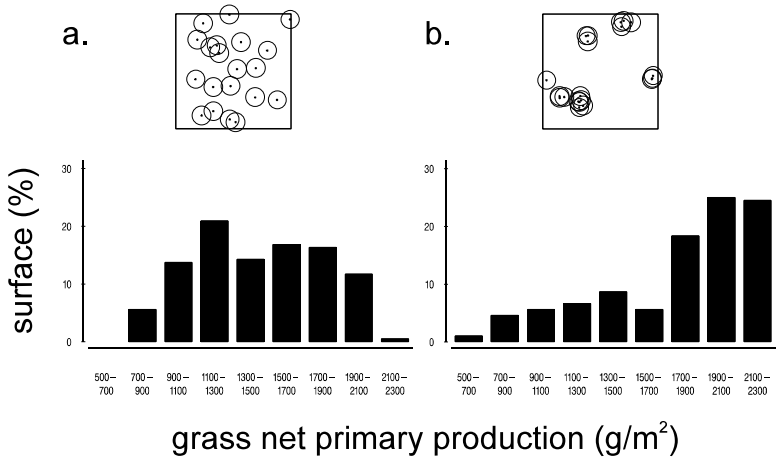

FIG. 6.9 – Differences in the simulated spatial distribution of grass net primary production over one vegetation cycle when trees are (a) randomly distributed, or (b) highly aggregated. Plots above graphs show the sites used for simulations (14×14 m), with their tree spatial distributions. Tree number is 20 and all trees are identical (3.61 m high, canopy area of 4 m^2).

decreasing towards zero : 14.33 $t{\cdot}ha^{-1}$ for grass NPP (corrected R^2=0.99, $F_{3.5}$=8097636, P<0.0001), 12.92 $t{\cdot}ha^{-1}$ for trees (corrected R^2=0.99, $F_{3,5}$=107726, P<0.0001) and 27.25 $t{\cdot}ha^{-1}$ for the total system (corrected R^2=0.99, $F_{3,5}$=93992, P<0.0001). These values are closed to those simulated with a cell size of 0.375×0.375 m.

4.5.Spatial patterns of NPP affected by tree spatial distribution

Figure 6.9 presents the effects of tree spatial distribution on grass NPP spatial heterogeneity. Overall grass production with aggregated trees (17.66 $t{\cdot}ha^{-1}$) was 20% higher than with randomly distributed trees (14.43 $t{\cdot}ha^{-1}$). When trees where randomly located (figure 6.9a), 93% of the site surface showed a grass NPP between 900 and 2100 $g{\cdot}m^2$. When trees where aggregated (figure 6.9b), high grass productions were more frequent : 67% of the surface showed a grass NPP above 1700 $g{\cdot}m^2$. Thus both grass NPP spatial distribution and mean values at the site scale were strongly influenced by tree spatial structure.

5. Discussion

The RATP model and its ability to simulate the distribution of light regime, carbon acquisition and transpiration within plant foliage had already been tested by its authors (Sinoquet et al., 2000). The radiation absorption submodel ability to reproduce grass radiation absorption had also been tested for a savanna grassland at Lamto (Le Roux et al., 1997). The production/water balance module of PEPSEE had been tested for savanna grasslands as well (Le Roux et al., 1996).

Our results showed that the model simulated quite accurately radiation, carbon and water processes. These tests were done with integrative variables (biomass, radiation

absorption, soil water contents, NPP) involving the whole or at least a large part of the processes implemented in the model. In addition, simulations were done using different sites with varying tree spatial structure, making use of available field data for the Lamto savannas. Hence, TREEGRASS appears able to simulate the effects of vegetation structure on NPP and water balance of Lamto savannas, despite the absence of nutrients and rainfall interception, and a simple tree architecture. However, these results also showed that the TREEGRASS model has some limits.

5.1. Plant radiation absorption

Tree PAR absorption efficiency was correctly simulated, except at the beginning of the cycle, for low tree LAI, probably because stems and branches were not represented in the model. In the field, these organs are able to absorb some radiation when leaves are not fully expanded. Jackson et al. (1990) reported a radiation interception efficiency of 0.25 for deciduous oaks without leaves. Stem material of numerous Texas savanna tree species showed a strong absorbance in a PAR spectral range, so that stem surfaces may have increased canopy PAR absorption efficiency by 10-40% when tree LAI was low (Asner et al., 1998a). This could be implemented in the model if reliable and simple data were available on tree architecture in Lamto savannas. Anyway, it was not a major problem in our simulations as radiation absorbed by branches would not have been converted into dry matter, though stems could alter the spatial distribution of radiation absorption. When tree LAI is sufficiently high, this problem can be neglected.

A previous work showed that the radiation absorption submodel had a tendency to overestimate grass PAR absorption at the beginning of the vegetation cycle (data not shown but see Le Roux et al, 1997). This was potentially due to the fact that the grass stratum was assumed to be continuous throughout the year, although the grass layer is composed of tufts that do not fully cover the soil during the first two months of the cycle. The importance of the grass fractional cover could be tested on a pure grass site, by explicitely taking into account grass spatial development at the begining of the cycle.

5.2. Carbon processes

This overestimation of the grass PAR absorption entailed an overestimation of grass production at the beginning of each cycle (figure 6.4).

The simulated reduction of grass NPP under tree clump was slightly higher than that observed in the field, this could be due to the fact that the model did not treat nutrients, as higher nutrient availability is expected under tree cover (Mordelet et al., 1993). As already mentioned, we plan to add nutrient processes in TREEGRASS.

5.3 Water processes

The overestimation of the grass radiation absorption could also be responsible for an underestimation of soil evaporation at the beginning of the vegetation cycle. This effect could explain why TREEGRASS overestimated the soil water content in layer 1 at the beginning of each cycle. Other reasons for this overestimation could be a possible different soil albedo after fire with the presence of ash during 1 to 3 weeks (Le Roux et al., 1994), and a change in the soil surface status at the end of the dry season that

would have increased the runoff. These two possibilities were not computed, sensitivity analyses are needed to test these hypotheses.

The seasonal course of water content in soil layer 2 under a tree clump was not tested because of lack of data. For the same reason, the partitioning of evapotranspiration between evaporation, grass and tree transpiration rates could not be tested. It is clear that it would be interesting to test the model ability to simulate the evaporation rate according to the tree spatial distribution, and the relative importance of tree and grass transpiration rates. In particular, comparing the simulated tree transpiration with measured sap flow rates (e.g. Howard et al., 1997) is needed. Grass transpiration is more difficult to measure : using gas exchange chambers (Tournebize et al., 1996), for instance, can alter the microclimate experienced by grasses.

Finally, it appeared that, despite of the absence of rainfall interception by the foliage, the model correctly simulated the grass behaviour in the absence of trees. A few data are available for rainfall interception by grass at Lamto and could be used to include this process in the model.

5.4. Importance of the size of grid cells

The smaller the cell size, the more accurate the representation of the tree crown shape, and the more accurate the simulation of competition for light. The ideal size would be the one under which there is no variation (in NPP for instance). 0.375×0.375 m was the smallest cell size that a computer could handle for the tests, and it seems that, from the non linear regression fit, it was very close to the ideal cell size. For larger sites, like those presented in Figure 6.9, with sizes compatible with the scale of an ecosystem study, the cell size limit for computers became 1×1 m. 1×1 m was thus applied to all test simulations as an acceptable compromise between precision and computer requirements. This does not mean that plots used for simulations should be small. The maximum plot size depends mainly on the type of vegetation : the more dense the vegetation, the higher the number of vegetation cells, and the longer the simulations.

5.5. Spatial heterogeneity of grass NPP and tree spatial distribution

Due to their size, trees have first access to light. When trees were aggregated, there were larger open areas, i.e. more grass surface where there was no or little tree influence. These open areas showed a high grass NPP. On the opposite, a random distribution was associated with more isolated trees, and thus entailed stronger interactions between trees and grasses. These results emphasize the interest to study effects of the vegetation spatial structure on radiation, carbon, and water fluxes. Knowing when fine tree spatial structure needs to be considered for the functioning of an ecosystem is one important purpose of TREEGRASS.

6. Conclusion

Tests described in this paper and using a 1x1m resolution were conclusive :

1. Seasonal variations in biomass, necromass and soil water contents in layers 1 and 2 were satisfactorily simulated by the model in the case of a pure grass site ;

2. Primary production values computed by the model were consistent with values reported in the literature ;

3. The model correctly simulated the seasonal course of the soil water content in layer 1 under tree clump ;

4. Tree PAR absorption efficiency was also correctly simulated.

As already mentioned, the model described in this paper must be considered as a first version. In the near future, we plan to add mechanistic computations for nitrogen processes, photosynthesis and a better tree architecture, in order to build a complete mechanistic model able to simulate daily savanna functioning. Breshears et al. (1997) found that, in New Mexico semiarid woodlands, two different tree species exploited soil water differently. A similar conclusion was raised by Le Roux and Bariac (1998) at Lamto. Other studies showed that grass species composition can be different under tree cover or in open areas (e.g. Belsky et al., 1993 ; Scholes and Archer, 1997). Thus, it appears necessary to introduce more species in our simulations, in order to account for functional diversity.

In the near future, TREEGRASS will be used to assess (1) the influence of tree spatial structure on total carbon and water fluxes at the site level (which is currently under progress) ; (2) the spatial and temporal distributions of production and water fluxes between individuals ; (3) the effects of different tree types (e.g. deciduous vs. evergreen, deep-rooted vs. shallow-rooted) on tree/grass interactions.

Acknowledgements

This work was supported by the European Terrestrial Ecosystem Modelling Activity (ETEMA) and by the Programme National de Recherche en Hydrologie (grant 99-PNRH 14, publication #189).

Chapitre 7

Seconde version de TREEGRASS

A model to predict 3D water balance and gross and net primary productions in tree/grass ecosystems, accounting for biodiversity and spatial vegetation structure

en préparation

G. Simioni, J. Gignoux/X. Le Roux

Introduction

Tree/grass systems exist as natural savannas, and as anthropogenic systems like orchards or silvo-pastoral systems. They are characterised by the coexistence of a continuous grass layer and a discontinuous tree layer. They occupy a large fraction of terrestrial surfaces (20% for savannas alone, Scholes and Hall 1996). They are very complex to study because of the spatial heterogeneity of their structure and function (Scholes and Archer 1997). and the occurrence of intense perturbations that are herbivory and fire (Frost et al. 1986). Tree/grass coexistence has received a lot of attention (e.g. Walker and Noy-Meir 1982, Gignoux 1994, Jeltsch et al. 1996). On the opposite, the influence of savanna particular structural features on annual carbon and water functioning have not been comprehensively studied so far. In particular, the tree/grass ratio (e.g. Scholes and Hall 1996, Simioni et al. 2001e), and the tree layer spatial structure (Simioni et al. 2001b) are strongly suspected to influence ecosystem net primary production (NPP). Functional diversity may also be an important aspect of savanna functioning. For instance, two coexisting tree species of the Lamto savannas (Ivory Coast) have different water uptake behaviours (Le Roux and Bariac 1998), production efficiencies (Simioni et al. 2001e), and phenologies (Simioni et al. 2001c).

While many studies attest the complexity of savannas, a rising opinion is that modelling may be the best approach to study tree/grass system complexity (Scholes and Archer 1997, Jeltsch et al. 1996). Different models were developed to study tree/grass coexistence (e.g. Eagleson and Segarra 1985 ; Jeltsch et al. 1996), landscape dynamics (the SAVANNA model, Coughenour 1994), long term carbon sequestration (Daly et al. 2000), or silvo-pastoral production (the GRASP model, McKeon et al. 1990, the ALWAYS

model, Berjez et al. 1999). But none of these approaches allows to study savanna fine spatial structure at an annual time scale.

Simioni et al. (2000) presented the three dimensioned (3D) TREEGRASS model. It was an original, spatially explicit model to study plant interactions in tree/grass systems. While this model was able to simulate mechanistically competition for light and water between plant individuals, it had several weak points. Its parameterisation suffered from a lack of data for trees and was limited to study one grass and one tree species at a time. Its representation of plant production lacked physiological detail, and did not account for nitrogen effects. And field data used to test the model did not allow a real spatial validation.

In this paper, we extended the TREEGRASS model. New features are C_3 and C_4 photosyntheses, leaf characteristics acclimation to leaf local radiation regime, and the possibility to account for several species at a time. This model was parameterised using recent field data sets. Model outputs were compared to original data sets, specifically collected to allow a spatial test of the model.

In the next sections, the description of the new version of the TREEGRASS model, TREEGRASS-2, its parametrisation for the Lamto savannas and its tests against field data are presented. The accuracy of the model to predict savanna carbon and water fluxes is discussed.

Model structure

Model overview

The main features of TREEGRASS-2 are (Figure 7.1) (new features appear in bold) :

1. TREEGRASS-2 simulates ecosystem production and evapotranspiration at the plant individual scale, and at an infra daily time step over one vegetation cycle.
2. Plant individual foliage and root system are represented in three dimensions (3D) within a 3D grid of cells. **Different tree and/or grass species can be represented at a time.**
3. A 3D radiation absorption is computed for PAR and infrared radiation, accounting for diffuse radiation and for reflections and transmissions by leaf and soil surfaces.
4. A 3D energy budget allows to estimate plant transpiration and soil evaporation.
5. **Plant photosynthesis is computed according to Farquhar et al. (1980) or Collatz et al. (1992) given each plant metabolic type (C_3 or C_4, respectively). Carbon losses through respiration and root exudates are computed as species specific fractions of gross photosynthesis.**
6. Carbon allocated to roots increases when the plant undergoes water stress.
7. **Tree leaf area index (LAI) is prescribed with measured data.** Grass leaf growth results from carbon allocated to leaves and leaf mortality rate.
8. **The model accounts for the temporal course of tree leaf traits : specific leaf area (SLA, $\mathbf{cm^2 \cdot g^{-1}}$), leaf nitrogen concentration (N) and leaf nitrogen per unit leaf area (N_a, $\mathbf{g \cdot m^{-2}}$). It also reproduces SLA, and N_a acclimation to local light environment.**

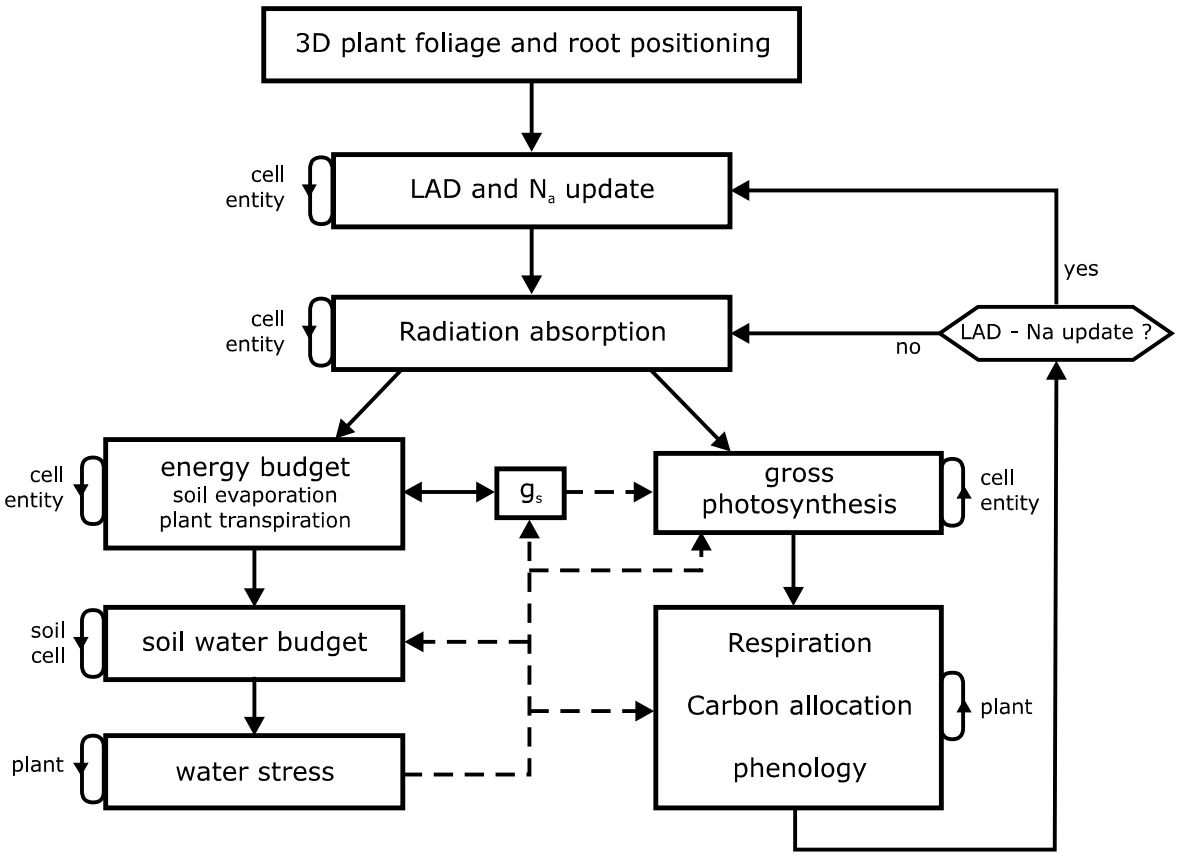

FIG. 7.1 – Main processes computed in TREEGRASS-2. Plain lines correspond to the flow chart. Dashed lines represent effect of water stress occurring the following time step. Loop level is indicated (plant, soil cell, or entity in each 3D grid cell, i.e. leaf type or soil surface). Leaf area density (LAD) and leaf nitrogen per unit leaf area (N_a) are updated in the 3D cell grid when a threshold variation has occurred.

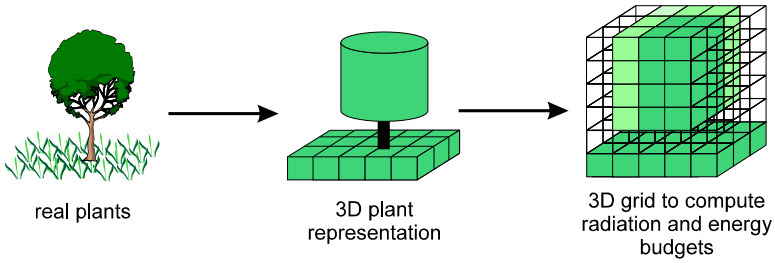

FIG. 7.2 – Spatial representation of plants in TREEGRASS (redrawn from Simioni et al. 2000). The second picture shows the simple plant structural features used to represent trees (i.e. simple cylindrical crown, crown radius, and total height and bole height). Though they do not appear on this figure, roots are represented in a similar way. the third picture represents the 3D grid used to compute the spatial distribution of plant foliage as used by the radiation/energy budget submodel (different levels of green correspond to different values of leaf area density (LAD)). Tree LAD is distributed using overlap coefficients between tree crown and cell volumes.

9. Plant transpiration is extracted from the soil according to root spatial location, and species vertical water extraction patterns. A soil water budget computes runoff and drainage. Soil water content determines plant water stress according to species specifications. Water stress decreases plant transpiration, photosynthesis and transfers plant water extraction to deep soil.
10. Fire occurs at fixed dates, removes all grass standing biomass and necromass, and makes all remaining tree leaves to fall.

Spatial representation

Space is represented as a three dimensioned grid of rectangular cells (Figure 7.2). Plant foliage is distributed within aboveground cells, plant roots are distributed within belowground cells. Branches and trunks are not explicitely represented. Grid horizontal precision and depths of vertical cell layers can be adjusted to fit with plant dimensions, but cell dimensions are fixed for a whole simulation. Cells containing plant foliage elements will be referred to as “vegetation cells”.

Individual plants are represented (Figure 7.2). A grass individual is assimilated to a grass pixel : it occupies one vegetation cell, and its roots are located in soil cells underneath. Thus the number of grass “individuals” depends on the number of cells in a horizontal section of the cell grid. There is no overlap between grass pixels.

A tree individual is characterised by its foliage and its root system. The foliage of an individual tree is assimilated to a cylinder in which leaf density is homogeneous. Tree total height, bole height (lower limit of foliage), and foliage crown radius are governed by allometric relations. Similarly, the root system of a tree is assimilated to a cylinder which depth is species dependent, and radius is determined by allometry with tree aboveground dimensions.

Tree foliage and roots are distributed in the vegetation and soil cells that overlap with foliage and root crowns. The fraction of a tree foliage or root that is placed in a given vegetation or soil cell is proportionned to the overlap between foliage or root crown

and the vegetation or soil cell. A tree can overlap with grasses and with other trees (i.e. share vegetation and soil cells).

For all grass and tree species, coarse and fine roots are ont differentiated.

To avoid side effects, the model assumes that the simulated plot is wrapped around.

Light absorption

The radiation absorption submodel was adapted from the RATP model of Sinoquet et al. (2001). Rays from several directions are directed into the cell grid. When a ray passes through a cell, it is attenuated following Beer's law, depending on the leaf area density (LAD), on leaf optical properties, and on the angular distribution of the vegetation entities (i.e. types of leaves : green or dead leaves of distinct species) present in the cell. Intercepted radiation is shared between these entities, assuming that the leaves are randomly and uniformly distributed. Light interception by twigs and branches is neglected.

Radiation interception computed for each ray is used to calculate exchange coefficients between sources and receptors. Sky, foliage and soil are both sources (respectively of direct and diffuse radiation, and of transmitted or reflected radiation) and receptors. For one day, five representative sun directions are computed (corresponding to daytime 6, 9 and 12 A.M., and 3 and 6 P.M.). These directions vary with the day of year and latitude. For diffuse and reflected radiation, the direction space is divided into solid angles, centered around representative heights and azimuths. Incident diffuse radiation is calculated assuming a standard overcast sky luminance distribution (Moon and Spencer, 1942). Sources of reflected radiation are calculated considering that reflections and transmissions are isotropic and depend only on the angular distribution of organs. Exchange coefficients between a source and a receptor are built in a progressive manner, adding the contribution of beams coming from the source when they meet the receptor.

These exchange coefficients are first calculated for diffuse and scattered radiation (depending thus only on the foliage characteristics and on the sky luminance distribution). For direct radiation, additional exchange coefficients are then computed for each time step, i.e. each sun direction. To save calculation time, exchange coefficients are computed only when a significant change in LAD (e.g. we used a threshold of 10%) of at least one individual has occurred.

Radiation fluxes intercepted by each entity in each cell are computed by using the radiosity method (Ozisik, 1981) : the flux intercepted by a given receptor is a linear combination of fluxes coming from the whole set of sources weighed by the exchange coefficients between the sources and the receptor. Intercepted fluxes (including multiple scattering) are thus written as a system of linear equations. Solving this system allows us to calculate radiation fluxes. Details on the calculation can be found in Sinoquet et al. (2001).

In addition, a sky openness index (fraction of sky not obstructed by upper foliage elements) is computed for each vegetation cell. It corresponds to the fraction of sun rays coming from all sky directions that reach the top section (top sky openness) or the bottom section (bottom sky openness) of a given vegetation cell. The computed sky openness can be compared to field estimates of sky openness (e.g. provided by hemispherical photographs).

Transpiration and evaporation

As in the first version of TREEGRASS, the energy budget is computed in three dimensions to determine, for each entity in each cell, the organ temperature that balances fluxes of received and lost heat :

$$R_{n_{jk}} - H_{jk} - E_{jk} = 0 \tag{7.1}$$

where $R_{n_{jk}}$ is the net radiation absorbed by entity j in cell k, and H_{jk} and E_{jk} are sensible and latent heat fluxes lost by entity j in cell k. Energy budgets are established for shaded and sunny surfaces. Energy storage by the plant is neglected. Net radiation absorption includes net balance for photosynthetically active radiation (Q), near infra-red radiation (NIR), and thermal infra-red radiation (TIR) emitted by leaves and soil. For instance, net radiation absorption by the sunny surface e of entity j in cell k can be written :

$$R^e_{n_{jk}} = I^e_{jk}(Q) + I^e_{jk}(NIR) + I^e_{jk}(TIR) - 2 \cdot \sigma \cdot (T^e_{jk})^4 \tag{7.2}$$

where $I(Q)$ and $I(NIR)$ are Q and NIR fluxes calculated by the radiation absorption submodel, $I(TIR)$ is the TIR absorbed by entity j in cell k, and the last term represents TIR emitted by the entity surface : T_{jk} is the surface temperature of entity j in cell k, and σ is the Stephan-Boltzman constant ($5.67 \cdot 10^{-8}$ W·m^{-2}·s^{-1}·K^{-4}). Sensible heat flux can be written :

$$H^e_{jk} = \rho \cdot C_p \cdot g_b \cdot (T^e_{jk} - T_a) \tag{7.3}$$

where ρ, C_p, and g_b are respectively the air density (kg·m^{-3}), the air specific heat (J·kg^{-1}·K^{-1}) and the aerodynamic conductance (m·s^{-1}) that depends on wind speed ; T_a is the air temperature and T^e_{jk} is the sunny surface temperature of entity j in cell k. Similarly, the latent heat flux can be expressed as :

$$E^e_{jk} = (\rho \cdot \frac{C_p}{\gamma}) \cdot g_w \cdot (e^e_{sjk} - e_a) \tag{7.4}$$

where parameters γ and g_w are the psychrometric constant (Pa·K^{-1}) and the leaf conductance (m·s^{-1}), respectively, e^e_{sjk} is the saturating vapour pressure at temperature T^e_{jk} estimated with the Tetens formula (1930), and e_a is the air water vapour pressure.

g_w is the combination of aerodynamic and stomatal conductances of lower and upper leaf surfaces (g^e_s and g^e_{ss}). These conductances depend on microclimatic factors. In this work, leaves are hypostomatous, g_{ss} is considered as nil, and the model proposed by Jarvis (1976) is used to compute g_s :

$$g^e_s = g_{sref} \cdot f_{VPD_l} \cdot f_Q \cdot f_{SI} \tag{7.5}$$

where g_{sref} is the reference stomatal conductance as a function of leaf nitrogen, f_Q is the response of the g_s/g_{sref} ratio to Q, f_{VPD_l} is the response of g_s/g_{sref} to vapour pressure deficit at leaf surface (VPD_l), and f_{SI} is the response of g_s/g_{sref} to water stress.

Similarly, an energy budget for each soil cell of the top soil layer is calculated taking into account a conductive heat flux G into the soil :

$$R_{n_{ks}} - G_{ks} = E_{ks} + H_{ks} \tag{7.6}$$

where G_{ks} is calculated as a fraction of $R_{n_{ks}}$ in soil cell ks, according to vegetation phenology (Le Roux, 1995). As for leaves, solving the soil energy budget requires the determination of the soil aerodynamic resistance and the soil surface resistance to water vapour transfer. The former depends on wind speed while the later depends empirically on the quantity of water evaporated since last rain from the upper soil layer (Amadou, 1994).

The overall energy budget for sunny and shaded surfaces of each entity j in each cell k (including soil cells) yields an equation system in which surface temperatures are the unknowns. The energy budget is solved using the Newton-Raphson algorithm by successive iterations. Further details are given by Sinoquet et al. (2001).

Evaporation, transpiration and absorbed Q obtained for each entity in each cell are summed up to calculate daily soil evaporation, and individual plant transpiration and absorbed Q.

Photosynthesis

Photosynthesis is computed for each leaf entity in each vegetation cells at each sun position for each time step using a photosynthesis submodel according to the metabolic pathway (C_3 or C_4). The C_3 and C_4 photosynthesis models correspond to those of Farquhar et al. (1980) and Collatz et al. (1992), respectively.

The C_3 photosynthesis model

In the model of Farquhar et al. (1980), according to the version proposed by Harley et al. (1992) (but without including the potential limitation due to the use of triose phosphate), net CO_2 assimilation rate A_n (μmol $CO_2 \cdot$ m$^{-2}\cdot$s^{-1}) is expressed as :

$$A_n = (1 - \frac{0.5 \cdot O}{\tau \cdot C_i}) \cdot min(W_c, W_j) - R_d \tag{7.7}$$

where W_c (μmol $CO_2\cdot$m$^{-2}\cdot$s^{-1}) is the carboxylation rate limited by the amount, activation state or kinetic properties of Rubisco, W_j (μmol $CO_2\cdot$m$^{-2}\cdot$s^{-1}) is the carboxylation rate limited by the rate of RuP_2 regeneration, τ is the specificity factor for Rubisco (Jordan and Ogren 1984), R_d (μmol $CO_2\cdot$m$^{-2}\cdot$s^{-1}) is the rate of CO_2 evolution in light that results from processes other than photorespiration, and O and C_i (Pa) are the partial pressures of O_2 and CO_2 in the intercellular air spaces, respectively.

W_c follows competitive Michaelis-Menten kinetics with respect to O_2 and CO_2 :

$$W_c = V_{cmax} \cdot \frac{C_i}{C_i + K_c \cdot (1 + \frac{O}{K_o})} \tag{7.8}$$

where V_{cmax} (μmol $CO_2\cdot$m$^{-2}\cdot$s^{-1}) is the maximum rate of carboxylation, and K_c and K_o (Pa O_2 and Pa CO_2) are Michaelis constants for carboxylation and oxygenation, respectively.

W_j is controlled by the rate of electron transport J (μmol$\cdot$m$^{-2}\cdot$s^{-1}) :

$$W_J = J \cdot \frac{C_i}{4 \cdot (C_i + \frac{O}{\tau})} \tag{7.9}$$

J depends on photosynthetically active photon flux density Q (μmol·m^{-2}·s^{-1}) :

$$J = \alpha \cdot \frac{Q}{\sqrt{1 + \frac{\alpha^2 \cdot Q^2}{J_{max}^2}}} \tag{7.10}$$

where J_{max} (μmol·m^{-2}·s^{-1}) is the light-saturated rate of electron transport, and α is the apparent efficiency of light energy conversion on an incident light basis (mol electrons per mol photons). The temperature dependence of R_d, τ, K_c, and K_o is described by :

$$(R_d,\, \tau,\, K_c,\, K_o) = e^{c - \frac{\Delta H_a}{R \cdot T_l}} \tag{7.11}$$

where ΔH_a (j·mol^{-1}) is the activation energy of the given parameter, R (8.3143 J·K^{-1}·mol^{-1}) is the gaz constant, T_l (K) is leaf temperature, and c is the dimensionless, scaling constant of the given parameter. Similarly, the temperature dependence of V_{cmax} and J_{max} is described by :

$$(V_{cmax},\, J_{max}) = \frac{e^{c - \frac{\Delta H_a}{R \cdot T_l}}}{1 + e^{\frac{\Delta S \cdot T_l - \Delta H_d}{R \cdot T_l}}} \tag{7.12}$$

where ΔS (J·K^{-1}·mol^{-1}) is an entropy term, and ΔH_d (J·mol^{-1}) is the deactivation energy of the given parameter. To account for the linear relationships commonly observed between leaf photosynthetic capacities and leaf nitrogen per unit leaf area N_a (g N·m^{-2}), the scaling factors c for V_{cmax}, J_{max}, and R_d are linearly related to $ln(N_a)$ as :

$$c = a_N + b_N \cdot ln(N_a) \tag{7.13}$$

The C_4 photosynthesis model

The C_4 photosynthesis model used to derive parameters from gas exchange measurements is the simplified model of Collatz et al. (1992).

Gross photosynthesis A is given as a function of Q, C_i, and T_l in a form of a pair of nested quadratic equations. The first equation is :

$$\theta \cdot M^2 - M \cdot (V_T + \alpha \cdot Q) + V_T \cdot \alpha \cdot Q = 0 \tag{7.14}$$

where V_T (μmol CO_2·m^{-2}·s^{-1}) is the temperature-dependent, substrate saturated rubisco capacity, α is the quantum efficiency, M (μmol CO_2·m^{-2}·s^{-1}) is the flux determined by the rubisco and light limited capacities, and θ is a curvature parameter that gives a gradual transition between Q and V_T limited fluxes. The limitation on the overall rate by M and the CO_2 limited flux is expressed likewise :

$$\beta \cdot A^2 - A \cdot (M + k_T \cdot \frac{C_i}{P}) + M \cdot k_T \cdot \frac{C_i}{P} = 0 \tag{7.15}$$

where k_T (μmol $CO_2 \cdot m^{-2} \cdot s^{-1}$) is the temperature-dependent pseudo-first order rate constant with respect with C_i, P is the atmospheric pressure (Pa), and β is analogous to θ and specifies the degree of co-limitation between M and the CO_2 limited flux. The smaller roots are the appropriate solutions for both quadratics. A_n is defined as :

$$A_n = A - R_T \tag{7.16}$$

where R_T is the temperature-dependent rate of leaf respiration.
Temperature dependencies follows :

$$V_T = \frac{V_{max} \cdot Q_{10-V_{max}}^{\frac{T_l-25}{10}}}{(1+e^{0.3\cdot(13-T_l)}) \cdot (1+e^{0.3\cdot(T_l-36)})} \tag{7.17}$$

$$R_T = \frac{R_d \cdot Q_{10-R_d}^{\frac{T_l-25}{10}}}{1+e^{1.3\cdot(T_l-55)}} \tag{7.18}$$

$$k_T = k \cdot Q_{10-k}^{\frac{T_l-25}{10}} \tag{7.19}$$

where $Q_{10-(V_{max},R_d,k)}$ are proportional increase of V_T, R_T, and k_T respectively, with a 10°C increase in temperature, T_l (°C) is leaf temperature, and V_{max}, k, and R_d are reference values for V_T, k_T, and R_T. Similarly to the C_3 photosynthesis model, V_{max}, k, and R_d can be related to N_a.

Coupling photosynthesis and stomatal conductance

Both C_3 and C_4 photosynthesis models are solved by coupling photosynthesis and stomatal conductance using the relation :

$$A_n = g_s \cdot \frac{1000}{1.6} \cdot \frac{C_s - C_i}{P} \tag{7.20}$$

where C_s is the air CO_2 concentration at leaf surface (Pa).

Photosynthesis inhibition by water stress

g_s reduction in case of water stress affects photosynthesis, but photosynthesis inhibition can also occur independently of stomatal closure for severe water stress (Chaves et al.).Non stomatal effects on photosynthetis were crudely implemented via a photosynthesis inhibition factor (PIF) that depends on the cumulative, multiplicative water stress since the plant is under water stress :

$$PIF = 10 \cdot \prod_t f_{SI_t} \tag{7.21}$$

The 10 value allows photosynthesis to be reduced by 50% in case of a constant f_{SI} value of 0.9 during 28 days, or a constant f_{SI} value of 0.5 during 4 days, or a constant f_{SI} value of 0.1 during less than 2 days.

Net carbon assimilation

For each plant, whole plant gross photosynthesis (GP_n) is computed as the sum of gross photosynthesis (A_n plus leaf respiration) for each vegetation cell where plant leaves are present.

Total plant respiration is computed simply as a constant, species dependent, fraction of gross photosynthesis (R_{coeff}). Thus whole plant net photosynthesis is :

$$NP_n = GP_n \cdot (1 - R_{coeff}) \tag{7.22}$$

This follows the opinion of Landsberg and Waring (1997) that computing respiration as a fixed fraction of gross photosynthesis would entail less errors than more detailed respiration models. This constancy of the carbon use efficiency is also supported by studies of Dewar (1996) and Dewar et al. (1998). Though most field estimations are for yearly production (Waring et al. 1998), results of Dewar (1996) and Dewar et al. (1998) theoretically apply for daily timesteps, at least when foliage is completely developed. The respiration coefficient also includes loss of carbon through root exudation, that can represent a substantial fraction of gross photosynthesis (Lynch and Whipps 1990, Johansson 1992).

Allocation

The proportion of NP_n allocated to shoots (η_s) is given by the empirical relation proposed by Landsberg and Waring (1997) :

$$\eta_s = 1 - \frac{\alpha_\eta}{1 + \beta_\eta \cdot f_{SI}} \tag{7.23}$$

For example, with $\alpha_\eta = 0.6$ and $\beta_\eta = 0.5$, a plant allocates 60% of carbon to shoots when $f_{SI} = 1$. This fraction decreases to 40% when the water stress is maximum ($f_{SI} = 0$). Such an effect of drought on root/shoot allocation has been reported in field studies (e.g. Durand et al. 1989) and is in accordance with the functional equilibrium theory (Brouwer 1983).

Grass foliage growth

Once net assimilated carbon has been allocated between shoots and roots, it is converted into dry matter depending on the organ fractional carbon content :

$$NPP_i = \frac{NP_{n_i}}{C_{content_i}} \tag{7.24}$$

where NPP_i (g dry matter) and $C_{content_i}$ are net primary production and fractional carbon content of organ i, and NP_{n_i}, is net photosynthesis allocated to organ i.

For each grass individual, variations in aboveground biomass and necromass are computed as (Le Roux, 1995) :

$$\begin{aligned} B_{l_t} &= B_{l_{t-1}} \cdot (1 - \Gamma_M) + NPP_{leaf} \\ N_t &= N_{t-1} \cdot (1 - \Gamma_D) + B_{l_{t-1}} \cdot \Gamma_M \end{aligned} \tag{7.25}$$

where B_l and N are above ground biomass and necromass (g·m^{-2}), Γ_M and Γ_D are above ground mortality and decomposition rates (g·g^{-1}·day^{-1}), and t is time (days). Based on field data for grasses, above ground mortality and decomposition rates are assumed to be zero after fire until grass individual LAI reaches 1, and constant afterwards (Le Roux, 1995). Grass green LAI is computed according to SLA values decreasing with increasing grass biomass values. A constant SLA is used for grass dead leaves.

N is computed empirically from field measurements. N_a is the ratio of N to SLA.

Tree foliage growth

Tree individual LAI is forced using field data (see parameterisation section), and assuming that all the remaining green leaves fall after fire occurrence. TREEGRASS-2 accounts for leaf acclimation to local radiation regimes.

At a given time step, leaf area density (LAD_t) is assumed constant throughout the whole canopy of a given tree individual. For each tree, it corresponds to the ratio of the LAI to the canopy depth. Leaf area LA_{it} at time t in cell i occupied by the foliage corresponds to :

$$LA_{it} = LAD_t \cdot V_i \tag{7.26}$$

where V_i is the volume shared by the tree canopy and cell i (overlap volume between tree foliage crown and vegetation cell i) where its foliage is present.

Leaf biomass is computed as :

$$B_{lt} = \sum_i \frac{LA_{it}}{SLA_{it}} \tag{7.27}$$

where SLA_{it} is the specific leaf area at time t in cell i where the tree foliage is present. SLA_{it} is computed as :

$$SLA_{it} = f_t \cdot f_{open} \tag{7.28}$$

where f_t is temporal variation of SLA since leaf flush, f_{open} is spatial variation of SLA with the mean sky openness of the corresponding entity in cell i (mean of top and bottom sky opennesses), as suggested by Simioni et al. (2001c).

As for grasses, N is computed empirically from field measurements, and, for each cell i, $N_{a_{it}}$ is the ratio of N to SLA_{it}.

As tree LAI is prescribed, leaf NPP is computed as the variation in leaf biomass (as long as LAI increases) :

$$NPP_{leaf} = B_{l_t} - B_{l_{t-1}} \tag{7.29}$$

Leaf NPP is nil if tree LAI decreases.

The corresponding assimilated carbon allocated to leaves is :

$$LeafC = NPP_{leaf} \cdot C_{content_{leaf}} \tag{7.30}$$

Carbon allocation to other organs is done as :

$$\begin{aligned} BranchC &= \eta_s \cdot NP_n - LeafC \\ RootC &= (1-\eta_s) \cdot NP_n \end{aligned} \tag{7.31}$$

If carbon allocated aboveground or even total assimilated carbon cannot fulfill leaf growth, the excess carbon needed by the leaf compartment is assumed to be taken from carbohydrate reserves. In such a case, it is assumed that branches and roots provide these reserves in equal proportions. The implicit reserve pool is replenished later in the year, when maximum LAI has been reached.

$BranchC$ and $RootC$ are converted into dry matter using branch and root specific carbon content values.

Soil water budget

Soil is divided into three strata, an upper layer (layer 1, the depth of which is defined so that this layer includes 90% of the grass roots), the layer 2 (down to the maximum plant rooting depth), plus the deep soil underneath.

Soil water extraction

Water evaporated from the soil is extracted from the upper layer cells. Water transpired by each individual is extracted from the soil cells occupied by the plant roots, using overlap coefficients between volumes of soil occupied by roots and soil cell volumes. The total transpiration T is extracted from layer 1 (T_1) and from layer 2 (T_2) for an individual ; values for T_1 and T_2 depend on the water stress index and are calculated as :

$$\begin{aligned} \frac{T_1}{T} &= (\frac{T_1}{T})_{max} \cdot f_{SI} \\ T_2 &= T - T_1 \end{aligned} \tag{7.32}$$

where $(\frac{T_1}{T})_{max}$ is a species specific parameter : the fraction of the plant total transpiration extracted in layer 1 under non-limiting water conditions.

Run-off and drainage

Run-off occurs if precipitation exceeds a threshold value and if the total LAI is below a threshold value. Drainage occurs from layer 1 to layer 2, and from layer 2 to deep soil when the soil water content of a given layer exceeds field capacity.

Water stress

In the model, for each plant, the stress index depends on the soil water content in the soil layer for which the species is sensible. Some species will be sensitive to soil water content in the upper layer, some to the soil water content in the whole soil column. Each soil cell in layer i (i can combine the two soil layers) has a corresponding stress index :

$$R_i \leq R_{l_i} \qquad f_{SI} = \frac{R_i - R_{wp_i}}{R_{l_i} - R_{wp_i}} \tag{7.33}$$

$$R_i > R_{l_i} \qquad f_{SI} = 1 \tag{7.34}$$

where R_i and R_{l_i} are the actual and threshold values of soil water content in layer i, and R_{wp_i} is the soil water content of layer i at wilting point.

A grass individual has its roots in only one soil pixel, its water stress index is thus determined by the water content in this pixel. On the opposite, the stress index for a tree individual is a combination of the stress indices of the different pixels where its roots are present. All soil pixels occupied by roots of a given tree contribute to its stress index in proportion to overlaps between the root crown volume and soil cell volumes.

Fire

Fire occurs at a prescribed date, according to field obervations. To avoid to model the kinetics of the allocation from roots to shoots after fire for grasses (Le Roux et al., 1997), leaf biomass is initialised to a minimum value, as proposed by Ciret et al. (1999).

Model tests for a West African savanna

The model was parameterised for the West african savanna of Lamto (Ivory Coast), and tested against field data collected during the 2000 vegetation cycle.

Parameterisation

Study site

The natural reserve of Lamto is located in Ivory Coast (6°13'N, 5°02'W). Mean monthly temperatures are constant throughout the year (27°C). Rainfall averages 1200 mm·y^{-1} and determines dry seasons (from November to March, and in August) and rainy seasons (from April to July, and from September to October). Soils are ferralsol (according to the FAO classification). Forests are present along streams, but most of the reserve is covered by savanna areas. In the savanna, the herbaceous layer is composed of perennial grasses mostly from the Andropogoneae family. Tree density varies along the catena, from almost pure grassland in bottomlands to dense shrub facies on plateaus. Trees are mainly composed of four species and can be found aggregated in clumps or isolated. Fire is set every year in early January and delimits the vegetation cycle.

Climatic data

Climatic data for the 2000 vegetation cycle (January 2000 to January 2001) were provided by the Lamto geophysical station. Global radiation, rainfall, wind speed, air temperature and air humidity were used as input variables. Atmospheric radiation was assumed to be constant. Basic radiation parameters are presented in Table 7.1. The model uses subdaily data of air temperature and humidity, corresponding to five sun positions, to account for daily variations. Daily global radiation is partitioned into the five sun positions assuming a sinusoidal evolution of global radiation during the day. Q and diffuse radiation are assumed constant fractions of global radiation. Wind speed was assumed constant throughout the day.

TAB. 7.1 – Radiation paramaters for the Lamto site.

Parameters	Values	References
PAR/global radiation ratio	0.48	Le Roux et al. 1997
Diffuse/global radiation ratio	0.60	Gauthier 1993
Atmospheric radiation ($W \cdot m^{-2}$)	350	Le Roux 1995
Leaf angular distribution		
Grass living leaves	erectophile	Le Roux et al. 1997
Grass dead leaves	planophile	Id.
Tree leaves	spherical	NA
PAR absorbances		
Ground	0.76	Le Roux et al. 1997
Grass living leaves	0.78	Id.
Grass dead leaves	0.35	Id.
Tree leaves	0.78	NA
PIR absorbances		
Ground	0.50	Le Roux et al. 1997
Grass living leaves	0.04	Id.
Grass dead leaves	0.05	Id.
Tree leaves	0.10	NA

NA : not available

Modelled plant species

Perennial grass species represent more than 80% of grass standing mass at Lamto (Le Roux 1995), and have similar N values (Abbadie 1984), photosynthetic capacities and stomatal behaviour (Le Roux and Mordelet 1995, Simioni et al. 2001e). Thus a generic grass was considered in the model, using common parameters measured on two species of the Andropogoneae family : *Hyparrhenia diplandra* and *Andropogon canaliculatus*. The two tree species are *Crossopteryx febrifuga* and *Cussonia arborea*. These two species present constrasting water extraction patterns (Le Roux and Bariac 1998), leaf gas exchange characteristics (Simioni et al. 2001e) and phenologies (Simioni et al. 2001c).

Tree allometry

The two tree species have similar allometric features. Each tree is characterised by its location (spatial position of the trunk), its total height (H_t m), and cylindrical leaf and root crown shapes. The basal leaf canopy surface (CS m^2) is given as (Gignoux, regression based on unpublished data) :

$$CS = 0.4372 \cdot H_t^{1.7228} \tag{7.35}$$

Bole height (height of the canopy bottom) is assumed to be half of H_t. Root crown radius (RCR m) depends on leaf crown radius (RC m), as suggested by Mordelet (1993) :

$$RCR = 1.5 \cdot RC \tag{7.36}$$

Tree architecture is assumed to be fixed during a vegetation cycle (i.e. fixed foliage and crown dimensions).

Leaf traits

Grass green LAI (LAI) is computed from leaf biomass B_l according to measured specific green leaf area (Le Roux 1995) :

$$LAI = (128 - 62 \cdot (1 - e^{-0.0102 \cdot B_l})) \cdot B_l \cdot 10^{-4} \tag{7.37}$$

Grass dead LAI depends on leaf necromass with a constant SLA of 144 cm^2·g^{-1}. When leaf mortality occurs, the rate of mortality Γ_M is 0.012 d^{-1}, and the rate of necromass decomposition Γ_D is 0.015 d^{-1}.

Temporal variations of minimal tree SLA (f_t) were empirically computed as (from data in Simioni et al. 2001c) :

$$\begin{array}{lrcl} C.febrifuga : & f_t & = & 155.024073 - 16.728854 \cdot ln(t) \\ C.arborea : & f_t & = & 144.488353 - 10.559472 \cdot ln(t) \end{array} \tag{7.38}$$

where t is time since leaf flush for the considered tree individual. Arbitrarily, leaf flush of a given tree occurs when its LAI reaches 0.15. Spatial variation of SLA with sky openness is computed as (Simioni et al. 2001c) :

$$\begin{array}{lrcl} C.febrifuga : & f_{open} & = & e^{5.710 - 0.356 \cdot ln(open)}/60.3 \\ C.arborea : & f_{open} & = & e^{4.964 - 0.007 \cdot open}/74.6 \end{array} \tag{7.39}$$

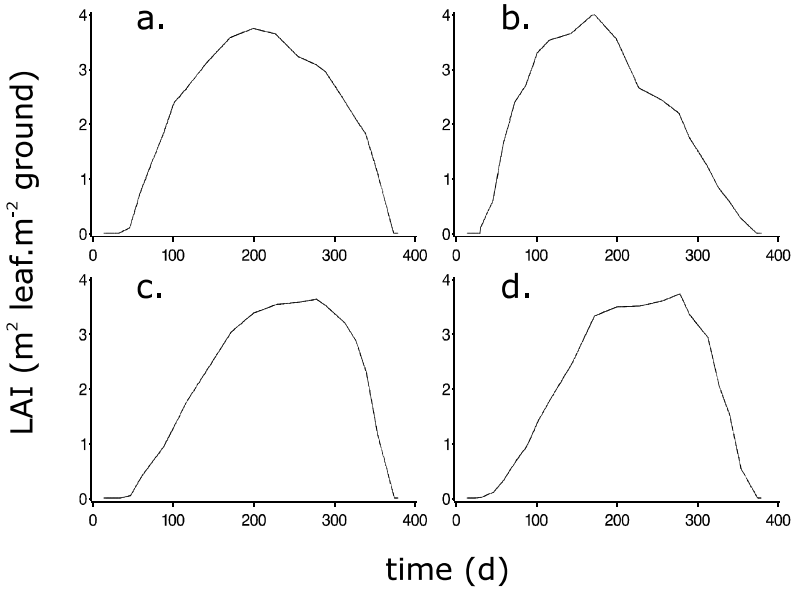

FIG. 7.3 – Temporal variations in individual tree leaf area index (LAI) used as inputs in TREEGRASS-2. Lines were linearly interpolated from mean measured data (Simioni et al. 2001c). (a.) and (b.) are LAI of isolated or clump *Crossopteryx febrifuga* individuals. (c.) and (d.) are LAI of isolated or clump *Cussonia arborea* individuals.

60.3 and 74.6 are minimum SLA values at the time of field measurements (i.e. corresponding to maximum sky openness), October 2000 (Simioni et al. 2001c).

N (%) is computed as a function of time since leaf flush from data in Abbadie (1984) for grasses, and Simioni et al. (2001c) for trees :

$$\begin{array}{lrcl} grasses: & N & = & e^{0.27832-0.00439\cdot N_a} \\ C.febrifuga: & N & = & 2.251752-0.242898\cdot ln(N_a) \\ C.arborea: & N & = & e^{0.641896-0.002806\cdot N_a} \end{array} \quad (7.40)$$

Tree LAI is forced using measured data of LAI temporal variation for the year 2000 (Simioni et al. 2001c), accounting for differences between clump and isolated trees (Figure 7.3).

Photosynthesis and stomatal conductance

Photosynthesis parameters are presented in Table 7.2. The reference stomatal conductance g_{sref} is a function of leaf N_a :

$$\begin{array}{lrcl} grasses: & g_{sref} & = & 0.075+0.166\cdot ln(N_a) \\ C.febrifuga: & g_{sref} & = & -0.118+0.251\cdot N_a \\ C.arborea: & g_{sref} & = & 0.116+0.114\cdot N_a \end{array} \quad (7.41)$$

Stomatal conductance response to Q was computed as (Simioni et al. 2001e) :

$$f_Q = a + b\cdot ln(Q) \quad (7.42)$$

TAB. 7.2 – Photosyntesis parameters for C_4 grasses, and C_3 trees : *Crossopteryx febrifuga* (CF) and *Cussonia arborea* (CA)

Parameters	Values		References
C_3 photosynthesis	CF	CA	
α (mol·mol^{-1})	0.24		Harley et al. 1992
c_{K_c}	35.79		Id.
c_{K_o}	9.59		Id.
c_τ	-3.9489		Id.
$a_{N-V_{cmax}}$	50.226449	50.546095	Simioni et al. 2001
$b_{N-V_{cmax}}$	0.996375	0.987913	Id.
$a_{N-J_{max}}$	36.224248	36.506946	Id.
b_{N-Jmax}	0.942307	0.757952	Id.
a_{N-Rd}	33.60206		Id.
b_{N-Rd}	0		Id.
ΔH_{a-K_c} (j·mol^{-1})	80.47·10^3		Harley et al. 1992
ΔH_{a-K_o} (j·mol^{-1})	14.51·10^3		Id.
$\Delta H_{a-\tau}$ (j·mol^{-1})	-28.99·10^3		Id.
ΔH_{a-R_d} (j·mol^{-1})	84.45·10^3		Id.
$\Delta H_{a-V_{cmax}}$ (j·mol^{-1})	116.3·10^3		Id.
$\Delta H_{a-J_{max}}$ (j·mol^{-1})	79.5·10^3		Id.
$\Delta H_{d-V_{cmax}}$ (j·mol^{-1})	202.9·10^3		Id.
$\Delta H_{d-J_{max}}$ (j·mol^{-1})	201·10^3		Id.
$\Delta S_{V_{cmax}}$ (j·K^{-1}·mol^{-1})	650		Id.
$\Delta S_{J_{max}}$ (j·K^{-1}·mol^{-1})	650		Id.
C_4 photosynthesis			
α	0.0657		Simioni et al. 2001
β	0.915		Id.
θ	0.7617		Id.
Q_{10-k}	1.8		Collatz, pers. com.
$Q_{10-V_{max}}$	2.1		Id.
Q_{10-R_d}	2		Id.
a_{N-k}	0.104367		Simioni et al. 2001
b_{N-k}	0.201284		Id.
a_{N-vmax}	15.640283		Id.
b_{N-vmax}	13.283342		Id.
a_{N-R_d}	0.778488		Id.
b_{N-R_d}	0		Id.

TAB. 7.3 – Soil water retention characteristics (mm) infered from data in Simioni et al. (2001).

soil layer	field capacity	limit content	wilting point
0-60 cm	100.5	55	26
60-170 cm	145	120	85
0-170 cm	245.5	175	111

With a =-0.764899, -0.743789, -0.410296 for grasses, *C. febrifuga*, and *C. arborea*, respectively, and b =0.252804, 0.244512, and 0.205952, for grasses, *C. febrifuga* and *C. arborea*, respectively (Simioni et al. 2001e).

Stomatal conductance response to VPD_l (Pa) is computed as (Simioni et al. 2001e) :

$$\begin{array}{lrcl} grasses: & f_{VPD_l} & = & 4.389 - 0.464 \cdot ln(VPD_l) \\ C.febrifuga: & f_{VPD_l} & = & 6.336 - 0.737 \cdot ln(VPD_l) \\ C.arborea: & f_{VPD_l} & = & 1.367 - 0.277 \cdot 10^{-3} \cdot VPD_l \end{array} \quad (7.43)$$

Respiration and allocation

No plant respiration data is available at Lamto except for grass and tree leaves (Simioni et al. 2001e). Waring et al. (1998) estimated NPP/GPP ratios for a range of temperate and nordic forests. They calculted carbon fractions lost from 0.45 to 0.55. We used a fration of 0.55 for the two tree species.

Very few respiration measurements were done on C_4 species, that were associated with carbon intake measurements. Byrd et al. (1991) made such a study. From their results, we calculated a respiration fraction of 0.43, assuming that respiration rates were identical day and night. This value is in accordance with data in Gifford 1994 for C_4 species. This value, conversely with data for trees, do not represent a NPP/GPP ratio, but only respiration. To account for a loss of carbon of about 12% as root exudate (carbon loss can represent 10 to 20% of gross photosynthesis, Johansson 1992), we increased the respiration fraction to 0.55 for grasses.

Allocation parameters were chosen so that plant allocated 60% of their assimilates to above ground parts without water stress and 40% with maximum water stress (Durand et al. 1989). Carbon contents for leaves are 0.420, 0.465 and 0.445 for grasses, *C. febrifuga*, and *C. arborea*, respectively (Simioni, unpublished data). Carbon contents for all other organs were set to 0.5.

Soil water storage and water flow

Values of soil water contents in layers 1 and 2 at field capacity and wilting point were estimated from field observations (Table 7.3). Aerodynamic soil resistance was prescribed. Soil surface resistance to water vapour transfer (SSR) depended on the amount of water evaporated since last rainfall from layer 1 (E_{cum}) (Amadou 1994) :

$$SSR = 80 \cdot e^{0.23 \cdot E_{cum}} \quad (7.44)$$

The conductive heat flux G in the soil was a constant fraction of net radiation (R_n) of the soil grass system (Le Roux 1995) :

$$\frac{G}{R_n} = 0.3 - 0.22 \cdot (1 - e^{-0.607 \cdot LAI}) \tag{7.45}$$

As suggested by Le Roux et al. (1995) and Le Roux and Bariac (1998), grasses and *C. febrifuga* water stress depends on the soil water content in layer 1, while *C. arborea* water stress depends on layers 1 and 2. The plant water extraction parameter $(\frac{T_1}{T})_{max}$ is 0.9, 0.7 and 0.5 for grasses, *C. febrifuga*, and *C. arborea* respectively (Le Roux et al. 1995, Le Roux and Bariac 1998). Runoff (mm) occurs if total LAI is lower than 2.5, and if precipitation P (mm) is higher than 22 mm :

$$Runoff = 0.1394 \cdot (P - 22) \tag{7.46}$$

Initialisations

The model does not account for growth initiation with carbohydrate and water reserves. To allow leaf growth to start, an initial leaf area was set for each grass plant. Le Roux et al. (1997) found that Lamto grasses could grow 10 g·m^{-2} of leaves in the obscurity during the first 50 days of the growing season. This value was measured in an open area (out of tree cover). An initial leaf biomass of 10 g·m^{-2} was set to grass pixel with no tree foliage above. This value decreases linearly to 2.5 for grass pixel completely under tree cover, corresponding to the range of decrease of grass tuft basal area under dense clumps (Simioni 2001, see Chapter 5). Intermediate values were set to grass pixels partially under tree cover.

Similarly, the soil water content in each soil cell was individually initialised. Simioni et al. (2001c) measured higher soil water contents in the upper soil layer under tree cover, than in open areas. Initial values of soil water contents in soil layer 1 were set to 52 mm for pixels in open areas (soil cell not under tree cover) up to 75 mm for soil cells completly under tree cover. Initial water contents in soil layer 2 were set to 128, according to field measurements.

Field data sets for model tests

TREEGRASS-2 was tested with field data collected during the 2000 vegetation cycle. Field data include :

1. Temporal dynamics of grass aboveground biomass, necromass, and phytomass measured on 1×1 m plots located in open areas, under tree clumps, or at intermediate distances from trees (unclosed tree cover) (Simioni 2001, Chapter 5). Data were measured using the non destructive point contact method at the beginning of the vegetation cycle, and by harvesting all grass plots at the end of the vegetation cycle.
2. Hemispherical photographs were taken in October above each grass plots used for the temporal survey. Sky openness values computed from hemispherical photographs were well correlated with grass above ground phytomass measured at the end of the vegetation cycle (Simioni 2001, Chapter 5). This data set allows to divide grass plots into sky openness (i.e. radiation level) classes.
3. Temporal dynamics of soil water contents in two soil horizons (0-60 cm, and 60-170 cm), measured in open areas and under tree clumps (corresponding to areas were the grass survey was conducted).

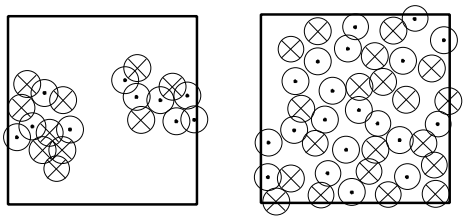

FIG. 7.4 – Maps of the two simulations used to test the model with 20 aggregated trees or 40 randomly located trees. *Crossopteryx febrifuga* ($\odot$) and *Cussonia arborea* ($\otimes$) individual canopies. All trees have the same size. Grass individuals are not represented.

Predicting grass growth accurately depends on the model ability to reproduce physiological, radiative, and soil processes. Predicting soil water contents accurately depends on the amount of soil evaporation and plant transpiration. Thus these field data present integrative variables to test the whole model accuracy. Moreover, these data allow to test the model ability to reproduce spatial variations in grass production and soil water contents.

Simulation and data analysis

Two simulations were carried out on sites of 16×16 m, with 20 trees in clump (test simulation 1), or 40 trees randomly distributed (test simulation 2) (Figure 7.4). All trees had the same dimensions (3.61 m height, 4 m^2 canopy cover). Basal grid cell size was 1×1 m. The grid was divided into four vertical layers : a grass layer, an empty layer, and two layers for tree foliage. Combining these two simulations allowed to cover a large range of tree/grass interactions from grass pixels under dense tree cover to grass pixels completely out of tree cover. The tree layer was equally partitioned between *C. febrifuga* or *C. arborea*. Tree individuals were randomly attributed to *C. febrifuga* or *C. arborea*.

In order to compare simulated and observed data, simulation outputs presented in this paper were :

1. temporal evolution of above ground biomass, necromass, phytomass, and top sky openness for each of the 512 grass pixels (256 pixels per simulation).
2. temporal evolution of soil water contents of each 512 soil cells from soil layer 1, and of each 512 soil cells from soil layer 2.
3. Additional standard outputs are plant individual GP_n, NPP, Q absorption, transpiration, leaf biomass, green and dead LAI, mean SLA, mean N, water stress, and soil evaporation.

For each grass pixel, a mean top sky openness was computed corresponding to the period of field measurement of sky openness (16th to 26th October 2000). Similarly, a mean grass aboveground phytomass was computed corresponding to the period of harvest of grass plots in the field (11th December 2000 to 4th January 2001). Simulated and observed relations between sky openness and grass aboveground phytomass were compared.

Grass pixels and field grass plots were then partitioned in sky openness classes (>80%, 70-80%, 60-70%, 30-40%, 20-30%, and <20%). For each classes, simulated and measured temporal dynamics of above ground biomass, necromass, and phytomass were compared.

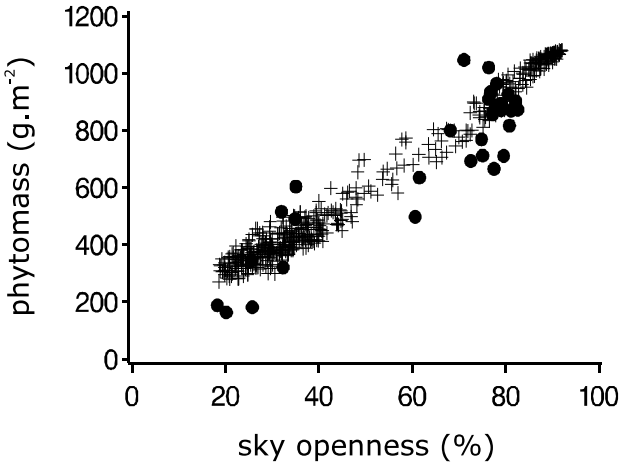

FIG. 7.5 – Simulated (+) and measured (•, Simioni 2001) relation between grass aboveground phytomass and sky openness for 1×1 grass plots. Field phytomass data were measured from 11/12/2000 to 04/01/2001, and sky openness from 16/10/2000 to 26/10/2000. Simulated data correspond to mean simulated values for the same periods.

In the field, the range of sky openness was 75-86% for open areas, and and 18-35% under tree clumps. Similarly to grass pixels, soil pixels corresponding to these classes were kept. For each of the two classes, simulated and measured temporal courses of soil water contents in soil layers 1 and 2 were compared.

Results

Model ability to reproduce spatial and temporal variations in grass production and soil water contents

The model reproduced well the spatial variations in grass phytomass with spatial variations in sky openness (Figure 7.5). Analysis of covariance showed no difference either for slope or for intercept between observed and simulated data ($P>0.05$, proc GLM, SAS inst.).

Temporal dynamics of grass aboveground biomass, necromass, and phytomass, by sky openness classes, were also well simulated (Figure 7.6), despite a slight overestimation of biomass at low sky opennesses (i.e. in shaded areas).

Temporal courses of soil water contents in soil layer 1 were well correlated for the two sky openness classes (Figure 7.7). Regression coefficient were lower for water contents in soil layer 2. However, regressions were done between mean observed and mean simulated data, but there is a high variability in observed values, and model outputs were almost always within the range of observed standard deviations.

Total annual primary production was 34.4 $t{\cdot}ha^{-1}$ for the simulation at 20 aggregated trees and 30.1 $t{\cdot}ha^{-1}$ for the simulation at 40 random trees. These data are in the range of NPP estimates in the field (Menaut and César 1979).

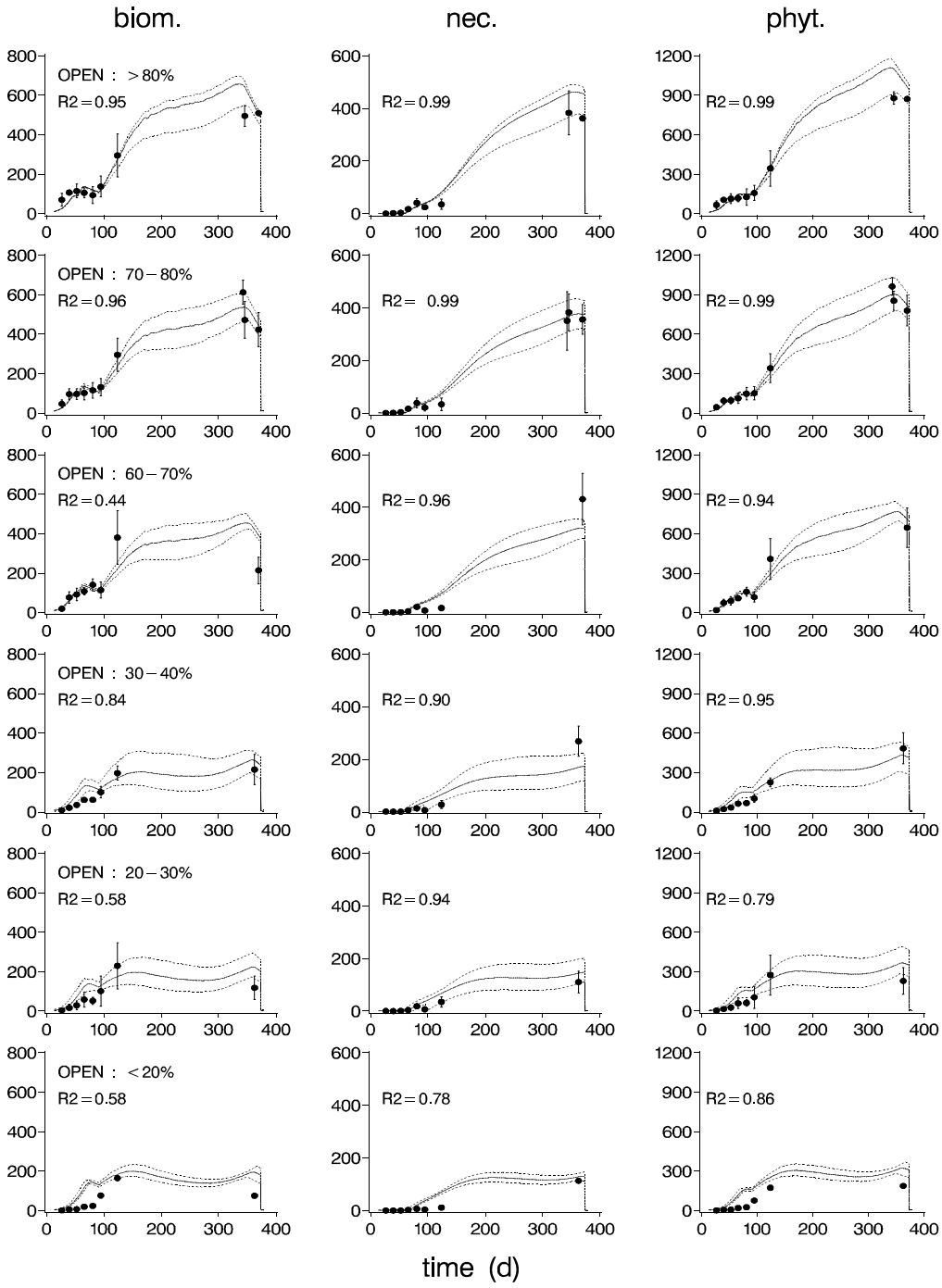

FIG. 7.6 – Temporal dynamics of measured (•, Simioni 2001) and simulated (lines) grass aboveground biomass, necromass, and phytomass ($g \cdot m^{-2}$) at different classes of sky openness (OPEN : >80%, 70-80%, 60-70%, 30-40%, 20-30%, and <20%). Bars represent standard deviations of observed values. Full lines represent average simulated values, dashed lines represent maximum and minimum simulated values. Regression coefficients correspond to signicant regressions ($P<0.05$) between mean observed and mean simulated data.

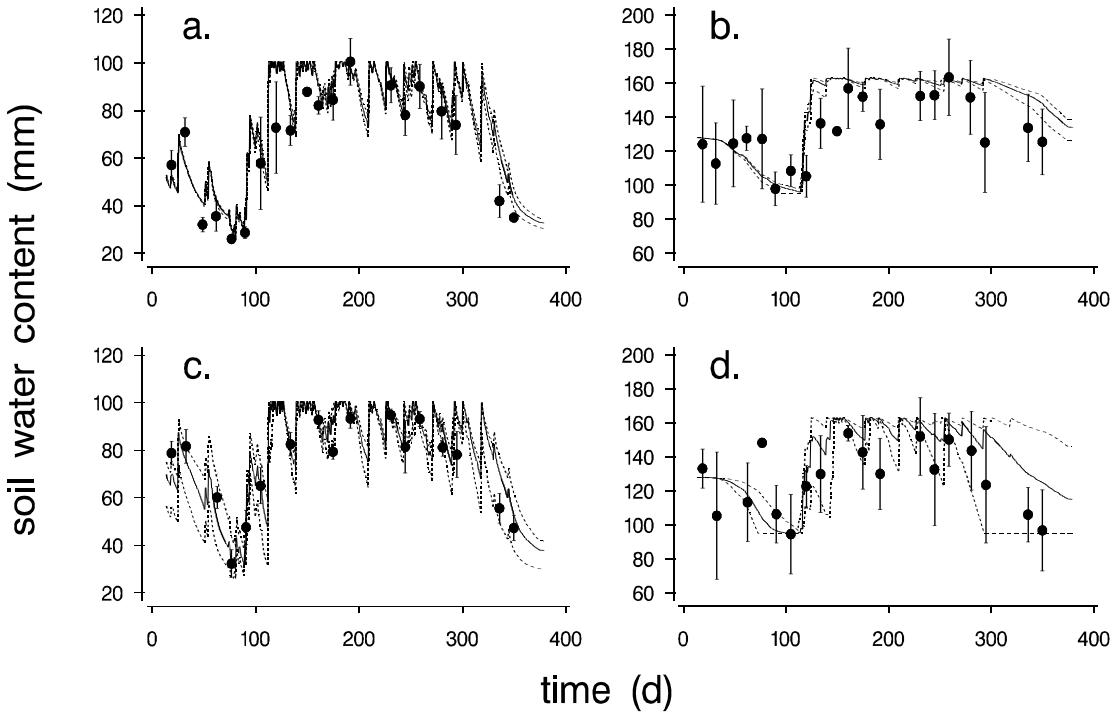

FIG. 7.7 – Observed (•, Simioni et al. 2001c) and simulated (lines) soil water contents in layer 1 (a. and c.) and 2 (b. and d.) for open (a. and b.) and tree clump (c. and d.) areas. Bars represent oberved standard deviation. Full line represent average simulated values and dashed lines represent maximum and minimum simulated values. Regression coefficients from significant regression between mean observed and mean simulated values were 0.86 (a.), 0.54 (b.), 0.83 (c.), and 0.41 (d.).

TAB. 7.4 – Simulated net primary production (NPP), transpiration, annual mean leaf nitrogen amount (N), light use efficiencies (LUE), water use efficiencies (WUE), and nitrogen use efficiencies (NUE), of *Crossopteryx febrifuga* and *Cussonia arborea*. Values are for test simulation 1 (see text), in which species were equally represented.

	C. febrifuga	*C. arborea*
NPP ($kg \cdot tree^{-1} \cdot y^{-1}$)	9.2	9.39
transpiration ($m^3 \cdot tree^{-1} \cdot y^{-1}$)	2.05	2.39
mean leaf N ($g\ N \cdot tree^{-1}$)	9.86	8.40
LUE ($g\ DM \cdot MJ^{-1}$ absorbed Q)	1.26	1.3
WUE ($g\ DM \cdot l^{-1}\ H_2O$)	4.51	3.94
NUE ($g\ DM \cdot g^{-1}\ N \cdot d^{-1}$)	2.82	3.5

Constrasts between *C. febrifuga* and *C. arborea*

From the test simulation 1, *C. febrifuga* presented a slightly higher WUE than *C. arborea*, a lower NUE, a similar LUE, and a higher leaf nitrogen mass (Table 7.4). NPP was similar between the two species, and *C. arborea* had a slightly higher annual transpiration. Trends were the same when looking at the results of the test simulation 2.

Discussion

Model ability to reproduce temporal and spatial variations in carbon and water fluxes

Spatially explicit models are scarce, and almost no model was ever tested with spatial data sets (but see Sinoquet et al. 2001 for the RATP model). In our study, simulated top sky openness above grass plots provided an index of the spatial heterogeneity of the tree layer. Using sky openness as a spatial reference, field measurements showed that grass standing biomass, necromass and phytomass were highly correlated to the shade level (i.e. value of sky openness, Simioni 2001, Chapter 5). Relation between grass standing phytomass and sky openness was very well simulated by TREEGRASS-2, showing its strong ability to reproduce the influence of tree cover on grass production. This represents a highly integrated test, as phytomass at the end of the vegetation cycle depends not only on the actual light availability, but also on the whole grass plot temporal dynamics (physiological processes and environmental effects).

As a matter of facts, the model also well reproduced temporal dynamics of grass standing biomass, necromass and phytomass, for different sky openness levels.

The last tests, comparing simulated and observed soil water contents, were satisfying, especially in soil layer 1. In soil layer 2, field measurements present a very high variability, and, if regression coefficients between observed and simulated soil moisture were not very high, model outputs are almost always in the range of observed standard deviations. TREEGRASS-2 simulated more variations in soil layer 2 under the tree clump than in open areas, reflecting tree ability to extract more water from the soil layer 2 than grasses.

If tests of the model were very satisfying, the use of the model is constrained by the important field data needed to parameterise it, in particular, the use of tree LAI as a

model input. But this allowed to avoid to compute the very complex carbon and water reserve management processes needed to reproduce well tree foliage development.

Effects of species functional diversity on carbon and water fluxes

The first version of TREEGRASS (Simioni et al. 2000) was limited to one grass and one tree species at a time. But ecosystems are composed of many species that can present constrasting features. As already stated, *C. febrifuga* and *C. arborea* have distinct water extraction patterns (Le Roux and Bariac 1998), gas exchange characteristics (Simioni et al. 2001c), phenologies, and leaf traits (Simioni et al. 2001c). Comparing the simulated NPP, transpiration, and resource use efficiencies of these two species in the test simulations showed that contrats in their WUE, NUE, and leaf acclimation resulted in similar annual NPP. This means that despite distinct foliage growth strategies, these present similar productivities. This counter-intuitive results highlights the importance to study effects of species functional diversity, because patterns detected at leaf scale, for instance, may not be representative of the whole vegetation functioning.

A model to study ecosystem structure and function

Savanna structure can be very variable considering climatic conditions, vegetation spatial structure, soil patchiness, and species composition and abundances. Whether and how these features influence savanna carbon and water processes has not been tested. TREEGRASS-2 provides and original opportunity to explore :

1. the vegetation spatial structure influence on carbon and water fluxes for the grass and tree components, and for the total system.
2. the importance of plant biodiversity and species abundances on ecosystem productivity.
3. the importance of climate variability.

Quatrième partie

Effets de la structure spatiale du couvert arbre sur les fonctionnements carboné et hydrique d'un écosystème de savane

Introduction

Cette partie est composée de deux chapitres, correspondant à deux publications, où sont présentés les résultats des expériences par simulations faites avec le modèle TREEGRASS.

Le Chapitre 8 s'appuie sur la première version du modèle (présentée au Chapitre 6), et présente une première exploration des effets potentiels de la structure spatiale de la strate ligneuse sur les flux de carbone et d'eau des composantes herbe et arbre.

La deuxième version de TREEGRASS est employée au Chapitre 9 afin d'étudier les effets de la structure spatiale de la strate arborée sur les efficiences d'utilisation des ressouces (lumière, eau et azote).

Les résultats des deux études étant complémentaires, une tentative de conceptualisation des effets observés est proposée à la fin du Chapitre 9. Par ailleurs, la publication présentée au Chapitre 9 n'est pas une version définitive.

Chapitre 8

Effets potentiels de la structure spatiale de la strate ligneuse sur la NPP et le bilan hydrique en savane

HOW DOES THE SPATIAL STRUCTURE OF THE TREE LAYER INFLUENCE WATER BALANCE AND PRIMARY PRODUCTION IN SAVANNAS ? RESULTS OF A 3D MODELLING APPROACH

à soumettre

G. Simioni, J. Gignoux, and X. Le Roux

Abstract

The spatially explicit and mechanistic model TREEGRASS was used to test effects of tree density, tree spatial distribution and tree size distribution on radiation absorption, net primary production (NPP) and water fluxes for a West African savanna. Annual photosynthetically active radiation (PAR) absorption efficiency, NPP, and transpiration of the tree layer increased with increasing tree density and decreased with increasing tree aggregation ; the grass layer showed the opposite trends. Total NPP (tree plus grass) remained stable for all tree densities and decreased slightly for aggregated tree distributions. Total transpiration increased with tree density and was not affected by tree aggregation. Changing the tree size distribution had no effect on radiation absorption, or carbon and water fluxes.

This study showed that fine scale vegetation structure can influence NPP and water fluxes. As such, it should be taken into account when assessing the functioning of tree/grass systems. However, the detailed fine scale structure of the tree layer is rarely available for savanna ecosystems. Thus we assessed the reliability of two common descriptors of savanna vegetation, leaf area index (LAI) and tree canopy cover, to predict

PAR absorption, NPP and evapotranspiration. Neither of these descriptors could adequately predict all the simulated effects. However, tree canopy cover reasonably estimated radiation absorption and carbon fluxes, whereas LAI was a good predictor of water fluxes. Therefore, mapping and monitoring approaches incorporating both LAI and tree canopy cover appear to be suitable alternatives to quantifying the fine scale vegetation spatial structure when assessing ecosystem function in savannas.

Key words : 3D ecosystem models, Lamto, Ivory Coast, spatial patterns, tree/grass interactions, LAI, tree cover, net primary production, evaporation, transpiration, 3D ray tracing

1.Introduction

Savanna ecosystems cover around 20% of terrestrial surfaces (Scholes and Hall 1996), and 40% of tropical surfaces (Solbrig et al. 1990). They are characterized by the coexistence of a continuous grass layer and a discontinuous tree layer (Scholes and Archer 1997), and thus display a high heterogeneity of vegetation structure (Menaut and César 1979). This heterogeneity is reflected in soil properties (e.g. Smith and Goodman 1986, Vetaas 1992), intensity of disturbances like fire (Menaut et al. 1990) or herbivory (Skarpe 1992), and availability of nutrients (e.g. Smith and Goodman 1986, Weltzin and Coughenour 1990, Vetaas 1992), water (Smith and Goodman 1986, Breshears et al. 1997a) and radiation (Breshears et al. 1997b). Furthermore, interactions exist between these parameters (Frost et al. 1986, Smith and Goodman 1986, Skarpe 1992). Such a complexity, in which spatial structure plays an important role, has led some authors to recognize that modelling experiments are critical to assessing ecosystem function in savannas (Jeltsch et al. 1996, Scholes and Archer 1997).

Neither ecosystem- nor global-scale models have tested the potential importance of the fine scale spatial structure of the vegetation (e.g. spatial location and shape of tree individuals, at a given leaf area index) on total (tree plus grass) water balance and net primary production (NPP), in savanna-like ecosystems. Most current models aimed at describing savanna function are not spatially explicit (but see the SAVANNA model, Coughenour 1994, and Jeltsch et al. 1996). SAVANNA is a landscape model that is partially spatially explicit at a local scale (one tree- and one grass-dominated areas per pixel). Whether and how the clumping of trees might influence ecosystem processes and hence determine the way grass and tree/grass areas have to be defined in a pixel remains to be determined (Coughenour, pers. com.). The model of Jeltsch et al. (1996) uses simplified processes compatible with simulations over long period (up to 300 years), but do not detail production and water processes occuring at fine time scales. Models simulating biome function at the global scale (e.g. Melillo et al. 1993, Woodward et al. 1995, or Sellers et al. 1996) cannot explicitly integrate local spatial patterns of vegetation, because of the large pixel size they must use. It is not yet clear how spatial variation within pixels might affect assessments of ecosystem processes. Thus there is a need for spatially explicit and mechanistic modelling approaches to test whether the fine scale spatial structure of the vegetation can influence NPP and water balance in tree/grass systems at a fine time scale (e.g. one vegetation cycle). If such an influence is demonstrated, then simple methods must be developed to represent the fine-scale distribution

of the vegetation in modelling efforts conducted at greater spatial and temporal scales.

In this paper, the three dimensioned (3D) model TREEGRASS (Simioni et al. 2000) was used to assess the effects of the fine scale spatial structure of the tree layer on NPP and water balance for small savanna areas (from 100 to 10000 m2) over one vegetation cycle. In a first section, we present the main features of TREEGRASS, parameterized for the humid savanna of Lamto (Ivory Coast), and the design of our simulation experiment. The effects of tree density, spatial distribution, and crown size distribution on NPP and water fluxes were tested at the ecosystem scale (annual NPP and evapotranspiration of the combined tree and grass components) and at the scale of the tree and grass components (annual total tree NPP and transpiration vs. annual total grass NPP and transpiration). Results were re-interpreted in order to test the ability of two common vegetation descriptors, leaf area index (LAI) and tree canopy cover, to predict NPP and water balance of tree, grass, and grass plus tree components at the ecosystem scale. Implications for vegetation monitoring and the representation of vegetation in models of mixed tree/grass ecosystems at larger scales are discussed.

2.Method

2.1.The TREEGRASS model

TREEGRASS is a spatially explicit, individual plant based model that simulates water fluxes and NPP for small tree/grass areas (tree plus grass layers) (100 to 10000 m2) over one to a few vegetation cycles, with a daily time step. Competition for light and water are treated mechanistically (i.e. most relationships used are biophysical). It includes submodels derived from the 3D RATP model (Radiation Absorption, Transpiration and Photosynthesis) (Sinoquet et al., 2001) that computes radiation and energy budgets within vegetation canopies, and from the PEPSEE model (Production Efficiency and Phenology in Savanna EcosystEms) (Le Roux et al. 1996) that simulates primary production and soil water balance in savanna grasslands. It works within the MUSE simulation framework (MUltistrata Spatially Explicit model) (Gignoux et al., 1996) that provides background algorithms for spatially explicit ecosystem modelling. A full description of TREEGRASS is presented in Simioni et al. (2000). Main features of TREEGRASS are :

1) Space is divided into a 3D grid of cells (Figure 8.1). Cell size can be defined to fit with the sizes of vegetation components. Above ground cells can contain homogeneous grass, tree or grass and tree foliage elements. There are three layers of below ground cells : layer 1 which includes 90% of grass roots ; layer 2, which contains all remaining grass roots ; and layer 3, the deep soil underneath.

2) The grass layer is divided into plots or pixels corresponding to grid cell basal dimensions. Each grass plant is relegated to its own pixel ; its foliage occupies one above ground cell and its roots are distributed in the two soil cells underneath. Each individual tree canopy is assumed to occupy a cylindrical volume, referred to as a foliage crown. Similarly, each individual tree root system is assumed to occupy a root crown. Tree height, bole (bottom of canopy), foliage and root crown radii, and peak leaf area index of individual trees are linked by allometric relations. Tree leaves and roots are located in above and below ground cells, according to overlap coefficients between crown cylinders and grid cells (Figure 8.1). Stems and branches are not explicitly represented. Two grass "in-

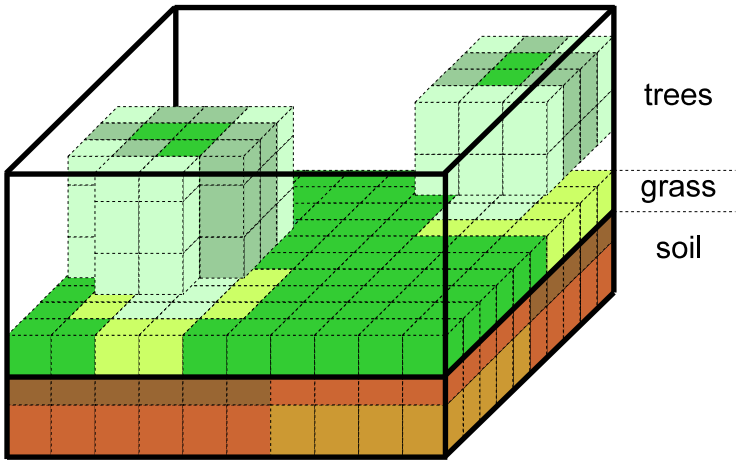

FIG. 8.1 – 3D representation of vegetation in the TREEGRASS model. Space is divided into a grid of cells (empty cells are not shown). Different shades of green/brown correspond to different leaf/root densities in above/belowground cells. A grass pixel occupies one above ground cell and the two soil cells underneath (100 grass pixels represented in this figure). Trees can occupy many above- and belowground cells, depending on their size (2 trees shown here). Stems and branches are not explicitly represented.

dividuals" (i.e. grass pixels) do not overlap. By contrast, tree crowns can overlap grass cells and other tree crowns. In the following, any cell containing leaves will be named "vegetation cell", and the different types of leaves sharing one vegetation cell will be referred to as "entities". Coarse and fine roots are not differentiated. Given the fine time resolution of the model, tree dimensions are assumed to be fixed over a simulation, only leaf area density (LAD) and root mass density can change within individual foliage and root crowns.

3) A radiation absorption submodel, adapted from Sinoquet et al. (2001) calculates the amounts of photosynthetically active radiation (PAR), near infrared radiation (NIR) and thermic infrared radiation absorbed or emitted at each time step by each entity in each vegetation cell, and by the soil surface. This submodel accounts for daily and yearly solar heights and azimuths, diffuse radiation, and reflection/transmission by foliage entities and soil. Radiation balance depends on leaf area density and leaf angle distributions in each vegetation cell, and species specific leaf optical properties. Radiation absorption is computed five times a day, accounting for diurnal variations in sun position and radiation intensity. In addition, this submodel was adapted to compute sky openness at the top of each vegetation cell (i.e. fraction of sky not obstructed by other foliage elements located above a vegetation cell).

4) The plant transpiration and soil evaporation submodel is also adapted from Sinoquet et al. (2001). For each entity in each vegetation cell, an energy budget is computed to determine the surface temperature that balances absorbed and emitted radiation, sensible heat flux and latent heat flux (leaf transpiration and soil evaporation). Transpiration and evaporation are derived from the energy budget equation. Transpiration thus depends mainly on net radiation at the leaf surface, leaf stomatal conductance and air vapour pressure deficit (VPD), while soil evaporation depends on net radiation at

the soil surface, soil surface conductance, and VPD. Stomatal conductance is computed according to Jarvis (1976), i.e. using a value of maximum stomatal conductance and empirical functions of the amount of leaf irradiance, VPD at leaf surface, and water stress experienced by the plant. Soil surface conductance depends on the time elapsed since the last rain date. Energy budget is also computed five times a day, to account for diurnal variations in radiation absorption, air VPD, and air temperature.

5) Amounts of transpired water for each entity in each vegetation cell are summed to yield individual plant transpiration rates. Plant water uptake depends on root spatial location, but not on root biomass or density (it is assumed that active and non active roots have identical spatial locations). Thus, soil moisture may not be identical in all soil cells from a same layer. Under non-limiting water conditions, water transpired by a given individual plant is extracted in layers 1 and 2 in cells where its roots are present. More water is extracted from layer 2 as water stress becomes more pronounced. The water stress experienced by each plant depends on the soil water content in layer 1, in cells where its roots are present.

6) When rainfall occurs, run-off is computed according to the degree of soil coverage by vegetation and rainfall amount. The remaining water is an input that increases soil water content in layer 1. Drainage occurs from layer 1 to layer 2, and into layer 3, when soil water content in a given layer exceeds field capacity.

7) Total absorbed PAR by each plant is converted into dry matter using the light use efficiency (LUE) approach (Monteith 1972, Monteith 1977). The actual LUE is computed according to a species dependent, maximum LUE constrained by water stress.

8) The ratio of the dry matter production allocated to roots versus shoots is computed as a function of the ratio of the actual to maximum LUE (Landsberg and Waring 1997) and thus depends on water stress. As water stress increases, the proportion of dry matter allocated to roots increases.

9) Grass leaf mortality is a function of grass phenology. The decomposition rate of dead leaves is assumed to be constant. Tree leaf mortality depends on the tree phenology and water stress.

2.2.Parameterization for the Lamto savanna

The Lamto natural reserve vegetation structure has been described by Menaut and César (1979). It is located in Ivory Coast, at 5°02' W and 6°13' N. Interannual rainfall variability is important with annual rainfall ranging from 800 to 1600 mm, with a mean of 1200 mm. Annual mean temperature is stable at about 27°C. The reserve presents a mosaic of forest along streams, and of savanna areas. Savanna areas present a high variability in the structure of the tree layer, from savanna grasslands to dense shrublands. Altitudes are comprised between 75 and 125 m. The topography is very smooth with a mean ground slope of about 5%. Soil is composed of 75-80% of sand and 7.5-15% of clay, it is classified as ferralsol (according to the FAO classification). Soil depth ranged from 1 to 2 m.

Daily radiation, rainfall, wind speed, and daily courses of air temperature and air himidity measured at Lamto were used as input variables and assumed to be spatially homogeneous on the site. The grass considered here was the C_4 perennial bunch grass *Hyparrhenia* spp. (Andropogoneae). The tree type represented in the model was *Crossopteryx febrifuga*, a dominant, deciduous, shallow-rooted species. 70% of this tree species

TAB. 8.1 – Main parameters used in the TREEGRASS model for simulations of the Lamto savannas.

parameters	values	references
PAR absorbances (fraction of incoming PAR)		
Ground	0.76	Le Roux et al. 1997
Grass green leaves	0.78	Id.
Grass dead leaves	0.35	Id.
Tree green leaves	0.78	NA
NIR absorbances (fraction of incoming NIR)		
Ground	0.50	Le Roux et al. 1997
Grass green leaves	0.04	Id.
Grass dead leaves	0.05	Id.
Tree green leaves	0.1	NA
Maximum stomatal conductances (mmol.m-2.s-1)		
Grass	230	Sueur 1995
Tree	230	NA
Maximum conversion efficiencies (g dry matter· MJ^{-1} absorbed PAR)		
Grass	2.28	Le Roux et al. 1997
Tree	1.6	A. Bégué, pers. com.
Fraction of roots in soil layer 1 (%)		
Grass	90	Le Roux 1995
Tree	70	Le Roux et al. 1995

NA : not available. (1) not available when simulations were performed but supported by recent field measurements (Simioni and Walcroft, unpublished data).

are located in soil layer 1 and remaining roots in soil layer 2. Tree root crown radius is 1.5 times the foliage crown radius, as suggested by Mordelet (1993). Important parameters in the context of this study are summurized in Table 8.1. A full description of the parameters used for the study site and tests against field data in open and shrubby areas can be found in Simioni et al. (2000).

2.3.Simulation experiment

All experimental simulations were done using representative plots of 196 m^2 (14x14 m). Plots were gridded into 1x1 m cells, thus involving 196 grass pixels. The accuracy of the 1x1 m resolution has been discussed in Simioni et al. (2000). The spatial structure of the tree layer on a plot is a combination of three components : tree density, spatial distribution and crown size distribution. One set of simulations was performed for each of these components (Figure 8.2). Each set was associated with the variation of only one parameter :

1. The effects of tree density were explored using a tree number on the whole plot ranging from 0 to 80 trees (i.e. from 0 to 4082 trees ha-1). For each density, a random tree spatial distribution was generated using a Poisson process. For all these simulations, a unique tree size was used (height=3.61m ; canopy area=4m^2).
2. Seven tree spatial distributions were tested, ranging from regular to highly aggregated in each of two densities (20 and 40 trees per plot). Regular distributions were generated using a sequential inhibition process (Gignoux et al. 1999), with an inhibition distance of 1.5 m (highly regular) or 0.5 m (loosely regular). Random distributions were generated as in (1). Aggregated distributions were generated by a Poisson cluster process (Gignoux et al. 1999) : parent points were generated, to which child points were associated. Child points were distributed with a normal distribution centered on parent point positions, using a mean tree number per clump of 8 and 2.5 for loosely and highly aggregated distributions respectively, and a mean clump radius of 2.8 m and 0.7 m for loosely and highly aggregated, respectively. The 'line' and the 'square' distributions were obtained by a random distribution within a 1 m wide line, and within a 4x4 m square. For all these simulations, a unique tree size was used as in (1.).
3. The effects of the tree size distribution were tested using four size class distributions : a unique tree size (3.61 m high), two size classes (trees split between two height classes : 2 m and 4.82 m), a normal size distribution (tree heights ranging from 1.91 m to 5.57 m) and a log-normal size distribution (tree heights ranging from 0.2 m to 14.85 m). For all these simulations, tree density (20 trees) and maximum tree LAI were constant, and tree spatial distribution was random as in (1.).

For all simulations, the model was run for one annual vegetation cycle (climatic data from January 1991 to January 1992), that starts and ends at dates when fire occurs. This vegetation cycle presented a typical annual rainfall, and corresponds to field measurements used to test TREEGRASS in Simioni et al. (2000). Climate conditions were thus identical for all experimental simulations. To quantify the effects of tree spatial structure on ecosystem function, model outputs included absorbed PAR, above and belowground NPP, transpiration and soil evaporation, and mean green LAI for the tree, grass, and the pooled tree plus grass component over the year.

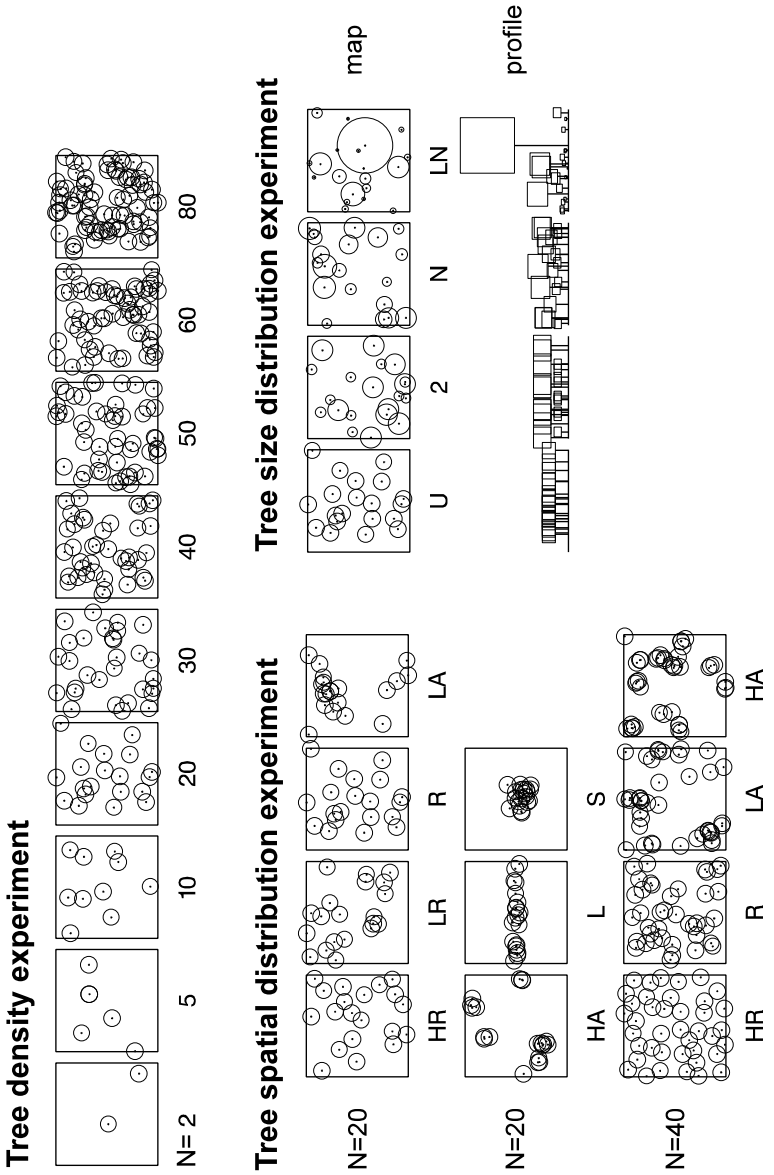

FIG. 8.2 – Maps of the 14x14 m sites used for the simulations with the TREEGRASS model. Tree canopies and trunks are represented by circles and dots on the maps, and by squares and sticks in the profile views. Grass individuals are not shown. N : number of trees per plot. Tree spatial distribution : HR, highly regular ; LR, loosely regular ; R, random ; LA, loosely aggregated ; HA, highly aggregated ; L, in line ; S, in square. Tree size distribution : U, unique size ; 2, two sizes ; N, normal ; LN, log-normal. Trees in density and size distribution experiments were randomly distributed and a unique density (20 trees) was used for the tree size distribution experiment. Individual tree size was unique for tree density and spatial distribution experiments.

2.4.LAI and tree canopy cover ability to describe NPP and water balance

In our simulations, when expressed at the total system scale, green LAI can be considered as a non-spatial parameter, as a given LAI value can correspond to various tree spatial distributions. By contrast, tree canopy cover (the ratio of projected crown surface to total plot area) implicitly includes spatial information because it depends on both tree density and tree spatial distribution (at a given tree density, tree cover decreases when overlap between tree crowns increases). Results of the simulations described above were re-interpreted in terms of annual averaged green LAI and tree cover. A regression analysis was done to assess LAI or tree canopy cover to predict grass, tree or grass plus tree PAR absorption efficiency, NPP, or transpiration. Best regression fits were searched for pooled data sets, including all simulation types. Regression coefficient values were used to compare LAI and tree cover reliability.

3.Results

3.1.Effects of tree spatial structure

Effects of tree density

Total PAR absorption efficiency (tree plus grass components over the whole plot) increased by 54% when tree density increased from 0 to 80 trees per plot (Figure 8.3). The increase in PAR absorption efficiency of trees overcompensated the decrease in grass PAR absorption efficiency. Total NPP remained roughly constant with increasing tree density, because the increase in tree NPP proportionately compensated the decrease in grass NPP (Figure 8.3). Annual total evapotranspiration increased 360 mm with increasing tree density. When tree density increased from 0 to 80 trees per plot, annual grass transpiration was reduced 390 mm, while annual tree transpiration increased 770 mm. Soil evaporation decreased slightly with increasing tree density (Figure 8.3). The decrease in grass PAR absorption efficiency, grass NPP, and grass transpiration with increasing tree density were all highly non-linear. Grass, tree, and total water use efficiencies (WUE, ratio of production to transpiration) decreased with increasing tree density. No effect of tree density was found on tree, grass and tree plus grass partitioning of NPP to above- and belowground parts. The overall above to belowground NPP ratio was 1.45.

Effects of tree spatial distribution

For aggregated distributions, grass PAR absorption efficiency was higher and tree PAR absorption efficiency lower than for random or regular distributions (Figure 8.4). These two trends did not fully compensate, and total PAR absorption efficiency by the tree plus grass vegetation decreased with increasing tree aggregation at both tree densities (-14% for 20 trees/plot, -10% for 40 trees/plot). Total NPP only slightly decreased with increasing tree aggregation (-7% for 20 trees per plot, -9% for 40 trees per plot), because the increase in grass NPP largely compensated the decrease in tree NPP (Figure 8.4). With increasing tree aggregation, soil evaporation and total evapotranspiration remained constant, with increases in grass transpiration being fully compensated by declines in tree transpiration. When tree aggregation increased, grass WUE increased

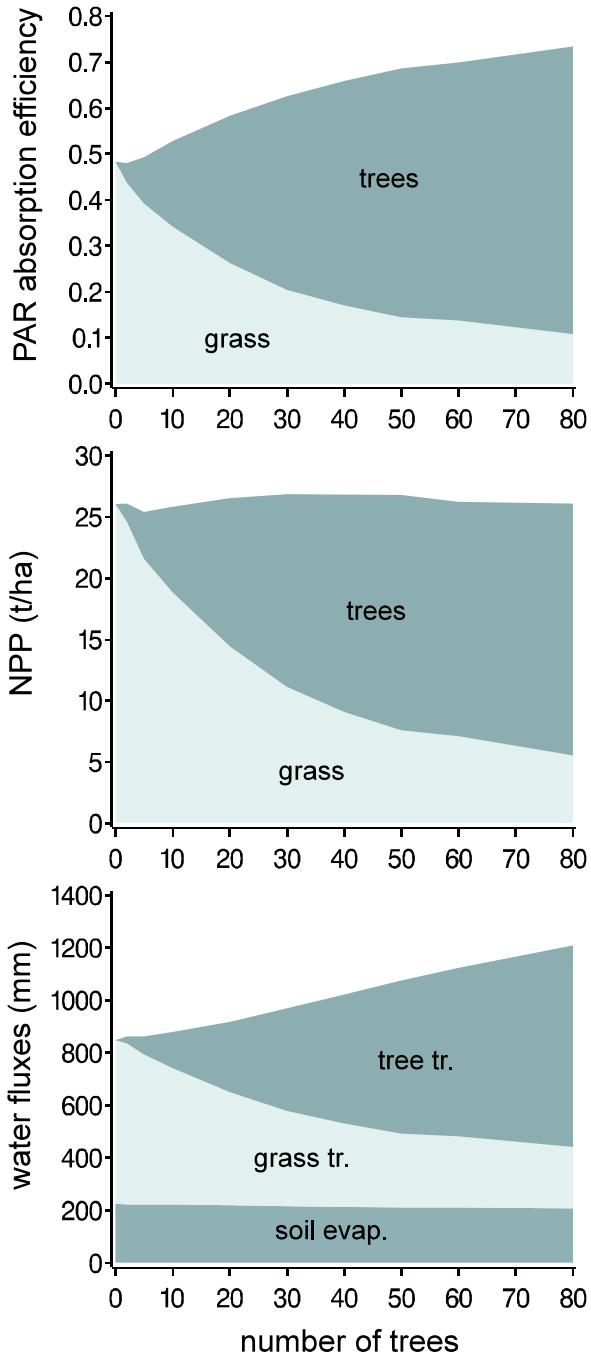

FIG. 8.3 – Predicted effects of tree density on system total annual absorption efficiency of photosynthetically active radiation (PAR), net primary production (NPP, above plus below ground) and water fluxes (tr., transpiration ; evap., evaporation).

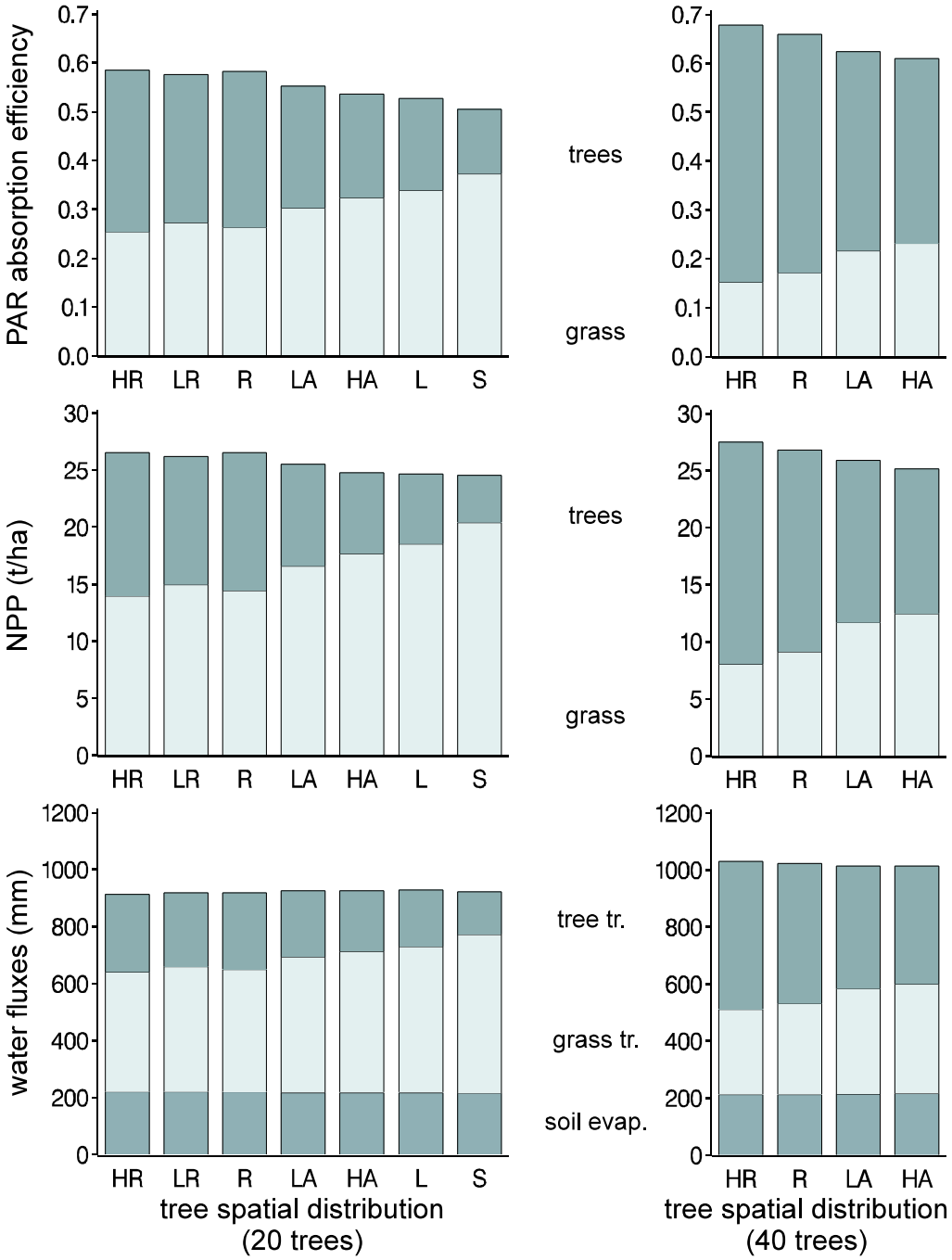

FIG. 8.4 – Predicted effects of tree spatial distribution on system total annual PAR absorption efficiency, NPP, and water fluxes at two tree densities (20 and 40 trees/plot). Abbreviations as in Figures 8.2 and 8.3.

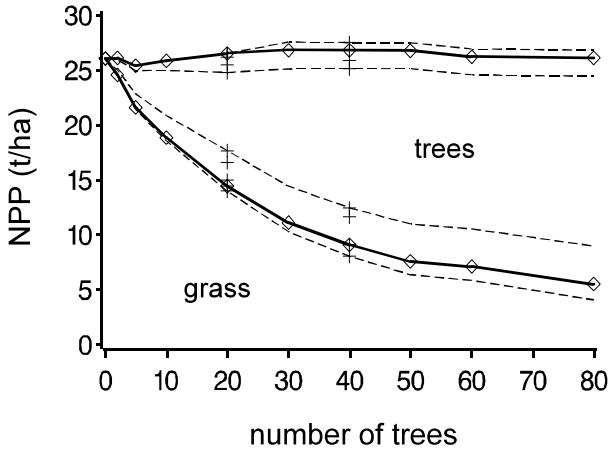

FIG. 8.5 – Influence of tree density and spatial distribution on annual grass, tree and total NPP. ⋄ results from the density experiment ; + results from the spatial distribution experiment. Solid lines : random tree distribution. Dashed lines : extreme tree distributions (highly regular and highly aggregated). Dashed lines were computed as linear interpolations of the random pattern curves. Bases for interpolation were spatial distribution effects at 20, 40 trees/plot, and 0 tree/plot (no expected effect of tree spatial structure).

slightly while that of tree decreased, whole system WUE was slightly decreased (results not shown). Qualitatively, similar results were obtained for the two tree densities studied.

Changing the tree spatial distribution only slightly influenced the response of total NPP to changes in tree density (Figure 8.5). But, it significantly affected the shape of the non-linear decrease in grass NPP with increasing tree density. Grass NPP decreased more importantly with aggregated tree distributions and less importantly with highly regular tree distributions.

Effects of tree size distribution

PAR absorption efficiency, NPP and transpiration rates of grasses and trees were insensitive to tree size distribution. Tree transpiration exhibited the highest change with changing tree size distribution (+9% from uniform to log-normal distributions).

3.2. LAI and tree cover as functional indicators

Annual PAR absorption efficiency, NPP, and transpiration of the grass layer were strongly correlated to grass green LAI and to tree canpoy cover (Figure 8.6). Unique relationships were obtained for the range of tree densities, spatial distributions, or crown size distributions examined. For the tree layer, PAR absorption efficiency and NPP were also strongly correlated to tree cover (Figure 8.7). By contrast, the relationship between tree PAR absorption efficiency and LAI, or NPP and tree LAI, was sensitive to the type of tree spatial distribution. At 20 trees/plot, from highly regular to highly aggregated tree distributions, tree NPP decreased by 43% while tree LAI was constant. Annual

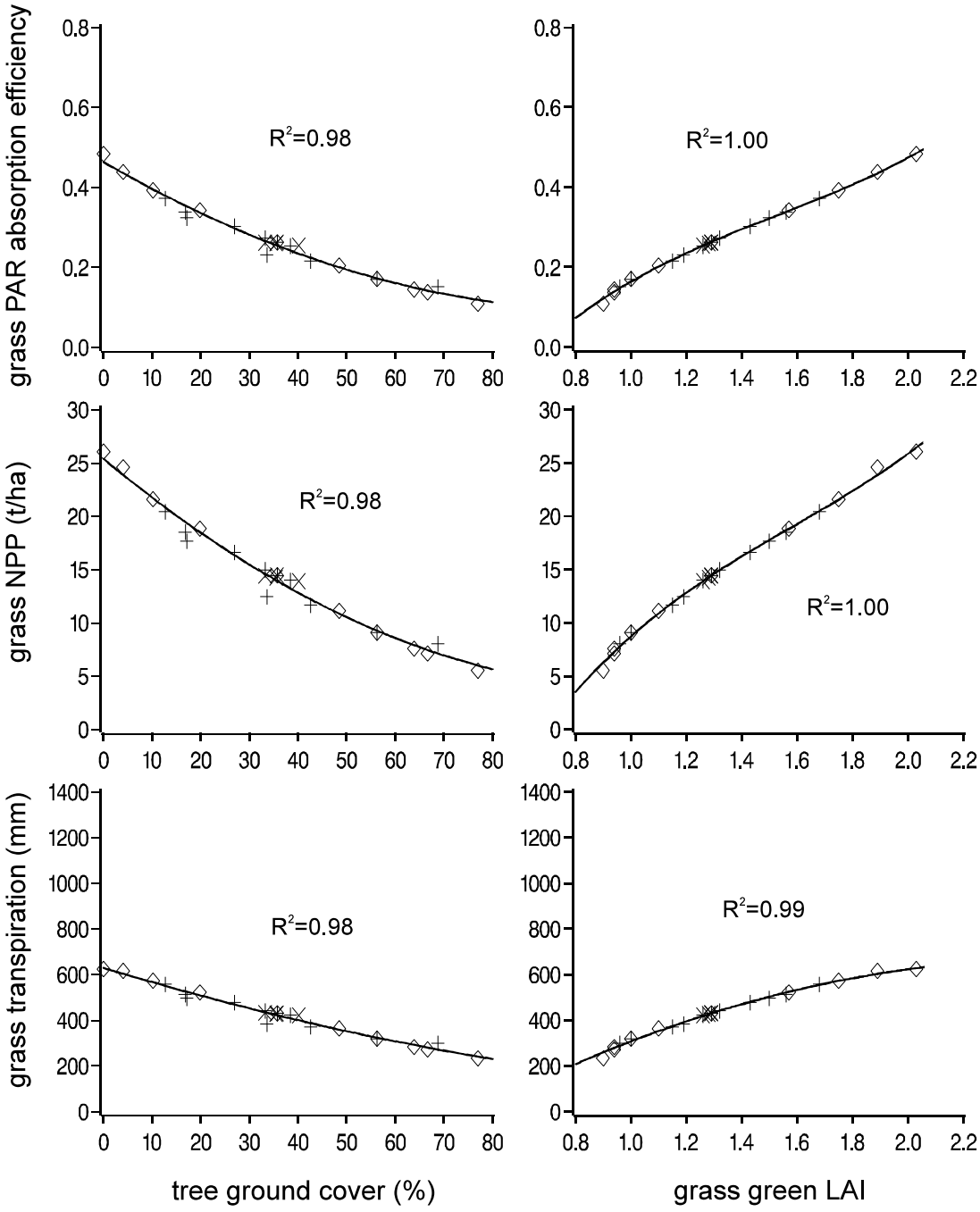

FIG. 8.6 – Variations in grass PAR absorption efficiency, NPP, and transpiration with tree cover and grass annual mean green LAI. ⋄ results from the density experiment ; + results from the spatial distribution experiment ; × results from the size distribution experiment. Lines represent best regression fits (best model regarding regression coefficient), all significant at $p<0.05$.

tree transpiration was highly correlated to tree LAI, while a weaker relationship was obtained when tree cover was used as the independent variable (Figure 8.7). Annual PAR absorption efficiency by the tree plus grass layers were well correlated with tree cover, but much less with total green LAI (Figure 8.8). Total NPP changed little but was significantly correlated to tree cover, but not to total green LAI. Soil evaporation, total transpiration and total evapotranspiration were highly correlated with total green LAI when data were pooled across all tree spatial or crown size distributions. By contrast, the correlation between total transpiration or total evapotranspiration and tree cover was sensitive to the type of tree spatial distribution.

4.Discussion

4.1.Effects of tree spatial structure on grass, tree and total NPP and transpiration

Effects of the tree spatial structure on NPP

In the last decade, two controversial issues regarding the influence of the tree layer structure (especially tree density) on the function of tree/grass systems have been raised : (i) how does grass and tree NPP change with changes in the structure of the tree layer ? and (ii) what is the influence of the structure of the tree layer on total (tree plus grass) ecosystem production ?

In many savannas, grass production declines when tree density increases (reviewed by Scholes and Hall, 1996). The observed shape of the grass NPP response curve with changes in tree density can be concave (e.g. Walker et al. 1972, Beale 1973), linear (Walker et al. 1986), or convex (Aucamp et al. 1983). These differences in shape are commonly attributed to differences in the potential site productivity (referred to as the potential grass production without trees) that depends on site fertility and rainfall (Scanlan and Burrows 1990) or to disturbance (e.g. grazing) regimes (McPherson 1992).

In our simulations, for a given (i.e. random) tree distribution, changes in tree and grass NPP with increasing tree density were non-linear. The decrease in grass NPP with increasing tree density was influenced by the tree spatial distribution (Figure 8.5). Soil fertility and rainfall were identical in all simulations, suggesting that, for a given site productivity, the relation between grass NPP and tree density can vary in response to the spatial structure of the tree layer.

In this humid savanna, this non-linearity is probably due to competition between trees for PAR. Trees have first access to light, but when tree density or aggregation increases, tree-tree competition for PAR increases as distances between trees decrease. Then, a tree individual absorbs less PAR on average (as can be inferred from Figures 8.3 and 8.4), and individual tree NPP decreases. This probably accounts for the decrease in tree PAR absorption efficiency with increasing tree aggregation (Figure 8.4), but also for the non linear increase in tree PAR absorption efficiency with a linear increase in tree density (Figure 8.3). As a result, the fraction of PAR reaching the grass layer deacreases non linearly with tree density and increases non linearly with tree aggregation, and grass NPP follows the same pattern.

Probably tree size distribution didn't affect importantly tree-tree competition for PAR, and this accounts for the observed stability of tree, grass and total PAR absorp-

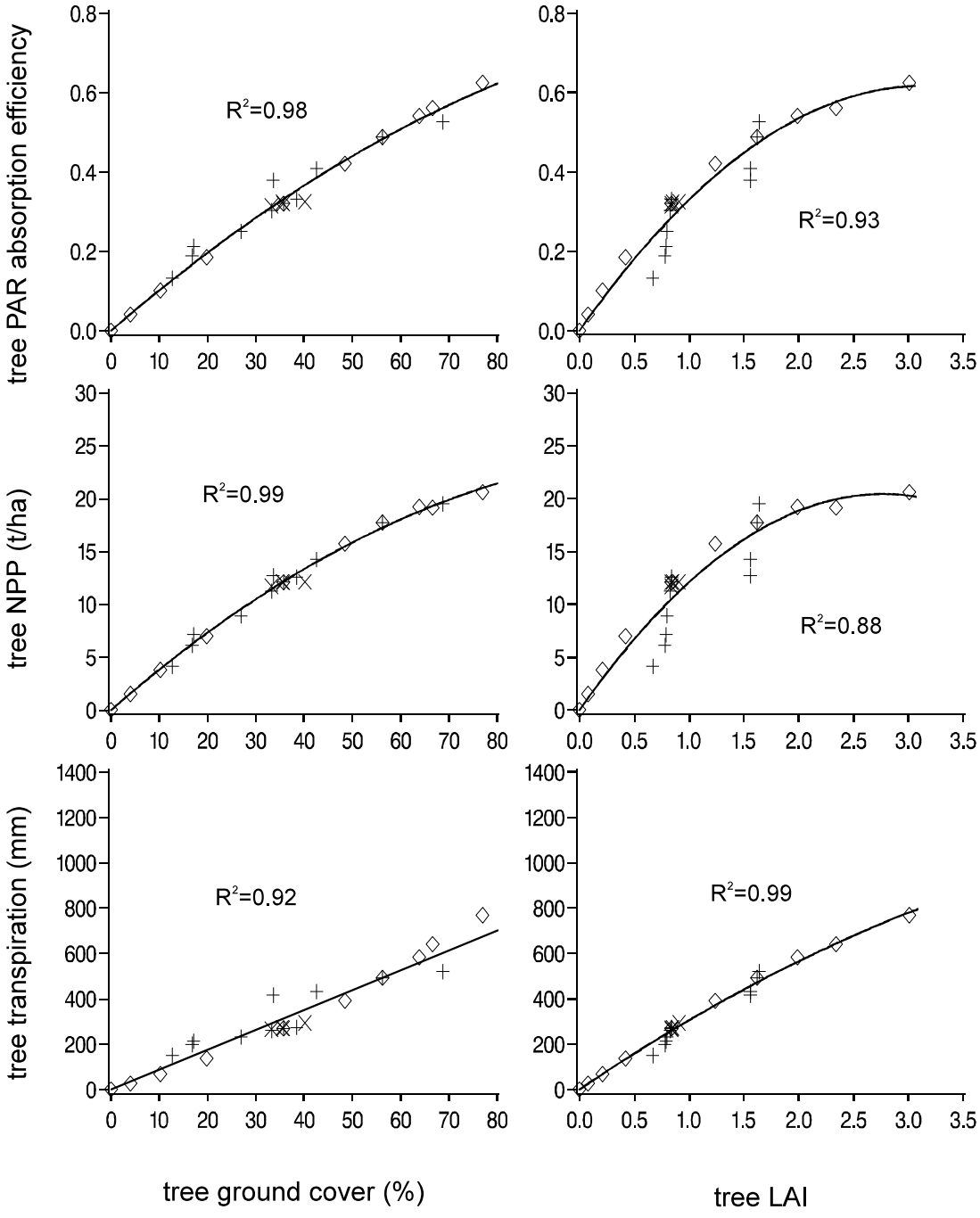

FIG. 8.7 – Variations in tree PAR absorption efficiency, NPP, and transpiration with tree cover and tree annual mean LAI. Legend as in Figure 8.6.

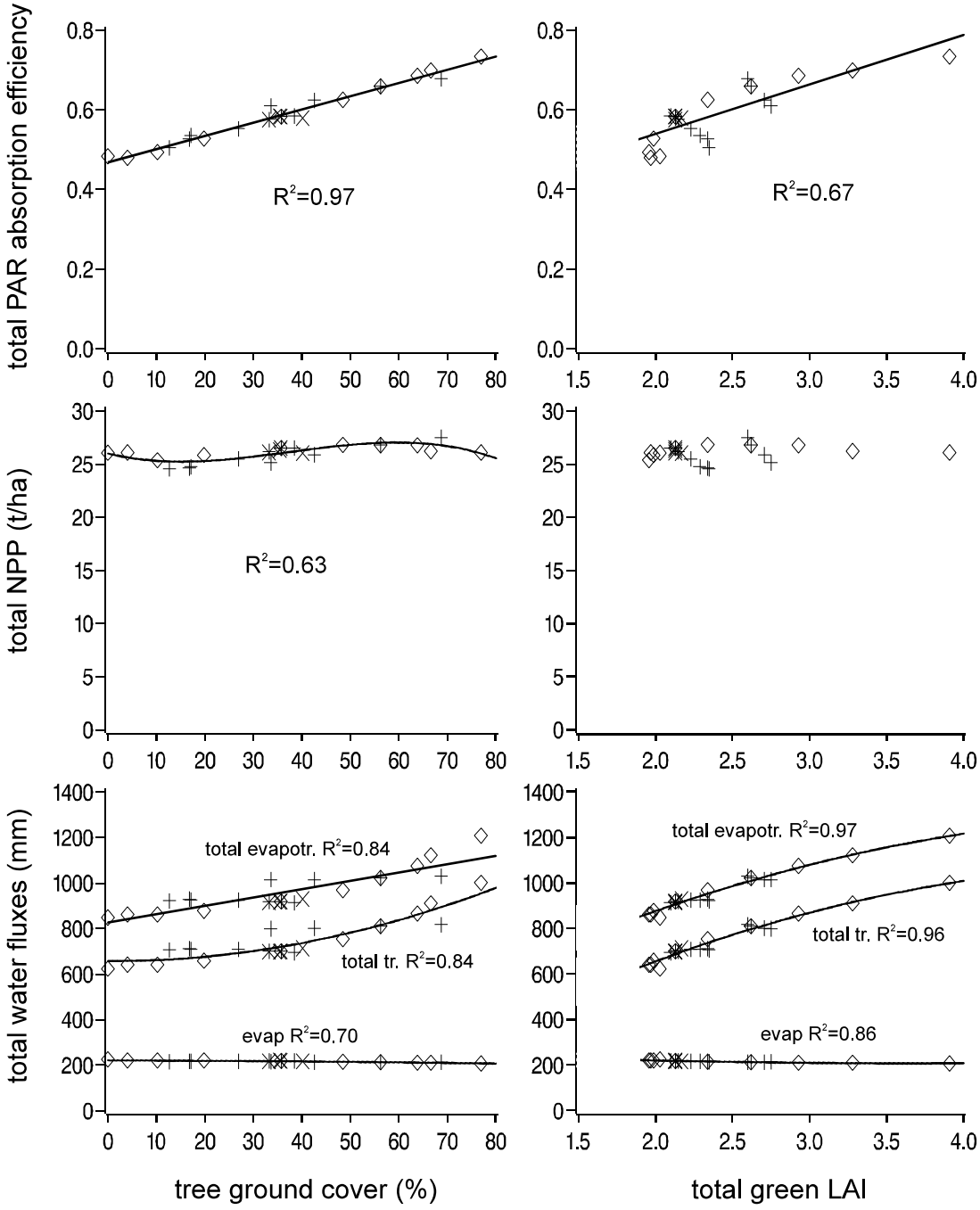

FIG. 8.8 – Variations in total PAR absorption efficiency, NPP, transpiration and evaporation, with tree cover and total annual mean green LAI. Legend as in Figure 8.6. (tr., transpiration ; evap., soil evaporation ; evapotr., evapotranspiration). No significant correlation was found between total NPP and total mean green LAI.

tion and NPP.

Increasing tree density or aggregation did not significantly change the simulated total NPP at the ecosystem scale. The strong increase in the PAR absorption efficiency of the tree layer with increasing tree density, simultaneous to the weaker decrease in the PAR absorption efficiency of the grass layer, entailed an increase in the PAR absorption efficiency of the whole system. Despite this, total NPP remained stable, because C_3 trees should have lower LUE than C_4 grasses under similar environmental conditions (Gosse et al., 1986 ; Prince, 1991) (Table 8.1). Whether this stability in total NPP is a general feature of ecosystems associating C_4 grass species and C_3 tree species, or is a peculiarity of Lamto savannas, needs to be tested (e.g. by applying the model to other sites). However, a savanna model comparison exercise was done within the SCOPE tree/grass modelling activity on an Australian savanna (House et al. in prep.). No model (including TREEGRASS) predicted any stability of total NPP when tree density increased. Thus, the occurrence of NPP stability depends on the savanna system considered.

Effects of tree spatial structure on water fluxes

Predicting the effects of vegetation cover on water fluxes at the soil-plant-atmosphere interface is important from a hydrological or meteorological point of view. However, there is little information available on the effect of tree density on grass, tree, and total transpiration in savannas. Our results are in accordance with experiments of Eastham and Rose (1988) who found that grass transpiration decreased with increasing tree density, and of Eastham et al. (1990) in which total tree transpiration increased with increasing tree density. Our simulated increases in total evapotranspiration with increasing tree density are consistent with field measurements in tropical agroforestry systems and the arid dehesas of South Spain. These studies found that evapotranspiration of tree/grass stands was greater than that of pure grass stands by about 100% (Tournebize et al. 1996), and by 25-65% (depending on year and site, Joffre and Rambal 1993).

Overall, grass and tree transpiration changed less than grass and tree NPP when tree density or aggregation increased. In the energy balance calculation, transpiration depends on net absorbed radiation (i.e. PAR plus IR), but IR radiation penetrates foliage better than PAR, and is thus less influenced by the vegetation structure. This led to a less spatially heterogeneous distribution of transpiration than production, reflected in the fact that water fluxes were better correlated with green LAI (a non-spatial vegetation descriptor) than to tree cover. This explains the stability of total transpiration with tree spatial distribution and with tree size distribution, as total green LAI did not change with these.

4.2.Consequences for tree/grass ecosystem functioning and for the mapping and monitoring of savannas

Implications in the context of woody plant expansion

Tree encroachment has been observed in many savannas worldwide (Polley et al., 1997 ; Archer et al. 2000), including at Lamto over the last 30 years (Gautier, 1989 ; Dauget and Menaut, 1992). If changes in tree cover occur in Guinea savannas, our results show that a change in the water balance, with an increase in the evaporative fraction

(i.e. annual evapotranspiration to rainfall ratio), can occur. Potential impacts of such a change on hydrology and climate need to be explored. A preliminary study coupling a simplified version of TREEGRASS with a hydrological model stressed the importance of taking into account the vegetation cover to predict water balance of a Sahelian savanna at the landscape scale (Boulain, 2000).

If no major change in annual total NPP is expected in the case of tree encroachment, the contribution of trees to total NPP can increase. Part of tree NPP is stored in woody organs, that don't, or only little burn when fire occurs, whereas all aboveground grass phytomass is released in the atmosphere with fire. Therefore, during a shift from grass-dominated to tree-dominated savannas, even if total system NPP is stable, less carbon would be released in the atmosphere. The study suggest that the magnitude of this effect depends on the tree spatial distribution, emphasizing the need to use adequate vegetation descriptors in field studies.

Tree cover and LAI as predictors of savanna function

Results of the simulations show that, if we focus only on total fluxes (water or NPP) at the system level, failure to consider the spatial structure of the vegetation will have little consequence. On the other hand, any study that needs to separate grass and tree functioning cannot ignore tree density and spatial distribution, as both strongly affect grass and tree PAR absorption efficiencies, NPP and transpiration. Simply measuring LAI, for example, would not be sufficient to characterize function in mixed tree/grass systems, in the absence of documenting tree aggregation. Other studies have stressed the importance of spatial patterns in the functioning of forest ecosystems (e.g. Pacala and Deutschman 1995, Gastellu-Etchegorry and Trichon 1998). Our results suggest that combining tree cover and LAI would be appropriate for describing tree spatial structure and predict its effects on carbon and water fluxes in savanna ecosystems.

4.3.Limits of model predictions

Spatial and temporal distribution of nutrient availability

Nutrients are known to greatly influence photosynthesis (Field and Mooney 1986), assimilate allocation (Wilson 1988, Ingestad and Agren 1991, Tan and Hogan 1998), and respiration (Ryan 1995). Cruz (1997) observed an increase of the light and nutrient use efficiencies of a C_4 grass under tree cover. All the simulations made in the present study assumed a constant light use efficiency (LUE) between grasses growing in open areas and under tree cover, but this did not affect the model ability to reproduce a decrease in grass production under tree cover (Simioni et al. 2000). Moreover, in various savannas (Belsky et al. 1989, Weltzin and Coughenour 1990, Vetaas 1992, Rhoades 1997), including Lamto (Mordelet et al. 1993), nutrient availability was found to be spatially heterogeneous, with nutrient-rich soils located under tree cover. Along with better water conditions, this higher nutrient availablity under tree cover explains grass NPP enhancement under tree cover observed in some savanna ecosystems (e.g. Weltzin and Coughenour 1990, Belsky et al. 1993).

Nutrients were not represented explicitly in this first version of TREEGRASS, for sake of simplicity. In the near future, we plan to include detailed physiological production processes (photosynthesis, respiration, carbon and nitrogen partitioning) and a soil

organic matter decomposition model (the SOMKO model, Gignoux et al. 2000), to account for account nitrogen processes.

Functional diversity of the grass and tree layers

Although the model TREEGRASS is able to represent plots with different plant species, only one grass species and one tree species were considered in the present study. This is a simplification of most real savanna ecosystems, because the specific composition of the grass layer can differ under tree cover and in open areas (Belsky et al. 1993, Scholes and Archer 1997). Furthermore, tree species that differ in their ability to acquire spatially heterogeneous resources can co-occur in savannas (Montaña et al. 1995, Breshears et al. 1997a, Le Roux and Bariac 1998, Jackson et al. 1999). In particular, two dominant tree species present at Lamto are known to have different water uptake behaviors (Konaté et al. 1998, Le Roux and Bariac 1998). Although beyond the scope of the present paper, the impact of the functional diversity (presence of different grass and/or tree species having distinct strategies of water uptake or growth) on the savanna functioning will have to be tested in future studies.

Tree architecture

In this study, tree-tree competition did not influence tree architecture (i.e. trees, whenever isolated or aggregated, had a cylindrical shape). But in forests or woodlands, tree crown shape can be influenced by the presence of neighbors (Sorrensen-Cothern et al. 1993, Moravie et al. 1997). Foliage crown shape can influence the acquisition of the light resource (Kuuluvainen and Pukkala 1989, Vales and Bunnel 1998) whereas species-specific plasticity of crown growth patterns sometimes partly determines the competitive ability of co-occuring tree species (Williams, 1996). A similar phenomenon is expected below ground (Eastham and Rose, 1990), and can be important to predict competition for water and nutrients. Thus, including tree shape plasticity in TREEGRASS could improve its predictive capacity.

Climatic variables

In the field, climatic variables are not always spatially homogeneous : temperature, VPD, and wind vary vertically and horizontally both at plot scale and within plant foliage (Tuzet et al. 1997, Daudet et al. 1999). However, explicit computations of feedbacks between plant function and air characteristics would be hardly integrated in an ecosystem model like TREEGRASS, because of computing time limitations. Moreover, the spatial distribution of microclimatic variables is not always of prime importance in determining the distribution of plant functioning. For instance, the spatial distribution of wind was found to have a negligible effect on transpiration and photosynthesis within an individual tree crown (Daudet et al. 1999).

5.Conclusion

Total evapotranspiration was sensitive and total NPP was insensitive to the spatial structure of the tree layer. However the balance between grass and tree functioning was

sensitive to both tree density and spatial distribution, but not to tree size distribution. Because these effects can be of prime importance for the whole system dynamics, further studies are needed to test interactions between carbon and water fluxes and three dimension ecosystem structure and dynamics at larger time and/or spatial scales.

Aknowledgements :

This work was supported by the Programme National de Recherche en Hydrologie (PNRH), and by the European terrestrial Ecosystem Modelling Activity (ETEMA).

Chapitre 9

Déterminisme des effets de la structure spatiale de la strate ligneuse sur les fonctionnements carboné et hydrique.

When and how the spatial structure of the tree layer can influence primary production, water balance, and resource use efficiencies of tree/grass systems ?

en préparation

G. Simioni, J. Gignoux/X. Le Roux

Introduction

Space is considered as a prominant factor influencing plant ecology (Tilman and Kareiva 1997, Murrell et al. 2001). Many works have related its importance on plant demography (e.g. Barot et al. 1999), coexistence (e.g. Chesson and Warner 1981), and population genetics (e.g. Antonovics and Levin 1980). Contribution of space in ecosystem production and water balance processes has drawn much less attention. Pacala and Deutschman (1995) showed that the interactions between plant individuals resulting from vegetation spatial patterns may have a critical impact on ecosystem productivity and species biomass. They argued that spatial patterns at the individual level are of critical importance for production at larger spatial scales, and that they should be accounted for in climate change studies. Simioni et al. (2001b) also showed that vegetation spatial structure could have strong impacts on ecosystem production and water balance. Plants are sessile organisms, and thus they interact only with their local environment. Thus all potential processes affecting plant individual functioning may have consequences at larger spatial scales. The role of space at the ecosystem level on carbon and water fluxes is not well understood, and, regarding the increasing concern about climate change, this gap has to be filled.

Among terrestrial ecosystems, savannas are probably among the most spatially heterogeneous. They are composed of a continuous grass layer underneath an heterogeneous tree layer. Several studies focused on the spatial patterns of the tree layer (e.g. Haase et al. 1996). Soil characteristics are also spatially heterogeneous : savanna trees are often considered as "islands of fertility" (Belsky et al. 1989, Weltzin and Coughenour 1990, Belsky 1994, Rhoades 1997). Termite mounds also contribute to the spatial heterogeneity of soil quality (Konate et al. 1998). The occurrence of strong perturbations like fire (Hochberg et al. 1994) and herbivory (Bailey et al. 1996), which intensities are also spatially heterogeneous, confers even more complexity to the pattern and process relations in savannas. These systems thus present an ideal support to study spatial patterns.

Predicting net primary production (NPP) and water balance in savannas is also of great importance for a variety of practical purposes like assessing savanna role in global production, linking vegetation cover and hydrology to manage water resources or managing silvo-pastoral farming systems.

Simioni et al. (2001b), using a spatially explicit model, TREEGRASS, highlighted the potential influence of tree density and spatial distribution on grass, tree, and total ecosystem productions and water balance in a West African savanna. They showed that tree spatial arrangement (degree of aggregation) could alter how ecosystem production was partitioned between the grass and tree components. However, TREEGRASS described plant production processes in a very simple way, and did not account for nitrogen effects, leaf acclimation to local light regime, and biodiversity.

In this paper, we investigate how the spatial structure of the tree layer can influence NPP, water balance, and resource use efficiencies. Our method consists in the use of an improved version of TREEGRASS (Simioni et al. 2001). In a first section, main features of the model and the simulation experiment design are presented. Predicted NPP, water balance, and resource (water, light and nitrogen) use efficiencies are interpreted in a form of a conceptual frame to characterise when and how vegetation spatial structure will influence ecosystem carbon and water fluxes.

Method

The TREEGRASS-2 model

Model overview

The TREEGRASS-2 model (Simioni et al. 2001e) is an improved version of the spatially explicit, individual based TREEGRASS model (Simioni et al. 2000). It has been designed to study the effects of spatial patterns on ecosystem production and water balance processes.

The main features of TREEGRASS-2 are :

1. TREEGRASS-2 simulates ecosystem production and evapotranspiration at the plant individual scale, and at a daily time over one vegetation cycle.
2. Plant individual foliage and root system are represented in three dimension (3D) within a 3D grid of cells. Different tree and/or grass species can be represented at a time. Plant foliage is distributed within aboveground cells, plant roots are distributed within belowground cells. Branches and truncs are not explicitely represented.

Grid horizontal precision and depths of vertical cell layers can be adjusted to fit with plant dimensions, but cell dimensions are fixed for a whole simulation. Cells containing plant foliage elements will be referred to as "vegetation cells". Individual plants are represented. A grass individual is assimilated to a grass pixel : it occupies one vegetation cell, and its roots are located in soil cells underneath. Thus the number of grass "individuals" depends on the number of cells in a horizontal section of the cell grid. There is no overlap between grass pixels. A tree individual is characterised by its foliage and its root system. A tree foliage is assimilated to a cylinder in which leaf density is homogeneous. Three height, bole (lower limit of foliage), and foliage crown radius are governed by allometric relations. Similarly, the root system of a tree is assimilated to a cyclinder which depth is species dependent, and radius is determined by allometry with tree aboveground dimensions. Tree foliage and roots are distributed in the vegetation and soil cells that overlap with foliage and root crowns. The fraction of a tree foliage or root that is placed in a given vegetation or soil cell is proportionned to the overlap between foliage or root crown and vegetation or soil cell. A tree can overlap with grasses and with other trees (i.e. share vegetation and soil cells). For all grass and tree species, coarse and fine roots are ont differentiated.

3. A 3D radiation absorption submodel (adapted from the RATP model of Sinoquet et al. 2001) computes absorption of photosynthetically active radiation (PAR) and infrared radiation for each sun and shade leaf or soil surface in each vegetation or soil cell, accounting for diffuse radiation and for reflections and transmission by leaf and soil surfaces. This submodel accounts for daily variations of incident radiation.
4. A 3D energy budget submodel (also adapted from Sinoquet et al. 2001) computes, for each sun and shade leaf or soil surface, in each vegetation or soil cell, surface temperature, stomatal conductance or soil surface conductace, and transpiration or soil evaporation. Stomatal conductance is computed according to Jarvis (1976), i.e. a species specific reference conductance is modulated by incident PAR, leaf vapour pressure deficit, and plant water stress. The reference stomatal condutance depends on leaf nitrogen concentration per unit leaf area (N_a).
5. Plant photosynthesis is computed according to Farquhar et al. (1980) or Collatz et al. (1992) given each plant metabolic pathway (C_3 or C_4) and depends on leaf N_a, leaf temperature, and stomatal conductance. A non stomatal inhibition of photosynthesis also occurs in case of severe water stress. Carbon losses through respiration and root exudates are computed as species specific fractions of gross photosynthesis, as suggested by Waring et al. (1998).
6. Carbon allocated to above- and below-ground parts, are computed for each plant using fractions that can be modified so that the fraction of carbon allocated to roots increases when the plant undergoes water stress.
7. Tree individual leaf area index is forced with measured data. Grass leaf growth results from carbon allocated to leaves and leaf mortality rate.
8. The model accounts for species specific temporal courses of tree leaf traits : specific leaf area (SLA, $cm^2 \cdot g^{-1}$), leaf nitrogen concentration (N) and N_a ($g \cdot m^{-2}$). It also reproduces SLA and N_a acclimation to local light environment (Le Roux et al. 1999b, Simioni et al. 2001c).

9. The soil is divided into two strata. Plant transpiration is extracted from the soil according to root spatial location and species vertical water extraction patterns. A soil water budget computes run-off and drainage. Soil water content determines plant water stress according to species sensitivities. Water stress influences plant transpiration, photosynthesis and plant water extraction pattern from the soil.
10. Fire occurs at fixed dates, and removes all grass standing biomass and necromass, and makes all remaining tree leaves to fall. Practically, fire delimits the beginning and the end of a simulation.

TREEGRASS-2 is fully described in Simioni et al. (2001a).

Model parameterization for a West African savanna

The model was parameterized and tested for a West African savanna (Lamto, Ivory Coast) as in Simioni et al. (2001a). The natural reserve of Lamto is located in Ivory Coast (6°13'N, 5°02'W). Mean monthly temperatures are constant throughout the year (27°C). Rainfall averages 1200 mm·year^{-1} and determines dry seasons (from November to March, and in August) and rainy seasons (from April to July, and from September to October). Soils are ferralsol (according to the FAO classification). Forests are present along streams, but most of the reserve is covered by savanna areas. In the savanna, the herbaceous layer is composed of C_4 perennial grasses, mostly from the Andropogoneae family. Tree density varies along the catena, from almost pure grassland in bottomlands to dense shrub facies on plateaus. Trees are mainly composed of four species and can be found aggregated in clumps or isolated. Fire is set every year in early January and delimits the vegetation cycle.

Grass species photosynthetic characteristics (Simioni et al. 2001e) and water behavior (Le Roux et al. 1995) of dominant species were fairly homogeneous. Thus one generic grass species representative of the Andropogoneae family is represented. Two codominant tree species were modelled : *Crossopteryx febrifuga* and *Cussonia arborea*. They were found to have contrasting gas exchange characteristics (Simioni et al. 2001e), water behaviors (Le Roux and Bariac 1998), phenologies and leaf traits (Simioni et al. 2001c). However it seems that these differences yield similar NPP for the two species and a slighlty higher transpiration for *C. arborea* (Simioni et al. 2001a).

The simulation experiment

Simulations performed

Simulations were performed for an annual vegetation cycle, starting and ending at dates corresponding to fire occurrence (i.e. in early January). Daily climate data for the 2000 vegetation cycle were used, as data needed to run the model (leaf trait temporal variation parameters, tree LAI temporal dynamics, initial soil water contents) were measured for the 2000 vegetation cycle (Simioni et al. 2001c).

Tree spatial structure is composed of tree density, tree spatial distribution, and tree size class distribution. Simioni et al. (2001b) found no effects of tree size class distribution on production and water processes. Thus this work focused the effects of tree density and spatial arrangement. Simulation plots are presented in Figure 9.1. All trees had the same dimensions (3.61 m high, 4 m^2 canopy cover). All simulations were done with a

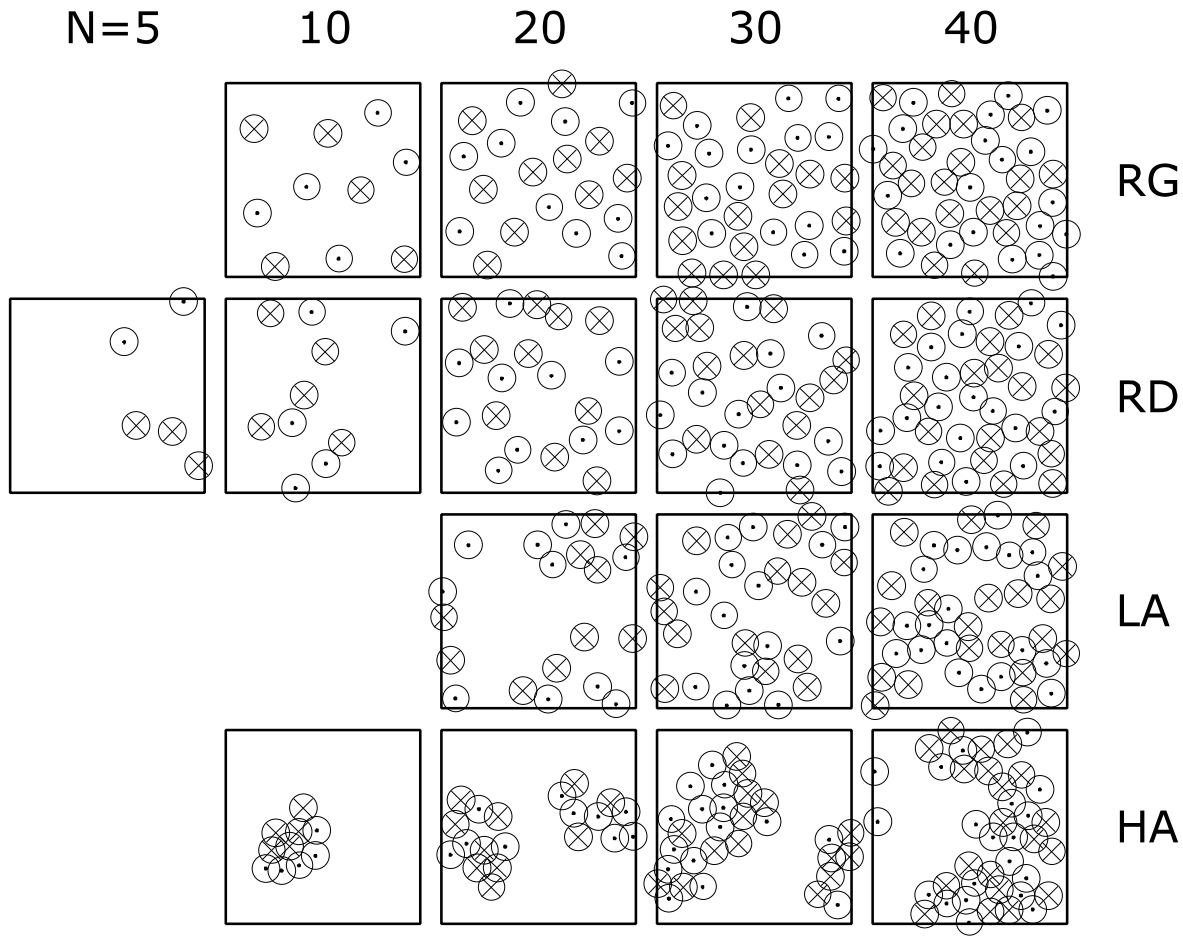

FIG. 9.1 – Maps of the simulation plots. Tree density ranges from N=0 (not shown) up to 40 trees per plot. Tree spatial distribution was regular (RG), random (RD), loosely aggregated (LA) or highly aggregated (HA). Each plot was 16×16 m. Tree indiviuals belong to two species : *Crossopteryx febrifuga* ($\odot$) or *Cussonia arborea* ($\otimes$). All trees had the same dimensions.

random mix of the two species, keeping an equal number of trees for each species. Each simulation plot was 16×16 m, with a basal grid cell size of 1×1 m, and 4 vertical grid strata : a grass stratum, an empty statum, and two strata for tree foliage. Tree density varied from 0 (pure grass site) to 40 trees per plot (i.e. 0 to about 1500 individuals/ha). At each tree density, simulations were done at regular, random and aggregated tree spatial distributions.

Random distributions were obtained using a Poisson random process respecting an inhibition distance between tree trunks of 1.92 m to prevent important overlap between tree canopies. Regular distributions were obtained using the same process but with higher inhibition distances, respectively 3, 3, 2.6, and 2.24 for tree densities of 10, 20, 30, and 40 (high tree densities did not allow important spacing between trees).

Aggregated distributions were obtained using a random Poisson process to generate parent points to which child points were associated randomly respecting a maximum

radius from parent points, and an inhibition distance between trees. Tree clump radius were 4.8 and 1.6 m for loosely and highly aggregated distributions. Mean number of trees per clump was set to 5 for both loosely and highly aggregated distributions. Inhibition distances between trees were 1.7 and 1.4 m for loosely and highly aggregated distributions, respectively. These aggregation parameters allowed to prevent excessive overlap between tree canopies, in order to respect a minimum light availability under tree cover, as was assessed in the field using hemispherical photographs (data not shown).

Model outputs and result presentation

Annual PAR absorption, NPP and transpiration were sorted for the tree and grass components by additioning all grass and tree individuals together. Annual total soil evaporation was computed as the sum of the amounts of water evaporated from all soil pixels.

LUE was computed as the ratio of NPP to absorbed PAR. Similarly, WUE was computed as the ratio of NPP to transpiration. NUE, for either the grass or the tree components, was calculated on a daily basis, as the ratio of daily production to leaf nitrogen mass. These daily NUE were weighted to account for the contribution of corresponding daily NPP to annual NPP. Daily weighted NUE were then summed to obtain annual grass and tree NUE, that thus represented a weighted mean daily NUE.

Results

Tree spatial structure effects on carbon and water fluxes

Tree PAR absorbtion increased, and grass PAR absorption decreased with increasing tree density (Figure 9.2). Dead leaf area contributed to one third of total green plus dead leaf area PAR absorption for the grass component at all densities. Total PAR absorption on a green plus dead leaf area basis was constant, while it increased up to 26% on a green only leaf area basis. The range of these trends were influenced by tree aggregation. Increasing tree aggregation increased grass PAR absorption up to 28% (at 30 trees/plot), and decreased tree PAR absorption up to 31% (at 10 trees/plot). Total system PAR absorption was only slightly affected by tree aggregation (-5.6% at 30 trees/plot, on a green only leaf area basis).

Grass and tree NPP showed the same trends than for PAR absorption. However, total NPP decreased with tree density by 19% for random tree distributions, but was less importantly affected by tree aggregation. The magnitude of changes in NPP with tree aggregation are presented in Figure 9.3.

Grass and tree transpiration also followed the same trends than PAR absorption and NPP, but were less sensitive to tree aggregation (Figure 9.2). The total system transpiration was wholely stable with tree density and tree aggregation (maximum change of 5.4% between regular and highly aggregated tree distributions at 40 trees/plot). Soil evaporation was fairly constant with tree density, with values between 260 and 280 mm (data not shown).

The range of grass and tree variations in PAR absorption, NPP and transpiration, were different between tree densities. Tree variations in PAR absorption, NPP and transpiration with tree aggregation were more pronounced at low tree densities, while

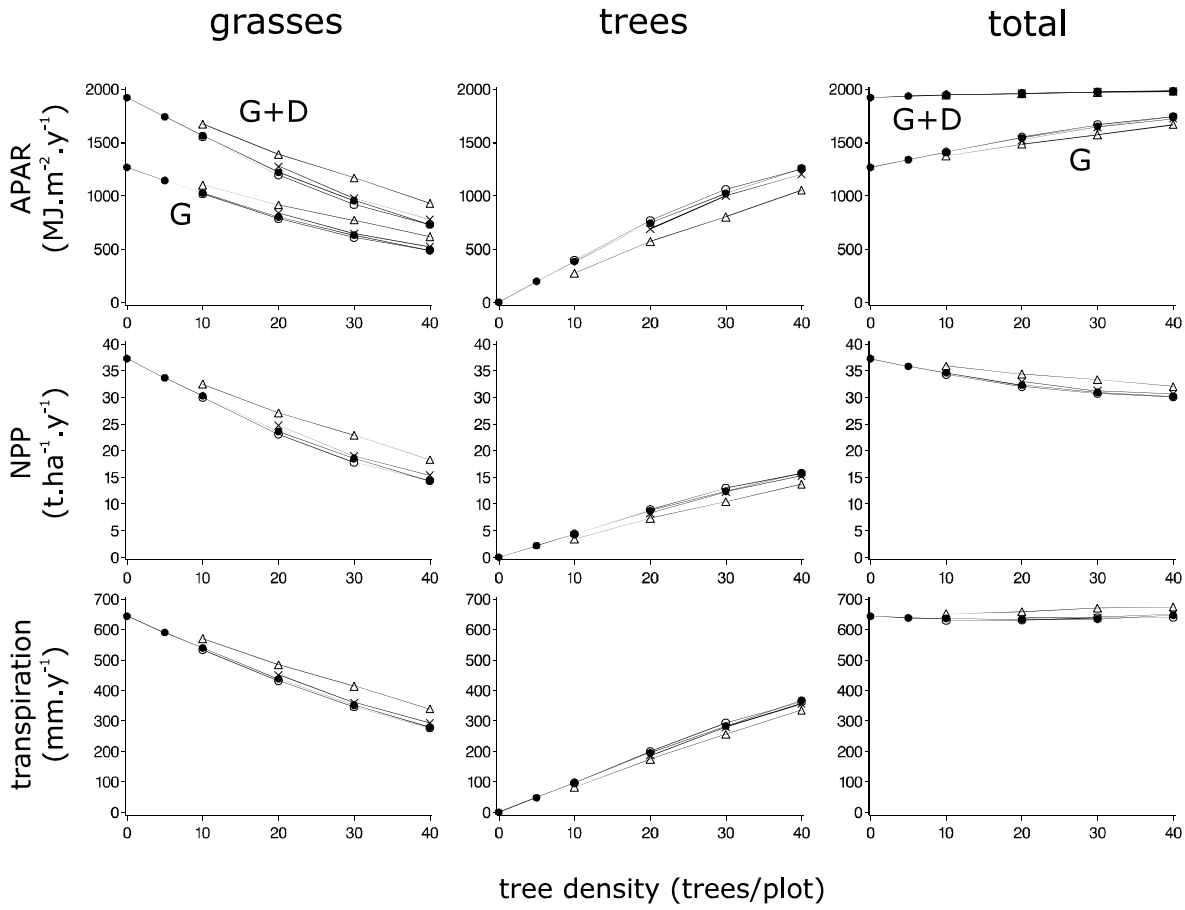

FIG. 9.2 – Predicted variations in annual grass, tree, and total system absorbed photosynthetically active radiation (APAR), net primary production (NPP), and transpiration (mm), with tree density. Effects of regular (○), random (●), loosely aggregated (×), and highly aggregated (△) tree distributions are presented. APAR is presented accounting for grass green leaf area (G) or grass green plus dead leaf areas (G+D).

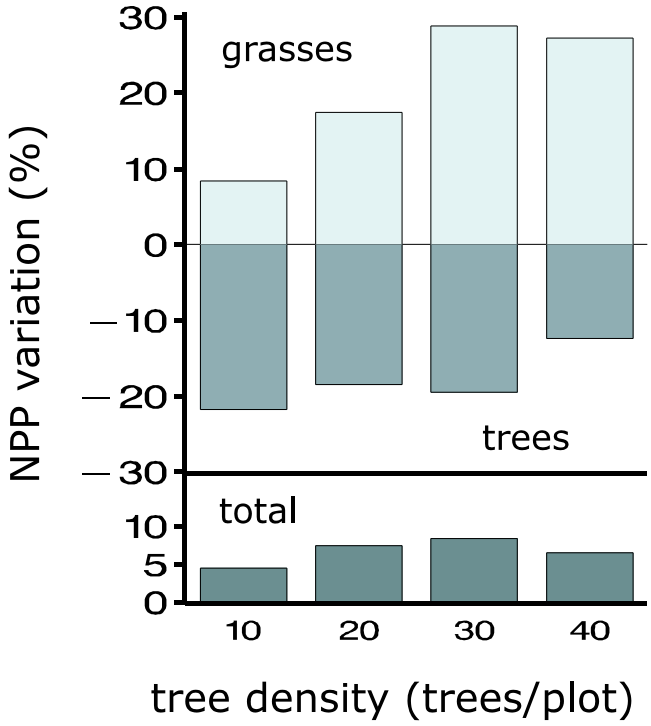

FIG. 9.3 – Percent of variation in grass, tree and total NPP when shifting from regular tree distribution to highly aggregated tree distributions, for different tree densities.

grass variations in PAR absorption, NPP, and transpiration were more important at high tree densities (see Figure 9.3 for NPP).

Tree spatial structure effects on resource use efficiencies

Grass LUE was constant with tree density at about 2.95 g DM·MJ^{-1} APAR on a green only leaf area basis (Figure 9.4). Grass LUE was not affected by tree aggregation. Tree LUE increased by 14% with tree density (for random tree distributions), but was wholely much lower than grass LUE with values around 1.2 g DM·MJ^{-1} APAR. Tree LUE was slightly affected by tree aggregation (+13% at 10 trees/plot). The shift from grass to trees as tree density increased made the total system LUE to strongly decrease (-41% on a green only leaf area basis, for random tree distributions, -22% on a green plus dead leaf area basis). Total system LUE was slightly affected by tree aggregation (+15% or +8.6% on a green only leaf area basis, or on a green plus dead leaf area basis, respectively, at 30 trees/plot).

Grass WUE decreased a little, while tree WUE was rather constant with tree density (-11% and 4% for random tree distributions, respectively). Grass and tree WUE were slightly affected by tree aggregation (+7.4% at 30 trees/plot, and -7.9 % at 10 trees/plot, respectively). But grass WUE (about 5.4 g DM·kg^{-1} H_20) was always higher than tree WUE (about 4.45 g DM·kg^{-1} H_20), and as tree density increased, whole system WUE decreased importantly. The whole system WUE was rather insensitive to tree aggregation.

Grass and tree NUE were rather insensitive to tree density and aggregation, but as

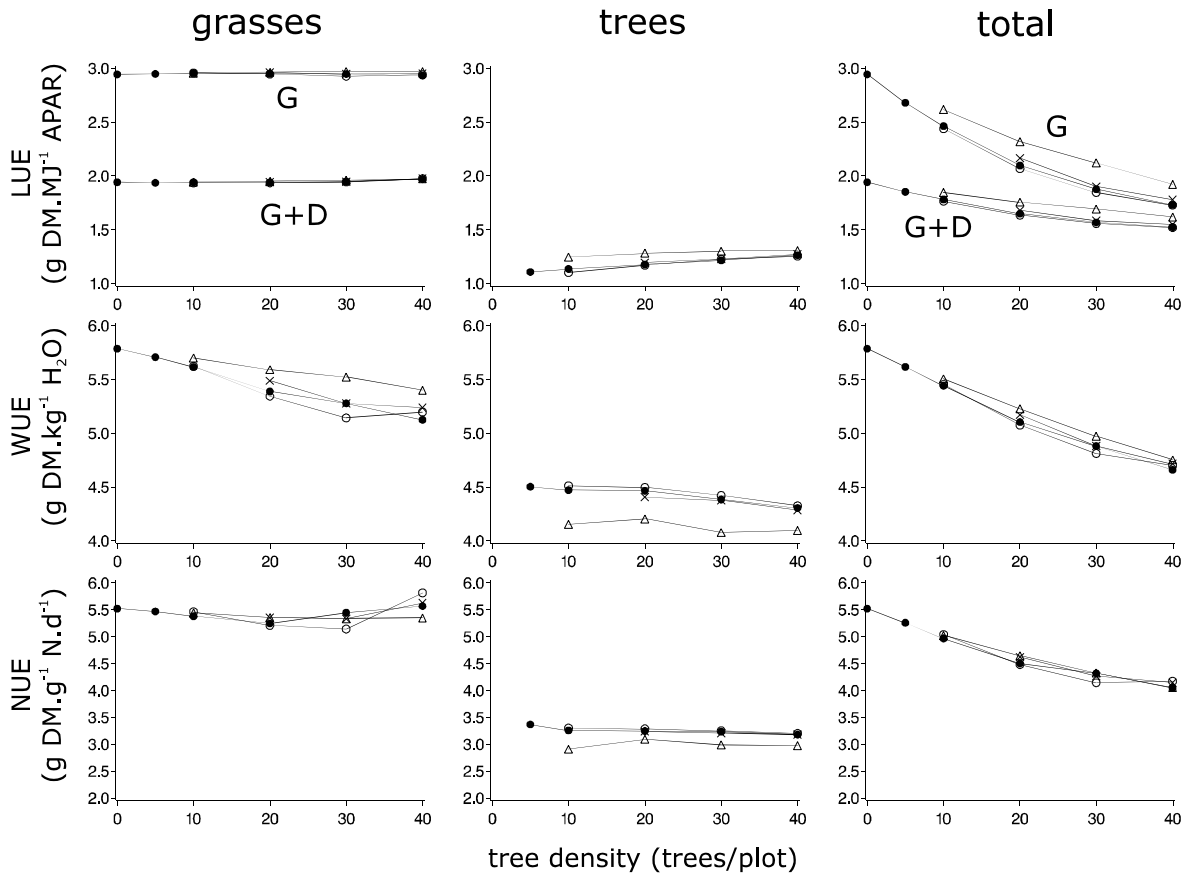

FIG. 9.4 – Predicted variations in annual grass, tree, and total light use efficiencies (LUE), water use efficiencies (WUE), and nitrogen use efficiencies (NUE), with tree density. Effects of regular (○), random (●), loosely aggregated (×), and highly aggregated (△) tree distributions are presented. LUE is presented accounting for grass green leaf area (G) or grass green plus dead leaf area (G+D).

grass NUE (about 5.2 g DM·g^{-1} N) was much higher than tree NUE (about 3.2 g DM·g^{-1} N), the whole system NUE decreased with tree density.

Discussion

Increasing tree density alters ecosystem performance

Water and nitrogen are strong limiting factors in savannas (Scholes and Archer 1997). But species have contrasting ability to use limiting resources. On a production basis, C_4 species are more efficient to use water, light, and nitrogen than C_3 species (e.g. Sage and Pearcy 1987). Species used for simulations do not except the rule : photosynthetic water and nitrogen use efficiencies (ratio of leaf net photosynthesis to leaf transpiration and leaf nitrogen) were largely higher for grasses than for trees (Simioni et al. 2001e). Model simulations reflect these results, though the difference between grass and tree NUE is lower than that measured at the leaf level. This must be due to grass self-shading (by green and dead leaves). When tree density increases, a larger fraction of resources are manipulated by the tree component. And because trees belong to the C_3 pathway, the whole system LUE, WUE and NUE decreased with increasing tree density. These trends are thus directly dependent on species efficiencies, and they do probably not persist in savannas associating C_3 trees and C_3 grasses (e.g. in Sahel). Indeed, changes in whole system resource use efficiencies depend on the resource use efficiencies of the species it is composed of, and of the abundances of these species. Species belonging to the same matabolic pathway may also present constrasting resource use efficiencies (see Ruimy et al. 1994 for LUE). As tree encroachment in savannas is a worldwide phenomemon (Archer et al. 2000), changes in ecosystem resource use efficiencies should be studied for the different types of savannas.

Ecosystem NPP variations with tree density depend on species productivity

The response of grass NPP to increasing tree density can be linear or non linear (see Scholes and Hall 1996). In this study, changes in grass NPP with changes in tree density were rather linear, while, for the same system, simulations done with the first version of TREEGRASS, grass NPP decreased non linearly with increasing tree density (Simioni et al. 2001b). This difference must be due to differences in grass productivity potentials. In the present work, grass computed LUE (on a green only leaf area basis) was 2.95 g dry matter·MJ^{-1} absorbed PAR, while the value used in Simioni et al. (2001b) was 2.28, and initial water conditions were better in the present work, allowing grasses to start growth earlier. Thus a more dense tree cover is needed to suppress grass production in this study than in Simioni et al. (2001b).

Another difference between this study and the previous experiment made with the first version of TREEGRASS is the change of total NPP with tree density. Simioni et al. (2001b) found a stable total NPP, while in this study, total NPP decreased with tree density. This must be due to differences in tree and grass productivity capacities. In Simioni et al. (2001b), grass LUE was lower, and tree LUE slightly higher than in the present work. Trees absorb more PAR than grasses, but have a lower LUE. The compensation between a higher absorbed PAR and a lower productivity may theoretically yield to an

increase, a constancy, or a decrease in total system NPP. The trend depends on the difference of productivity between trees and grasses. For low differences, total NPP may increase, and for high differences, total NPP will decrease with increasing tree density.

The overall transpiration was constant, instead of a strong increase in the previous study. This may be due to the lowest stomatal conductance at low N_a values. N_a depends of the light level, being lower for shade leaves. As tree density increased, the shade of a tree by its neighbours increased, making its overall N_a decreasing, and thus its overall stomatal conductance decreased. The same process applies for grasses. This resulted in a constant system transpiration.

Contrasts in species productivity conditions the influence of the tree spatial structure on ecosystem function

Simioni et al. (2001b) provided a first evidence of the potential influence of tree spatial arrangement on carbon and water fluxes. The present work provides more detail on how and when these effects occur. Between NPP and transpiration, NPP was the most sensitive to tree spatial distribution. Tree NPP varied more with tree spatial distribution at low tree densities. At low densities, competition between trees can be inexistent (completly isolated tree) or on the opposite can be extremely high (dense tree clumps). When tree density increases, the range of spatial distributions is constrained, and trees cannot escape competition with each other. Thus relative effects of tree spatial distribution on tree function will be more important at low tree densities.

On the opposite, the effects of the tree spatial distribution on grass NPP are more important when tree density increases. At very low tree densities, the ratio of grass to tree NPP is so high that any change in tree spatial distribution will change very little the grass production. Then a trade off appears, because when tree density is very high, no change of tree spatial distribution is possible, and thus the effect on grass is constant. This results in a range of tree densities for which changing tree spatial distribution is still sensible enough to induce important changes in grass NPP. This can be summurized in a conceptual frame.

The combination of tree density and spatial distribution can be viewed as an area of possibilities in the form of a triangle (Figure 9.5a). Limits of this area are 1) no trees (bottom), 2) excessive overlap between tree canopies at maximum tree aggregation (left) and 3) excessive overlap between tree canopies at maximum tree density (top). At the lower part (low densities) of the triangle is a zone of maximum effect of tree spatial arrangement on tree functioning (Figure 9.5b). The upper limit of this zone is probably determined by tree ability to “escape” competition (i.e. by having distinct phenologies, water uptake behaviors, etc.). At an intermediate tree density level is a zone of maximal effect of tree spatial distribution on grass functioning (Figure 9.5c). The factors that determine the extent of this last zone depends on the resource use efficiencies of the coexisting tree and grass species. The combination of species capacities result in various tree/grass ratio in terms of NPP or water balance. The more symmetric the tree/grass ratio, the more important the overlap between grass and tree zones of maximal effects. In systems where grasses present a very high production capacity compared to trees, overlap may not occur (Figure 9.5d). In Simioni et al. (2001b) the tree/grass ratio was rather well balanced at 20 trees/plot in terms of NPP, and changing the spatial distribution of trees affected importantly both tree and grass NPP (overlap, like in Figure 9.5e).

In the present study, the ratio was balanced at 40 trees/plot. But with such a density, tree-tree interactions are strong even at regular distributions. Thus only a small overlap between tree and grass zones of maximal effect occurred.

Conclusion

This paper completed well the results of Simioni et al. (2001b) that showed that ecosystem function could be influenced by the tree layer spatial structure. This work showed that ecosystem resource use efficiencies can be strongly altered when tree density increases, while resource use efficiencies of the tree and grass components were relatively stable. It also provided some clues about conditions determining the effects of tree spatial structure on ecosystem NPP and water balance. Tree spatial structure will have the strongest effects on both grass and tree components when grass and tree species present similar productivities. These results strongly suggest to study species functional attributes in the different savannas of the world, especially those associating C_3 grasses and C_3 trees to confirm the trends developped in this paper. They also suggest to study all factors affecting species productivity capacities, such as climate or herbivory, as species may respond differently to environmental limitations.

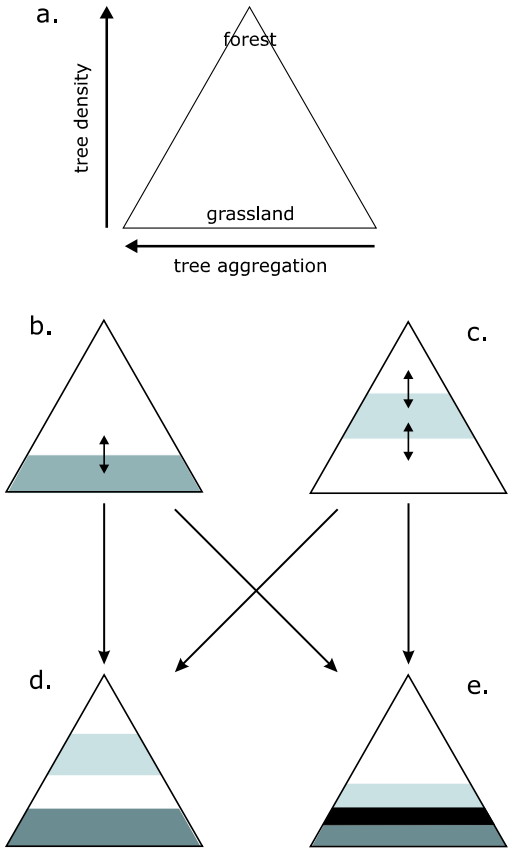

FIG. 9.5 – Simple representation of tree spatial distribution effects on production patterns. Savannas can be seen as a combination of tree densities and tree aggregation (a.). When tree density increases, less aggregation patterns are possible, because of the reduced land area allocated to a tree individual. This means that the most important tree aggregation effects on tree production will occur at low tree densities and a zone of maximal impact on trees can be drawn (b.). The effects of changing tree aggregation on the grass layer production is maximal when the tree/grass ratio is balanced, and a zone of maximal impact on grass can be drawn, which upper and lower limits depend on the difference of productivity between grasses and trees (c.). When grasses are more productive than trees, a balanced tree/grass ratio is found only at high tree densities, and zones of maximal impact on grasses and trees correspond to distinct tree densities (d.). On the opposite, when tree and grass have similar productivity, the two zones of maximal impact will overlap, and the tree spatial distribution will have strong effects on both tree and grass components (e.).

Conclusion & Perspectives

Chapitre 10

Conclusion et perspectives

Détailler pour simplifier

Objectifs et réalisations

La Figure 10.1 présente l'approche "bottom up" adoptée au cours de cette thèse, avec, pour chacune des étapes, les réalisations correspondantes à l'étude de la structure spatiale de la strate arborée.

Détailler les processus permet de distinguer, dans un contexte donné, ceux jouant un rôle prépondérant de ceux qui sont négligeables. Si des effets importants d'un processus sont mis en évidence avec TREEGRASS à une échelle spatiale et temporelle fines, et qu'il apparaît profitable d'en tenir compte à des résolutions spatiales ou temporelles plus grossières, des simplifications sont nécessaires.

TREEGRASS devrait permettre de calibrer de telles simplifications. Ainsi, l'utilisation de TREEGRASS en temps qu'outil de référence devrait permettre d'opérer des simplifications *a posteriori* des processus, c'est à dire en pouvant quantifier la marge d'erreur due à la simplification, par rapport à une situation de référence.

Simplifications à des fins de changement d'échelle

> *"The importance of processes governing fine-scale spatial heterogeneity implies that biospheric models will agree with nature only if they are phenomenological (e.g. fitted to data) at large scale, or if scaling rules are discovered that allow one to derive system-level properties from individual-level processes."*
>
> Pacala and Deutschman 1995

De fait, les résultats de cette thèse permettent de proposer deux pistes de simplification : l'utilisation de descripteurs de végétation que sont le LAI et le recouvrement arbre, et celle des efficiences d'utilisation de la lumière.

LAI et recouvrement arbre

Au Chapitre 8, il a été montré que le recouvrement arbre (tree cover) était bien corrélé aux flux annuels de carbone, et que le LAI moyen annuel était bien corrélé aux flux d'eau. Cela suggère que pour prédire les flux de carbone et d'eau, il n'est pas nécessaire

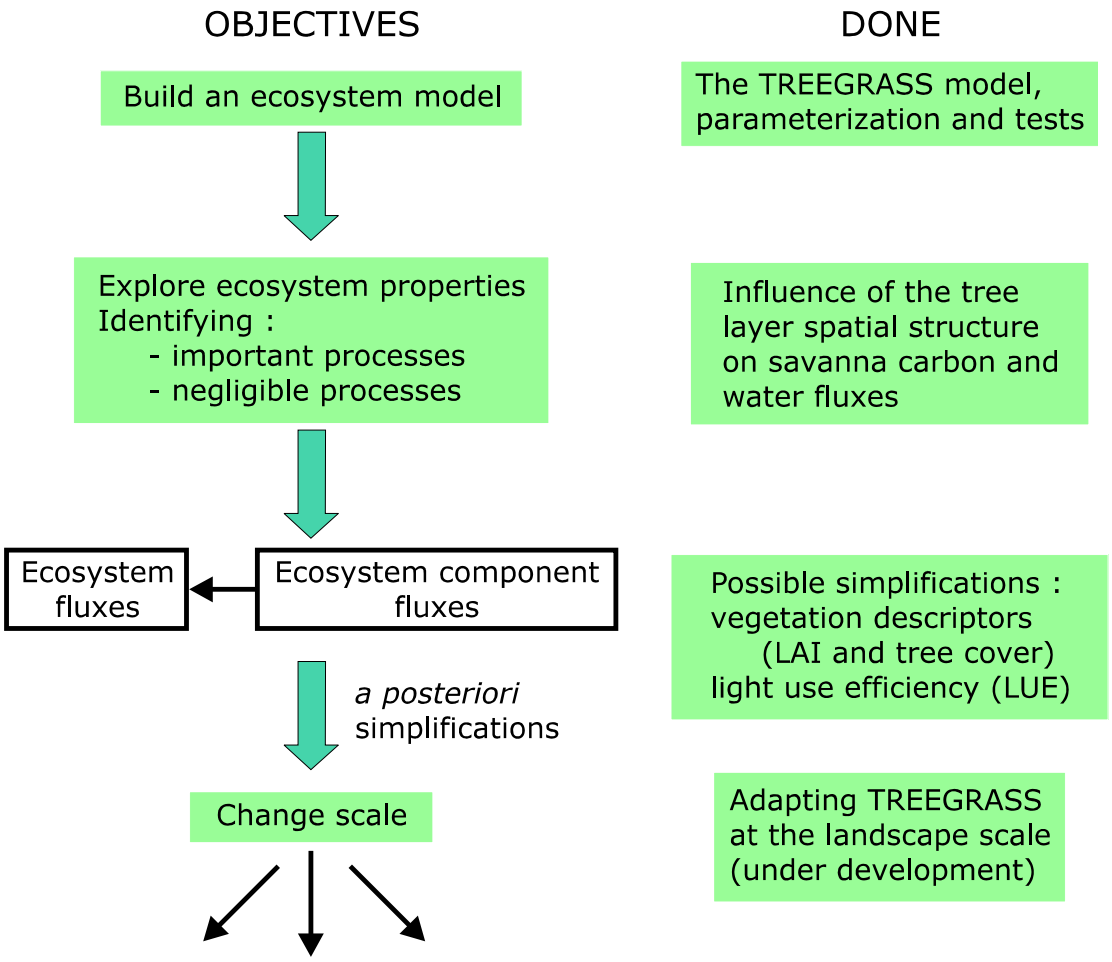

FIG. 10.1 – Démarche contextuelle de la thèse et réalisations.
Background objectives and thesis achievements.

de connaître la structure spatiale fine de la végétation, mais que l'utilisation conjointe du recouvrement arbre et du LAI devrait permettre des estimations correctes de ces flux.

Une partie du travail de thèse de Nicolas Boulain, au laboratoire d'écologie de l'ENS, est justement de mettre au point une méthode de changement d'échelle pour tenir compte de l'influence de la structure spatiale des arbres sur le fonctionnement carboné à l'échelle d'un bassin versant. C'est une première tentative d'utiliser TREEGRASS à des fins de changements d'échelle.

Efficience d'utilisation de la lumière (LUE)

La LUE est utilisée par certains modèles de végétation pour prédire la production (ex. Ruimy et al. 1996). Au Chapitre 9, il a été montré que la LUE de l'écosystème peut varier avec la structure spatiale de la strate ligneuse, et donc qu'on ne peut appliquer une seule valeur à l'échelle de l'écosystème. En revanche, il a été montré que les valeurs de LUE sont stables pour chacune des composantes herbe et arbre. Connaître les LUE des composantes et les abondances relatives de ces composantes dans l'écosystème devrait permettre de mieux paramétrer les savanes dans les modèles de végétation utilisant ce type d'approche.

L'intérêt d'intégrer les processus à l'échelle de l'écosystème

Une partie des résultats acquis aux cours de cette thèse n'auraient pu être présentée si l'on ne s'était attaché à intégrer les processus sous-tendant le fonctionnement de l'écosystème. L'estimation des efficiences d'utilisation des ressources, et les bilans de carbone annuels respectifs des deux espèces d'arbre en sont de bons exemples.

Efficiences d'utilisation des ressources

Leur calcul implique de pouvoir estimer :
- la production herbe, arbre, ou totale ;
- la quantité de resource utilisée (lumière, eau, azote).

Qui dépendent de nombreux processus mettant en jeu les réactions de l'écosystème à des changements de structure. Réactions qui ne peuvent être extrapolées simplement à partir de mesures à l'échelle d'une plante, par exemple, puisque cela n'intègre pas la compétition entre plante.

Production des espèces d'arbre

Des mesures d'échanges gaseux foliaires, de phénologie, de trait foliaires et de mode d'extraction de l'eau du sol suggéraient des contrastes significatifs entre *Crossopteryx febrifuga* et *Cussonia arborea*. Or lorsqu'elles sont présentes à égales abondances, ces espèces présentent des productions annuelles très proches. Là également, ce n'est que lorsque l'on tient compte de l'ensemble des processus et des feedbacks opérant à l'intérieur de l'écosystème que l'on peut savoir dans quelles mesures des contrastes vont se compenser au cours d'un cycle de végétation.

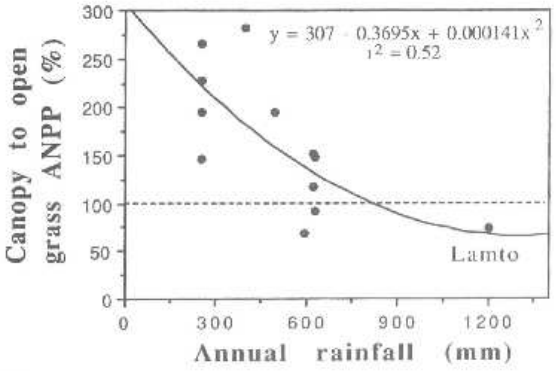

FIG. 10.2 – Effets du couvert arbre sur la production herbe, en fonction des précipitations annuelles (d'après Mordelet et Le Roux 2001).
Tree cover influence on grass production at different annual rainfall levels (after Mordelet and Le Roux 2001)

Autres aspects du fonctionnement à intégrer

La composition spécifique

Les résultats présentés au cours de cette thèse sont valables pour des associations de type herbes C_4 et arbres C_3.

Les plantes à métabolismes C_4 ou C_3 présentent des caractéristiques très différentes. Il serait donc intéressant de reproduire l'étude pour des associations de type C_3-C_3, courantes dans certains types de savane (au Sahel par exemple). On peut également aller plus loin et ne pas s'intéresser qu'aux simples différences herbes-arbres, mais étudier

Variabilité climatique et interaction herbes-arbres

Le couvert arbre peut avoir différents effets sur la production herbe. La Figure 10.2 suggère une facilitation de la production herbe par le couvert arbre en zone de savane sèche, et une suppression en zone de savane humide. Or ces zones ne diffèrent pas seulement par la pluviométrie, mais également par les espèces en présence ou le type de sol. Distinguer l'influence de chacun de ces facteurs devrait permettre de mieux comprendre les différences de réaction de la production herbe au couvert arbre dans différents types de savane.

Un deuxième aspect concerne les expériences par contraste des expériences par gradient. Chaque point dans la Figure 10.2 correspond à une comparaison entre une situation "sous couvert arbre" avec une situation "hors couvert arbre" (contraste), sans que le couvert arbre soit quantifié. Au cours de la thèse, on a pu quantifié le couvert arbre au moyen de photos hémisphériques (gradient entre zones ouverte et complètement recouverte). Avec TREEGRASS, en étudiant la répartition spatiale de la production herbe intra-site (pour chaque pixel herbe), on peut simuler la relation entre production herbe et recouvrement arbre le long d'un gradient de recouvrement arbre.

A étudier : d'autres aspects du fonctionnement des savanes

Les changements climatiques

Le rôle que peuvent jouer les savanes dans le cadre des changements climatiques reste malconnu. TREEGRASS, dans son état actuel, ne permet pas une étude rigoureuse des effets de l'augmentation du CO_2. Celui-ci est en effet susceptible d'agir non seulement sur la photosynthèse, mais sur la respiration, les teneurs en azote des organes, sur l'allocation des assimilats aux différents organes des plantes ... et sur le fonctionnement du sol lié à la matière organique.

Etudier les effets des changements climatiques sur le fonctionnement des savanes en partant du modèle TREEGRASS nécessiterait donc :

- de coupler le modèle TREEGRASS avec un modèle de décomposition de la matière organique du sol (par exemple le modèle SOMKO, Gignoux et al. 2000, développé au laboratoire d'écologie de l'ENS) ;
- de développer les aspects de la physiologie des plantes liés notamment à l'absorption des nutriments par les racines, et à l'allocation des assimilats ;
- de changer d'échelle spatiale si l'on veut pouvoir étudier la question à l'échelle du paysage ou du biome.

La coexistence herbes-arbres

La question de cette coexistence est importante dans le contexte d'augmentation du couvert ligneux dans l'ensemble des savanes du globe (Archer et al. 2000). Différentes causes de cette coexistence ont été avancées (Skarpe 1992), parmi lesquelles l'importance des perturbations telles que le feu ou l'herbivorie. Dans tous les cas les mécanismes s'opèrent à des échelles de temps assez grossière.

En partant du modèle TREEGRASS il faudrait :

- développer des méthodes de changement d'échelle temporelle ;
- inclure les effets des perturbations ;
- coupler TREEGRASS avec un modèle de démographie des arbres (ex. Gignoux 1994).

La modélisation comme moyen d'intégrer les processus

Manipuler la complexité de l'écosystème

Je rejoins l'opinion de Luo et Reynolds (1999) selon laquelle, pour connaître comment les écosystèmes peuvent réellement réagir à des perturbations (ces auteurs se placent dans le contexte d'une augmentation de CO_2 atmosphérique), il est nécessaire d'utiliser des approches intégratrices d'un grand nombre de processus. Je pense également que ce n'est qu'en tentant d'"embrasser" la complexité du réel comme on tend à le faire avec TREEGRASS, qu'on pourra mettre en évidence des phénomènes n'apparaissant qu'avec un nombre d'interactions et de feedbacks élevé au sein d'un système.

Or manipuler la complexité d'un écosystème est extrêmement difficile voire impossible par des approches expérimentales classiques. Quand bien même on peut expérimentalement manipuler la biodiversité en environnement contrôlé, les moyens à mettre en oeuvres sont colossaux, et le nombre de réplicats est toujours limité. Manipuler la

structure spatiale d'un écosystème est impossible en savane, sachant que l'on ne trouvera jamais deux parcelles naturelles ne variant que par la densité ou le degré d'agrégation des arbres. Enfin, seuls des modèles peuvent permettre d'appréhender des processus opérants à des échelles de temps très vastes (plusieurs siècles, par exemple).

Un modèle tel que TREEGRASS, fournit, pour une simulation sur un cycle de végétation, les caractéristiques de production, de transpiration, de surface foliaire, de teneur en azote, de stress hydriques... par individu plante et par jour, et pour les teneurs en eau des cellules de sol. Aucun suivi de végétation sur le terrain ne peut fournir un tel niveau de détail.

TREEGRASS : un modèle lourd, mais polyvalent et évolutif

Construire un modèle tel que TREEGRASS requiert un investissement important en terme de (i) programmation, (ii) de données de terrains (nécessaires pour paramétrer et valider), et (ii) de mise en oeuvre (besoin d'ordinateurs puissants). C'est en outre, dans son état actuel, un modèle délicat à manipuler à cause du grand nombre de paramètres qu'il nécessite, et qui limite son utilisation à des sites bien documentés.

Cependant, TREEGRASS offre la possibilité d'étudier de nombreux aspects du fonctionnement de l'écosystème. Par exemple :

- on s'est pour l'instant centré sur les effets de la structure spatiale de la strate ligneuse sur les flux de carbone et d'eau, on peut aussi s'intéresser à la répartition intra-écosystème de ces flux ;
- le modèle peut être utilisé pour étudier l'influence de la biodiversité sur les flux ;
- ou encore l'influence de la variabilité climatique ;
- l'importance de l'architecture des courones des arbres ;
- ...

TREEGRASS n'a pas été conçu comme un modèle éphémère, mais comme un outil évolutif devant permettre d'intégrer par étape un nombre croissant de processus. Avec deux versions en trois ans, on a pu montrer que ce type de modèle est réalisable.

Indissociabilité entre modélisation et expériences de terrain

Les intérêts à utiliser des modèles d'écosystèmes ne valent que si ces modèles peuvent être correctement paramétrés et testés. Or paramétrisation et tests nécessitent de nombreux jeux de données. D'où l'intérêt des sites d'étude de référence fortement documentés, tels que la savane de Lamto.

La première version de TREEGRASS a tiré profit des informations déjà disponibles sur le site de Lamto. Ces informations ont dû être complétées pour construire la deuxième version. Les informations acquises sur les arbres ont tenté de "rattraper" le retard par rapport à la strate herbacée. D'autres expériences faites au cours de la thèse, dont les données n'ont pas encore été analysées, apporteront d'autres informations sur l'architecture et les flux transpiratoires de *Crossopteryx febrifuga* et *Cussonia arborea*. L'ensemble de ces expériences a aussi été l'occasion d'initier un suivi de la végétation à long terme.

Les mesures d'échanges gazeux foliaires et d'azote foliaire sont des données rares pour des espèces de savane, mais indispensables pour paramétrer des modèles de végé-

tation, que ce soit à l'échelle de l'écosystème (ex. TREEGRASS) ou du biome (ex. Sellers et al. 1997).

Bibliographie

[1] Abbadie, L., 1983. Aspects fonctionnels du cycle de l'azote dans la strate herbacée de la savanne de Lamto. Thèse de Doctorat, University Paris 6, 158 pp.

[2] Abbadie, L. 1984. Evolution saisonnière du stock d'azote dans la strate herbacée d'une savane soumise au feu en Côte d'Ivoire. Acta oecologica, Oecologia Plantarum 5 :321-334.

[3] Abbadie, L., Lepage, M., and Le Roux, X. 1992a. Soil fauna at the forest-savanna boundary : role of termite mounds in nutrient cycling. In : Nature and dynamics of forest-savanna boundaries. Furley, P. A., Proctor, J., and Ratter, J. A. Eds. Chapman et al. pp. 473-484.

[4] Abbadie, L., Mariotti, A., and Menaut, J. C. 1992b. Independance of savanna grasses from soil organic matter for their nitrogen supply. Ecology 72 :608-613.

[5] Amadou, M., 1994. Analyse et modélisation de l'évapotranspiration d'une culture de mil en région sahélienne. Thèse de Doctorat, University Paris 11, 106 pp.

[6] Amundson, R. G., Ali, A. R. and Belsky, A. J. (1995). Stomatal responsiveness to changing light intensity increases rain-use efficiency of below-crown vegetation in tropical savannas. J. Arid Environ. 29, 139-153.

[7] Anten, N. P. R., Schieving, F. and Werger, M. J. A. (1995). Patterns of light and nitrogen distribution in relation to whole canopy carbon gain in C_3 and C_4 mono- and dicotyledonous species. Oecologia 101, 504-513.

[8] Anten, N. P. R., Werger, M. J. A. and Medina, E. (1998). Nitrogen distribution and leaf area indices in relation to photosynthetic nitrogen use efficiency in savanna grasses. Plant Ecology 138, 63-75.

[9] Antonovics, J., and Levin, D. A. 1980. The ecological and genetic consequences of density-dependent regulation in plants. Annu. Rev. Ecol. Syst. 11 :411-452.

[10] Archer, S., T. W. Boutton, and K. A. Hibbard. 2000. Trees in grasslands : biogeochemical consequences of woody plant expansion. Pages in press in Schulze, E.-D., Harrison, S. P., Heimann, M., Holland, E. A., LLoyd, J., Prentice, I. C., and Schimel, D., editors. Global biogeochemical cycles in the climate system. Academic Press, San Diego.

[11] Asner, G. P. and Wesman, C. A. (1997). Scaling PAR absorption from the leaf to landscape level in spatially heterogeneous ecosystems. Ecological Modelling 101, 145-163.

[12] Asner, G. P., Wessman, C. A., Archer, S., 1998a. Scale dependance of absorption of photosynthetically active radiation in terrestrial ecosystems. Ecol. Appl., 8 : 1003-1021.

[13] Asner, G. P., Wessman, C. A., and Schimel, D. S. 1998b. Heterogeneity of savanna canopy structure and function from imaging spectrometry and inverse modeling. Ecological Applications 8 :1022-1036.

[14] Aucamp, A. J., J. E. Dankwerts, W. R. Teague, and J. J. Venter. 1983. The role of Acacia karoo in the false thornveld of the Eastern Cape. Journal of Grassland Society of Southern Africa 8 :151-154.

[15] Bailey, D. W., Gross, J. E., Laca, E. A., Rittenhouse, L. R., Coughenour, M. B., Swift, D. M., and Sims, P. L. 1996. Mechanisms that resut in large herbivore grazing distribution patterns. J. Range Manage. 49 :386-400.

[16] Barot, S., Gignoux, J. and Menaut, J.-C. 1999. Demography of a savanna palm tree : predictions from comprehensive spatial pattern analyses. Ecology 80 :1987-2005.

[17] Baruch, Z., and Bilbao, B. 1999. Effects of fire and defoliation on the life history of native and invader C-4 grasses in a Neotropical savanna. Oecologia 119 :510-520.

[18] Baruch, Z. and Fernández, D. S. (1993). Water relations of native and introduced C_4 grasses in a neotropical savanna. Oecologia 96, 179-185.

[19] Baruch, Z., Ludlow, M. M., Davis, R., 1985. Photosynthetic responses of native and introduced C_4 grasses from Venezuelan savannas. Oecologia, 67 : 388-393.

[20] Beale, I. F. 1973. Tree density effects on yields of herbage and tree components in south-west Queensland mulga (*Acacia aneura* F. Meull.) scrub. Tropical Grasslands 7 :135-142.

[21] Belsky, A. J., 1994. Influences of trees on savanna productivity : tests of shade, nutrients, and tree-grass competition. Ecology, 75(4) : 922-932.

[22] Belsky, A. J., R. G. Amundson, J. M. Duxbury, S. J. Riha, A. R. Ali, and S. M. Mwonga. 1989. The effects of trees on their physical, chemical, and biological environments in a semi-arid savanna in Kenya. Journal of Applied Ecology 26 :1005-1024.

[23] Belsky, A. J., S. M. Mwonga, R. G. Amundson, J. M. Duxbury, and A. R. Ali. 1993. Comparative effects of isolated trees on their undercanopy environments in high- and low-rainfall. Journal of Applied Ecology 30 :143-155.

[24] Bergez, J. E., Etienne, M., and Balandier, P. 1999. ALWAYS, a plot-based silvopastoral system model. Ecol. Modelling 115 :1-17.

[25] Bolton, J. K. and Brown, R. H. (1980). Photosynthesis of grass species differing in carbon dioxide fixation pathways. Plant Physiology 66, 97-100.

[26] Boot, R. G. A. and den Dubbelden, K. C. (1990). Effects of nitrogen supply on growth, allocation and gas exchange characteristics of two perennial grasses from inland dunes. Oecologia 85, 115-121.

[27] Borchert, R. (1994). Soil and stem water storage determine phenology and distribution of tropical dry forest trees. Ecology 75, 1437-1449.

[28] Boulain, N. 2000. Modélisation de l'interaction végétation-hydrologie de surface en zone sahélienne : effets du régime des précipitations et de l'occupation des sols. Mémoire de DEA, Université Paris 6, 33 pages.

[29] Brady 1973

[30] Breshears, D. D. and Barnes, F. J. (1999). Interrelationships between plant functional types and soil moisture heterogeneity for semiarid landscapes within the grassland/forest continuum : a unified conceptual model. Landscape Ecology 14, 465-478.

[31] Breshears, D. D., O. B. Myers, S. R. Johnson, and S. N. Martens. 1997a. Differential use of spatially heterogeneous soil moisture by two semiarid woody species : *Pinus edulis* and *Juniperus monosperma*. Journal of Ecology 85 :289-299.

[32] Breshears, D. D., Nyhan, J. W., heil, C. E. and Wilcox, B. P. (1998). Effects of woody plants on microclimate in a semiarid woodland : soil temperature and evaporation in canopy and intercanopy patches. International Journal of Plant Science 159, 1010-1017.

[33] Breshears, D. D., P. M. Rich, F. J. Barnes, and K. Campbell. 1997b. Overstory-imposed heterogeneity in solar radiation and soil moisture in a semiarid woodland. Ecological Applications 7 :1201-1215.

[34] Brouwer, R., 1983. Functional equilibrium : sense or nonsense ? Neth. J. Agric. Sci., 31 : 335-348.

[35] Byrd, G. T., Sage, R. F. and Brown, R. H. (1992). A comparison of dark respiration between C_3 and C_4 plants. Plant Physiology 100, 191-198.

[36] César, J. 1971. Etude quantitative de la strate herbacée de la savane de Lamto (moyenne Côte d'Ivoire). Thèse de doctorat, Université Paris 6.

[37] César, J., et Menaut, J.-C. 1974. Le peuplement végétal des savanes de Lamto (Côte d'Ivoire). Bulletin de liaison des chercheurs de Lamto n° spécial 2, 161 pages.

[38] César, J. 1992. La production biologique des savanes de Côte d'Ivoire et son utilisation par l'homme. Thèse d'Etat. Institut d'élevage et de médecine vétérinaire des pays tropicaux, CIRAD.

[39] Chabot , B. F., Jurik, T. W. and Chabot, J. F. (1979). Influence of instantaneous and integrated light-flux density on leaf anatomy and photosynthesis. Amer. J. Bot. 66, 940-945.

[40] Chapin, F. S. I. and Kedrowski, R. A. (1983). Seasonal changes in nitrogen and phosphorus fractions and autumn retranslocation in evergreen and deciduous taiga trees. Ecology 64, 376-391.

[41] Chaves M. 1991. Effects of water deficit on carbon assimilation. Journal of Experimental Botany 42 :1-16.

[42] Chesson, P. L., and Warner, R. R., 1981. Environmental variability promotes coexistence in lotery competitive systems. Am. Nat. 17 :923-943.

[43] Ciret, C., Polcher, J., Le Roux, X., 1999. An approach to simulate the phenology of savanna ecosystems in the LMD general circulation model. Global Biogeochemical Cycles, 13 : 603-622.

[44] Collatz, G. J., Ribas-Carbo, M. and Berry, J. A. (1992). Coupled photosynthesis-stomatal conductance model for leaves of C_4 plants. Aust. J. plant Physiol. 19, 519-38.

[45] Coquillard, P. et Hill, D. R. C. 1997. Modélisation et simulation d'écosystèmes, des modèles déterministes aux simulations à évènements discrets. Masson, Paris. 273 pages.

[46] Coughenour, M. B., 1994. Savanna - Landscape and regional ecosystem model. Documentation. Fort Collins, Colorado State University, 47 pp.

[47] Crane, W. S. B. and Banks, J. C. G. (1992). Accumulation and retranslocation of foliar nitrogen in fertilised and irrigated Pinus radiata. Forest Ecology and Management 52, 201-223.

[48] Cruz, P. 1997. Effect of shade on the growth and mineral nutrition of a C_4 perennial grass under field conditions. Plant and Soil 188 :227-237.

[49] De Jong, K., 1983. Research on the water balance in a savannah ecosystem. A study for two soil types at Lamto, Ivory Coast. Internal report, ENS, 73 pp.

[50] Daly, C., Bachelet, D., Lenihan, J. M., Neilson, R. P., Parton, W. and Ojima, D. (2000). Dynamic simulation of tree-grass interactions for global change studies. Ecological Applications 10, 449-469.

[51] Daudet, F.A., X. Le Roux, H. Sinoquet, and B. Adam. 1999. Wind speed and leaf boundary layer conductance variation within tree crown - Consequences on leaf-to-atmosphere coupling and tree functions. Agricultural and Forest Meteorology 97 :171-185.

[52] Dauget, J. M., and J. C. Menaut. 1992. Evolution sur 20 ans d'une parcelle de savane boisée non protégée du feu dans la réserve de Lamto (Côte-d'Ivoire). Candollea 47 :621-630.

[53] Delmas, J. 1967. Recherches écologiques dans la savane de Lamto (Côte d'Ivoire). Les sols et leur valeur agronomique. La Terre et la Vie 3 :216-227.

[54] Delmas, R., Lacaux, J. P., Menaut, J.-C., Abbadie, L., Le Roux, X., Lobert, J., and Helas, G. 1995. Nitrogen compound emission from biomass burning in a tropical african savanna, FOS/DECAFE 1991 experiment (Lamto, Ivory Coast). Journal of Atmospheric Chemistry 22 :175-193.

[55] Devineau, J. L., Lecordier, C. et Vuattoux, R. 1984. Evolution de la diversité spécifique du peuplement ligneux dans une succession préforestière de colonisation d'une savane protégée des feux (Lamto, Côte d'Ivoire). Candollea 39 :103-134.

[56] Dewar, R. C. (1996). The correlation between plant growth and intercepted radiation : an interpretation in terms of optimal plant nitrogen content. Annals of Botany 78, 125-136.

[57] Dewar, R. C., Medlyn, B. E., McMurtrie, R. E., 1998. A mechanistic analysis of light and carbon use efficiencies. Plant Cell Env., 21 : 573-588.

[58] Dreyer, E., Le Roux, X., Montpied, P., Daudet, F.-A., and Masson, F.. 2001. Temperature response of leaf photosynthetic capacity in seedlings from seven temperate tree species. Tree Physiol. 21 :223-232.

[59] Durand, J. L., Lemaire, G., Gosse, G., Chartier, M., 1989. Analyse de la conversion de l'énergie solaire en matière sèche par un peuplement de luzerne (*Medicago sativa* L.) soumis à un déficit hydrique. Agronomie, 9 : 599-607.

[60] Eagleson, P. S. and Segarra, R. I., 1985. Water-limited equilibrium of savanna vegetation systems. Water Resour. Res., 21(10) : 1483-1493.

[61] Eamus, D. (1999). Ecophysiological traits of deciduous and evergreen woody species in the seasonally dry tropics. Trends in Ecology and Evolution 14, 11-16.

[62] Eastham, J., and C. W. Rose. 1988. Pasture evapotranspiration under varying tree planting density in an agroforestry experiment. Agricultural Water Management 15 :87-105.

[63] Eastham, J., and C. W. Rose. 1990. Tree/pasture interaction at a range of tree densities in an agroforestry experiment. I. Rooting patterns. Australian Journal of Agricultural Research 41 :683-695.

[64] Eastham, J., C. W. Rose, D. A. Charles-Edwards, D. M. Cameron, and S. J. Rance. 1990. Planting density effects on water use efficiency of trees and pasture in an agroforestry experiment. New Zealand Journal of Forestry Science 20 :39-53.

[65] Edwards, G. E., and Huber, S. C. 1981. C_4 pathway. In : Biochemistry of plants : a comprehensive treatrise (eds M. D. Hatch and N. K. Boardman). Vol. III. Academic Press, New York, London.

[66] Ehleringer, J. and Björkman, O. (1977). Quantum yields of CO2 uptake in C_3 and C_4 plants : dependence on temperature, CO_2 and O_2 concentration. Plant Physiology 59, 86-90.

[67] Ellsworth, D. S. and Reich, P. B. (1992). Leaf mass per area, nitrogen content and photosynthetic carbon gain in *Acer saccharum* seedlings in contrasting forest light environments. Functional Ecology 6, 423-435.

[68] Ellsworth et al. 1994

[69] Farquhar, G. D., Von caemmerer, S. and Berry, J. A. (1980). A biochemical model of photosynthesic CO2 assimilation in leaves of C3 species. Planta 149, 78-90.

[70] Field, C. B. (1983). Allocating leaf nitrogen for the maximization of carbon gain : leaf age has a control on the allocation program. Oecologia 56, 341-347.

[71] Field, C. and Mooney, H. A. (1983). Leaf age and seasonal effects of light, water, and nitrogen use efficiency in a California shrub. Oecologia 56, 348-355. Field, C. and Mooney, H. A. (1986). The photosynthesis-nitrogen relationship in wild plants. In On the economy of plant form and function (ed. T. J. Givnish), pp. 25-55. Cambridge Univresity Press.

[72] Field, C. and H. Mooney. 1986. The photosynthesis-nitrogen relationship in wild plants. Pages 25-55 in Givnish, G. T., editor. On the economy of plant form and function. Cambridge University Press.

[73] Fordyce I. R., Duff G. A., Eamus D. 1995. The ecophysiology of Allosyncarpia ternata (Myrtaceae) in northern Australia : tree physiognomy, leaf characteristics and assimilation at contrasting sites. Aust. J. Bot. 43 :367-377.

[74] Frack et al. 2001

[75] Fraser, G. W., C. D. Canham, and K. P. Lertzman. 1999. Gap Light Analyser (GLA) : Imaging software to extract canopy structure and gap light transmission indices from true-colour fisheye photographs, users manual and program documentation. Copyright (c) 1999 : Simon Fraser University, Burnaby, British Columbia, and the Institute of Ecosystem studies, Millbrook, New York.

[76] Frost, P., E. Medina, J. C. Menaut, O. Solbrig, M. Swift, and B. Walker. 1986. Responses of savannas to stress and disturbance. Biology International 10 :1-82.

[77] Gamon, J. A., Field, C. B., Goulden, M. L., Griffin, K. L., Hartley, A. E., Joel, G., Penuelas, J. and Valentini, R. (1995). Relationships between NDVI, canopy structure, and photosynthesis in three Californian vegetation types. Ecological Applications 5, 28-41.

[78] Garnier and Dajoz 2001

[79] Gastellu-Etchegorry, J. P., and V. Trichon. 1998. A modeling approach of PAR environment in a tropical rain forest in Sumatra : application to remote sensing. Ecological Modelling 108 :237-264.

[80] Gauthier, H. 1993. Echanges radiatifs et production primaire dans une savane humide d'Afrique de l'Ouest (Lamto - Côte d'Ivoire). Mémoire de DEA, CESR University Paul Sabatier Toulouse, 37 pp.

[81] Gautier, L. 1989. Contact forêt-savane en Côte d'Ivoire centrale : évolution de la surface forestière de la réserve de Lamto (sud du V-Baoulé). Bulletin de la société botanique de France 136 :85-92.

[82] Gautier, L. 1990a. carte du recouvrement ligneux de la réserve de Lamto. Conservatoire et jardin botanique de la ville de Genève.

[83] Gautier, L. 1990b. Contact forêt-savane en Côte d'Ivoire centrale : évolution du recouvrement lineux des savanes de la réserve de Lamto (sud du V-Baoulé). Candollea 45 :627-641.

[84] Gifford, R. M. 1994. The global carbon cycle : a viewpoint on the missing sink. Australian Journal of Plant Physiology 21, 1-15.

[85] Gignoux, J. 1994. Modélisation de la coexistence herbes/arbres en savane. Thèse de Doctorat, Univeristy Paris 6, 273 pages.

[86] Gignoux, J., Clobert, J. and Menaut, J. C. (1997). Alternative fire resistance strategies in savanna trees. Oecologia 110, 576-583.

[87] Gignoux, J., C. Duby, and S. Barot. 1999. Comparing the performances of Diggle's tests of spatial randomness for small samples with and without edge effect correction : application to ecological data. Biometrics 55 :156-164.

[88] Gignoux, J., J. House, D. Hall, D. Masse, H. Nacio, and L. Abbadie. 2000. Design and test of a generic cohort model of soil organic matter decomposition : the SOMKO model. Global Ecology and Biogeography, in press.

[89] Gignoux, J., Menaut, J.-C., Noble, I. R., Davies, I. D., 1996. A spatial model of savanna function and dynamics : model description and preliminary results. In : Prins, H. H. T., Brown, N. (Ed.), Dynamics of tropical communities, the 37th symposium of the British Ecological Society, Blackwell Science, pp. 361-383.

[90] Gosse, G., C. Varlet-Grancher, R. Bonhomme, M. Chartier, J. M. Allirand, and G. Lemaire. 1986. Production maximale de matière sèche et rayonnement solaire intercepté par un couvert végétal. Agronomie 6 :47-56.

[91] Gower, S. T. and Norman, J. M. (1991). Rapid estimation of leaf area index in conifer and broad-leaf plantations. Ecology 72, 1896-1900.

[92] Gulmon, S. L. and Chu, C. C. (1981). The effects of light and nitrogen on photosynthesis, leaf characteristics, and dry matter allocation in the Chaparral shrub, *Diplacus aurantiacus*. Oecologia 49, 207-212.

[93] Haase, P., Pugnaire, F. I., Clark, S. C., and Incoll, L. D. 1996. Spatial patterns in a two-tiered semi-arid shrubland in southeastern Spain. J. Veg. Sci. 7 :527-534.

[94] Harley, P. C., Thomas, R. B., Reynolds, J. F. and Strain, B. R. (1992). Modelling photosynthesis of cotton grown in elevated CO2. Plant, Cell and Environment 15, 271-282.

[95] Haxeltine, A. and Prentice, I. C. (1996). BIOME3 : An equilibrium terrestrial biosphere model based on ecophysiological constraints, resource availability, and competition among plant functional types. Global biogeochemical cycles 10, 693-709.

[96] Hesla, B. I., Tieszen, H. L. and Boutton, T. W. (1985). Seasonal water relations of savanna shrubs and grasses in Kenya, East Africa. J. Arid Environ. 8, 15-31.

[97] Hochberg, M. E., Menaut, J. C. and Gignoux, J. (1994). The influence of tree biology and fire in the spatial structure of the West African savannah. Journal of ecology 82, 217-226.

[98] Howard, S. B., Ong, C. K., Black, C. R., Khan, A. A. H., 1997. Using sap flow gauges to quantify water uptake by tree roots from beneath the rooting zone in agroforestry systems. Agrofor. Syst., 35 : 15-29.

[99] Ingestad, T., and G. I. Agren. 1991. The influence of plant nutrition on biomass allocation. Ecological Applications 1 :168-174.

[100] Isichei, A. O. and Muoghalu, J. I., 1992. The effects of tree canopy cover on soil fertility in a Nigerian savanna. J. Trop. Ecol., 8 : 329-338.

[101] Jackson, L. E., Strauss, R. B., Firestone, M. K., Bartolome, J. W., 1990. Influence of tree canopies on grassland productivity and nitrogen dynamics in deciduous oak savanna. Agriculture, Ecosystems and Environment, 32 : 89-105.

[102] Jackson, P.C., F. C. Meinzer, M. Bustamante, G. Goldstein, A. Franco, P. W. Rundel, L. Caldas, E. Igler, and F. Causin. 1999. Partitioning of soil water among tree species in a Brazilian Cerrado ecosystem. Tree Physiology 19 :717-724.

[103] Jarvis, P. G. 1976. The interpretation of the variations in leaf water potential and stomatal conductance found in canopies in the field. Philosophical Transactions of the Royal Society of London Series B. 273 :593-610.

[104] Jeltsch, F., S. J. Milton, W. J. R. Dean, and N. van Rooyen. 1996. Tree spacing and coexistence in semi-arid savannas. Journal of Ecology 84 :583-595.

[105] Jeltsch, F., Milton, S. J., Dean, W. R. J. and Van Rooyen, N. (1997). Analysing shrub encroachment in the southern Kalahari : a grid-based modelling approach. J. Appl. Ecol. 34, 1497-1508.

[106] Joffre, R. and Rambal, S., 1988. Soil water improvement by trees in the rangelands of southern Spain. Acta cologica (col. Plant.), 9(4) : 405-422.

[107] Joffre, R., and S. Rambal. 1993. How tree cover influences the water balance of mediterranean rangelands. Ecology 74 :570-582.

[108] Johansson, G. 1992. Release of organic carbon from growing roots of meadow fescue (*Festuca pratensis* L.). Soil Biol. Biochem. 24 :427-433.

[109] Jordan, D. B., and Ogren, W. L. 1984. The CO_2/O_2 specificity of ribulose 1,5-bisphosphate carboxylase/oxygenase. Planta 161 :593-610.

[110] Kelliher, F. M., Leuning, R., Raupach, M. R. and Schulze, E.-D. (1995). Maximum conductances for evaporation from global vegetation types. Agricultural and Forest Meteorology 73, 1-16.

[111] Kirschbaum, M. U. F. (1999). CenW, a forest growth model with linked carbon, energy, nutrient and water cycles. Ecological Modelling 118, 17-59.

[112] Knoop, W. T. and Walker, B. H., 1985. Interactions of woody and herbaceous vegetation in a southern african savanna. J. Ecol., 73 : 235-253.

[113] Konaté, S., X. Le Roux, D. Tessier, and M. Lepage. 1998. Influence of large termitaria on soil characteristics, soil water regime, and tree leaf shedding pattern in a West African savanna. Plant and Soil 206 :47-60.

[114] Korzukhin, M. D. and Ter-Mikaelian M. T., 1996. An individual tree-based model of competition for light. Ecol. Modelling, 79 : 221-229.

[115] Kuuluvainen, T., and T. Pukkala. 1989. Simulation of within-tree and between-tree shading of direct radiation in a forest canopy : effect of crown shape and sun elevation. Ecological Modelling 49 :89-100.

[116] Lacey, C. J., Walker, J. and Noble, I. R. (1982). Fire in Australian tropical savannas. In Ecology of tropical savannas (ed. H. Walker), pp. 246-272. Springer Verlag.

[117] Landsberg, J. J., and R. H. Waring. 1997. A generalised model of forest productivity using simplified concepts of radiation-use efficiency, carbon balance and partitioning. Forest Ecology and Management 95 :209-228.

[118] Lata, J.-C. 1999. Interactions entre processus microbiens, cycle des nutriments et fonctionnement du couvert herbacé : cas de la nitrification dans les sols d'une savane humide de Côte d'Ivoire sous couvert à *Hyparrhenia diplandra*. Thèse de Doctorat, Université Paris 6, 197 pages.

[119] Le Provost, E., 1993. Structure et fonctionnement de la strate herbacée d'une savanne humide (Lamto, Côte d'Ivoire). Mémoire de DEA, University Paris 11, 38 pp.

[120] Le Roux, X. 1995. Etude et modélisation des échanges d'eau et d'énergie sol-végétation-atmosphère dans une savane humide (Lamto, Côte d'Ivoire). Thèse de Doctorat, Université Paris VI, 203 pages.

[121] Le Roux, X., and T. Bariac. 1998. Seasonal variation in soil, grass and shrub water status in a West African humid savanna. Oecologia 113 :456-466.

[122] Le Roux, X., T. Bariac, and A. Mariotti. 1995. Spatial partitioning of the soil water resource between grass and shrub components in a West African humid savanna. Oecologia 104 :147-155.

[123] Le Roux, X., H. Gauthier, A. Bégué, and H. Sinoquet. 1997. Radiation absorption and use by humid savanna grassland : assessment using remote sensing and modelling. Agricultural and Forest Meteorology 85 :117-132.

[124] Le Roux, X., Grand, S., Dreyer, E., Daudet, F.-A., 1999. Parameterisation and testing of a biochemically based photosynthesis model for walnut (Juglans regia) trees and seedlings. Tree Physiol., 19 : 481-492.

[125] Le Roux, X. and Mordelet, P. (1995). Leaf and canopy CO2 assimilation in a West African humid savanna during the early growing season. Journal of Tropical Ecology 11, 529-545.

[126] Le Roux, X., Polcher, J., Menaut, J.-C., Monteny, B. A., 1994. Radiation exchanges above West African moist savannas : seasonal patterns and comparison with a GCM simulation. J. Geophys. Res., 99(D12) : 25857-25868.

[127] Le Roux, X., Sinoquet, H. and Vandame, M. (1999b). Spatial distribution of leaf dry weight per area and leaf nitrogen concentration in relation to local radiation regime within an isolated tree crown. Tree Physiology 19, 181-188.

[128] Le Roux, X., A. Tuzet, O. Zurfluh, J. Gignoux, A. Perrier, and B. A. Monteny. 1996. Modélisation des interactions surface/atmosphère en zone de savane humide. Pages 303-317 in Hoepffner, M., Lebel, T., and Monteny, B., editors. Interactions surface continentale/atmosphère : l'expérience HAPEX-SAHEL. ORSTOM Editions.

[129] Leriche, H., Le Roux, X., Gignoux, J., Tuzet, A., Fritz, H., Abbadie, L. and Loreau, M. (2001). Which functional processes control the short-term effect of grazing on net primary production in grasslands ? Oecologia 129, 114-124.

[130] Leuning, R. (1990). Modelling stomatal behaviour and photosynthesis of *Eucalyptus grandis*. Australian Journal of Plant Physiology 17, 159-75.

[131] Littleboy, M. and McKeon, G. M., 1997. Evaluating the risks of pasture and land degradation in native pastures in Queensland - Appendix 2 - Subroutine GRASP : Grass Production Model. Indooroopilly : Rural Industries Research and Devlopment Corporation.

[132] Luo, Y. Q. and Reynolds, J. F. (1999). Validity of extrapolating field CO2 experiments to predict carbon sequestration in natural ecosystems. Ecology 80, 1568-1583.

[133] Lynch, J. M., and Whipps, J. M. 1990. Substrate flow in the rhizosphere. Plant Soil 129 :1-10.

[134] McKeon, G. M., Day, K. A., Howden, S. M., Mott, J. J., Orr, D. M., Scattini, W. J. and Weston, E. J. (1990). Northern Australian savannas : management for pastoral production. Journal of Biogeography 17, 355-372.

[135] McNaughton, S. J. 1993. Biodiversity and function of grazing ecosystems. In : Biodiversity and ecosystem function. E.-D. Schulze and H. A. Mooney Eds Springer-Verlag, Ecological studies, Berlin. pp. 361-408.

[136] McPherson, G. R. 1992. Comparison of linear and non-linear overstory-understory models for ponderosa pine : a conceptual framework. Forest Ecology and Management 55 :31-34.

[137] Medina, E., 1982. Physiological ecology of neotropical savanna plants. In : Huntley and Walker (Ed.), Ecology of tropical savannas, pp. 308-335.

[138] Medina, E. and Francisco, M., 1994. Photosynthesis and water relations of savanna tree species differing in leaf phenology. Tree Physiol., 14 : 1367-1381.

[139] Melillo, J. M., D. A. McGuire, D. W. Kicklighter, B. Moore, C. J. Vorosmarty, and A. Schloss, 1993. Global climate change and terrestrial net primary production. Nature 363 :234-240.

[140] Menaut, J.-C., 1974. Chutes de feuilles et apport au sol de litière par les ligneux dans une savane préforestière de Côte d'Ivoire. Bulletin d'Ecologie, 5 : 27-39.

[141] Menaut, J.-C., Abbadie, L., Lavenu, F., Loudjani, P., and Podaire, A. 1991. Biomass burning in West African Savannas. In : Global biomass burning - Atmospheric, climatic and biospheric implications. Levine, J. S. Ed. MIT Press. Cambridge, Mass.pp. 133-142.

[142] Menaut, J.-C., Abbadie, L., and Vitousek, P. 1993. Nutrient and organic matter dynamics in tropical ecosystems. In : Fire in the environment : its ecological, climatic and atmospheric chemical importance. P. J. Crutzen, J. G. Goldammer eds. John Wiley and Sons, pp. 215-231.

[143] Menaut, J.-C. and César, J., 1979. Structure and primary productivity of Lamto savannas, Ivory Coast. Ecology, 60 : 1197-1210.

[144] Menaut, J. C., J. Gignoux, C. Prado, and J. Clobert. 1990. Tree community dynamics in a humid savanna of the Côte d'Ivoire : modelling the effects of fire and competition with grass and neighbours. Journal of Biogeography 17 :471-481.

[145] Millard, P. and Nielsen, G. H. (1989). The influence of nitrogen supply on the uptake and remobilization of stored N for the seasonal growth of apple trees. Annals of Botany 63, 301-309.

[146] Minski, M. L. 1965. Matter, Minds and Models. International Federation of Iformation Processing Congress 1 :45-49.

[147] Monnier, Y. 1968. Les effets des feux de brousse sur une savane préforestière de Côte d'Ivoire. Etudes Eburnéennes IX. 259 pages.

[148] Montaña, C., B. Cavagnaro, and O. Briones. 1995. soil water use by coexisting shrubs and grasses in the southern Chihuahuan desert, Mexico. Journal of Arid Environments 31 :1-13.

[149] Monteith, J. L. 1972. Solar radiation and productivity in tropical ecosystems. Journal of Applied Ecology 2 :747-766.

[150] Monteith, J. L. 1977. Climate and the efficiency of crop production in Britain. Philosophical Transactions of the Royal Society of London Series B 281 :277-274.

[151] Moon, P. and Spencer, D. E., 1942. Illumination from a non-uniform sky. Trans. Illum. Eng. Soc., 37 : 707-712.

[152] Moravie, M.-A., J.-P. Pascal, and P. Auger. 1997. Investigating canopy regeneration processes through individual-based spatial models : application to a tropical rain forest. Ecological Modelling 104 :241-260.

[153] Mordelet, P. 1993a. Influence des arbres sur la strate herbacée d'une savane humide (Lamto, Côte d'Ivoire). PhD. Thesis, University Paris 6, 150 pp.

[154] Mordelet, P., 1993b. Influence of tree shading on carbon assimilation of grass leaves in Lamto savanna, Côte d'Ivoire. Acta cologica (col. Plant.), 14(1) : 119-127.

[155] Mordelet, P., L. Abbadie, and J. C. Menaut. 1993. Effects of tree clumps on soil characteristics in a humid savanna of West Africa (Lamto, Côte d'Ivoire). Plant and Soil 153 :103-111.

[156] Mordelet P., Le Roux X. 2001. Tree/grass interactions. In Menaut J.-C., Abbadie L., and Lepage M. (Eds) Lamto : structure, function and dynamics of a savanna ecosystem. Ecological studies, Springer Verlag, Berlin (in prep.).

[157] Mordelet, P. and Menaut, J.-C., 1995. Influence of trees on above-ground production dynamics in a humid savanna. J. Veg. Sci., 6 : 223-228.

[158] Murrell, D. J., Purves, D. W., and Law, R. 2001. Uniting pattern and process in plant ecology. TREE 16 :529-530.

[159] Naeem, S., Thompon, L. J., Lawler, S. P., Lawton, J. H. and Woodfin, R. M. (1994). Declining biodiversity can alter the performance of ecosystems. Nature 368, 734-736.

[160] Owen Smith, N. 1988. Megaherbivores. The influence of very large body size on ecology. Cambridge University Press.

[161] Ozisik, N. M., 1981. Radiative transfer. Wiley Interscience, New York, 575pp.

[162] Pacala, S. W. and Deutschman, D. H., 1995. Details that matter : the spatial distribution of individual trees maintains forest ecosystem function. Oikos, 74 : 357-365.

[163] Parton, W. J., 1996. The CENTURY model. In : Powlson, D. S., Smith, P., Smith, J. U. (Ed.), Evaluation of soil organic matter models, Springer Verlag, Berlin, pp.283-294.

[164] Parton, W. J., Scurlock, J. M. O., Ojima, D. S., Gilmanov, T. G., Scholes, R. J., Schimel, D. S., Kirchner, T., Menaut, J.-C., Seastedt, T., Garcia Moya, E., Kamnalrut, A., Kinyamario, J. L. 1993. Observations and modelling of biomass and soil organic matter dynamics for the grassland biome worldwide. Global Biogeochemical Cycles 7 :785-809.

[165] Parton, W. J., Stewart, J. W. B. and Cole, C. V. (1988). Dynamics of C, N, P and S in grassland soils : a model. Biogeochemistry 5, 109-131.

[166] Pearcy, R. W. and Ehleringer, J. (1984). Comparative ecophysiology of C3 and C4 plants. Plant, Cell and Environment 7, 1-13.

[167] Polley, H. W., H. S. Mayeux, H. B. Johnson, and C. R. Tischler. 1997. Viewpoint : Atmospheric CO2, soil water, and shrub/grass ratios on rangelands. Journal of Range Management 50 :278-284.

[168] Pressland, A. J. (1975). Productivity and management of Mulga in South-western Queensland in relation to tree structure and density. Australian Journal of Botany 23, 965-976.

[169] Prince, S. D. 1991. A model of regional primary production for use with coarse resolution satellite data. International Journal of Remote Sensing 12 :1313-1330.

[170] Prior L. D., Eamus D., Duff G. A. 1997. Seasonal and diurnal patterns of carbon assimilation, stomatal conductance and leaf water potential in Eucalyptus tetrodonta saplings in a wet-dry savanna in Northern Australia. Aust. J. Bot. 45 :241-258.

[171] Puyravaud, J.-P., Menaut, J.-C., and Abbadie, L. 1990. Herbaceous phytomass dynamics of two Ivorian savannas measured by the harvest method. Its relationship to rainfall. Tropical Ecology 36 :167-176.

[172] Reich, P. B., Walters, M. B. and Ellsworth, D. S. (1992). Leaf life-span in relation to leaf, plant, and stand characteristics among diverse ecosystems. Ecological Monographs 62, 365-392.

[173] Reich et al. 1994

[174] Reich, P. B., Ellsworth, D. S., Walters, M. B., Vose, J. M., Gresham, C., Volin, J. C. and Bowman, W. D. (1999). Generality of leaf trait relationships : a test across six biomes. Ecology 80, 1955-1969.

[175] Rhoades, C. C., 1997. Single-tree influences on soil properties in agroforestry : lessons from natural forest savanna ecosystems. Agroforestry Systems, 35 : 71-94.

[176] Riou, G. 1974. Les sols de la savane de Lamto. Bulletin de liaison des chercheurs de Lamto, numéro spécial.

[177] Roland, J.-C. 1967. Recherches écologiques dans la savane de Lamto (Côte d'Ivoire). Le cycle annuel de la végétation herbacée. La Terre et la Vie 3 :228-237.

[178] Ruimy, A., Dedieu, G. and Saugier, B. (1996). TURC : A diagnostic model of continental gross primary productivity and net primary productivity. Global Biogeochimical Cycles 10, 269-285.

[179] Ruimy, A., Saugier, B., and Dedieu G. 1994. Methodology for the estimation of terrestrial net primary production from remotely sensed data. Journal of Geophysical Research 99 :5263-5283.

[180] Running, S. W. (1994). Testing forest-BGC ecosystem process simulations across a climatic gradient in Oregon. Ecol. Applications 4, 238-247.

[181] Ryan, M. G. 1995. Foliar maintenance respiration of subalpine and boreal trees and shrubs in relation to nitrogen content. Plant, Cell and Environment 18 :765-772.

[182] Sage, R. F. and Pearcy, R. W. (1987). The nitrogen use efficiency of C_3 and C_4 plants. II. Leaf nitrogen effects on the gas exchange characteristics of Chenopodium album (L.) and Amaranthus retroflexus (L.). Plant Physiology 84, 959-963.

[183] San José, J. J., Fariñas, M. R. and Rosales, J. (1991). Spatial patterns of trees and structuring factors in a Trachypogon savanna of the Orinoco Llanos. Biotropica 23, 114-123.

[184] SAS Institute, 1990. SAS/STAT user's guide, SAS institute, Cary.

[185] Scanlan, J. C., and W. H. Burrows. 1990. Woody overstorey impact on herbaceous understorey in *Eucalyptus* spp. communities in central Queensland. Australian Journal of Ecology 15 :191-197.

[186] Scholes, R. J., and S. R. Archer. 1997. Tree-Grass interactions in savannas. Annual Review of Ecology and Systematics 28 :517-544.

[187] Scholes, R. J. and Hall, D. O., 1996. The carbon budget of tropical savannas, woodlands and grasslands. In : Hall, D. O., Breymeyer, A. I., Mellilo, J. M., Agren, G. I., (Ed.), Global change : effects on coniferous forests and grasslands, SCOPE, Wiley and Sons, pp. 69-100.

[188] Schulze, E.-D., Kelliher, F. M., Körner, C., Lloyd, J., and Leuning, R. 1994. Relationships among stomatal conductance, ecosystem surface conductance, carbon assimilation rate, and plant nitrogen nutrition : a global ecology scaling exercise. Annu. Rev. Ecol. Syst. 25 :629-660.

[189] Sellers, P. J., L. Bounoua, J. Collatz, D. A. Randall, D. A. Dazlich, S. O. Los, J. A. Berry, I. Fung, C. J. Tucker, C. B. Field, and T. G. Jensen. 1996. Comparison of radiative and physiological effects of double atmospheric CO2 on climate. Science 271 :1402-1406.

[190] Sellers, P. J., Dickinson, R. E., Randall, D. A., Betts, A. K., Hall, F. G., Berry, J. A., Collatz, G. J., Denning, A. S., Mooney, H. A., Nobre, C. A., Sato, N., Field, C. B. and Henderson- Sellers, A. (1997). Modeling the exchanges of energy, water, and carbon between continents and the atmosphere. Science 275, 502-509.

[191] Senft, R. L., Coughenour, M. B., Bailey, D. W., Rittenhouse, L. R., Sala, O. E., and Swift, D. M. 1987. Large herbivore foraging and ecological hierarchies. Landscape ecology can enhance traditional foraging theory. BioScience 37 :789-799.

[192] Simioni, G., 2001. Importance de la structure spatiale de la strate arborée sur les fonctionnements carboné et hydrique des écosystèmes herbes-arbres. Exemple d'une savane d'Afrique de l'Ouest. Thèse de doctorat.

[193] Simioni, G., Gignoux J./Le Roux X. 2001a. A model to predict 3D water balance and gross and net primary productions in tree/grass ecosystems, accounting for biodiversity and spatial vegetation structure. En préparation.

[194] Simioni, G., Gignoux, J., and Le Roux, X. 2001b How does the spatial structure of the tree layer influence water balance and primary production in savannas? Results of a 3D modelling approach. A soumettre.

[195] Simioni, G., Gignoux, J., Le Roux, X., and Appé, R. 2001c. Spatial and temporal variations in leaf area index, specific leaf area, and leaf nitrogen of two co-occurring savanna tree species. A soumettre.

[196] Simioni, G., Gignoux, J., Le Roux, X. and Leriche, H. (2001d). TREEGRASS, A 3D process-based model for simulating the functioning of tree-grass ecosystems : potential for herbivory studies. International Symposium on Silvopastoral Systems, Second Congress on Agroforestry ans Livestock Production in Latin America (ed. M. Ibrahim), San Jose, Costa Rica.

[197] Simioni, G., X. Le Roux, J. Gignoux, and H. Sinoquet. 2000. TREEGRASS : a 3D, process-based model for simulating plant interactions in tree-grass ecosystems. Ecological Modelling 131 :47-63.

[198] Simioni, G., Walcroft, A., Le Roux, X., and Gignoux, J. 2001e. leaf gas exchange characteristics and water- and nitrogen- use efficiencies of dominant grass and tree species in a West African savanna. A soumettre.

[199] Simoes, M. and Baruch, Z., 1991. Responses to simulated herbivory and water stress in two tropical C_4 grasses. Oecologia, 88 : 173-180.

[200] Sinoquet, H. and Bonhomme, R., 1992. Modeling radiative transfer in mixed and row intercropping systems. Agric. For. Meteorol., 62 : 219-240.

[201] Sinoquet, H., Le Roux, X., Adam, B., Ameglio, T. and Daudet, F. A. (2001). RATP : a model for simulating the spatial distribution of radiation absorption, transpiration and photosynthesis within canopies : application to an isolated tree crown. Plant, Cell and Environment 24, 395-406.

[202] Sinoquet, H., Le Roux, X., Améglio, T., Daudet, F.-A., 2000. Modélisation de la distribution spatiale du microclimat lumineux, de la transpiration et de la photosynthèse : application à un arbre isolé. In : Maillard, P., and Bonhomme, R., (Ed.), Fonctionnement des peuplements végétaux sous contraintes environnementales, INRA Editions, Paris, Série Les Colloques, pp. 185-199.

[203] Skarpe, C. (1991). Spatial patterns and dynamics of woody vegetation in an arid savanna. Journal of Vegetation Science 2, 565-572.

[204] Skarpe, C. 1992. Dynamics of savanna ecosystems. Journal of Vegetation Science 3 :293-300.

[205] Smith, T. M., and P. S. Goodman. 1986. The effect of competition on the structure and dynamics of *Acacia* savannas in southern Africa. Journal of Ecology 74 :1031-1044.

[206] Sobrado M. A. 1991. Cost benefit relationships in deciduous and evergreen leaves of tropical dry forest species. Funct. Ecol. 5 :608-616.

[207] Sobrado M. A. 1996. Leaf photosynthesis and water loss as influenced by leaf age and seasonal drought in an evergreen tree. Photosynthetica 32 :563-568.

[208] Solbrig, O., J. C. Menaut, M. Mentis, H. H. Shugart, P. Stott, and D. Wigston. 1990. Savanna modelling for global change. Biology International 24 :3-45.

[209] Sorrensen-Cothern, K. A., E. D. Ford, and D. G. Sprugel. 1993. A model of competition incorporating plasticity through modular foliage and crown development. Ecological Monographs 63 :277-304.

[210] Stuart-Hill, G. C. and Tainton, N. M., 1989. The competitive interaction between *Acacia karroo* and the herbaceous layer and how it is influenced by defoliation. J. Appl. Ecol., 26 : 285-298.

[211] Sueur, J., 1995. Comparaison des échanges gazeux foliaires de différents génotypes d'une graminée de savane (Hyparrhenia diplandra). Mémoire de DEA, ENS Lyon, 26 pp.

[212] Tan, W. X., and G. D. Hogan. 1998. Dry weight and N partitioning in relation to substrate N supply, internal N status and developmental stage in jack pine (*Pinus banksiana* Lamb.) seedlings : implications for modelling. Annals of Botany 81 :195-201.

[213] Tilman, D., and Kareiva, P. 1997. Spatial ecology : the role of space in population dynamics and interspecific interactions. Princeton University Press.

[214] Tissue, D. T., Griffin, K. L., Thomas, R. B. and Strain, B. R. (1995). Effects of low and elevated CO_2 on C_3 and C_4 annuals. II. Photosynthesis and leaf biochemistry. Oecologia 1995.

[215] Tournebize, R., H. Sinoquet, and B. Bussière. 1996. Modelling evapotranspiration partitioning in a shrub/grass alley crop. Agricultural and Forest Meteorology 81 :255-272.

[216] Tuzet, A., J. F. Castell, A. Perrier, and O. Zurfluh. 1997. Flux heterogeneity and evapotranspiration partitioning in a sparse canopy : the fallow savanna. Journal of Hydrology 189 :492-493.

[217] Ullman, I., 1985. Diurnal courses of transpiration and stomatal conductance of sahelian and saharian acacias in the dry season. Flora, 176 : 383-409.

[218] Vales, D. J., and F. L. Bunnel. 1998. Relationships between transmission of solar radiation and coniferous forest stand characteristics. Agricultural and Forest Meteorology 43 :201-223.

[219] Vetaas, O. R. 1992. Micro-site effects of trees and shrubs in dry savannas. Journal of Vegetation Science 3 :337-344.

[220] Von Caemmerer, S., and Farquhar, G. D. 1981. Some relationships between the biochemistry of photosynthesis and the gas exchange of leaves. Planta 153 :376-387.

[221] Vuattoux, R. 1970. Observations sur l'évolution des strates arborée et arbustive dans la savane de Lamto. Annales de l'Université d'Abidjan, série E 3 :285-315.

[222] Vuattoux, R. 1976. Contribution à l'étude de l'évolution des strates arborée et arbustive dans la savane de Lamto (Côte d'Ivoire), deuxième note. Annales de l'Université d'Abidjan, série C XII :35-63.

[223] Walker, B. H., Ludwig, D., Holling, C. S., Peterman, R. M., 1981. Stability of semi-arid savanna grazing systems. J. Ecol., 69 : 473-498.

[224] Walker, B. H. and Noy-Meir, I. (1982). Aspect of the stability and resilience of savanna ecosystems. In Ecology of tropical savannas (ed. W. B. H. Huntley), pp. 556-590. Springer Verlag.

[225] Walker, J., R. M. Moore, and J. A. Robertson. 1972. Herbage response to tree and shrub thinning in *Eucalyptus populnea* shrub woodlands. Australian Journal of Agricultural Research 23 :405-410.

[226] Walker, J., J. A. Robertson, and L. K. Penridge. 1986. Herbage response to tree thinning in a *Eucalyptus crebra* woodland. Australian Journal of Ecology 11 :135-140.

[227] Walker, J., Sharpe, P. J. H., Penridge, L. K. and Wu, H. (1989). Ecological field theory : the concept and field tests. Vegetatio 83, 81-95.

[228] Waring, R. H., Landsberg, J. J. and Williams, M. (1998). Net production of forests : a constant fraction of gross primary production ? Tree Physiology 18, 129-134.

[229] Weishampel, J. F. and Urban, D. L., 1996. Coupling a spatially-explicit forest gap model with a 3-D solar routine to simulate latitudinal effects. Ecol. Modelling, 86 : 101-111.

[230] Weltzin, J. F., and M. B. Coughenour. 1990. Savanna tree influence on understory vegetation and soil nutrients in northwestern Kenya. Journal of Vegetation Science 1 :325-334.

[231] Williams, M. 1996. A three-dimensional model of forest development and competition. Ecological Modelling 89 :73-98.

[232] Williams R. J., Myers B. A., Muller W. J., Duff G. A., and Eamus D. 1997. Leaf phenology of woody species in a North Australian tropical savanna. Ecology 78 :2542-2558.

[233] Wilson, J. B. 1988. A review of evidence on the control of shoot :root ratio, in relation to models. Annals of Botany 61 :433-449.

[234] Wilson , K. B., Baldocchi, D. D., and Hanson, P. J. 2001. Spatial and seasonal variability of photosynthetic parameters and their relationship to leaf nitrogen in a deciduous forest. Tree Physiol. 20 :565-578.

[235] Woodward F. I., and Smith T. 1995. Predictions and measurements of the maximum photosynthetic rate Amax, at the global scale. pp. 491-509 in Schulze E. D., Caldwell M. M. (Eds) Ecophysiology of photosynthesis. Springer Verlag, Berlin.

[236] Woodward, F. I., T. M. Smith, and W. R. Emanuel, 1995. A global land primary productivity and phytogeography model. Global Biogeochemical Cycles 9 :471-490.

[237] Wright S. J., and Cornejo F. H. 1990. Seasonal drought and leaf fall in a tropical forest. Ecology 71 :1165-1175.